NASA CR-2001-210260

2000 RESEARCH REPORTS

NASA/ASEE SUMMER FACULTY FELLOWSHIP PROGRAM

JOHN F. KENNEDY SPACE CENTER
AND
UNIVERSITY OF CENTRAL FLORIDA

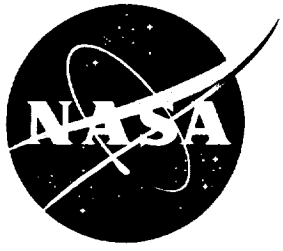

2000 RESEARCH REPORTS

NASA/ASEE SUMMER FACULTY FELLOWSHIP PROGRAM

JOHN F. KENNEDY SPACE CENTER

UNIVERSITY OF CENTRAL FLORIDA

EDITORS:

Dr. E. Ramon Hosler, University Program Director
Department of Mechanical, Materials and Aerospace Engineering
College of Engineering
University of Central Florida

Mr. Gregg Buckingham, NASA/KSC Program Director
University Programs Office
John F. Kennedy Space Center

NASA Grant No. NAG10-280

Contractor Report No. CR-2001-210260

November 2000

PRIMARY/CW/IN/99

PREFACE

This document is a collection of technical reports on research conducted by the participants in the 2000 NASA/ASEE Summer Faculty Fellowship Program at the John F. Kennedy Space Center (KSC). This was the sixteenth year that a NASA/ASEE program has been conducted at KSC. The 2000 program was administered by the University of Central Florida (UCF) in cooperation with KSC. The program was operated under the auspices of the American Society for Engineering Education (ASEE) and the Education Division, NASA Headquarters, Washington, D.C. The KSC program was one of nine such Aeronautics and Space Research Programs funded by NASA Headquarters in 2000.

The basic common objectives of the NASA/ASEE Summer Faculty Fellowship Program are:

a. To further the professional knowledge of qualified engineering and science faculty members;
b. To stimulate an exchange of ideas between teaching participants and employees of NASA;
c. To enrich and refresh the research and teaching activities of participants institutions; and,
d. To contribute to the research objectives of the NASA center.

The KSC Faculty Fellows spent ten weeks (May 15 through July 21 or June 5 through August 11, 2000) working with NASA scientists and engineers on research of mutual interest to the university faculty member and the NASA colleague. The editors of this document were responsible for selecting appropriately qualified faculty to address some of the many research areas of current interest to NASA/KSC. A separate document reports on the administrative aspects of the 2000 program. The NASA/ASEE program is intended to be a two-year program to allow in-depth research by the university faculty member. In many cases a faculty member has developed a close working relationship with a particular NASA group that had provided funding beyond the two-year limit.

TABLE OF CONTENTS

5/cw/10/-3

2000 NASA/ASEE SUMMER FACULTY FELLOWSHIP PROGRAM

JOHN F. KENNEDY SPACE CENTER
UNIVERSITY OF CENTRAL FLORIDA

DEVELOPING A NEW SAMPLING AND ANALYSIS METHOD FOR HYDRAZINE AND MONOMETHYL HYDRAZINE:

Using a Derivatizing Agent with Solid Phase Microextraction

Dr. John Allen
Instructor of Chemistry
Southeastern Louisiana University
Rebecca Young
KSC Colleague

ABSTRACT

Solid phase microextraction (SPME) will be used to develop a method for detecting monomethyl hydrazine (MMH) and hydrazine (Hz). A derivatizing agent, pentafluorobenzoyl chloride (PFBCl), is known to react readily with MMH and Hz. The SPME fiber can either be coated with PFBCl and introduced into a gaseous stream containing MMH, or PFBCl and MMH can react first in a syringe barrel and after a short equilibration period a SPME is used to sample the resulting solution. These methods were optimized and compared. Because Hz and MMH can degrade the SPME, letting the reaction occur first gave better results. Only MMH could be detected using either of these methods. Future research will concentrate on constructing calibration curves and determining the detection limit.

1. Introduction

Fueling rockets and the space shuttle constitutes more dangers than just the threat of the fuel igniting. The fuel itself may be toxic as in the case of hypergols. Hypergols can contain hydrazine, N_2H_4, or more commonly monomethyl hydrazine, $CH_3N_2H_3$. Hypergols are used in the thrusters of single use rockets, solid rocket boosters of the space shuttle, and in the space shuttle orbiter. Both fuels cause acute poisoning and are known to be carcinogens in addition to being corrosive[1,2]. In addition, both are gases that can easily make large areas dangerous to the health of people working near the region. Therefore great care must be exercised when using hypergols containing hydrazine or its analogs. Due to its reactivity and toxicity, development of simple, fast, accurate methods of monitoring monomethyl hydrazine and hydrazine are necessary.

There have been several different methods used for detecting hydrazine and monomethyl hydrazine such as reacting hydrazine or its analogs directly with acetone, and analyzed the resultant product by the means of gas chromatography/mass spectroscopy instrumentation[3]. Many of these methods must be first standardized with a known concentration of analyte. In order to accomplish the analysis there must be a method to standardized the known concentration of analyte, which is simple, accurate, and reproducible. The standard method for analyzing monomethyl hydrazine and hydrazine is a coulometric titration involving scrubbing with sulfuric acid. The coulometric titration is very accurate, but complicated and time consuming. The scrubbing at low vapor concentrations may take several hours.

One possible new method to resolve the problem, involves reacting hydrazine or monomethyl hydrazine with a derivatizing agent in a sealed container such as a syringe and introducing the sample with solid phase microextraction (SPME) into a gas chromatograph/mass spectrometer (GC/MS) for determination. Another method involves coating the SPME with the derivatizing agent, inserting the SPME into the sample stream for a set length of time to allow the derivatizing agent to react with any analyte, and then injecting the SPME into the injection port of the GC/MS. While coating the SPME with the derivatizing agent has the positive characteristic of being simpler, it does expose the SPME to the corrosive effect of the analyte gas stream. These two methods will be optimized and analyzed in regard to simplicity, time, reproducibility, and practicality. Problems will be investigated and solved if possible. Finally recommendations on the ability of using this method as compared to the standard method will be made.

An advantage of SPME is that no solvent is used to introduce the sample into the injection port, which simplifies the method and reduces the chances of errors being introduced into the analysis. Both methods involving the use of SPME could decrease sampling time if the reaction with the derivatizing agent is fast or the equilibrium constant is large[4]. Also fewer solutions and wet chemistry is involved compared to the coulometric titration, since the only solution or chemical needed is the derivatizing agent.

The derivatizing agent selected in this case is pentafluorobenzoyl chloride (PFBCl), which has been used with hydrazine(Hz) and monomethyl hydrazine(MMH) in headspace sampling using a GC/MS for the determination of pesticides in apple juice[5]. Pentafluorobenzoyl chloride reacts quickly with monomethyl hydrazine and hydrazine forming several different derivatives. In the equations below, hydrazine is most likely to form hz-PFB(tetras) and monomethyl hydrazine may react with three PFBCl molecules to form the most likely derivative, MMH-PFB(tris), although bis derivatives for both may also form as well.

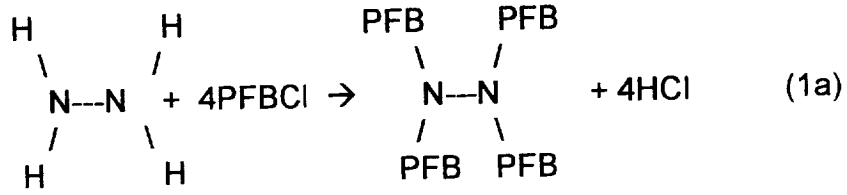

(1a)

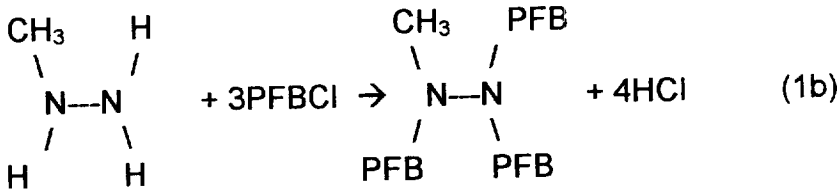

(1b)

2. Methods

As indicated, a SPME fiber will be used to introduce a sample into the injection port of a GC/MS. The gas chromatograph used was a Varian Star 3600 with a mass spectrometer (Varian Saturn 2000) and 8200 autosampler with SPME option, which allowed the separation of the derivatives from the derivatizing agent and identification of the derivatives by mass spectroscopy. The mass spectrum was compared to literature values for the monomethyl hydrazine and hydrazine derivatives in order to identify the correct peak on the chromatogram.

The heart of SPME is a fused silica fiber coated with a polymer. This fiber is attached to a plunger contained in a syringe-like body. This allows the coated fiber to be exposed or drawn into the needle for protection and to preserve the sample (Figure 1). Different polymers can be coated on the fiber, to have a broad range of samples that can be absorbed on the SPME. The choice of polymer is an important step in formulating the analysis. Several different polymers were compared in development of the method.

Figure 1. Schematic of the Operation of a SPME

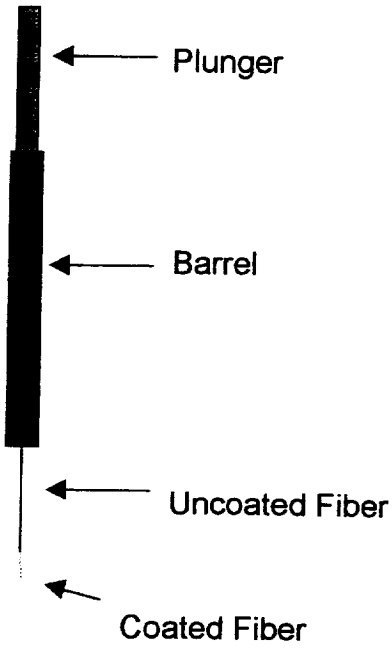

SPME can be used with liquids or gases. The needle of the SPME apparatus is used to pierce the septum of the sample container and to protect the fiber from physical damage. After the SPME is inserted into the sample the SPME fiber is extended into either the liquid, the headspace above the liquid, or into a gas chamber. Equilibrium is established between the polymer coating and the sample after a set period depending on the equilibrium constant. After which, the fiber is withdrawn and the SPME is removed from the sample container. And finally inserted, and the fiber exposed, into the injection port of the gas chromatograph where the heat from the injection port causes the equilibrium to shift to favor desorption of the analyte from the fiber onto the column[4].

Two different techniques are used with SPME. The first involves coating the SPME fiber with a derivatizing agent by absorbing from headspace or dipping the SPME fiber into the liquid derivatizing agent. The hydrazine or analog will react forming the derivative on the surface of the fiber coating. The SPME apparatus can then be placed on the autosampler to be inserted into the injection port. Variables such as absorption of derivatizing agent, exposure time in analyte gas stream, transportation time of SPME, and possible side reaction must be optimized or determined.

An alternative to coating the SPME is to allow the reaction to occur before absorption occurs. This sidesteps any problems exposing the SPME to hydrazine or monomethyl hydrazine. The method consists of adding a known volume of derivatizing

agent to a syringe, drawing up a known volume of gas containing the analyte, allowing the gas to mix with the derivatizing agent to form the derivative, and finally injecting the solution into a vial, into which a SMPE may be inserted to extract a sample. Problems can arise if the air is not excluded when the derivatizing agent is drawn. The needle used to draw the derivatizing agent must not be used again in adding the analyte gas to the syringe. A different needle is needed for the analyte gas. Mixing must be complete to insure that all of the analyte has reacted. Finally, the needle must not allow the derivatizing agent or the analyte gas to leak out of the barrel, which can be accomplished by using a gas tight syringe with a lock mechanism on the inlet of the syringe.

3. Results

In developing a new method for the analysis of Hz and MMH vapor samples, the choice of SPME polymer is a primary variable, from coating favoring polar compounds to ones resembling a liquid layer.
Polydimethylsiloxane(PDMS)/polydivinylbenzene(DVB) coating has been used for a similar derivatizing agent and was the first choice[6]. In fact, most of the following experiments were performed with a PDMS/DVB coated SPME. However, this polymer was found to be noisy and degraded easily. As a substitute, polyacrylate coating was used and found to be superior. Future experiments will be performed with the polyacrylate coated SPME.

The second most important parameter to be determined is the derivatizing agent. Hydrazine and monomethyl hydrazine are too reactive and light massed to be determined directly. Rutschmann and Buser reacted PFBCl with Hz, MMH, and unsymmetrical dimethylhydrazine to form derivatives that were analyzed with GC/MS[5]. Based on these results, PFBCl was the first choice for a derivatizing agent.

During another experiment the SPME was observed to form a coating limiting the number of absorbance sites on the polymeric coating. The trials in Figure 2 were performed at random but appear to decrease with each injection of the SPME into the derivatizing agent. Afterwards a modification to the gas chromatograph was added cleaning the SPME by inserting the fiber into the injection port at high temperatures (230°C for PDMS based SPMEs and 250°C for polyacrylate SPMEs) for 15 minutes. The chromatograms of these cleaning steps revealed more PFBCl remaining as well as degradation products. This could have been the reason for the gradual decrease in response as seen in Figure 2.

Figure 2. Effective coating of SPME by dipping into PFBCl vs. Time

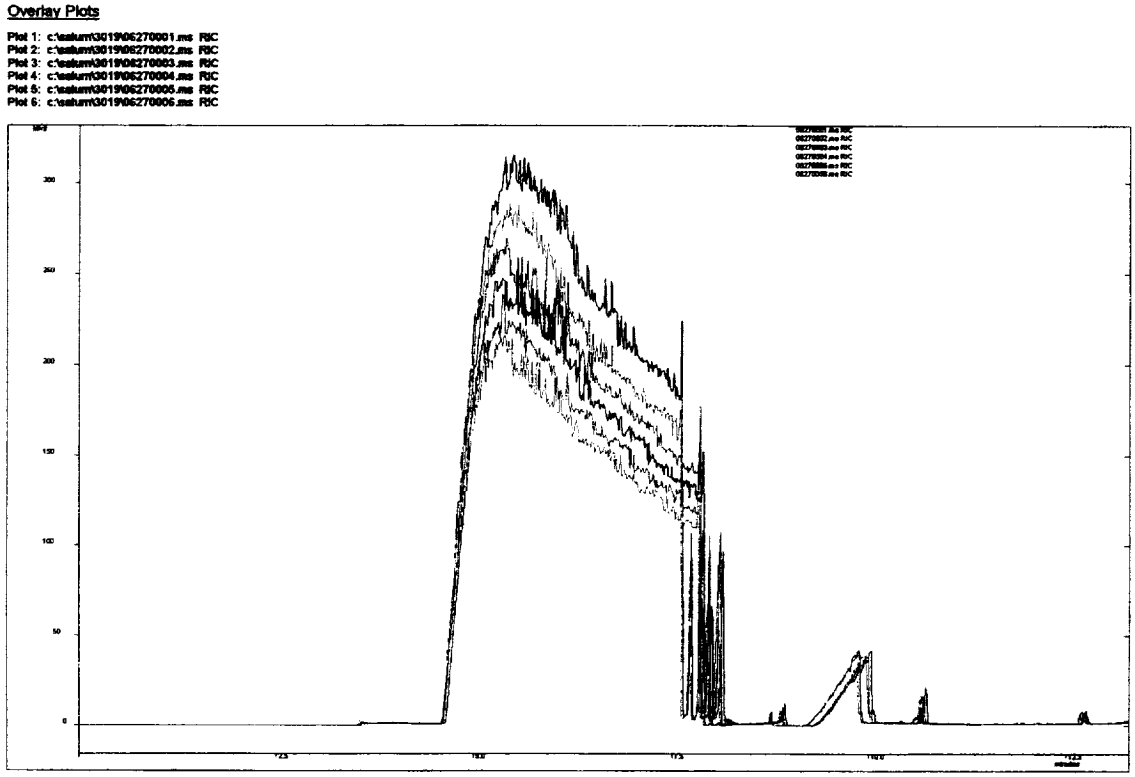

Chromatograms were preformed consecutively. The top two chromatograms were dipped in PFBCl for 30sec. The next two were dipped in PFBCl for 5 mins. And the bottom two chromatograms were dipped for 1 min.

In order to find the peak corresponding the presence of MMH-PFB or Hz-PFB in the respective determination, a sample containing 200 μL of PFBCl and 0.2 μL of the liquid analyte were mixed. The resulting solutions were sampled by a poyacrylate SPME. The mixture containing Hz-PFB did not show a peak corresponding to this compound, while the MMH-PFBCl solution gave a peak at 21 minutes corresponding to MMH-PFB(tris) (Figure 3) The compound was identified by the 416, 195, 117 m/z peaks in the mass spectrum, which correspond to what is expected of MMH-PFB(tris), even though the 167 m/z peak and the molecular mass peak are absent[5].

Figure 3. Chromatogram using SPME on a Solution Containing PFBCl and 200 µL of Liquid Monomethyl Hydrazine.

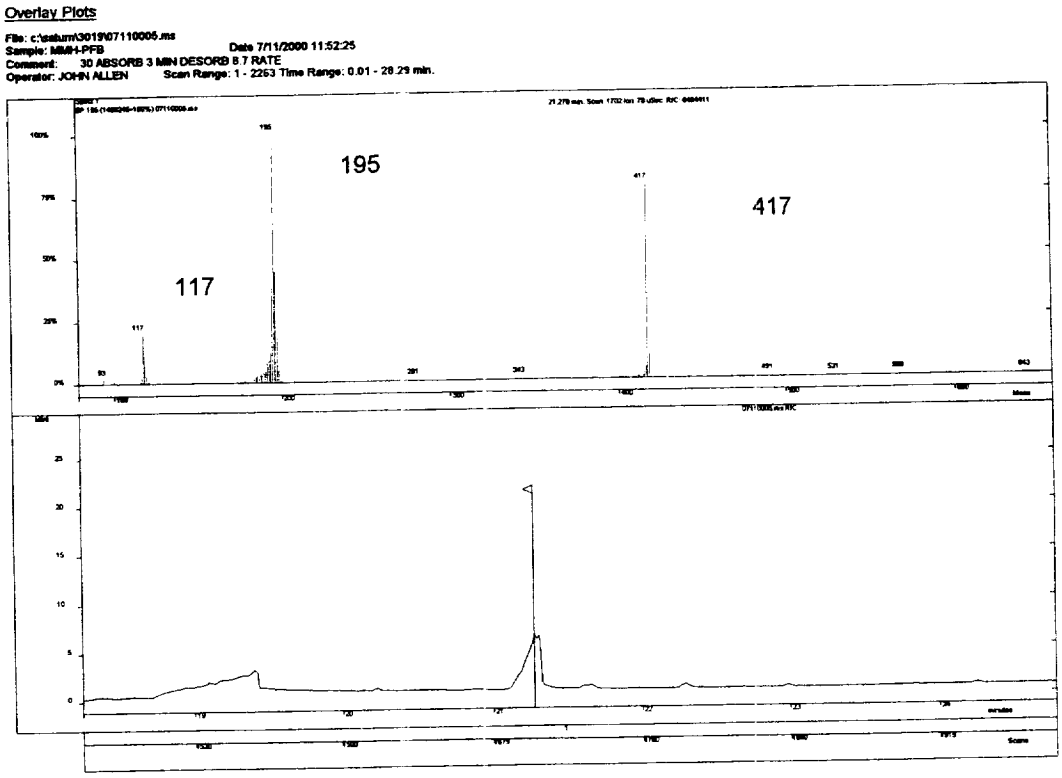

Normally, the derivatizing agents coat the SPME fibers subsequently, the fiber is exposed to the analyte to capture the analyte as a derivative on the polymeric coating of the fiber. This is the approach taken for the first method examined. PFBCl is a volatile liquid, which is used as a derivatizing agent for GC/MS. There are two procedures for coating the SPME fiber, either absorbance of the derivatizing agent from the headspace for a set time or dipping the fiber for a set time in the liquid PFBCl. Adsorbing the PFBCl on the fiber involved inserting the fiber for a set time into the headspace of a PFBCl solution. There were no dramatic increases in amount absorb after 5 minutes adsorbing time. Sampling hydrazine gas streams using this method were performed. Hz may have formed derivatives with the derivatizing agent but also attacked the SPME fiber itself. Therefore this method was abandoned in favor of dipping the SPME into the PFBCl liquid to insure a thick coating of derivatizing agent. Hz should not come into contact with the bare SPME polymer coating. The amount of time necessary to have a thick coating on the SPME (Figure 2) indicates in a short time (30 seconds) the fiber absorbs a thick coating of derivatizing agent. However, experiments exposing these fibers to Hz demonstrate that the Hz can still damage the fiber.

Since Hz and MMH can damage the fiber and render the SPME inoperable, a new method where the analyte and the derivatizing agent are mixed and react before coming

into contact with the SPME was developed. A know amount of PFBCl was drawn into a gas tight locking syringe. A known volume of MMH or Hz is bubbled through the liquid PFBCl and mixed by shaking the syringe. A white smoke can be seen at first, which gradually disappears. The chromatograph of a series of different concentrations of MMH using this method contains peaks with the same retention time as the sample containing liquid MMH (Figure 4). However, there was no correlation to concentration of MMH. The problems may be due to changes in concentration in the headspace of the MMH used to provide the gas. This sample was a sealed bottle of MMH. Also the needle used to draw the sample was stainless steel, which reacts with MMH. The concentrations drawn may have become nonlinear.

Figure 4. Chromatogram of Different Concentrations of Headspace Gaseous MMH Premix with PFBCl Sampled with a SPME.

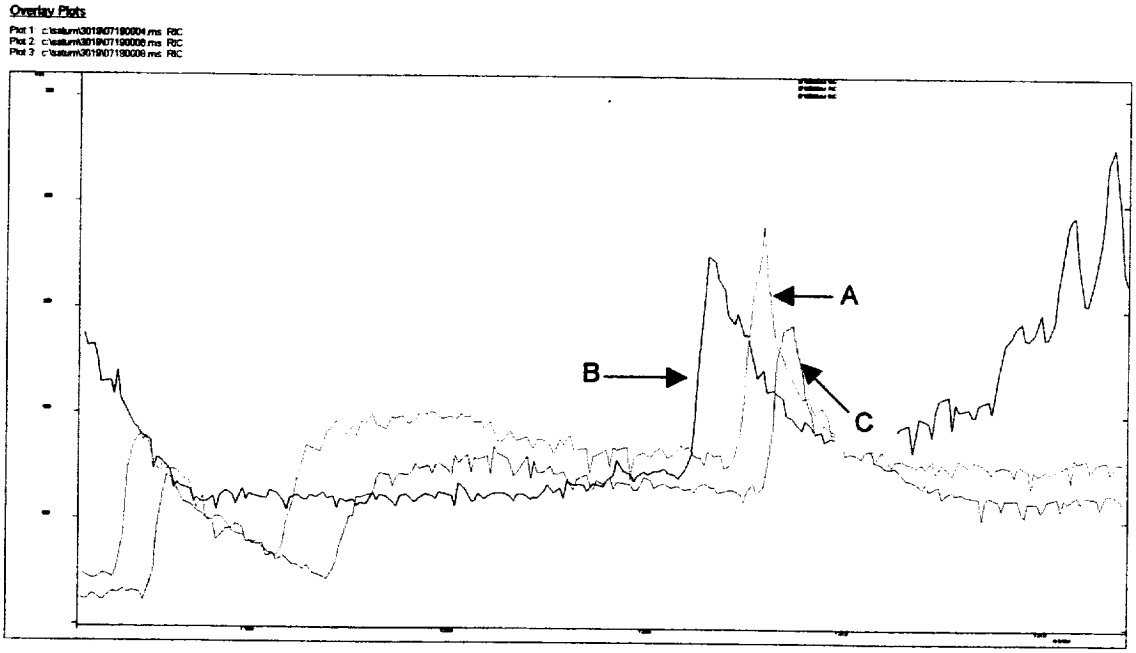

A: 100 μL MMH B: 200 μL MMH C: 300 μL MMH

4. Conclusion and Future Research

The derivative of MMH and PFBCl has been identified in the chromatogram, which was one of the goals of the project. No such derivative has been found for hydrazine and PFBCl, which would mean that major changes to the method or use of a different method should be used for the determination of Hz. Further modifications for the determination of MMH must be performed on the reaction first technique before it can become useful. Results indicate that for the detection limit needed for this technique (10 ppb) to be viable, larger volumes of analyte gas must be used. A better choice of syringe to increase the volume of analyte gas along with a more accurate transfer of reagents should allow a calibration curve to be constructed.

References

[1] Hannum, J. E. "Recent Developments in the Toxicology of Propellant Hydrazines"; Chemical Propulsion Information Agency, Laurel, MD, 1982.

[2] Ellis, Diane L.; Zakin, Mitchell R.; Bernstein, Lawrence S.; Rubner, Michael F. *Anal. Chem.* 68, **1996**, 817-822.

[3] Holtzclaw, James R.; Rose, Susan L.; Wyatt, Jeffrey R. *Anal.Chem.* 56, **1984**, 2952-2956.

[4] Pawliszyn, Janusz "Solid Phase Miceroextraction: Theory and Practice", Wiley-VCH, Inc. New York, NY, 1997.

[5] Rutschmann, Marcel Andre; Buser, Hans-Rudolf *J. Agric. Food Chem.* 39, **1991**,176-181.

[6] Martos, Perry A.; Pawliszyn, Janusz *Anal. Chem.*70, **1998**, 2311-2320.

52/IW/IN/32

ASEE/NASA SUMMER FACULTY FELLOWSHIP PROGRAM

JOHN F. KENNEDY SPACE CENTER
UNIVERSITY OF CENTRAL FLORIDA

UTILIZATION OF KSC PRESENT BROADBAND COMMUNICATIONS DATA SYSTEM FOR DIGITAL VIDEO SERVICES

Alfred S. Andrawis

Associate Professor
Electrical Engineering Department
South Dakota State University
Brookings, SD 57007
E-mail: Alfred_Andrawis@sdstate.edu

KSC Colleague

Po Tien Huang

YA-D5
Kennedy Space Center, Florida 32899
E-mail: PoTien.Huang-1@ksc.nasa.gov

ABSTRACT

This report covers a visibility study of utilizing present KSC broadband communications data system (BCDS) for digital video services. Digital video services include compressed digital TV delivery and video-on-demand. Furthermore, the study examines the possibility of providing interactive video on demand to desktop personal computers via KSC computer network.

UTILIZATION OF PRESENT KSC BROADBAND COMMUNICATIONS DATA SYSTEM FOR DIGITAL VIDEO SERVICES

Alfred S. Andrawis

1. INTRODUCTION

Existing analog television standards are in the process of being phased out and replaced with digital television (DTV) standards such as SMPTE 259M (digital NTSC) and SMPTE 292 (high definition television, HDTV). The present broadband communication data system (BCDS) of the Kennedy Space Center (KSC) is designed to distribute analog NTSC video. The modulation scheme presently used on KSC BCDS is vestigial side-band modulation (VSB).

Compressed DTV utilizes the transmission bandwidth more efficiently than NTSC analog TV. Furthermore, compression enables the utilization of other types of service such as video-on-demand (VOD) and interactive video-on-demand (IVOD). For KSC employee training and certification, VOD and IVOD are important types of DTV service.

One interesting feature of DTV is its compatibility with computer networks. Computer networks has the advantage of delivering DTV to computer terminals without having specialized modulation such as QAM. Hence, making DTV accessible from any desktop PC is a bonus feature for the system. Furthermore, personal computers are more suitable for IVOD in training courses and distant learning.

This study address the possibility of simultaneously transmitting VSB analog signals and quadrature amplitude modulation (QAM) signals on existing BCDS. QAM signals are capable of delivering all types of DTV including VOD. VSB signals may gradually be phased out leaving behind QAM signals. Furthermore, the study investigates the possibility of integrating KSC BCDS and computer network.

2. OVERVIEW OF PROPOSED ANALOG AND DIGITAL TELEVISION DELIVERY SYSTEM

KSC network topology is a centralized design i.e. all down links, OTV, off-air channels and head-end hardware are located in one location (CIF 339). It is likely that the proposed DTV terminal equipment will co-exist in the same location and share the same network. Maintenance and operation of this topology is relatively easier than other topologies such as distributed topology. The negatives of a centralized approach are cost, size, delay, and network bandwidth.

The most common DTV modulation scheme in CATV is quadrature amplitude modulation (QAM). The standard levels of QAM modulation are 64-QAM and 256-QAM. The bandwidth of both QAM levels is to fit in a regular 6 MHz NTSC channel. The bit-rate that can be transmitted through 64-QAM modulator is 27.8 Mbps, while a 256-QAM modulator input bit rate is 38.8 Mbps [1]. Furthermore, the level of encoding will determine the number of video streams that could be sent through a modulator. For example, if an encoding rate of 3.85 Mbps

is chosen, the maximum number of streams that can be multiplexed to fit one 6 MHz 256 QAM signal is 10 MPEG II streams.

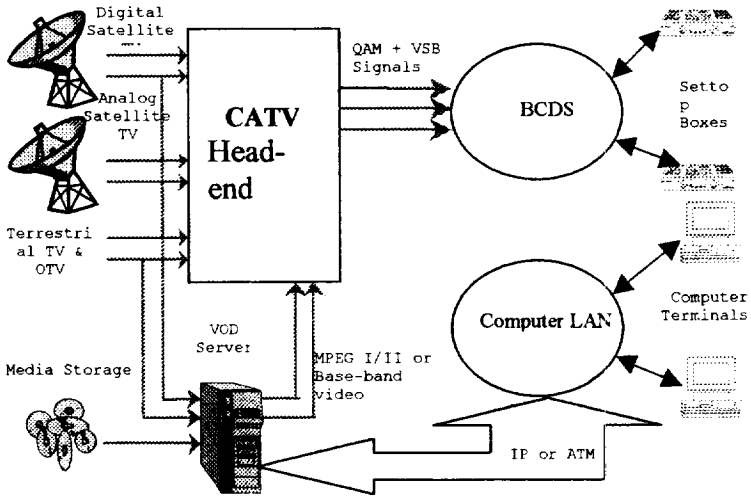

Figure 1: Proposed KSC analog and digital television delivery network

Figure 1, illustrates a possible scenario of KSC BCDS integrated with KSC computer local area network (LAN). The head-end delivers video to BCDS in several formats including: VSB for NTSC analog TV and 64/256 QAM for DTV. DTV may include satellite and terrestrial DTV, compressed OTV as well as VOD. Moreover, head-end delivers DTV to KSC computer LAN in either IP or ATM format. This IP or ATM stream may consist of satellite and terrestrial DTV, compressed OTV, VOD and I-VOD [3].

Some of the advantages for feeding IP or ATM DTV to KSC computer network are the following:

1. Reduce the load on QAM modulators.
2. Increase the accessibility of KSC employees to DTV services including VOD.
3. Facilitate the use of interactive VOD, which is used, for instructional purposes.
4. Allow out-of-site training for other NASA personnel.

3. SYSTEM COMPONENTS

KSC owns several General Instruments (GI) CATV components. The proposed VOD system could be implemented by utilizing present GI components. Certainly, additional components will be needed to build DTV and VOD delivery system.

VOD, like other interactive services, requires real time communications between the settop clients (Digital Consumer Terminal, DCT) and the application server. The settop box in possession of KSC is GI model # DCT2000. This settop box in addition to GI NC1500 Network

Controller, Modular Processing Unit (MPS), in combination with OM1000 (Out of Band modulators) and RPD1000 (Return Path Demodulators) can provide VOD service to BCDS clients [2]. This network uses a combination of the in-band, out of band, and return path signals for the delivery of VOD and other interactive services. The frequency spectrum of the system is shown in Figure 2 [3]. The in-band channel is primarily the source of the streamed MPEG-2 services, both broadcast and on-demand. It is also used to send JPEG and MPEG stills used to construct the User Interface for various applications (i.e. a selection template for videos, or an email template). The out of band (OOB) channel and the return path form the data channels for the network. The OOB data path provides 2.048Mbps to the DCTs at one of three fixed frequencies (73.75, 75.25, and 104.2MHz). The OOB band carries data in an MPEG-2 compliant transport and is the source for system wide information such as virtual channel maps, and code objects. The OOB also serves as the downstream data path and can provide as much as 1.5Mbps of data to a population of settops. The return path is constructed as a series of channels (up to 20) between 8MHz and 12MHz. Each channel is capable of carrying 256Kbps of data from the settop modulators (found in DCT2000 terminal) to the demodulators in the headend. Access control and interfaces to the billing system are provided by the DAC6000.

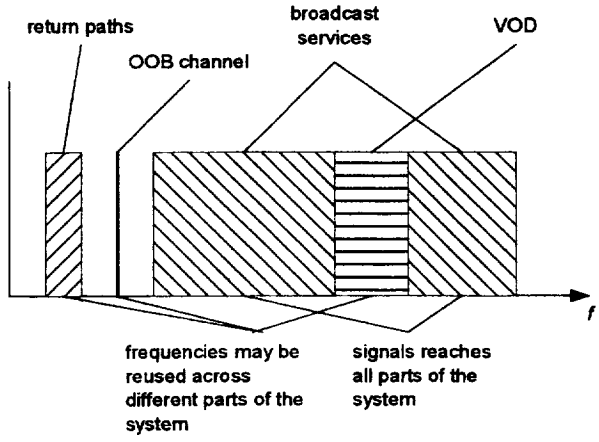

Figure 2: Proposed BCDS Frequency Spectrum

3.1. VOD on the DCT2000

The architecture for a DCT2000 interactive network is shown in Figure 3. VOD applications running on DCT2000 terminal use a combination of in-band, out of band, and return path (8 – 12MHz) for delivery of services to subscribers on a session basis. The in-band data path is primarily used for the delivery of the video service and various log-on and selection screens. The real-time data network is comprised of the out of band, as facilitated by the OOB Modulator (OM1000), and the return path demodulators (RPD1000). The interactive network is made possible with the introduction of the network controller (GI's NC1500 or equivalent).

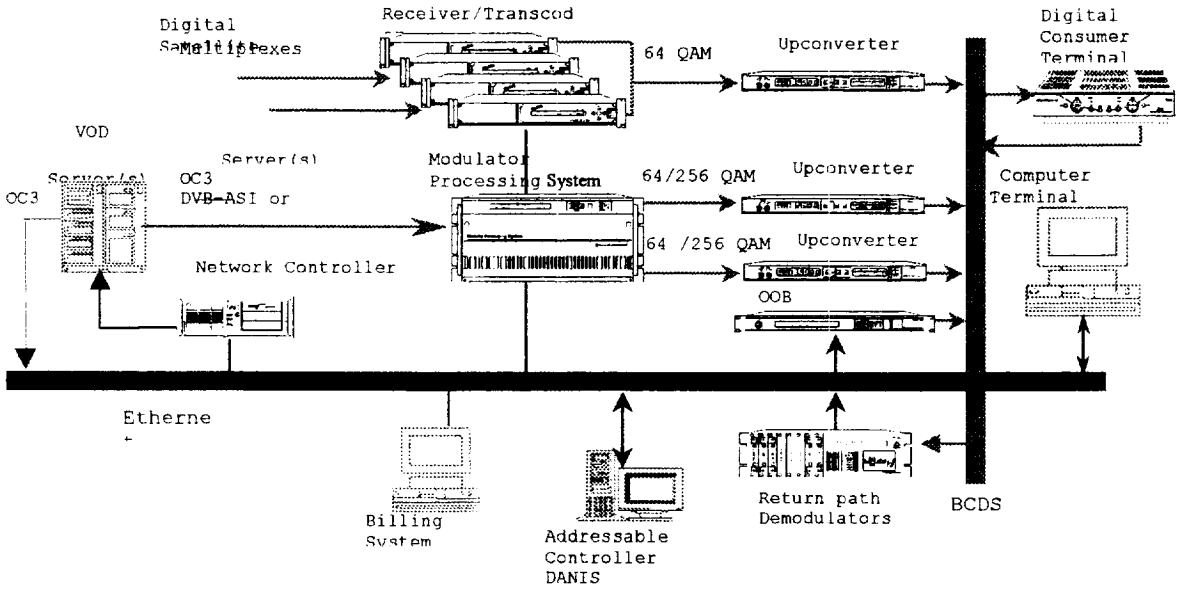

Figure 3: Proposed BCDS VOD System Architecture

The network controller is a hybrid fiber coax (HFC) network controller that enables interactive applications with a Digital Consumer Terminal (DCT2000). The network controller enables interactive sessions between application servers and the DCTs by translating Internet Protocols (IP) to deliver data packets to the DCTs through the out of band data channel. The return path serves as the upstream data path where the network controller aggregates demodulated data bursts from DCTs and routes the data to the appropriate server. The network controller also provides advanced features such as settop provisioning (assigns terminal IP addresses), upstream frequency management, and statistical monitoring of key settop transmission parameters. With the network controller, application servers can communicate directly with DCT settop terminals using IP protocols. The applications require no knowledge of the HFC network that exists between as the network controller facilitates the processing necessary for successful communications.

In a typical BCDS VOD session, as in Figure 4, the user navigates through server supplied selection and information screens with the remote handheld or keyboard. Commands are sent in data packets from the settop and are received by the VOD server through the network controller and return path demodulator. Once the network controller received any data packet, it immediately sends an acknowledgement, over the out of band channel, to the appropriate settop. If the settop does not receive an acknowledgement within a pre-configured timeframe, it simply resends the command packet back the upstream channel. Upstream communications are enabled through a modified version of the Aloha protocol. As this protocol is contention based (i.e. any terminal in the system is free to communicate on a particular channel at any time, without knowledge of other terminal transmission) acknowledgments are key in maintaining responsive

interactive sessions. Once the video selection has begun, the viewer can employ fast forward, pause, and rewind commands in the same manner.

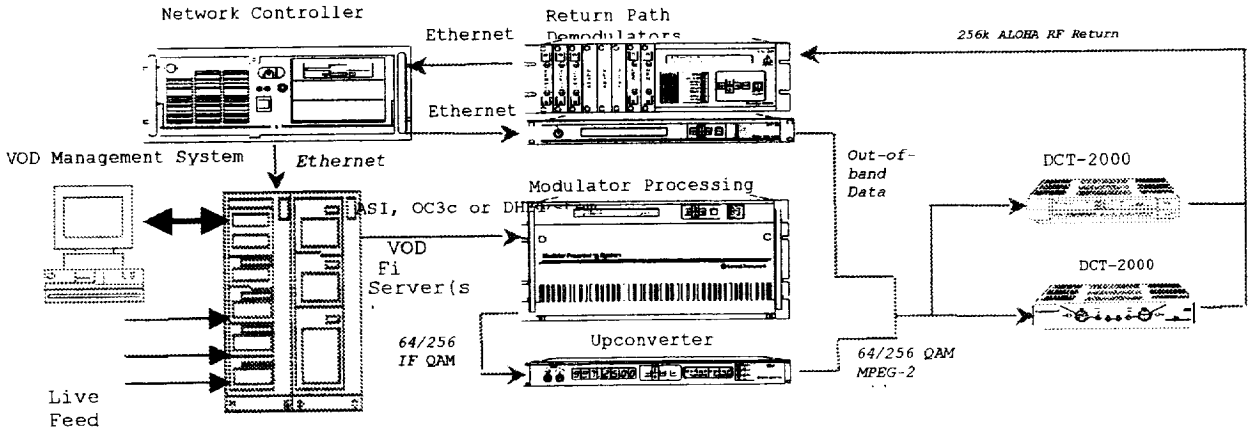

Figure 4: Simplified BCDS VOD Session.

In a typical computer network VOD session, as in Figure 5, only users with VOD IP addresses can navigate through server supplied selection and information screens with their keyboard. Commands are sent in data packets from the PC and are received by the VOD server through the network controller and computer network headend. Once the network controller received any data packet, it immediately sends an acknowledgement, to the appropriate user. Once the video selection has begun, the viewer can employ fast forward, pause, and rewind commands in the same manner.

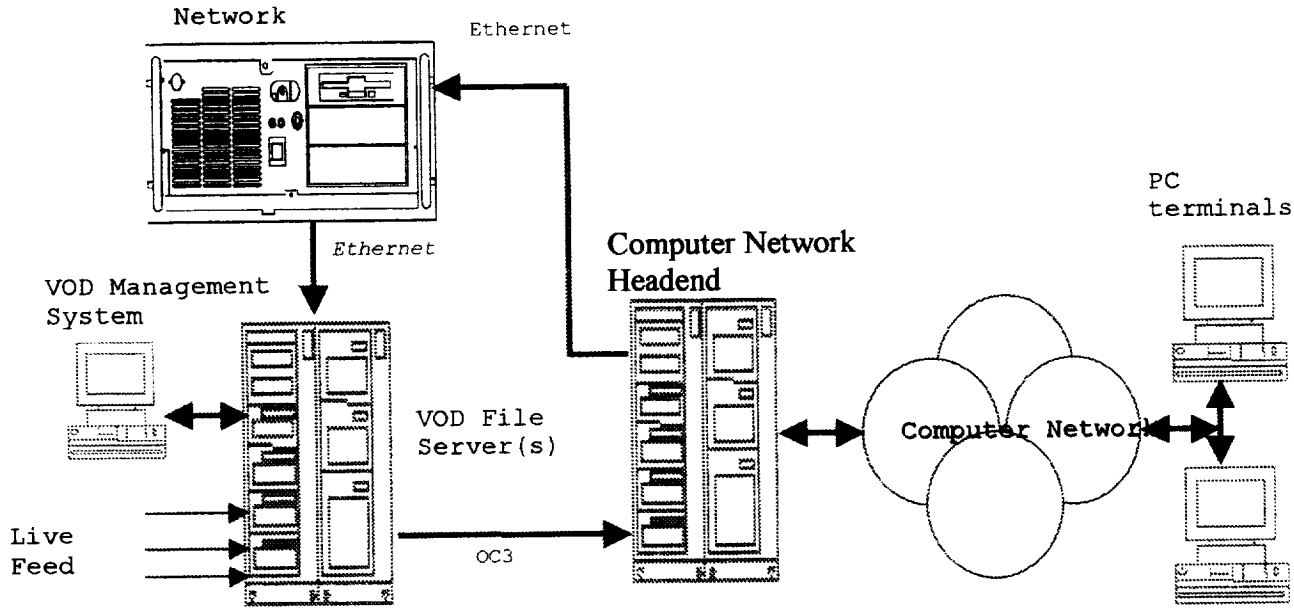

Figure 5: Simplified Computer Network VOD Session.

3.2. VOD File Server

The video server is resposible for storage and management of the VOD system's content, as well as delivary of video streams (such as off-air and OTV) in response to subscribers' commands.

The server must be integrated with the headend, network and existing DCTs. The video server should be able to deliver compressed (MPEG-1 or MPEG-2) video data streams over both digital and analogue distribution networks [4-5]. The digital output is to deliver video to KSC's administrative computer network as well as operational computer network. The digital output also modulates several QAM carriers to be delivered through the BCDS. The capacity of each QAM carrier depends on the compression level of the video signal.

The video sizes and the disk capacity of the video server determine the total number of video titles, which can be stored. The size of a particular video depends on its duration and on the bit-rate at which the video was encoded. However, the number of simultaneous viewers of a particular title is also determined by the arrangement of the video storage

The number of simultaneous video streams which can be delivered by a video server is determined by the number of interactive video modules (IVMs), the video delivery media, the video bit-rates and the number, and speed of the content disks.

The video server software includes a video pump (VP) to continuously access and deliver content from disk to the front-channel network and a video manager (VODM) to control video streams assigned to the video pumps. Figure 5 depicts an illustration of single VP vs. multiple VP server software.

4. FUTURE WORK

Several parameters should be investigated. The value of these parameters depends on the specifics of KSC BCDS and the desired quality of service. These parameters include:

- QAM M-level should be determined experimentally (64 or 256).
- QAM signal level w.r.t. analog VSB should be determined experimentally:
  64 QAM allowable levels are: -18 dBm to +5 dBm
  256 QAM allowable levels are: -12 dBm to +5 dBm.
- QAM signal & VSB signal cross modulation effects should be determined experimentally.
- Number of MPEG I & MPEG II PC clients with a given QOS should be estimated.

5. CONCLUSIONS

Digital video services including video on demand could be added to existing KSC BCDS. No major modifications are needed to adapt for the change. Furthermore, video-on-demand services could also be delivered to selected clients of computer networks. These selected clients could be inside or outside KSC campus. The addition of DTV to computer networks will increase the accessibility to distant learning and certification.

ACKNOWLEDGMENTS

The author would like to express his appreciation to Po T. Huang and Chuck Brown for allowing him the opportunity to participate in their ongoing project. Moreover, the author is greatly indebted to Professor Ramon Hosler, and Cassandra Spears for organizing the program and its activities.

REFERENCES

[1] D. Kunert, "What to look for in a video-on-demand system," Private & Wireless Cable, October 1998.

[2] General Instruments Co. Web Page: http://www.gi.com/BUSAREA/DNS/digint/digint.html.

[3] General Instruments Co. "Video on demand on the GI interactive network," White Paper, General Instruments Co., June 24, 1999.

[4] Concurrent Computer Co., "MediaHawk video server technical description," White Paper, Concurrent Computer Co., May 1999, http://www.ccur.com/.

[5] nCUBE Co., "Introducing MediaCUBE 4, An evolutionary and innovative video server system from nCUBE," White Paper, nCUBE Co. http://www.ncube.com/vod-nvodsolutions/vodsolutions.html.

LIST OF ACRONYMS AND ABBREVIATIONS

ASI	Asynchronous Serial Interface
ATM	Asynchronous Transfer Mode
ATVEF	Advanced TV Enhanced Features
BCDS	Broadband Communication Data System
CMT	Cable Modem Terminal system
DAC	Digital Addressable Controller
DANIS	Digital Access Network Interface Subsystem
DCT	Digital Consumer Terminal
DHEI	Digital Headend Expansion Interface (standard developed by General Instruments)
DOCSIS	Data Over Cable Service Interchange Specification
DTV	Digital Television
HCT	Headend Configuration Tool
HDTV	High Definition Television
HFC	Hybrid Fiber Coax
IRT	Integrated Receiver Transcoder
IVM	Interactive Video Module
IVOD	Interactive Video-On-Demand
MPEG	Moving Picture Experts Group (video compression standard)
MPS	Modulator Processing System
NC	Network Controller
OC-3	Optical Carrier level 3 (155Mbps)
OM	Digital QPSK Out-of-band Modulator
OOB	Out Of Band
OTV	KSC Operation Television
QAM	Quadrature Amplitude Modulation
RPD	Return Path Demodulator
VOD	Video-On-Demand
VP	Video Pump
VSB	Vestigial Side-Band Modulation

S3/:04, 4V/31

2000 NASA/ASEE SUMMER FACULTY FELLOWSHIP PROGRAM

JOHN F. KENNEDY SPACE CENTER
UNIVERSITY OF CENTRAL FLORIDA

PROCESS ENGINEERING TECHNOLOGY CENTER INITIATIVE

Martha A. Centeno
Associate Professor
Department of Industrial and Systems Engineering
Florida International University
Daisy Correa

ABSTRACT

NASA's Kennedy Space Center (KSC) is developing as a world-class Spaceport Technology Center (STC). From a process engineering (PE) perspective, the facilities used for flight hardware processing at KSC are NASA's premier factories. The products of these factories are safe, successful shuttle and expendable vehicle launches carrying state-of-the-art payloads. PE is devoted to process design, process management, and process improvement, rather than product design. PE also emphasizes the relationships of workers with systems and processes. Thus, it is difficult to speak of having a laboratory for PE at K.S.C. because the entire facility is practically a laboratory when observed from a macro level perspective. However, it becomes necessary, at times, to show and display how K.S.C. has benefited from PE and how K.S.C. has contributed to the development of PE; hence, it has been proposed that a Process Engineering Technology Center (PETC) be developed to offer a place with a centralized focus on PE projects, and a place where K.S.C.'s PE capabilities can be showcased, and a venue where new Process Engineering technologies can be investigated and tested. Graphics for showcasing PE capabilities have been designed, and two initial test beds for PE technology research have been identified. Specifically, one test bed will look into the use of wearable computers with head mounted displays to deliver work instructions; the other test bed will look into developing simulation models that can be assembled into one to create a hierarchical model.

1. INTRODUCTION

A *Spaceport Technology Center* (STC) encompasses a variety of systems supporting the development and utilization of technologies required to access space [1]. In this context, a *system* is understood as the set of people, processes, hardware, software, and infrastructure grouped to accomplish a common goal or objective. Similarly, *technology* shall be understood as the practical application of knowledge to produce something entirely new or in an entirely new way [4].

The vision of the KSC Spaceport Technology Center has been defined based on the classification of the many systems that function at K.S.C. The classification has led to the following three functionality visions of the STC:

1. *Launch and Launch Vehicle Processing Systems*. The STC will seek the development and application of technologies and expertise required to provide reliable and safe launch vehicles to access space.

2. *Payload and Payload Carrier Processing Systems*. The STC will seek the development and application of technologies and expertise required to enable cost effective payloads and payload carriers processing.

3. *Landing and Recovery Systems*. The STC will seek the development and application of technologies and expertise required to safely land and/or recover a launch vehicle or payload.

To achieve its visions, the STC will concentrate technology development in five areas, called *Spaceport Technology Development Initiatives* (STDI). The following STDI areas have been identified: a) Command, Control, and Monitor Systems, b) Range Systems, c) Fluids and Fluid Systems, d) Materials Evaluation, and e) Process Engineering.

Technological complexities make it impossible to look at these five STDI as 100% independent initiatives. There is a technological overlap among them; hence, three *technology areas* have been identified as important to the STC: 1) Information Systems, 2) Simulation (discrete and continuous), and 3) Biological Payload Processing Systems.

From observing the various processes that take place at a spaceport, it is easy to see that Process Engineering (PE) methods, techniques, and tools must be used to manage these processes effectively. PE is devoted to process design, process management, and process improvement, rather than product design. PE also emphasizes the relationships of workers with systems and processes. PE has demonstrated its value in industry for several decades; however, spaceport processes have many unique aspects that require development of innovative Process Engineering (PE) modeling and analysis technologies. Many of the PE techniques have demonstrated their robustness for large-scale, high-volume manufacturing and service systems; but spaceport processes include depot-level maintenance processes, high-performance system test and checkout procedures, and low-volume manufacturing processes not found in traditional industrial settings. Nevertheless, K.S.C. has successfully used PE techniques and it seeks to contribute to the development of new PE techniques tailored to the space industrial sector. It has

become necessary to show and display how K.S.C. has benefited from PE, how K.S.C. has contributed to the development of PE, and how K.S.C. may contribute to PE development.

From a process engineering (PE) perspective, the facilities used for flight hardware processing at KSC are NASA's premier factories. The entire K.S.C. facility is practically a PE laboratory when observed from a macro level perspective, which means that it is difficult to speak of PE laboratory in the traditional definition of a laboratory. Hence, it has been proposed that a Process Engineering Technology Center (PETC) be developed, so that it

a) Offers a centralized focus on PE projects,

b) Showcases PE capabilities at K.S.C., and

c) Provides a venue where new Process Engineering technologies can be investigated and tested.

This report describes the current status of this effort. Section 2 discusses the showcasing aspect of it, whereas Sections 3 and 4 discuss two initial test beds for PE technology research; Specifically, Section 3 looks into the use of wearable computers with head mounted displays to deliver work instructions, and Section 4 looks into developing simulation models that can be assembled into one to create a hierarchical model. Last, but not least, Section 5 presents the next steps in this effort.

1.1 OBJECTIVES

A key aspect of the KSC Spaceport Technology Center is to design, analyze, model, and develop advanced technology for spaceports of the future, but not actually operate the spaceports. The STC will be the research, development, and technology organization for spaceports anywhere. Every STC must include in its mission the development of effective communication mechanisms so that the developed technologies can be adequately disseminated. With this in mind, this effort sought to:

1. Investigate means to showcase PE successes and to market the existence of the Process Engineering Technology Center (PETC).

2. Investigate feasible and worthwhile test beds for new or improved PE technologies for space vehicle processing and space processes management.

2. SHOWCASING PROCESS ENGINEERING

The various previous PE efforts at KSC were investigated, and close collaboration with Dynacs was initiated. Dynacs is a NASA subcontractor that specializes in the production of graphics. The symbiotic relationship with Dynacs required that

a) PE success stories be identified.

b) Dynacs' staff be educated as to what process engineering is all about in the context of KSC.

c) Dynacs be given design guidelines and feedback, so that the final graphical product is effective in conveying the PETC message.

The projects in Table 1 have been chose as candidates for success stories. Discussions are still going on and should be finalized by the end of August. Material on these projects has been collected, and it is been reviewed.

A seminar on Process Engineering was prepared and delivered. Original presentation has been given to Daisy Correa. Through this seminar, it was clearly establish the kind of story that we needed the graphics to convey. Basically, these graphics should tell:

Project Title	POC
Upgraded APU Spares Process Simulation	JoAnn Archer, Janet Parker,
Ground Processing Scheduling System	Jim Tulley
Goal Performance Evaluation System	
SFC/DC System	Tim Barth
EPICS	Darcy Miller
Shuttle World Class Surveillances	Tim Obrien, Jean Flowers
ROCA	Tim Barth
K.S.C. Screcard Metrics	Michael Bell
Vision Spaceport	Carey McCleskey
Human Factors Event Evaluation Model	Donna Blankmann-Alexander

Table 1: Candidates for the PE Hall of Fame

1.- *What has PE done for K.S.C. lately?* With this graphics, a variety of poster, videos, and presentation could be done to demonstrate PE capabilities at K.S.C. The graphics, hence, should be multipurpose for posters, flyers, trade shows, and so forth.

2.- *What is going on right now that is PE supported?* This implies that the graphics are not a one in a lifetime, static deal; rather, part of the graphics effort is to develop a template to show case PE successes as time passes.

3.- *What will PE do for the future of K.S.C.?* This implies showcasing the current capabilities as well as the research potential in the PE area.

These requirements were further discussed in a series of meetings. An important clarification

was the form that the initial deliverables would take. Since the target audience is both internal as well as external, it was decided that Dynacs would

1. *Design graphics and a poster to tell the PE store*. This poster could vary in size.

2. *Design graphics and posters for each area under PE*. Five areas have been identified, following the scheme used in the K.S.C. Annual Technology Report: a) Process Modeling and Analysis, b) Systems Analysis, c) Engineering Management Systems, d) Human Factors Engineering, and e) Work Measurement.

3. *Design a template for a success story*. The template would be filled by the person in charge of the project, and then Dynacs beautifies it. It is expected that the template would be ready by the end of August.

It is expected that the list of candidates as well as the graphics developed by Dynacs will be presented to the KSCIENet Group so that the group provides feedback.

In addition to the graphics, it is necessary to have the means to display such graphics. At this moment it has not been finalized, but the usage of one of the Collaborative Engineering Environment (CEE) rooms is being considered. If none of these rooms can be used, then it will be necessary to purchase some equipment and equip a new room or have a portable show.

The minimum requirements for a PE showcasing are sketched in Figure 1. At least two large display devices are needed to have the capability of showing material directly from a computer and, at the same time, showing material incoming from another media (e.g. videos, other computers, slides, and so forth). There is a need to have a portable PC to house PE software tools that cannot reside on the K.S.C. wide network. Some software licenses is limited, while other software cannot run through the network. The laptop should have network connectivity, so it can connect to servers on the K.S.C. network as needed. There should be a touch screen that enables easy management of the display equipment as well as of the various PE shows. Table 2 gives a preliminary estimate on the cost of the minimum hardware needed; these estimates are not official quotes.

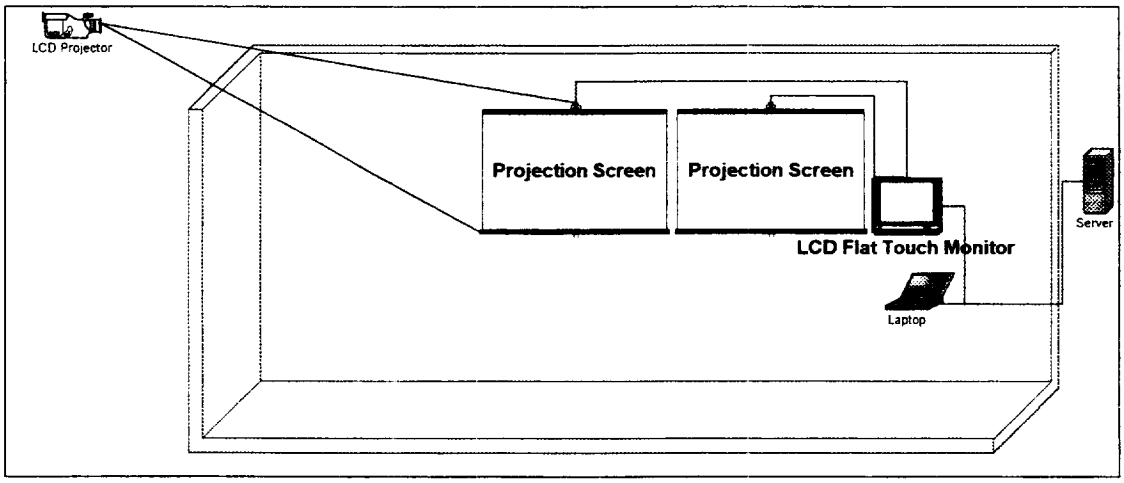

Figure 1: Minimum Showcasing Requirements

Description	qty	unit cost	total cost
Dell Latitude CPx. It inlcudes a Pentium III processor, 650 MHz with 14.1 XGA TFT Display, 512 MB SDRAMM, 2DIMMS, 18GB HD, Windows NT 4.0 SP5, Logitech Mouse with wheel Xirxom RealPort CardBUs Ethernet 1-/1-- + modem 56K, 24X max/ 10X min CD ROM drive, C/Dcok II Expansion station with TRING card, MS Office professional, Carrying case, 3-year on-site parts & labor, Second Li-Ion battery, 250 MB zip drive.	1	$6,070	$6,070
TLP B2 LCD projector, 1,000 ANSI lumens, true xga 1024x768, 5.8, plug-n-play, PC, MAC, and video input, contrast 400:1built-in 1w moaural speakerx1, 5.8 lbs (Figure 2).	1	$5,500	$5,500
P401LC Digtial Information Display, 40 inch rear projection unit, 800x600 dots, vga, svga, xga, and video,i I/O BNC female x 1, RGB for PC infrared remot, wired remote, 32(w)x35(h)x15.6(d) inches, stackable, wall or floor, 75 lbs (Figure 4).	2	$10,000	$20,000
Elo Intuitive 1825L 18" LCD Touch monitor. 1280x1024 at 60Hz, contrast ratio 150:1 19.6(w)10.3(d)x15(h), analog input video (Figure 3).	1	$1,500	$1,500
		Total	**$33,070**

Table 2: Estimates for Showcasing Hardware

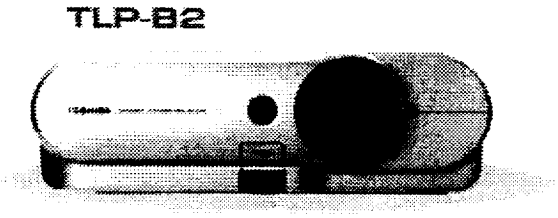

Figure 2: LCD Portable Projector

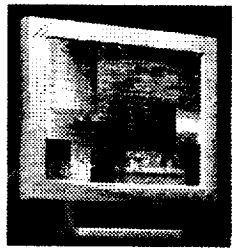

Figure 3: Touch Screen

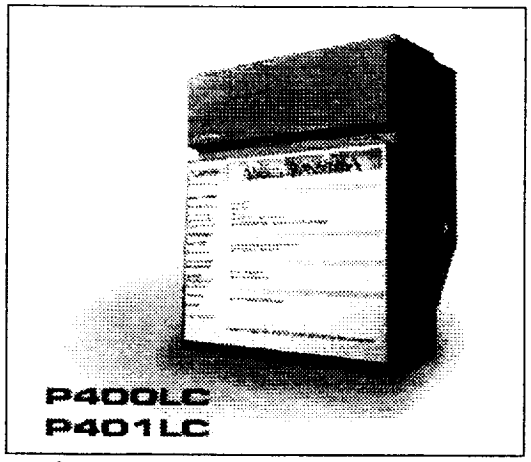

Figure 4: Projection Screen (Panel)

Teresa Lawhorn manages one CEE room that has the necessary hardware for displaying PE shows via PC and Internet. That particular room does not have the necessary wall space to display large posters on a continuous basis, but it could be utilized to store the posters when they are not in display. K.S.C. is currently building two more CEE rooms that may be used for this purpose as well; thus, the purchase of the projection screens, the touch screen, and the LCD projector may not be necessary; however, the purchase of the laptop is necessary even if existent CEE rooms are used because certain PE tools are not accessible through the network. All the CEE rooms have a port to which a laptop can be connected in a plug-n-play fashion.

3. WORK INSTRUCTIONS DELIVERY TEST BED

The delivery of Work Instructions was proposed as an initial test bed. More specifically, we set out to research how to deliver Work Instructions, when working under hazardous conditions requiring the use of safety suit. The initial line of thinking was to use Head Mounted Displays to delivery the work instructions to technicians while suited in the SCAPE suit. This idea came about from a meeting that took place at JSC about one year ago. At that meeting, the discussion was focused on EVA suits and Mars Surface EVA suits. However, those suits are not readily accessible here at K.S.C., but the SCAPE suit is; hence, it was proposed that the SCAPE suit be used to test ideas on how to deliver work instructions to a suited worker (technician or astronaut).

Initial research and meetings with individuals familiar with both the SCAPE suit and the Work Instruction Delivery System has led to a shift in the focus of the initial proposal. Instead of pursuing the testing on the SCAPE suit itself, it is necessary to first test the feasibility and effectiveness of using the display and delivery technologies in existence. This has led to the consideration of a delivery system based on a wearable computer, rather than just on a head mounted display device. In other words, the new focus is to convert at least one work instructions document, so that it can be delivered via a wearable computer with a head mounted display device. If this effort is successful, then the resulting tested technology could be used by a worker wearing a suit (SCAPE or EVA) or by a worker working in a confined area such as the aft of the shuttle.

Wearable computers are currently available in the market with varying degrees of capabilities. Technically speaking, wearable PCs are being developed with the ultimate goals of hands-free mobility and real-time support. Because wearable PCs can be small, lightweight, powerful, and either touch- or voice-activated, they are perfect for work conditions that are fast-paced or cramped, as well as for tasks that demand constant attention for safety and effectiveness. A person using wearable PCs is able to review maintenance manuals and access specifications while having tools in hand. There are several prototypes in the market; however, Xybernaut®'s Mobile Assistant IV® is seems to be the most complete wearable today. However, the MA IV could work with several HMD, not only with the one that it comes with. Among these alternatives are the Eglass (Figure 5) and the V-Cap 1000 (Figure 6). A complete evaluation of these devices can be found in http://www.stereo3d.com/hmd.htm#chart.

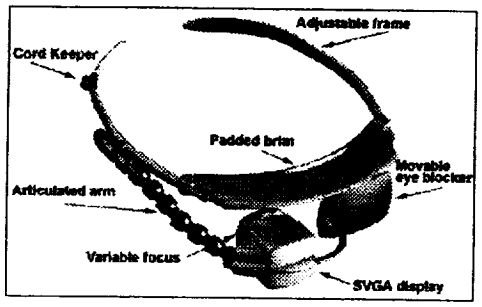

Figure 5: Eglass

Figure 6: V-Cap 1000

Part #	Description	qty	Unit Cost	Total Cost
XYB-00304	MA IV Deluxe. It includes a CPU, Pentium 233 MHz, 160MB RAM, 4.3 GB HAD, a floppy drive, a Xyberview HMD, two Lithium-ion rechargeable batteries with holders, a battery charger AC adapter, an 11" mini keyboard, a belt with battery pouch, a mini port replicator (floppy drive, keyboard), IBM voice LinkAssist Intro, Norton AntiVirus, Operating system (win98, win 200 or winNT), and 90 days labor, 1 year parts.,	1	$6,995	$6,995
FPD-00100	Flat panel display	1	$1,525	$1,525
SWE-00310	Smart writer software	1	$121	$121
BWA-00102	Vest with cable sleeves, CPU, battery, flat panel, and mini port holsters	1	$257	$ 257
BWA-00200	CPU holster for belt	1	$61	$ 61
BWA-00202	Flat panel display holster for belt	1	$ 48	$ 48
CAM-00100	Video camera	1	$ 294	$ 294
CAM-00201	Nogatech USB video capture adapter for HMD and FPD	1	$ 93	$ 93
CAS-00100	Carrying case	1	$ 247	$ 247
CDD-00101	24x Addonics CD-ROM with PCMCIA connection	1	$ 360	$ 360
COM-00200	Linksys wired LAN connection	1	$ 180	$ 180
PRF-00100	Full port replicator (docking station)	1	$ 158	$ 158
SWE-00200	LinkAssist Developer's kit	1	$1,495	$1,495
SWE-00300	Stefra Video Control 98 video software	1	$ 49	$ 49
	Shipping and handling	1	$ 75	$ 75
			Total	*$11,958*

Table 3: Estimate for MA IV

4. HIERARCHICAL SIMULATION TEST BED

Model reusability has for long been a research topic in computer simulation. With the advances achieved in software technologies, model reusability is now approaching feasibility. However, there are still several issues that are not yet fully understood. For instance, methodologies to adequately break large systems into smaller subsystems are far from been standard. Methodologies on how to couple and coordinate the interaction between two are more

models are just now maturing.

Daisy Correa, Grant Cates, and a team from UCF are currently working on a Macro Level Model of the Space Shuttle Processes. It is proposed that this model be used to explore new methods for simulation model modularization as well as simulation models coupling and decoupling. An initial step in model reusability is the addition of a user interface that enables users of the model to change input parameters with ease and without needing to change the model themselves. The software used by the UCF team (ARENA) offers a full scale Visual Basic language that allows the development of user interfaces as well as the ability to integrate other applications with the simulation model.

This model offers another research opportunity in the area of Goal Driven Simulation (GDS). GDS seeks to automatically adjust the inputs to the model to attain a goal specified by the user of the model. There are a couple of algorithms that have been developed by a team of researchers led by Dr. Centeno at F.I.U. These algorithms could be tested on this model.

5. WHERE TO GO NEXT

The thing to do next is to work in parallel in the finalization of the showcasing of PE successes as well as in the initialization of the tests beds. It is recommended that

a) A meeting be set up with the K.S.C. IENet group to discuss the graphics produced by Dynacs. This meeting can take place last week of August.

b) At the same meeting, the PE projects to be part of the PE @ K.S.C. Hall of Fame should be discussed and a selection be made.

c) Purchase show case hardware as recommended

d) Purchase wearable computer, and establish a formal team of two or three persons (one from USA) that will work in converting one WAD to be displayed via the wearable computer. The team requires someone knowledgeable in work instruction documents, someone knowledgeable in the information system used by USA to generate work instructions, and someone that can convert such document to a wearable PC database.

e) Develop a user interface for the simulation model developed by the UCF team.

f) Test principles of Goal Driven Simulation with the simulation model developed by the UCF team.

6. REFERENCES

[1] Kennedy Space Center Implementing NASA's Strategies, KDP-KSC-5-2000, Rev.: Basic 3/98

[2] Kennedy Space Center Roadmap, KDP-KSC-S-2001, Rev.: Basic 3/98

[3] U.S. Congress, Office of Technology Assessment, "Reducing Launch Operations Costs: New Technologies and Practices", OTA-TM-ISC-28, Washington, D.C.: U.S. Government Printing Office, September 1988

[4] Office of the Chief Technologist, NASA Technology Plan, 1998

[5] Spaceport Technology Center Concept, White paper, Tim Barth, Summer 2000.

2000 NASA/ASEE SUMMER FACULTY FELLOWSHIP PROGRAM

JOHN F. KENNEDY SPACE CENTER
UNIVERSITY OF CENTRAL FLORIDA

Designing Extraterrestrial Plant Growth Habitats With Low Pressure Atmospheres

Kenneth A. Corey
Associate Professor
Department of Plant & Soil Sciences
University of Massachusetts

Colleague: Raymond M. Wheeler

ABSTRACT

In-situ resource utilization, provision of human life support requirements by bioregenerative methods, and engineering constraints for construction and deployment of plant growth structures on the surface of Mars all suggest the need for plant growth studies at hypobaric pressures. Past work demonstrated that plants will likely tolerate and grow at pressures at or below 10 kPa. Based upon this premise, concepts are developed for the design of reduced pressure atmospheres in lightweight, inflatable structures for plant growth systems on Mars with the goals of maximizing design simplicity and the use of local resources. A modular pod design is proposed as it could be integrated with large-scale production systems. Atmospheric modification of pod clusters would be based upon a pulse and scrub system using mass flow methods for atmospheric transport. A specific modification and control scenario is developed for a lettuce pod to illustrate the dynamics of carbon dioxide and oxygen exchange within a pod. Considerations of minimal atmospheric crop requirements will aid in the development of engineering designs and strategies for extraterrestrial plant growth structures that employ rarefied atmospheres.

1. INTRODUCTION

Advanced life support systems for people working and living for extended durations remote from Earth-based resources will eventually include the use of plants for sustainable bioregeneration of oxygen, water, and food (3,7). Systems for the production of crop plants in enclosed environments may involve a number of different scenarios with respect to atmospheric management. Certainly, inclusion of plants in human habitation structures would also have positive if undefinable psychological value. The pressure and composition of the Earth's atmosphere has been modified over the aeons to become suitable for a wide range of organisms. While plants and people coexist and provide reciprocal requirements for one another, they do not share the same atmospheric limits, nor do they have the same optima for partial pressures of gases. This suggests the consideration of developing plant growth habitats that are isolated atmospherically from human habitats.

A primary, long-term goal of sustaining life in remote space locations is to minimize the amount of mass and therefore energy required to launch and maintain life support systems. If one considers only the atmospheric requirements of people, the lower limit of ppO_2 for human comfort during routine activities is on the order of 15 kPa or the equivalent of a 3000 meter altitude. While we could safely breath a pure atmosphere of oxygen at a total pressure of 15 kPa, the fire hazard would pose an unacceptable risk. If a quenching gas in the form of nitrogen, argon, or some combination of inert gases and water vapor (~1 to 4 kPa, depending on temperature and relative humidity) is added to the extent that oxygen comprises no greater than a mole fraction of 0.3, then the total atmospheric pressure requirement would be 50 kPa or about one half atmosphere pressure.

On the other hand, plants can tolerate and perhaps thrive in an environment with oxygen partial pressures as low as 2 to 5 kPa (2,5,9-13,14,15-22). In addition, there is evidence that a diluent gas is not necessary for normal plant function (1). A structure devoted solely to plants will contain relatively large quantities of water and is not likely to contain combustible materials as a human habitat would. Exceptions to this may be with crops such as wheat that would not be harvested until an advanced stage of senescence when the moisture content is relatively low. Therefore, an examination of total pressure limits for plants suggest that minima are much lower than those for people. Furthermore, if one considers maximizing the use of local resources such as energy, then it would be desirable to make use of ambient light. Light intensities in near-Earth space to regions on the Martian surface would provide sufficient photosynthetic photon flux to support plant growth. In order to harvest ambient light, it would be desirable to have a structure with maximum transparency. This structural consideration then leads to the question of what materials would be sufficiently transparent and strong to contain a plant growth atmosphere that would have a higher pressure than the near vacuum of space, the atmosphereless surface of the Moon, or the low pressure (~ 7 mb or < 1 kPa) atmosphere of the Martian surface. In order to construct a plant growth habitat that meets these requirements, it is likely that the materials will be thin and perhaps incapable of holding very high pressure gradients. Therefore, it would be desirable to achieve as low a total pressure gradient as possible to minimize the structural strength required for such structures.

Based upon the premise that the use of low pressure atmospheres will have applications in future plant growth systems in extraterrestrial habitats (2,7-12,18,20,22), the goals of this report are to: 1) discuss key considerations related to tailoring atmospheric designs to specific plant growth requirements, 2) propose an approach for designing minimal atmospheric scenarios for crop growth structures, and 3) develop a feasible modular and scaleable structural design for growing crop plants on the Martian surface.

2. *MARTIAN RADIATION ENVIRONMENT*

Mars is half again as far from the sun as is the Earth with an incident solar flux at the atmospheric boundary of about 42 % that of Earth (Table 1). Plant growth and development is strongly dependent upon spectral quality of the radiation in the waveband from 440 to 720 nm. This amounts to approximately 30 % of the total radiation incident at the atmospheric boundary of Earth. In addition, there is very little attenuation of the visible wavelengths by atmospheric absorption. Assuming that similar proportions reach the surface of Mars, there may be about 860 $\mu mol/m^2 s$ of photosynthetically active radiation (PAR) at the Martian surface, depending on latitude and season. While this amount would certainly be sufficient for productive culture of most plants, there are two major factors limiting the availability of this photon flux. First, there is the attenuation brought about by the material of a greenhouse structure. In order to maximize plant growth, one would want to select a material that has strength, flexibility, maximum transmittance to visible light, and good insulating properties to minimize heating requirements for the large temperature differences the habitat will have to maintain on the surface of Mars. Suppose an optimistic scenario is assumed and material and energy resources resulted in a greenhouse that cut the incident PAR in half. The resulting value of 430 $\mu mol/m^2 s$ would be a workable PAR for modest growth rates of some crop species. However, the occurrence of dust storms for several weeks could decrease the PAR to levels at or slightly below the light compensation point of most crop stands (Table 1). This would necessitate the use of supplemental lighting systems; perhaps combined with the use of crop plants genetically selected or engineered for adaptation to either low light compensation points or extended tolerance of irradiance near the light compensation point.

Of particular concern on the Martian surface will be the higher than Earth levels of UV-B and UV-C radiation (Table 1). Estimates of biological stress of this radiation on organisms (e.g. DNA damage frequency) led to strategies and recommendations for UV mitigation which included elimination of all wavelengths below 290 nm (6). High energy UV mitigation will likely be an important requirement for plant growth structures.

3. *AUTONOMOUS PLANT GROWTH STRUCTURES*

A desirable engineering objective in providing human life support by bioregenerative means would be to establish plant growth systems that could be initiated and then mechanized and controlled with minimal further human input until harvest. Such structures would essentially be isolated and not permit entry by humans without preconditioning at low pressure and provision of supplemental oxygen. Even with technologies for advanced mechanization (i.e. robotics), it will be necessary to have some human input in the set-up, monitoring, and management of growth systems; particularly with planting and harvest operations. One of the first problems to consider is what size and shape should a specific growth structure or module be to withstand atmospheric pressure gradients, and enable human handling for set-up, planting, and harvest operations. Modularization of a system provides for ease of human handling, gives a degree of robustness to the system if a failure occurs in a part, and it enables designs of atmospheric environments tailored for different plant species. Also, a plant and harvest scheme would still necessitate subsystems for management of atmospheric constituents, thermal regime, nutrient delivery system, and the water cycle. This report will focus on management of atmospheric variables with considerations of other subsystems that influence those variables.

Table 1. Comparison of solar flux on Earth and Mars.

Variable	*Earth*	*Mars*
Mean Distance from Sun (10^6 km)	149.60	227.94
Solar Constant (W m^{-2})	1380	579[a]
Photosynthetically Active Radiation (W m^{-2})	418	181[b]
(μmol m^{-2} s^{-1})	2000	860
Photosynthetically Active Radiation During Global Dust Storm (W m^{-2})[c]	-----	27
(μmol m^{-2} s^{-1})	-----	128
Ultraviolet Radiation (W m^{-2})[d]		
UV-C (200 – 280 nm)	0	3.4
UV-B (280 – 315 nm)	2.0	7.9
UV-A (315 – 400 nm)	56.8	31.1

[a] Kuhn and Atreya, 1979, J. Mol. Evol. 14: 57-64.
[b]Assumes similarity to visible portion of solar spectrum of Earth. There is very little atmospheric attenuation of the visible portion of the spectrum on Earth and attenuation is less on Mars.
[c]Estimate assumes 6.5 % of Earth incident radiation of 1380 W m^{-2} as reported by Drake, ed., 1998, NASA, EX13-98-036. A value of 30 % of that value was assumed to be in the visible portion (400 to 700 nm).
[d]Cockell and Andrady, 1999, Acta Astronautica 44: 53-62.

4. *GROWTH MEDIUM AND NUTRIENT DELIVERY SYSTEM*

A critical consideration in the design of structures is the type of nutrient delivery system to be employed. Minimizing the partial pressure of oxygen would necessitate the use of a delivery system that maximizes oxygen availability to the root system. Additional complications arise if growth structures are designed for μG applications (i.e. formation of liquid-phase bridges across pores that impede oxygen diffusion). Consideration of gravity-based systems would then involve a choice of solution culture, solid matrix culture (soil or synthetic), and aeroponics. With solution culture, dissolved oxygen can often become limiting to root systems under normoxic conditions in variations ranging from large bulk solutions to nutrient film technique.

Aeroponic systems would perhaps have an advantage over those of solution culture, as root systems would be bathed with the atmosphere of the habitat and oxygen diffusion barriers at the surfaces of roots would be limited to the proportion of the root surface area covered with liquid phase water. The latter is presumably controllable by the rate of application of water from a system of nozzles or other means of spray or drizzle application. However, the rate of water application will be governed largely by stage of crop development and the root to atmosphere water potential gradient at low pressure; which, in turn should be controllable by temperature and humidity regulation such that absorption rates are always in excess of transpiration rates. A

major disadvantage of a system involving spray is the gradual buildup of salt residues. In an inflatable structure, such residues could alter the intensity of the photon flux incident on the plant canopy, could perhaps lead to equipment corrosion, and would add a step to material recovery.

Finally, a solid matrix system would be desirable for in-situ resource use (e.g. Martian soil), air-water relations, structural support, and, depending upon the medium, chemical buffering. Oxygen diffusion will depend largely on the nature and distribution of pores and channels and the relative abundance of water 'bridges' that may form at different moisture contents for a specific solid medium. Intuitively, a desirable solid medium (i.e. one with high oxygen diffusivity over a range of water contents) would have better oxygen delivery than solution culture but not as good as an aeroponic system. Under good circumstances of air filled pores, diffusion rates of oxygen are still less than one-third of those in free air (23). In addition, the use of a soil-based medium would impose a heavy structural load on individual pods. Perhaps a lightweight, synthetic medium with both good aeration and drainage properties could be used in this context.

5. GEOMETRY OF STRUCTURES

It is well established from engineering principles that the stress on a vessel or structure is directly proportional to the internal pressure. The hoop stress formula describes the maximum hoop (tangential) stress in the wall of a thin cylinder. While this formula simplifies the forces and configuration of a hypothetical structure, which will presumably be more complex, it does provide a rationale for the stress load on a structure as it is related to internal pressure. Stress is also related to the mass and nature of the material and it will be of interest to minimize the mass required to contain a specific pressure gradient between internal and external atmospheres or the vacuum of space.

The strongest geometric configuration of a structure to minimize the stress load is a spherical shape. However, a spherical geometry would automatically place a constraint on the size of the structure, since a volume-efficient design would necessitate that the diameter of the sphere would be limited by the 'height' of the crop canopy and accompanying support materials if one also wishes to minimize head space volumes. The volume/area ratio of spheres increases linearly with the radius of the sphere. Inefficient planting configurations (i.e. high volume/area) would require larger inputs of start-up and maintenance masses for atmospheric management. Alternatively, ellipsoidal shapes would provide for more volume-efficient designs and with favorable, but less than ideal structural strength properties. The geometry of ellipsoids is considerably more complex than that of spheres, since all three axes can vary. Ellipsoidal shapes can be tailored to the height of the crop canopy and will enable volume:area ratios of less than unity. Low volume/area ratios for spheres are only possible for radii less than a meter.

An individual unit or module (spheres or ellipsoids) of a structure will be referred to as a pod. The following sections represent an attempt to develop a conceptual architectural design for the production and management of plants in modular, scaleable structures consisting of clusters of pods. Designs are driven by the goals of local resource use, minimization of energy inputs, and the use of low pressure, modified atmospheres. Therefore, simplicity of design and function is a primary concern in integrating many of the design requirements. The ensuing discussions also provide rationales for selecting certain design options and then proceed to develop them into a proposal for a functional modular system.

6. POD DESIGN

An individual pod will need to have the capabilities for introducing atmospheric gases, water, and nutrients, should have minimal leakage of atmosphere, provide structural support for the plants, allow maximum interception of incident radiation, should be easy to plant and harvest,

and should maximize the production of consumables in a given volume. All of these design requirements will be addressed in some way. It will be assumed that inflatable materials with high strength and transparency are available and that such materials can be sealed to minimize leakage of atmospheric gases. Human handling could be facilitated by a modular system where each individual pod or cluster of pods could be easily attached or detached. Minimization of the number of penetrations is important to minimize the potential for leakage at joints. It is proposed that each pod have a major seal along the equatorial axis and one penetration that allows for the transport and exchange of both liquid and gaseous fluids. Liquid fluids (water or nutrient solutions) could be introduced via a reservoir at the top of a control tower (Figure 1). To minimize energy expenditure in getting the water to the top of the control tower, the air circulation pattern may be designed to flow to the top of the tower and down through the top of an inner conical or cylindrical column. At the top of the inner truncone or cylinder, the air flows through condensing coils or plates and the condensate collects in a reservoir sized to be more than large enough to provide water to fill the water supply matrix in every pod. A supply line runs from the supply reservoir in a helical pattern down the inner wall of the outer truncone. Pod clusters (Figure 1) would be arranged down the helix in a nonoverlapping manner to maximize interception of incident radiation. If the control tower is large enough to provide for more than one circumferential loop, either the angle of the helix or the slant of the truncone could be designed to eliminate shading of lower loop clusters by upper loop clusters.

During a given water supply event, water or solution flows by gravity down the helical supply line to fill each cluster of pods. In the event that water resupply is necessary before sufficient condensate is available in the supply reservoir, additional water needs could be obtained from the water and atmosphere resupply reservoir at the base of the truncones.

7. ATMOSPHERIC MODIFICATIONS

A part of the atmospheric control system involves maintaining sufficient water vapor pressures for plant growth. The region between the cones could be atmospherically sealed from the pod clusters and the resupply reservoir at the bottom could be heated to the boiling point. Using total atmospheric pressures in the range of 7 to 20 kPa would only require heating to temperatures in the range of 25 to 55 C. Such temperatures may be attained passively with an external supply reservoir equipped with a transparent top and superenriched with carbon dioxide or Mars atmosphere to provide conditions for a runaway local greenhouse effect. During the Martian day, it would be possible to trap heat in the reservoir. It would be necessary to minimize the loss of gained heat during the Martian night with a method for providing an insulated cover over this exposed reservoir. Such insulation requirements also apply to the arrays of pod clusters. This heated water and carbon dioxide mix could be used to supply each control tower in a large-scale array. In future missions, if it is determined that Mars has sufficient surface or subterranean water, this reservoir could be supplied by one of a number of methods. Alternatively, start-up water for the facility will need to be brought to the site, or made as a product of the Sebatier process from hydrogen that is brought to the site. The Sebatier process enables great flexibility in supply of direct human needs and start-up and maintenance needs for a plant growth facility.

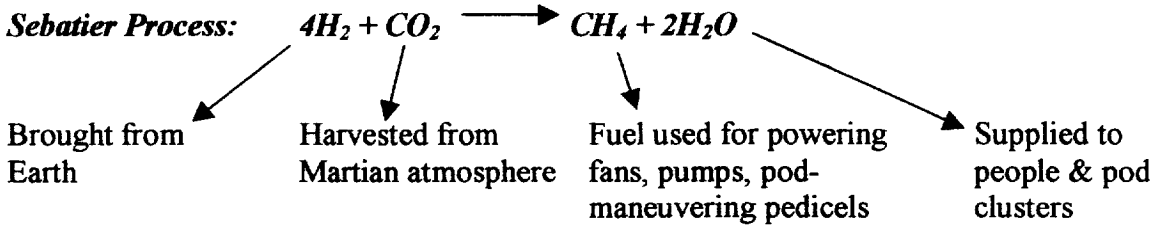

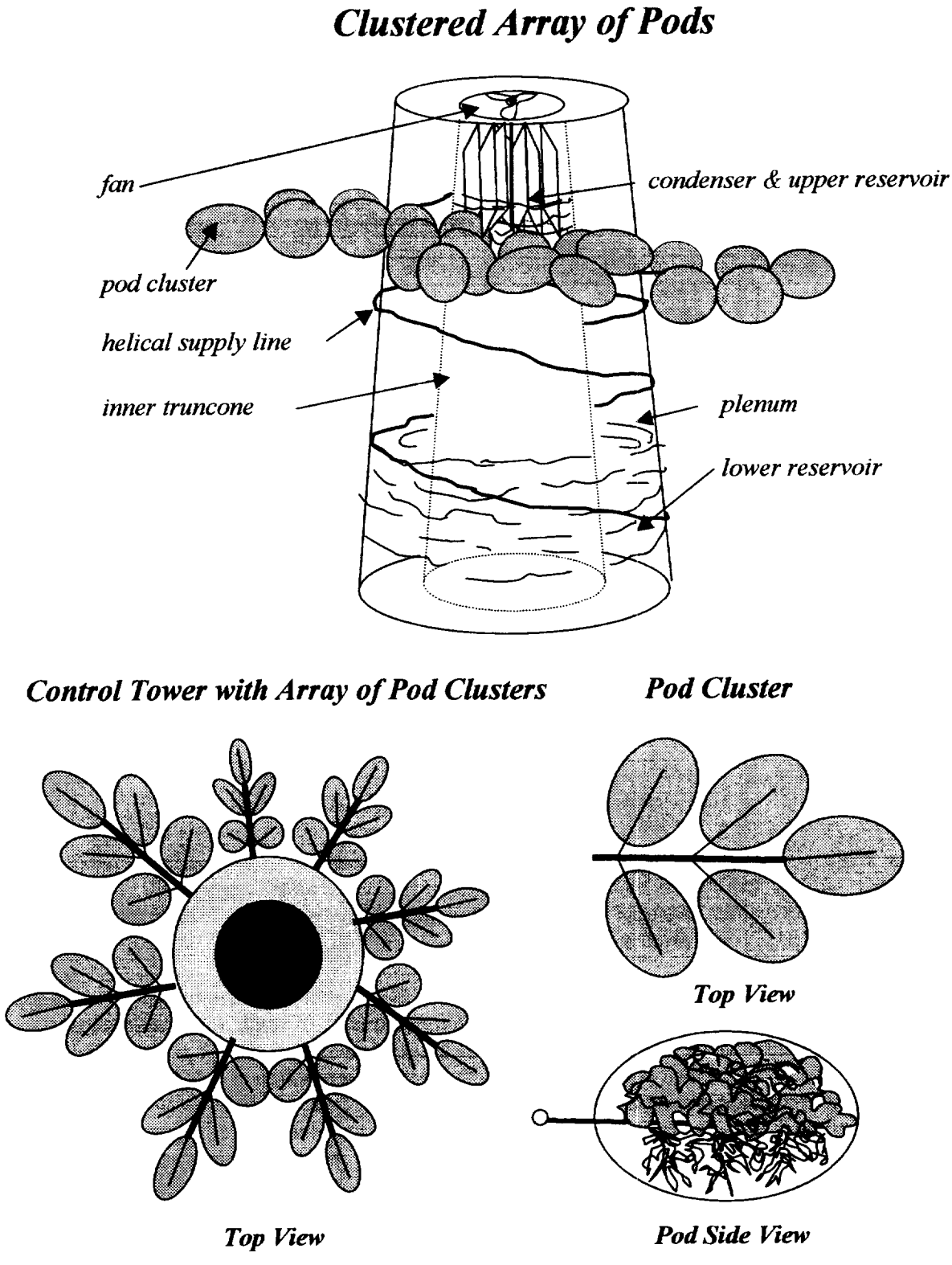

Figure 1. Schematics of clustered array of pods (CAPS), pod cluster, and lettuce pod.

During a particular atmospheric recharge event or 'pulse', the necessary makeup gas mix can be introduced to the space between the truncones via the atmospheric processing facility and reservoir located on the inside of the inner truncone below the upper supply reservoir (Figure 1). The particular ratio of oxygen, carbon dioxide, and diluent gas (if needed) will be specifically tailored for the crop and stage of development as determined by past and future research results. A generalized chart was developed to illustrate the possible range of needs for atmospheric gases (Figure 2).

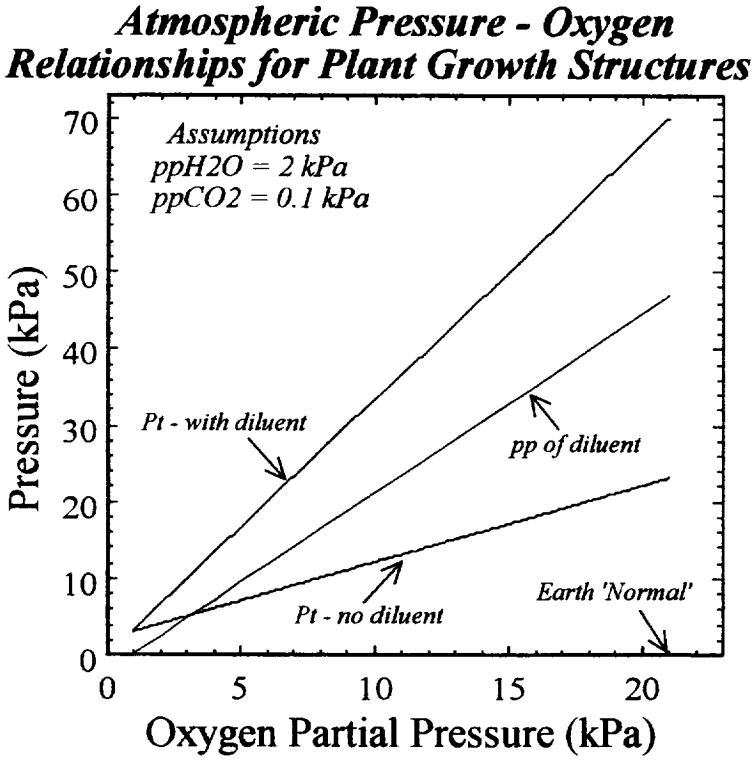

Figure 2. Total atmospheric pressure (P_t) and diluent gas requirements for a range of partial pressures. Total pressure with a diluent gas was computed based upon an upper safety limit of 0.3 mole fraction oxygen. The assumed partial pressure of water vapor would correspond to a temperature of 21 C and a relative humidity of 80%..

This information applies to a thermal regime of 21 C, a relative humidity of 80 %, and a partial pressure of carbon dioxide of 0.1 kPa. The partial pressure of water vapor under these conditions is approximately 2 kPa. The next step is to select an oxygen partial pressure value, which can only be determined with any assurance by complete growth tests. However, the limited literature available on this subject suggests that many plants will function normally, and perhaps have growth enhancements at ppO_2 in the range of 5 to 10 kPa (10,11,16). Studies are needed to address the safe oxygen partial pressures at which to grow crop plants. Considerable work will be needed to define curves analogous to Pasteur effect functions for different crops and stages of development. It is well established that plants vary widely in tolerance to anoxic conditions. Perhaps species and genotypes can be selected for anoxia tolerance. Combined with a knowledge of the saturation vapor pressure at normal growth temperatures, the theoretical limit of plant growth for a species tolerant of anoxia could perhaps be as low as 2 kPa. This is suggested by the y-intercept of the line for no diluent gas (Fig. 2).

Total atmospheric pressures of pods could be as low as 7 kPa for plants with intermediate tolerance to anoxic conditions and the absence of a diluent gas. If one selects a mole fraction of 0.3 as an upper safety limit for ppO_2, then a diluent such as nitrogen or argon (concentrated from the Martian atmosphere) would be used as a quenching gas, bringing the total atmospheric pressure up to 18 kPa. However, the 0.3 mole fraction safety limit for oxygen is based upon studies of ignitable and combustible materials combined with human occupancy. In addition, work stimulated by the Apollo 1 accident demonstrated that the ignition and propagation of a flame is inversely proportional to the total pressure for a constant mole fraction of oxygen (4). Thus, in the absence of combustable materials (excepting dried plant material) and people, the high water content and the low total pressure all suggest that the diluent gas may be omitted or allowed to be considerably lower than those suggested by Figure 2.

In the proposed system of transient atmospheric pulse and scrub (TAPS), the partial pressures and total pressures will be allowed to swing across relatively wide ranges (i.e. 0.1 kPa < $ppCO_2$ < 1.0 kPa and 5.0 kPa < ppO_2 < 10 kPa). Such wide swings minimize the number of control events. Hypothetical scenarios of the dynamics of carbon dioxide and oxygen swings in spherical and ellipsoidal lettuce pods are illustrated in Figure 3.

This figure was generated by first retrieving a set of net photosynthesis and dark respiration values for 15 and 28 days after planting for a lettuce crop (Wheeler et al., 1994). A linear interpolation for all the intermediate day points was used to calculate the number of moles of carbon dioxide consumed during the light period or evolved during the dark period. Conversely, for the sake of simplification and demonstrating the concept, the moles/m^2 oxygen evolved during the light or consumed during the dark was based upon the assumption of an assimilation quotient (AQ) of 1 and a respiratory quotient (RQ) of 1. The assumption for the AQ is generally quite good, but the RQ is more dependent on the species and stage of development and will generally be in the range of 0.8 to 1. An additional simplifying assumption was the use of a 12 h light/12 h dark cycle, an approximation of what would occur during a Martian equinox at all latitudes. Using an average temperature of 20 C, an ellipsoidal pod volume of 0.4 m^3, and an average total atmospheric pressure of 14 kPa, the ideal gas law was applied to calculate daily predicted partial pressure increases or decreases in carbon dioxide and oxygen. For carbon dioxide, when the partial pressure decreased to a lower setpoint limit of 100 Pa, the system was pulsed to raise it to an upper setpoint limit of 1000 Pa. As crop growth occurs, the pulse frequency increases (Figure 3A &3C). Some research has been conducted on crop tolerance to high $ppCO_2$ and perhaps this upper setpoint will be found to be conservatively low. For oxygen, a lower setpoint limit of 4000 Pa was selected (i.e. as would occur following a scrub event or other means of atmospheric modification) as a starting point and then allowed to increase without a scrub event (Fig. 3B & 3D).

Once the particular atmospheric gas design is chosen, the volume between the cones could be pressurized sufficiently to provide, when opened, the appropriate pressure and composition of gas atmosphere to all of the pods via mass flow. Mass flow pulsing of the system would also facilitate gas exchange and oxygen penetration into the root zone, particularly critical since relatively low partial pressures of oxygen may be used.

From a practical management standpoint, scrubbing of oxygen could physically take place within the atmosphere of the truncone and delivered to a compressor for storage and later used directly for human habitat atmospheres. It may be desirable to have time separation of pulse and scrub events, since the selected setpoints will be reached at different times and the atmospheres of the pod and truncone volumes will need to be opened and closed to enable appropriate atmospheric modifications by mass flow.

9. REFERENCES

1. Andre, M. and Ch. Richaux. 1986. Can plants grow in quasi-vacuum? In: CELSS 1985 Workshop, NASA Publication TM 88215, 35-404.
2. Andre, M., and D. Massimino. 1992. Growth of plants at reduced pressures: experiments in wheat-technological advantages and constraints. Adv. Space Res. 12: 97-106.
3. Boston, P.J. Low-pressure greenhouses and plants for a manned research station on Mars. J. British Interplanetary Soc. 54: 189-192.
4. Botteri, B.P. 1967. Fire protection for oxygen enriched atmosphere applications. Fire Hazards and Extinguishment Conference, Brooks Air Force Base, Texas, AFAPL-CONF-67-10.
5. Bjorkman, O. 1966. The effect of oxygen concentration on photosynthesis in higher plants. Physiol. Plant. 19: 618-633.
6. Cockell, C.S. and A.L. Andrady. 1999. The Martian and extraterresrial UV radiation environment – 1. Biological and closed-loop ecosystem considerations. Acta Astronautica 44: 53-62.
7. Corey, K.A., P.A. Fowler, and R.M. Wheeler. 2000. Plant responses to rarified atmospheres. Inflatable Greenhouse Workshop. NASA TM 2000-208577.
8. Corey, K.A. 1999. Testing plant responses to rarified atmospheres for inflatable greenhouses. Amer. Soc. for Engineer. Educ. SFFP. Contract .
9. Corey, K.A., D.J. Barta, M.A. Edeen, and D.L. Henninger. 1997. Atmospheric leakage and method for measurement of gas exchange rates of a crop stand at reduced pressure. Adv. Space Res. 20 (10): 1861-1867.
10. Corey, K.A., D.J. Barta, and D.L. Henninger. 1997. Photosynthesis and respiration of a wheat stand at reduced atmospheric pressure and reduced oxygen. Adv. Space Res. 20 (10): 1869-1877.
11. Corey, K.A., M.E. Bates, and S.L. Adams. 1996. Carbon dioxide exchange of lettuce plants under hypobaric conditions. Adv. Space Res. 18 (4/5): 265-272.
12. Daunicht, H.J. and H.J. Brinkjans. 1992. Gas exchange and growth of plants under reduced air pressure. Adv. Space Res. 12: 107-114.
Drake, ed., 1998, NASA, EX13-98-036.
13. Ehleringer, J.R. 1979. Photosynthesis and photorespiration: Biochemistry, physiology, and ecological implications. HortScience 14: 217-222.
14. Gerbaud, A. and M. Andre. 1989. Photosynthesis and photorespiration in whole plants of wheat. Plant Physiol. 89: 61-68.
15. Musgrave, M.E., W.A. Gerth, H.W. Scheld, and B.R. Strain. 1988. Growth and mitochondrial respiration of mungbeans (*Phaseolus aureus* Roxb.) germinated at low pressure. Plant Physiol. 86: 19-22.
16. Musgrave, M.E. and B.R. Strain. 1988. Response of two wheat cultivars to CO_2 enrichment under subambient oxygen conditions. Plant Physiol. 87: 346-350.
17. Quebedeaux, B. and R.W.F. Hardy. 1976. Oxygen concentration: Regulation of crop growth and productivity. In: Carbon Dioxide Metabolism and Plant Productivity, R.H. Burris and C.C. Black, eds., University Park Press, Baltimore, Maryland.
18. Ohta, H., E. Goto, T. Takakura, F. Takagi, Y. Hirosawa, and K. Takagi. 1993.
Measurement of photosynthetic and transpiration rates under low total pressures. American Society of Agricultural Engineering Paper No. 934009.
19. Parkinson, K.J., H.L. Penman, and E.B. Tregunna. 1974. Growth of plants in different oxygen concentrations. J. Expt. Bot. 25: 135-145.
20. Rule, D.E. and G.L. Staby. 1981. Growth of tomato seedlings at sub-atmospheric pressures. HortScience 16: 331-332.
21 Siegel, S.M. 1961. Effects of reduced oxygen tension on vascular plants. Physiol. Plant. 14: 554-557.
22. Schwartzkopf, S.H. and R.L. Mancinelli. 1991. Germination and growth of wheat in simulated Martian atmospheres. Acta Astronautica 25: 245-247.
23. Taylor, S.A. 1949. Oxygen diffusion in porous media as a measure of soil aeration. Soil Sci. Soc. Amer. Proc. 14: 55-61.
24. Wheeler, R.M., C.L. Mackowiak, J.C. Sager, N.C. Yorio, W.M. Knott, and W.L.Berry. 1994. Growth and gas exchange by lettuce stands in a closed, controlled environment. J. Amer. Soc. Hort. Sci. 119: 610-615.

2000 NASA/ASEE SUMMER FACULTY FELLOWSHIP PROGRAM

JOHN F. KENNEDY SPACE CENTER
UNIVERSITY OF CENTRAL FLORIDA

Evaluating Education and Science at the KSC Visitor Complex

Lance K. Erickson
Professor
Applied Aviation Sciences
Embry-Riddle Aeronautical University

ABSTRACT

As part of a two-year NASA-ASEE project, a preliminary evaluation and subsequent recommendations were developed to improve the education and science content of the Kennedy Space Center Visitor Complex exhibits. Recommendations for improvements in those exhibits were based on qualitative descriptions of the exhibits, on comparisons to similar exhibit collections, and on available evaluation processes. Because of the subjective nature of measuring content in a broad group of exhibits and displays, emphasis is placed on employing a survey format for a follow-on, more quantitative evaluation. The use of an external organization for this evaluation development is also recommended to reduce bias and increase validity.

Evaluating Education and Science at the KSC Visitor Complex

Lance K. Erickson

2. Introduction

The primary objective of this project is the preliminary evaluation of the educational and science content within the developing and continuing exhibits at the KSC Visitor Complex (KSCVC). To achieve more than a simple critique of the perceived impact or the content within the exhibits, a more in-depth procedure is required, however. Such a procedure would not only provide an assessment of the exhibit content, but would examine the impact of the exhibit on the public.

Because the exhibits at the Visitor Complex are also intended to stimulate and engage the viewer, evaluation methods that are used for more traditional educational programs, such as classroom curricula, are not appropriate. Structure for a more quantitative evaluation of the exhibit content should therefore be directed towards feedback through an outcomes and/or process evaluation. Using survey techniques, the feedback process could identify strong and weak elements in the exhibits, and identify visitor interests, visitor expectations and visitor demographics. This information could be used to help plan future exhibits and measure the success of NASA in bringing visitors to the Kennedy Space Center. Feedback from the surveys could also provide a measure of how effectively the important elements of NASA's history, vision and mission were conveyed.

3. Project Description

Four primary phases were used in this evaluation project. Those were:

1. Project definition
2. Exhibit review
3. Evaluation summary
4. Final report

1. The first step in this project was the project definition. This was outlined during preparation for the first summer of the project. A schedule of development and final product was agreed on which was the final report and recommendations.

2. The second step in the project included exhibit reviews of the KSC Visitor Complex: once during the summer 1999 period, and again during the first part of the 2000 summer program because of the numerous changes in the exhibits. Those review summaries are included in the 1999 project paper and are also mentioned below.

   In addition to the KSCVC review, a comparative description of the Smithsonian Air & Space Museum, and the Adler Planetarium in Chicago exhibits were included in the first summer paper. These reviews were intended to provide a comparison of the content and structure of related exhibits.

3. Following the exhibit review, an evaluation process was identified that could assess qualitative information transfer between exhibits and the visitors. This would measure how

effective the exhibits are in getting NASA's message across to the visiting public. The recommended method for affectivity and consistency is survey sampling.

4. This paper, the final project report, outlines recommendations for ongoing evaluation of the educational and science content within the KSCVC and related initiatives. Summaries of earlier work, and several NASA strategic statements are also included for a more complete background and rationale for the recommendations.

4. Exhibit Content: The NASA Message

In August 1967, NASA opened the Kennedy Space Center's visitor center, Spaceport USA. The visitor's center served to underscore the importance of space flight operations for our nation, and the Kennedy Space Center's role in those operations. Since then, the role of the Kennedy Space Center in the U.S. space program and the space flight operations at the Kennedy Space Center have expanded. These increases have been reflected in the size of and attendance at the visitor's center. The visitor center has also provided the public access to important historical artifacts, records, and information on current and past space flight projects. At the same time, NASA's overall efforts to inform the public of its character and mission and its interest in helping extend science literacy in the public have expanded in scope.

NASA's story and the related messages, which are a significant part of the NASA public outreach, continue to benefit both the public and NASA. Information on the role of space exploration and of technology advancement in our lives not only increases public interest in NASA, but it helps the Agency improve the public's understanding of the importance of science. As an example, the message outlined in the NASA vision statement "NASA is an investment in America's future. As explorers, pioneers, and innovators, we boldly expand frontiers in air and space to inspire and serve America and to benefit the quality of life on Earth." [1] underscores the importance of NASA's role in the future of America. Because of the importance of informing the public of its mission, the NASA story is emphasized in this project as a vital element in the educational and science contents of the KSCVC exhibits.

An outline of the NASA message and the need to transfer information to the public can be found in several sources, including *Communicating NASA's Knowledge* report [2] and *Space Science Education and Public Outreach* [3]. Additional education and information guidelines for the NASA are provided in the NASA Strategic Plan and the four Strategic Enterprise strategic plans. Each of the four Strategic Enterprise areas (Aero-space Technology, Earth Science, Human Exploration and Development of Space, and Space Sciences) provides plans and objectives for education and outreach [4]. Included in the Space Science education and public outreach description, as an example of the efforts throughout NASA to increase public awareness in their mission and in science, advocates "to make education at all levels and the enhanced public understanding of science integral parts of the Space Science missions and research programs."

A coherent NASA message and story that would be informative and exciting to the public requires careful study and development. Establishing that message and the NASA story also requires a close look at the historical record, and a comprehensive review of the space exploration, education and technology development plans throughout NASA. For the NASA story and message to be effectively integrated into the KSCVC exhibits, a serious effort should

be made to develop and help transfer those important concepts to the exhibits developer. This could be done internally or contracted externally, but constitutes a crucial part of the education and science elements of the KSCVC exhibits.

5. Exhibit Content: The KSC Role

The role of the Kennedy Space Center in NASA's space exploration programs and technology transfer efforts are also important contributions that need to be conveyed to the public. This is especially so for those who are interested enough in NASA-KSC to visit the Kennedy Space Center. Providing those visitors with informative, relevant, and stimulating information is necessary for the continuing public support of our nation's space flight initiatives. Public education is vital in the continuing support of NASA, and for support of the space flight projects and supporting programs found at the Kennedy Space Center.

Keeping the public informed of the importance of NASA programs and the role of the Kennedy Space Center in those programs should be one of the primary messages within the KSCVC exhibits. Concurrent information on the economic vitality of the space programs is also important for public support of NASA and the space flight programs. Emphasis on public education is reiterated in the Visitor Complex mission statement, "to tell the NASA story and inspire all people to support the exploration of space."

It follows that information on the KSC role in both NASA and international space flight programs should also be included in the KSCVC exhibits. Because of the changing nature of the roles and responsibilities of the Kennedy Space Center, it is recommended that these exhibit messages be reviewed regularly, and updated with current project and program information. In addition, the increasing participation and importance of the Russian collaboration in the International Space Station strongly suggests that the KSCVC multilingual information include the Russian language.

6. Exhibit Content: Evaluation

Determining the means and method of the follow-on evaluation was an important preliminary step in this project. Because of the difficulty in defining the character of educational or scientific content within a broad medium (display and exhibit material in this case), a sampling survey was identified as the most effective format. Relatively consistent results from a sampling survey should provide a measure of information that is retained by the participant – the visiting public - provided the objectives are well defined. To that end, it is recommended that the objectives of the evaluation process be developed early and clearly. How those objectives are measured or satisfied is important also, and must be detailed in the evaluation development process.

Unquestionably, a survey of the visitors at the KSCVC should be targeted to the specific interests of NASA and the Kennedy Space Center. However, this survey sampling could be developed to identify not only what information or messages are successfully broadcast, but also how the visitors perceive the exhibits, displays, and/or facilities, and what their expectations are or were. Additional queries could be included to measure the visiting public's opinions on a wide range of subjects for a variety of applications. Those may include:

- NASA space flight programs and their importance
- NASA-KSC accessibility (physical & virtual)
- Strengths and weaknesses of the KSCVC
- Youth program interest
- Additional conveniences desired
- Major detractions from visiting KSC
- Comments

Since the focus of this project is education and science evaluation, the emphasis of the survey is suggested to concentrate on the measurement of the process of knowledge transfer. However, it is recognized that an important component of the exhibits/displays within the KSCVC is the element of attraction: the inspiration that accompanies a well-designed exhibit. The survey instrument should, therefore, remain sufficiently flexible to measure both the content of the exhibit/display message, and its effect.

Emphasis for this evaluation is on the learning potential and on increasing science literacy at the KSCVC. This leads to several general recommendations on the evaluation survey in these areas. The first and most fundamental recommendation is that the survey process evaluate the successful or unsuccessful transfer of information through questions specific to the exhibits and their content. Second, the survey instrument should solicit open responses to the displays and/or exhibits and their perceived impact. These "comment" sections could be targeted to individual exhibits/displays or could be aimed at an entire exhibit, or even an overall opinion on the visitor's satisfaction with the exhibit and/or facility. The open response sections could also provide important insight into related areas such as the strengths and weaknesses of the exhibits, facilities that may be lacking, or suggestions for improvements.

Some of the most important aspects of the evaluation process are the specification of the objectives and the definition of the elements to be measured. Defining the objectives is important to understanding the outcome of the survey and should be established early in the evaluation planning. Just as important is the development of the principal elements to be measured - the metrics. Guidelines for these defining steps are provided by the survey developer, and help establish the priorities and procedures for the evaluation. Development of the central elements to be measured would then follow in a collaborative agreement between the three key participants: the survey developer, NASA, and the exhibit developer/contractor. Specific objectives and key evaluation elements, although impossible to stipulate before the development and agreement process, would aim at a continuing evaluation process if following these recommendations. General objectives and evaluation elements are suggested below for initial direction to the evaluation development process.

<u>Objectives:</u>

- Develop master plan for current & future exhibits & facilities
- Develop coherent NASA story and message
- Identify desired level of content in education & science to be evaluated
- Determine desired level of broadcasting the NASA messages
- Establish ongoing review of exhibit content
- Relate visitor experience and expectations to exhibits & facility

Evaluation elements:

- Educational content (was information retained?)
- Science content (is science representative of NASA's efforts?)
- Science literacy improvement (scientific principles available and understood?)
- Exhibit impact (engaging & memorable exhibit?)
- NASA message delivery (was message conveyed & correct?)

Because survey instrument design is best structured by organizations that develop surveys professionally, the evaluation process, whether simple or elaborate, should be developed with the assistance of a professional group familiar with educational exhibits. Input from the principals (NASA and exhibit developer/contractor) is essential throughout the development process for obvious reasons. With that in mind, the following suggestions for evaluation of the KSCVC exhibits are compiled below, based primarily on the exhibit review walkthroughs in 1999 and 2000.

Early Space Exploration

Early space flight is covered fairly well in this exhibit, although several sections lack significant detail and space history integration. A survey could identify the effectiveness of the 1960's displays in helping the visitor identify with or understand the early manned missions. The Mercury launch room exhibit could also be examined to help visitors identify its location and presentation times. Some effort should be made to link the early exploration history to the space flights of the future within other exhibits in the KSCVC.

Rocket Garden

The Rocket Garden is currently under redesign, with additional displays and facilities planned. A necessary addition should be an educational section that would introduce the principles of the rocket, rocket propulsion, and how those principles are related to these early rockets and engines on display. This should also include the Space Shuttle and possibly the International Space Station propulsion systems for continuity. Historical information would also be useful for integrating these displays with NASA's past, present and future space exploration programs.

Exploration in the New Millennium

Emphasis in this exhibit should be on the NASA exploration programs, especially those planned for the future. Unfortunately, little information is actually available on the numerous programs and projects planned. Most of the display content is on past missions, or undefined exploration concepts. A tie-in among the displays would be nice, but elaboration on NASA's future exploration programs is essential – and in keeping with the exhibit name. Science content is lacking in general and nearly nonexistent for astronomy, astrophysics and cosmology programs which are some of the most exciting and innovative projects that NASA has planned. Although there is an interactive astronomical display within the exhibit area, little is presented on the remarkable discoveries of the universe and our origin. Improvements could also be made by including the NASA-KSC efforts in manned space flight efforts (life support, bioregeneration, etc.) and other projects relating to NASA's future exploration projects.

Space Shuttle Plaza

The Space Shuttle mockup (Orbiter, ET & SRB) is a popular and effective exhibit that could be improved dramatically by

1. placing it in or near the Rocket Garden, and
2. improving the information detail on the STS systems, functions and history with strategically placed panels.

LC-39 Observation Gantry

Survey feedback could identify strong and weak areas within the LC-39 tour stop. This would be an appropriate exhibit to list coming launches and the locations of the respective ELV & Shuttle launch pads in more dramatic detail.

Apollo-Saturn V Center

This exhibit hall is rich in history and hardware from the Apollo program, and also includes some Space Shuttle information. The large floor space is well suited for additional displays that could be used to inform and engage visitors about NASA's initiatives related to lunar (and planetary) exploration. The expanse beneath the Saturn V could be used for a multitude of display/exhibits on the NASA lunar exploration initiatives (past, present and future), and a display of the fundamentals of our Moon. This hall is an ideal location and environment for stimulating the visitor's curiosity about NASA's lunar (and planetary) space exploration.

International Space Station Center

The ISS exhibits are useful in showing the station scale and some specifics, although the building space is too small for the displays on both floor levels. A review of the ISS modules displayed should be considered and updates including expanded information related to the content & function of the station components/modules should be included.

Attention should be paid to the Space Station Processing Facility overlook because of its potential for informing as well as inspiring the public about the very important ISS program, and because of the stark nature of the room. A detailed proposal for reworking the overlook room has been presented to the exhibits contractor and NASA representatives. The proposal appears very useful in improving the educational/informational nature of the display.

Overall, the exhibits throughout the KSCVC appear to have some of the basic background information on NASA programs and history. However, many of the exhibits lack the scientific detail that would engage the visitor's curiosity, or relate the various displays/events to a higher-order message such as NASA's space exploration strategies. One example of this is the Mars Viking Lander display within the Exploration of the New Millennium exhibit. Only two sentences are provided near the display for what could be a wealth of information on a spacecraft that has provided us with insight into the climate and atmospheric makeup, not only of Mars, but other terrestrial planets. This display could also be used as an introduction to subsequent and future Mars missions. Another example of the weakness in the science detail is the Robot Scouts' lack of significant findings of NASA's exploration missions that have proved rewarding to scientists and exciting to the public because of the extraordinary discoveries. Exciting images, unexpected findings and dramatic data have come from numerous space flight missions including Galileo, Cassini, Magellan, Hubble, COBE, Pathfinder, and Clementine, to name just a few.

In contrast, an example of a well designed, detailed, informative and engaging exhibit can be seen in the Liberty Bell 7 exhibit that is currently on tour (housed in the KSCVC IMAX building from June to September 2000). The traveling exhibit provides not only extensive background on the Mercury program, flights and hardware, but accentuates the learning experience with several simple interactive stations. One of these stations is a crude mockup of the Mercury capsule that children and adults can sit in and get a feeling for the cramped capsule environment.

7. Evaluation survey

At the focus of this project is the recommendation for a survey process to evaluate the learning experience within the KSCVC exhibits. This method of evaluation provides the flexibility of reviewing specific elements of a program or exhibit, and/or identifying much broader concepts. However, the usefulness of the survey evaluation is highly dependent on the defined objectives and goals of the project, and the sampling methods. The first of these, objectives and goals, would require careful coordination between the three principals: NASA, the survey developer, and the exhibit developer/contractor. Sampling methods also require coordination, but more often come under the direction of the survey developer. Similar visitor survey techniques are employed in other exhibit evaluations, including NASA's traveling exhibit displays [5] and the Chicago Adler Planetarium (Dr. Evalyn Gates, June 1999, private communication).

This evaluation process would be most effective as a periodic review because of the changing nature of the KSCVC exhibits, and the variations in the visitor population. With changing exhibits and changing needs for both NASA and the exhibits developer/contractor, the survey instruments would likely have to be updated regularly.

The instrument could have many forms, but with long-term evaluation in mind, the surveys could be distributed and collected through the mail, on-site handouts, and online formats (see, for example the KSC home site survey at http://pao.ksc.nasa.gov/pasurvey/paform.cfm). It is possible that a combination of these could decrease cost and increase flexibility of the process.

Effectiveness of this evaluation process would be strengthened significantly if the process were incorporated into the multi-year development plan for the KSCVC and exhibits. With a well-defined direction for the exhibits from long-term planning, an effective evaluation of the content and impact of exhibits would benefit NASA managers, the exhibit developer/contractor, and most of all, the visiting public.

The survey instrument and process should be developed and monitored by an organization/corporation that specializes in learning and exhibit evaluation. Development of the instrument externally would also for minimal bias in the evaluation process by virtue of independence from the exhibits developer/contractor. However, responsibility for the survey instrument should be determined by the combined requirements and needs of the three concerned groups: NASA-KSC, the exhibits developer/contractor, and the survey developer.

After reviewing several exhibit evaluation organizations, the Institute of Learning Innovations in Annapolis, Maryland appears to have relevant experience in reviewing, recommending and

evaluating the educational/learning elements in the KSCVC exhibits. The non profit organization's web contact can be found at www.ilinet.org.

8. Educational Initiatives at KSC

Education is one of the essential elements of the Kennedy Space Center Visitor Complex because of its Center's function - to inform and inspire the visitors about the present and future NASA space flight programs, and about NASA's history. Educational programs are found throughout the Kennedy Space Center relating to training, on-site degree programs, internships, outreach efforts and more. To strengthen these programs, and provide overlap with a number of education initiatives currently operating at the KSCVC, an initiative could be developed that would broaden NASA's involvement with regional educational institutions and the educational community. This program could also be used to draw local, national, international, and visiting youth to participate in evening, weekend and summer space schools. The program would be focused on the NASA and KSC space exploration efforts.

The space school, focusing on the NASA-KSC space programs at KSC but incorporating other fields of science, could be funded by the participants, operated through the KSCVC, and taught with the assistance of local colleges and universities. Teaching expertise could come from the college and university faculty who elect to participate. Key faculty would be responsible for transferring information from NASA and NASA-KSC operations personnel to their undergraduate/graduate students, who, in turn, would teach the visiting youth.

Several internship/co-op teaching programs at local schools could be employed for teaching the classes. Additional instruction and education components could also be provided by K-12 teachers interested in the program. A collaborative university program structure is already in place at the Kennedy Space Center that could provide direction and possibly organization for the agreements between NASA-KSC, the colleges/universities, and the KSCVC personnel, for operation of the school. Those organizational entities include the KSC Education Division and The Florida Space Institute.

Emphasis for the school would be related to ongoing NASA space flight programs, and more specifically, NASA-KSC space operations programs and projects. Because tours throughout the NASA-KSC site have limited access, especially for children and young adults, the school would need basic infrastructure including buildings, classrooms, simulators, and theatres.

The advantages of the space school would benefit all participants: NASA & NASA-KSC, KSCVC, local colleges and universities, primary and secondary schools, and, of course, the young students/participants. Such a space school could serve to attract youth from throughout the state and the nation, and extend the NASA experience for visiting families, generally for the weekend and evening sessions. The space school could also satisfy the natural curiosity of a greater number youth in space and space exploration beyond the KSCVC experience, and it could expand NASA's contact with youth interested in space, science and engineering. Program advantages also include increased university student involvement with NASA programs and increased faculty experience with NASA scientists, engineers and managers. Members of the space school operations staff, consisting of the NASA-KSC education representatives, KSCVC operations personnel, and participating colleges, universities and

schools, could develop the fundamental structure of the space school and its educational outcomes. Additional details of the school funding and related responsibilities could establish the working relationships between the principals. Curricular details could be established and coordinated through the NASA-KSC University Programs office.

9. Summary

Recommendations for detailed evaluation of the KSCVC exhibits have been outlined in the preceding sections, emphasizing the educational and science content. To provide a more effective evaluation process for the Visitor Complex exhibits, additional recommendations have been introduced for strengthening contact between the visiting public and NASA. A compilation of those recommendations are summarized below.

- A periodic evaluation survey process and instrument should be developed for evaluating the KSCVC exhibit educational effectiveness through an independent organization, with input from both NASA and the exhibit contractor representatives. A well defined purpose and specific function for the evaluation survey would be required, although specific survey content and construction would be the purview of the evaluation organization.

- Increased science detail should be included in exhibits throughout the KSCVC to reflect the NASA story and NASA's mission and strategic initiatives, especially those efforts that are supported at the Kennedy Space Center.

- NASA's story and mission concepts should be presented within the Visitor Complex exhibits to provide the public with informative and exciting information on NASA's future efforts and its role in improving life on Earth. These statements would be integrated into the most widely attended areas within the KSCVC and provide the public with insight into NASA's current efforts as well as the role of the Kennedy Space Center in the development and exploration of space.

- A necessary prerequisite to an effective presentation of the NASA story is a careful study that would construct an accurate, faithful representation of NASA's history and future. This study should be established as soon as practicable to enhance current exhibits and support future exhibit development.

- Emphasis on new exhibit development and exhibit improvements should include NASA future programs, general space exploration plans, and specific NASA-KSC space flight operations. Science emphasis should be extended to offer the visitors intellectual stimulation, inspiration and entertainment from NASA's space operations. Because of the importance of the four NASA exploration initiatives, those areas should be effectively underscored within the KSCVC exhibits.

Educational initiatives should be developed that extend the NASA-KSC experience beyond the walls of the KSCVC exhibits. These initiatives could overlap already-existing programs, and provide revenue for its operation in relatively simple fashion. Funding structure would also enable the expertise and participation of local education groups, and NASA personnel.

1. References

[1] **NASA Vision Statement**
http://businessworld.ksc.nasa.gov/BusinessWorld/html/strategic_planning.html

[2] **Communicating NASA's Knowledge: A Report of the Communicate Knowledge Process Team**, 1998, NP-1998–08-240-HQ

[3] **Space Science Education and Public Outreach**
http://spacescience.nasa.gov/educatio/index.html

[4] **NASA Strategic Enterprises**
http://education.nasa.gov/enterprs1.htm

[5] **NASA Exhibits Program,** NASA NPG-1387.1, November 9, 1999

2000 NASA/ASEE SUMMER FACULTY FELLOWSHIP PROGRAM

JOHN F. KENNEDY SPACE CENTER
UNIVERSITY OF CENTRAL FLORIDA

PRMS Data Warehousing Prototype

Eranna K. Guruvadoo
Assistant Professor
Bethune-Cookman College

KSC Colleagues
Neil Spears
PRMS Database Administrator
Cary Peaden
PRMS Project manager

ABSTRACT

Project and Resource Management System (PRMS) is a web-based, mid-level management tool developed at KSC to provide a unified enterprise framework for Project and Mission management The addition of a data warehouse as a strategic component to the PRMS is investigated through the analysis, design and implementation processes of a data warehouse prototype. As a proof of concept, a demonstration of the prototype with its OLAP's technology for multidimensional data analysis is made. The results of the data analysis and the design constraints are discussed. The prototype can be used to motivate interest and support for an operational data warehouse.

PRMS Data Warehousing Prototype

Introduction

Project and Resource Management System (PRMS) is a web-based, mid-level management tool for project and mission resource planning and workflow tracking. It is being designed at Kennedy Space Center (KSC) to provide a unified enterprise framework for Project and Mission management ranging from Document Management associated with KSC Missions and Contracts, Project Plans, Schedules, Task Orders, Purchase Requests, Delivery Orders, Maintenance Requests, Program Operating Plans, Configuration Control Boards, to Configuration Change Request and Performance Appraisals. The addition of a Strategic Management Subsystem to PRMS for upper-level management has been envisioned. One component of such subsystem should provide analytical capabilities on historical data acquired through the use of PRMS. This should provide considerable insight into projects managed at KSC.

The objective of this project is to investigate into the feasibility of a data warehousing system to support the Strategic Management Subsystem. To this end, an analysis of the PRMS database has been performed and a data warehouse prototype has been designed, developed and demonstrated as a proof of concept.

This paper is organized as follows: Section I describes the analysis and logical design performed for the project. Section II describes the implementation of the data warehouse prototype, followed by discussion on the design processes and a conclusion.

Section I

Analysis and Logical Design

The design and development process of a data warehousing system is a complex, multi-layered, iterative approach. The design workflow starts by identifying the business drivers and the types of data analysis to be performed. The data requirements for the front-end applications drive the design of the data warehouse schema and the data storage requirements. Once the data sources are identified, the Extraction, Transformation and Load (ETL) processes are designed. In short, the user requirements drive the design processes.

Constraints. The recent NASA 2000 Reorganization that was implemented at KSC has shifted interest and support for the PRMS development. Consequently, it was difficult to solicit requirements from upper management. In addition, due to the ten weeks limitation of this project, the data sources considered are only those available at the PRMS development servers. Data from other sources (e.g. Accounting Dept.) would require considerable negotiation and time to acquire.

Accounting Codes. Projects are authorized from NASA Headquarters and are identified by an 11-digit NASA Program Code in the Agency Wide Coding Structure (AWCS) database. At KSC, projects are sub-allocated to various organizations. An Activity Classification Number (ACN) scheme of up to 15-alphanumeric characters is used to classify and record accounting activities relating to different projects. A description of the ACN scheme and its relation to program code and funding source is attached in the Appendices – Activity Classification Number.

Data Sources

The PRMS database has accumulated about nine months data for only four projects. This volume of data is considered too low for a data warehouse. Consequently, the data from the monthly downloaded files (October 1999 – June 2000) from the STAR System (Accounting) to the PRMS System were selected. The data was moved to some temporary tables on the PRMS Database. The associated tables and descriptions are shown in the Appendices – PRMS_OLAP Source Data

Selected Measure

The DDOCCS File (downloadable from STAR System) contains six classes of expenses - Authorized, Allocated, Allocated –Reserved, Obligated, Costed and Disbursed, and their cumulative aggregates for the month-to-date, quarter-to-date and year-to-date. The Disbursed Expense is selected as the Measure of interest for the prototype because it represents the final transaction while the other expense classes represent transient states, although they may have significant importance to account management. However, any other expenses could have been selected as a Measure without affecting the schema design.

Data Granularity Level

Although the DDOCCS File contains detailed expense data to the lowest ACN-Level, only the first 8 or 10 alphanumeric characters of ACN code have been considered. The alphanumeric character after the decimal are allocated by Resource Analysts for different projects (see Appendices for detailed description of ACN). Currently, there is no consistent coding scheme used by the Resource Analyst. For example, an item like travel expense, different coding schemes have been observed.

Data Warehouse Schema

A star schema has been selected for the prototype. The structure of the Fact Table (Fact_Exp) and the Dimension Tables (Time_Dim, ACN_Dim, Program_Dim) and other shadow tables are as follow:

Fact_Exp (**FactKey**, Time_Key, Prog_Key, AcnKey, Classification, Dis_Exp)

Acn_Dim (**AcnKey**, TheAcn, Rc_Description, Organization)

Time_Dim (**TimeKey**, TheDate, Year, Quarter, Month)

Prog_Dim (**ProgKey**, Program_Code, Prog_Description, Classification, Upn_Fpn_Code, Upn_Break_1, Upn_Break_2)

Pcode_Fcode_inter_table(**ProgKey**, **Fund_Source_Code**)

Fund_Source (**Fund_Source_Code**, Fund_Src_Description)

The field named classification in the Fact_Exp and Prog_Dim tables is used to classify the expense as UPN of FPN. The schema with all the field descriptions are shown in the Appendices – PRMS_OLAP FACT and Dimension Tables.

Section II

Implementation

The data warehouse prototype has been implemented on an NEC Server – Net Express 5800 with the following specification:

Server Name:	AIS8
Domain Name:	Renaissance
Processor:	Dual Pentium II – 333 Mhz
RAM:	0.5 GB
Disk Space	4.5 GB
Operating System:	MS Windows NT 4.0

Microsoft SQL Server 7.0 has been used to implement the data warehouse prototype. The tables were created using the Enterprise Manager. The Extraction, Transformation and Loading (ETL) processes were done using the Data Transformation Services (DTS) of SQL server 7.0 in addition to stored procedures. The source code for the stored procedures is available on the AIS8 Server

The OLAP Server Services of MS SQL Server 7.0 were used to specify the dimensions in the dimension tables and the to build the Expense Cube. MS Excel Pivot-table was used as a front-end application to view the data.

The architectural design and implementation of the data warehouse prototype was presented to the PRMS Development Team, followed by a demonstration of the OLAP operations (drill down/up, slicing and dicing etc.)

Result and Discussion

The data warehouse prototype designed can be used, even in its minimal design form, to educate or stimulate the interest of project managers or higher-level management in the benefits of having a data warehouse. The ability to interactively analyze on-line data along multiple dimensions should provide tremendous insight into project management

In the analysis and design process of this prototype, several important factors have been identified that would likely influence an operational data warehouse. These factors will be briefly discussed next.

Ensuring data quality is a cornerstone to guarantee the usefulness of a data warehouse as a source of data for decision-making. The data acquired through the STAR System, upon close examination, shows serious quality problem. For example, some ACN codes are only partial; some expense items do not even have ACN codes. Some disbursed expense items have negative entries. The ETL process for the prototype data warehouse was completed without much emphasis on the data cleansing. Therefore, no assurance can be given to its data quality.

If the PRMS is to be used as a source of data for a potential future data warehouse, the following observation is relevant. Although the PRMS has all the capabilities built in its front-end applications to capture the necessary data, many of the data entry fields are still optional. Either these fields are made mandatory, or triggers have to be implemented to supplement user entries.

In addition, only a much larger set of projects would generate enough data for a data warehouse. Using the downloadable files from the STAR System would provide all expense transactions. However, additional sources need to be identified across the Center and acquired to provide the data for the dimensions.

Ideally, an enterprise data warehouse is more desirable. This raise several issues about enterprise data planning that are consistent and usable across the Center and perhaps across NASA. Given the complexities of NASA Accounting System, this is not a trivial task.

Conclusion

A strategic component to the PRMS has been investigated through the analysis and design of data warehouse prototype. The data warehousing system has been implemented using the Data Warehouse Framework of Microsoft SQL Server 7.0 and the OLAP capabilities have demonstrated through Microsoft Excel Pivot Table as a front-end application. The design and implementation processes have provided tremendous insight into the data requirements and data quality for a future operational data warehouse. The prototype can be use as a selling point to motivate interest and support for an enterprise data warehouse.

Acknowledgement

This project was made possible through the help and assistance of the PRMS Development Team, in particular, Neil Spears – the Database Administrator for his valuable time and help, and Cary Peaden – the Project Manager for guidance.

Appendices

ACN – ACTIVITY CLASSIFICATION NUMBER

An activity-related code of reference number (up to 15 digits) assigned by the CFO colocated Resources Analysts to activities of management interest. It is an identifier utilized to classify and record input data and provide a basis for reporting.

- **1st 2 DIGITS OF ACNs are as follows for**

  DIRECT FUNDS - Organization that established the **ACN – PH, JJ, FF,...**
  SUBALLOTTED FUNDS - **SA** for Sub-Authorization – for funds received from HQs Or other NASA Centers that have a Method of Authorization (**MA**) code.
  REIMBURSABLE FUNDS – CW for Center-Wide – for reimbursable funds from other Gov't or non-Gov't Agencies that have a Reimbursable Agreement Number (RAN) and a Reimbursable Code (RC).

- **3rd DIGIT OF ACN IS ALWAYS A DASH (-).**

- **4th thru 5th DIGIT AFTER THE DASH (-).**

  - **DIRECT FUNDS AND SUBALLOTED FUNDS** – 1st 5 or 7 DIGITS AFTER THE DASH (Digits 4 thru 8 or 4 thru 10 are known in the system as basci ACNs).

    1st 5 or 7 digits of the basic ACN after the dash (-) are the same as the 11-digit NASA HQs Program Code in the Agency-Wide Coding Structure (AWCS) database system.

XXXXXXXXXXX	PROGRAM CODE (11 digits)	
XXX	UPN or UNIQUE PROJECT NUMBER	(4th thru 6th)
XXXXX	UPN and Sub-break 1	(4th thru 8th)
XXXXXXX	UPN and Sub-break 2	(4th thru 10th)
XXXX	FPN or FACILITY PROJECT NUMBER	(4th thru 7th)

    Depending on the number of digits in the basic ACN, noted above, the next digit must be a decimal (.) to establish sub-ACNs for an activity.

    Resource Analysts determine the Alphanumeric characters following the decimal (.)

- **REIMBURSABLE FUNDS** – 1st 2 or 3 DIGITS AFTER THE DASH (digits 4 thru 6 are known in the system as basic ACNs)

  1st 2 digits (1992 and prior years) or 3 digits (1993 and subsequent years) of the basic ACNs after the dash (-) for reimbursable activity are the same as the unique KSC IDENTIFIER assigned by the STARS Financial Management System for tracking and reporting.

  The 6th or 7th digit must be a decimal (.) to establish sub ACNs for the reimbursable activity.

  Resource Analysis determine the alphanumeric characters following the decimal (.)

PRMS_OLAP FACT and Dimension Tables

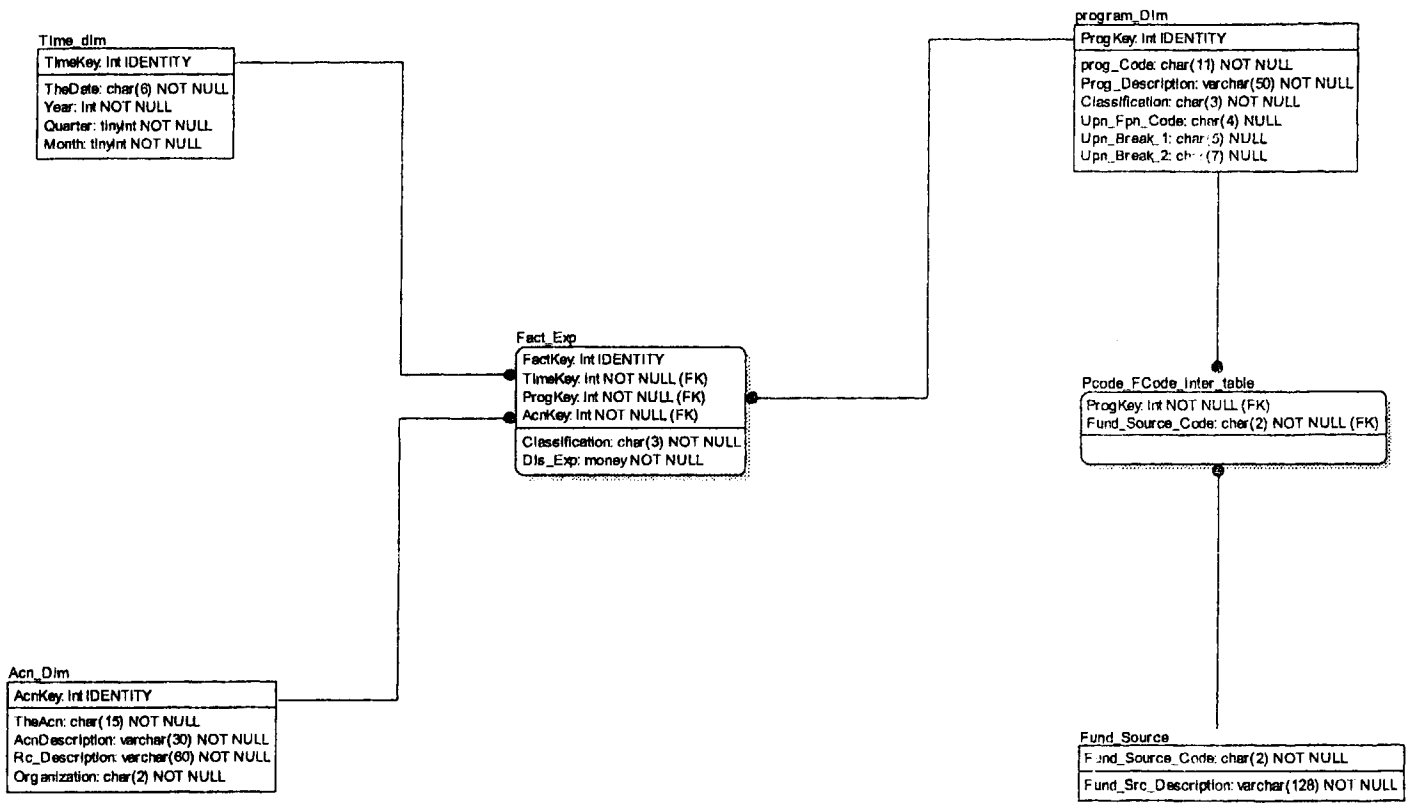

PRMS_OLAP Source Data

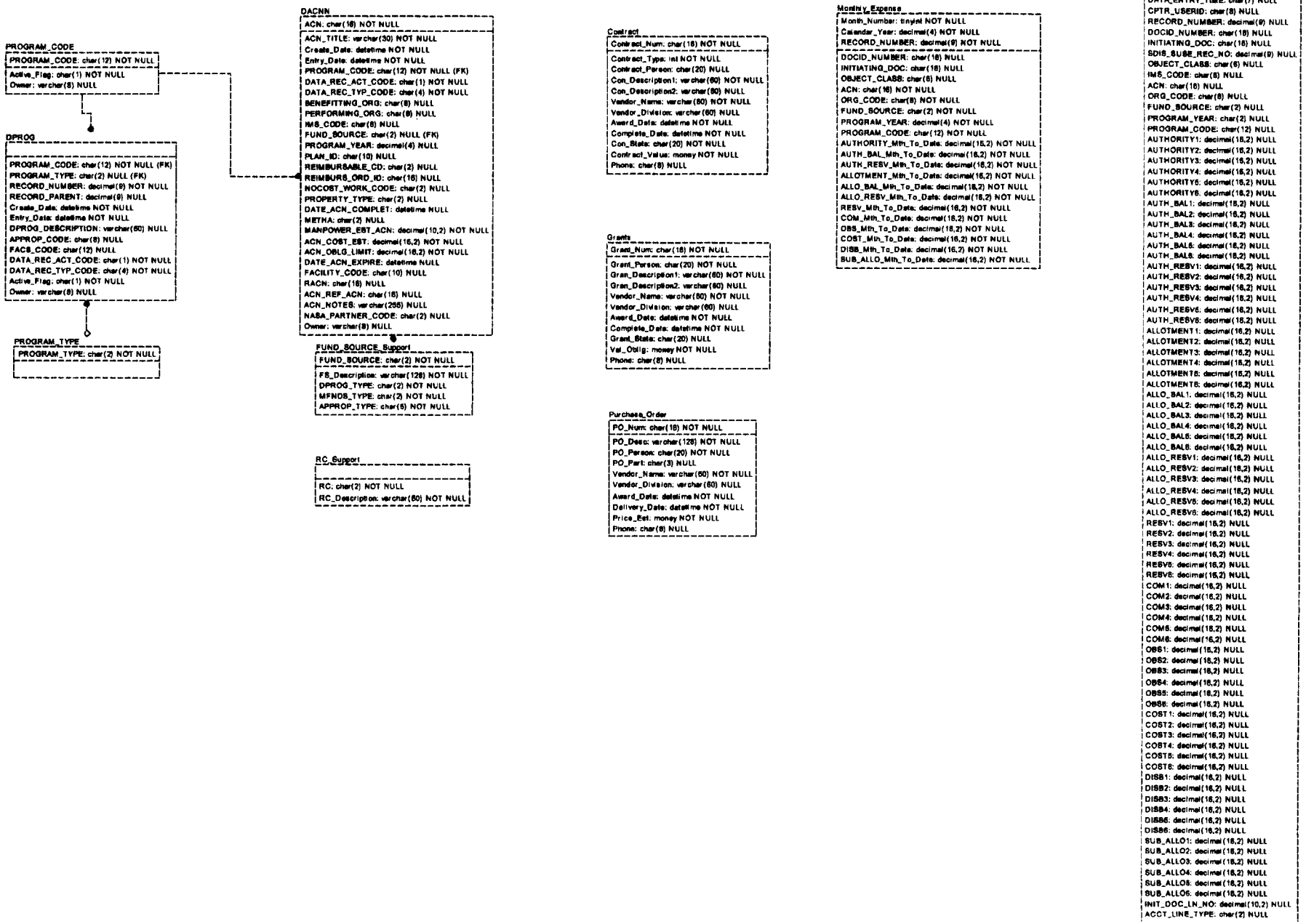

References

1. *Project and Resource Management System (PRMS) User's Guide, Release 3A, Feb 17, 2000*; SE&T Directorate, KSC, NASA.

2. Giovinazzo, W. A. 2000. *Object-Oriented Data Warehouse Design – Building a Star Schema*, Prentice Hall.

3. Agosta, L. 2000. *The Essential Guide to Data Warehouse*, Prentice Hall.

4. Microsoft Training and Certification: *Designing a Data Warehouse in MS SQL Server 7.0*, Microsoft Corporation, 1999.

Final Report

Summer Faculty Fellowship, Summer, 2000

Dr. Michael D. Hampton, Department of Chemistry, University of Central Florida, Orlando, FL
mhampton@mail.ucf.edu

The objectives for this summer faculty fellowship were first to repair the Kratos XSAM 800 X-ray Photoelectron Spectrometer (XPS) and then to utilize the instrument to participate in ongoing research projects at KSC and in the researcher's own laboratory at UCF.

The first 6 weeks were used in repairing the instrument. Working both alone and with the Kratos service engineer, a number of hardware problems, largely associated with the sample stage control system, were corrected. Defective parts were identified and fixed in the computer driver boards, the stage power supply, and the driver interface. The power supply was completely replaced. After four weeks of work, the instrument was functional. This occurred on a Wednesday. The following Friday the instrument had to be completely shut down because the power to the O & C Building was to be turned off. The instrument was properly secured.

On Monday, the instrument was powered up and the original problems returned. After another 2 weeks of work, a software problem was identified. This problem caused the computer to use a defective port for the sample stage control. It was circumvented by rewriting the startup routine.

The final 3 weeks of the fellowship were spent using the XPS to analyze samples being studied in the Langley materials project (Martha Williams) and a catalyst project (Dr. Orlando Melendez). During this time, several sample analysis requests from other groups at KSC also came in and those samples were run as well.

The summer faculty fellowship also allowed many contacts to be made. After meeting with the sensors group, two projects were identified for collaboration and white papers are being prepared. One project aims to develop small, very sensitive hydrogen detectors and the other to develop a broad area, easily monitored, zero power consumption hydrogen detector.

In addition to the work mentioned above, the XPS was utilized in a study underway in Dr. Hampton's laboratory at UCF. Attached is a preliminary report on that project. The other two authors listed on the paper are Dr. Giannuzzi, a colleague who handles the FIB and TEM and Janice Lomness, a doctoral graduate student jointly directed by Dr. Hampton and Dr. Giannuzzi.

51/CW/1M/26

The Role of Water in the Storage of Hydrogen in Metals

Dr. Michael D. Hampton and Janice K. Lomness, Department of Chemistry
and Dr. Lucille A. Giannuzzi, Department of Mechanical, Materials, and Aerospace Engineering
University of Central Florida, Orlando, FL 32816

Introduction

One major problem with the use of hydrogen is safe and efficient storage. In the pure form, bulky and heavy containers are required greatly reducing the efficiency of its use. Safety is also a great concern. Storage of hydrogen in the form of a metal hydride offers distinct advantages both in terms of volumetric efficiency and in terms of safety. As a result, an enormous amount of research is currently being done on metal-hydrogen systems. Practical application of these systems to storage of hydrogen can only occur when they are very well understood.

Processes such as purging and cooling, that involve the loss of large amounts of hydrogen are very expensive. This expense could be greatly reduced if the hydrogen normally lost could be captured. Metal hydrides are strong contenders for this application as well.

Most metals and alloys react directly and reversibly with hydrogen to form metal hydrides. One major obstacle encountered with the application of these materials for hydrogen storage is their inability to absorb hydrogen under reasonable conditions. This problem has been attributed to the formation of oxide and/or hydroxide surface layers resulting from exposure to air. Because the surface contamination acts as a barrier to hydrogen, some form of surface treatment is necessary for initial activation and stable hydriding properties to be achieved. Several approaches have been taken to overcome the difficulty of initial activation and improve hydriding characteristics.

One method reported involved the use of a dilute solution of HCl to etch the surface of Mg_2Ni[1]. In this study it was found that the HCl etch resulted in the removal of MgO and dissolved away NiO from the surface. The new surface was composed mainly of metallic porous nickel microspheres that had a high catalytic activity towards hydrogen chemisorption.

Another study reported was the use of aqueous fluoride to remove oxides and/or hydroxides from the surface of La-Ni-Al and Mg-Ni alloys[2]. Suda reported that fluoride treatment of $LaNi_{4.7}Al_{0.3}$ produced a Ni-rich sub-surface under a surface of LaF_3. It was proposed that the LaF_3 protected the lower layer from contamination while cracks in the fluoride layer provided a path for hydrogen molecules to diffuse to the Ni-rich sub-surface where dissociation into atomic hydrogen occurs.

Previous work in this laboratory has shown that water and water vapor treatment of Mg_2Ni provided very rapid activation for hydrogen uptake and greatly improved hydriding and dehydriding properties[3]. Alloy activated using the liquid water absorbed hydrogen at relatively low temperatures, 413 K, at 827 kPa H_2 resulting in a hydrogen content approaching the theoretical maximum. Water vapor treatment also essentially caused complete activation of the alloy.

The literature is full of references to the deleterious effects of oxide and hydroxide layers on the reactivity of metals and alloys with hydrogen. Water is commonly listed as a poison to hydrogen storage systems[4]. In light of the studies above, more work is obviously required on the role of oxides and hydroxides in the interaction of metals and alloys with hydrogen.

It has been shown that a pressure of 10^{-6} torr at room temperature is equivalent to a temperature of 350 – 400°C at atmospheric pressure[5]. Since surface analysis techniques utilize vacuum in this range, it is likely that surface hydroxides are commonly destroyed in the process of analysis. Thus, the role of hydroxides in hydrogen storage systems is not well understood.

In this paper, the preliminary results of a study of the surfaces of magnesium nickel alloys will be presented. Alloys that have been rendered totally unreactive with hydrogen as well as those that have been activated with liquid water and with water vapor were studied. Data obtained from XPS analysis, with samples held in vacuum for the shortest possible time to minimize the hydroxide degradation will be presented. Furthermore, TEM data on samples prepared in a new way that largely protects the surface from the high vacuum will be discussed.

Experimental

The Mg_2Ni alloy was purchased from Aldrich Chemical Company as Hy-Stor 301. This alloy is slightly magnesium enriched, with a formula of $Mg_{2.35}Ni$, in order to prevent disproportionation of Mg_2Ni to Mg and $MgNi_2$. Water used was deionized with a Culligan ion-exchange system and then further purified with a Barnstead B-Pure polishing system. The hydrogen (ultra high purity grade) and argon (high purity grade) were used without further purification.

XPS studies were done on a Kratos XSAM 800 XPS (NASA, Kennedy Space Center) using a Mg anode operating at 15 mamp and 14 kV. Samples were mounted on C tape and evacuated for the minimum time, 10-25 min, before analysis. The C tape allowed for a strong elemental C peak

for adjustment and alignment of the spectra. The surfaces of samples to be analyzed by TEM were sputter coated with an EMITECH K550 Au-Pd sputter coater. Samples for analysis with TEM were obtained with an FEI FIB 200 TEM focused ion beam. Surface structures were determined using a Philips EM430 TEM operating at 300 keV.

TEM analyses were done using the FIB lift out technique[6]. Particles were sputter coated with Au-Pd to protect the outer surface from spurious sputtering due to FIB imaging an to protect the surface from the high vacuum. Preliminary trench FIB cuts were milled, producing a specimen 10 μm long x 5 μm wide x 1 μm thick. The specimen was milled to electron transparency (~100 nm thick) before finishing cuts were made at the sides. The freed specimen was lifted-out and placed on a carbon coated Cu grid using a hydraulic micromanipulator and a light optical microscope.

Hydrogen uptake and release data were obtained by the method published elsewhere, see reference 3. See this reference also for data handling and deactivation procedures.

The liquid water treatment of short treatment time samples involved swirling the ground alloy in deionized water for 30 sec then allowing the alloy to settle for 1.5-2 min. The water was decanted and the alloy was allowed to dry either by standing in air for 12 hr or by drying at reduced pressure for 20 min at room temperature then increased temperature to 323 K over 40 min. Longer duration water treatment was done in an evaporating dish with constant stirring using a magnetic stirring bar. In order to expose samples to humidity, the ground alloy was placed on a watch glass, spread out and placed in air at 100% relative humidity for the required time.

Results and Discussion

XPS data obtained on the as-received, deactivated, liquid water treated, and water vapor treated alloy are shown in Table 1. In all of the spectra the Ni 2p peak was small indicating that in all of these samples a very small amount of Ni was present in the sampling depth of the XPS.

The as-received material had a relatively large amount of C (33 atomic %) and O (54 atomic %), a small amount of Mg (12 atomic %) on the surface. The position and shape of the Mg 2p peak (Fig. 1) indicates that the Mg on the surface was mostly in the oxidized form, though a small amount of metallic Mg did show. After 20 min etching with an Ar^+ beam, the Mg 2p peak broadened towards low binding energy (Fig. 1) indicating the presence of more elemental Mg. This change possibly indicates that the contaminating surface layer on the as-received alloy was thin and became more transparent with etching. After etching, the amount of Mg increased and the amount of C decreased with no significant change in the O or Ni content indicating that the surface contaminant may have been an organic compound that was mostly removed by etching.

After deactivation, the surface contained less than half the C originally present, indicating the possible removal of an organic contaminant. Deactivation resulted in the surface Mg more than doubling and the O increasing by ~ 3 atomic %. After etching, Mg increased further and O and C dropped. The Mg 2p peak (Fig. 2) indicated the presence of mostly metallic Mg with some possibly bonded to a low electronegativity element. After etching, the Mg 2p peak was centered at a binding energy of 50 eV indicating that the Mg was split between Mg and Mg^{2+}. These results suggest that residual organic contaminant was removed by etching. Elemental Mg could result from the surface coating being thin enough that the XPS detected electrons from underlying alloy. Splinter[7] showed that the limiting thickness of an oxide coating on the surface of Mg resulting from the interaction with water vapor was 11 monolayers, thinner than the XPS analysis depth.

These changes in the as-received alloy are consistent with the removal of an organic surface contaminant and the establishment of an MgO coating. The lack of reactivity with hydrogen confirmed that the coating present was continuous and wide spread enough to be protective.

Sample	Atomic % Mg	Atomic % C	Atomic % O	Atomic % Ni
As-Rec'd.	11.8	33.6	53.8	0.7
As-Rec'd., Etched	20.9	25.5	53.1	0.5
Deact.	28.4	14.4	56.7	0.5
Deact., Etched	34.5	11.2	53.7	0.6
LWTR	23.8	8.7	67.1	0.4
LWTR, Etched	29.9	11.3	58.3	0.52
WVTR	25.2	15.6	58.9	0.3
WVTR, Etched	31.4	13.3	54.7	0.6

Table 1. XPS data. LWTR = liquid water treated samples, WVTR = water vapor treated samples.

Treatment of the deactivated alloy with water, either the liquid or vapor, resulted in a decrease in the amount of Mg and an increase in the amount of O present in the surface layer. This caused an increase in the O:Mg ratio as expected if $Mg(OH)_2$ was formed from MgO. As expected, the decrease in Mg and increase in O were greatest for the liquid water treated sample due to the more vigorous reaction conditions. The alloy was reactive with hydrogen after treatment with both liquid water and water vapor indicating that the new coating was permeable to hydrogen.

In samples treated with liquid water and those treated with water vapor, the Mg 2p peak indicated the presence of mostly metallic Mg before etching (Fig. 4, 5). After etching the Mg 2p peak shifted to higher binding energy in both samples indicating the presence of more oxidized Mg. In the liquid water treated sample, there was a small amount of metallic Mg remaining. The water vapor treated sample had essentially only oxidized Mg after etching. These data indicate that somehow surface Mg is becoming reduced to elemental Mg in a very thin film. Etching removed this film revealing the oxidized magnesium underneath.

While the XPS results are inconclusive, they do suggest that the as-received alloy was contaminated with an organic compound that was largely removed in the deactivation process. The XPS data neither support nor disprove the presence of a layer of MgO on the surface of the deactivated alloy. This is not surprising since a very thin coating would be expected. The XPS data do lend some support to the idea that a coating of magnesium hydroxide is present on the surface of the treated alloy samples. However, the pressure in the analysis chamber of the XPS during the analysis of each sample was no higher than 5×10^{-8} torr which is sufficiently low to cause the decomposition of magnesium hydroxide if it was present. The large changes in surface composition and peak positions after etching suggest a strong interaction of the samples with the vacuum of the XPS, further complicating the results.

Thus, it was necessary to seek a different analytical technique. While the FIB and TEM are high vacuum instruments, the first step in sample preparation is coating the sample with Au/Pd, thus protecting the surface from the vacuum. Further sample preparation involves milling out electron transparent wafers of sample. While this process exposes the surface of the alloy to vacuum on two sides, the top is still protected.

The bright field TEM images of the deactivated, liquid water, and water vapor treated Mg_2Ni alloy samples obtained using the FIB LO method are shown in Fig. 5, 6, and 7, respectively. Diffraction patterns obtained from the surface layers are shown in the insets of Fig. 6 and 7. The bright field (BF) images show a substantial change in the characteristics of the surface upon treatment with liquid water and water vapor, with formation of surface layers about 470 nm and 130 nm thick, respectively. This supports the results obtained from XPS analysis of the alloy and confirms that the alloy surface was more affected by the liquid water treatment than by the water vapor treatment. The surface of the liquid water treated sample shows more texture than that of the water vapor treated sample though the surface layers are identical in contrast. The diffraction patterns obtained for the liquid water and water vapor treated samples indicate that the surface layers are polycrystalline. The surface layer of the water vapor treated sample exhibited more diffraction spots than that of the liquid water treated sample, probably because this layer was not as thick as the water treated sample surface. Some of these diffracted spots may be from the bulk Mg_2Ni. Preliminary analysis of the diffraction patterns indicates the presence of $Mg(OH)_2$ in the surface layer of the liquid water and water vapor treated Mg_2Ni samples.

The analysis of the electron diffraction patterns is still in progress. It is expected that the presence of magnesium hydroxide will be confirmed. When thi happens, it will be the first time that the presence of $Mg(OH)_2$ on the surface of an alloy has been conclusively shown. It will also be the first demonstration that hydroxides on the surface of magnesium nickel alloy is useful and important for the application of these alloys for the storage of hydrogen.

Acknowledgements

The authors thank NASA and the members of the Chemistry Group at Kennedy Space Center for their help and encouragement. The NASA/ASEE Summer Faculty Fellowship provided to Dr. Hampton for the summer, 2000 was invaluable in this work.

---

[1] H-Y Zhu, C-P Chen, Y-Q Lei, J Wu, and Q-D Wang, *J Less Common Metals,* 1991;174:873.

[2] X. Wang, A.i Inoue, H. Watanabe, T. Ebihara, and S. Suda, *Surface Structure of Highly Reactive Hydriding Materials Produced by Surface Treatment,* Reprinted from Research Reports of Kogakuin University, 1992;No73:57, F.-J. Liu, G. Sandrock, and S. Suda, *J. Alloys and Compounds,* 1992;190:57, F.-J. Liu, G. Sandrock, and S. Suda, *Z. Physik. Chemie,* 1994;183:163, S. Suda, *Mechanism of Hydrogen Uptake on the F-treated Surface of* $LaNi_{4.7}Al_{0.3}$*-alloy,* Reprinted from Research Reports of Kogakuin University, 1993;No74:29, F-J Liu, M. Ito, and S. Suda, *The Effects of Chemical Treatment on the Activation Properties of* $laNi_{4.7}Al_{0.3}$*-Hydride,* Reprinted from Research Reports of Kogakuin University, 1992;No72:85.

[3] M. D. Hampton, and J. K. Lomness, *Int. J. Hydrogen Energy,* 1999;24:175, M.D. Hampton, R. Juturu, and J. Lomness, *Int. J. Hydrogen Energy, .* **24(10)**, 981 (1999).

[4] for example, see F-J. Liu, G. Sandrock, and S. Suda, *J.I Alloys and Compounds,* **190**, 57 (1992) and G. Sandrock and P. Goodell, *J. Less Common Metals,* **73**, 161 (1980).

[5] K. Hirokawa and Y. Danzaki, *Surf. and Interfac. Anal.*, **4**, 63 (1982).

[6] L. Giannuzzi, J. Drown, S. Brown, R. Irwin, and F. Stevie, *Mat. Res. Symp. Proc.*, **480**, 19 (1997).

[7] s. Splinter, *The Initial Interaction of Water Vapour With Magnesium and Magnesium Alloy Surfaces,* Ph. D. Dissertation, University of Western Ontario, London, Ontario, March, 1994.

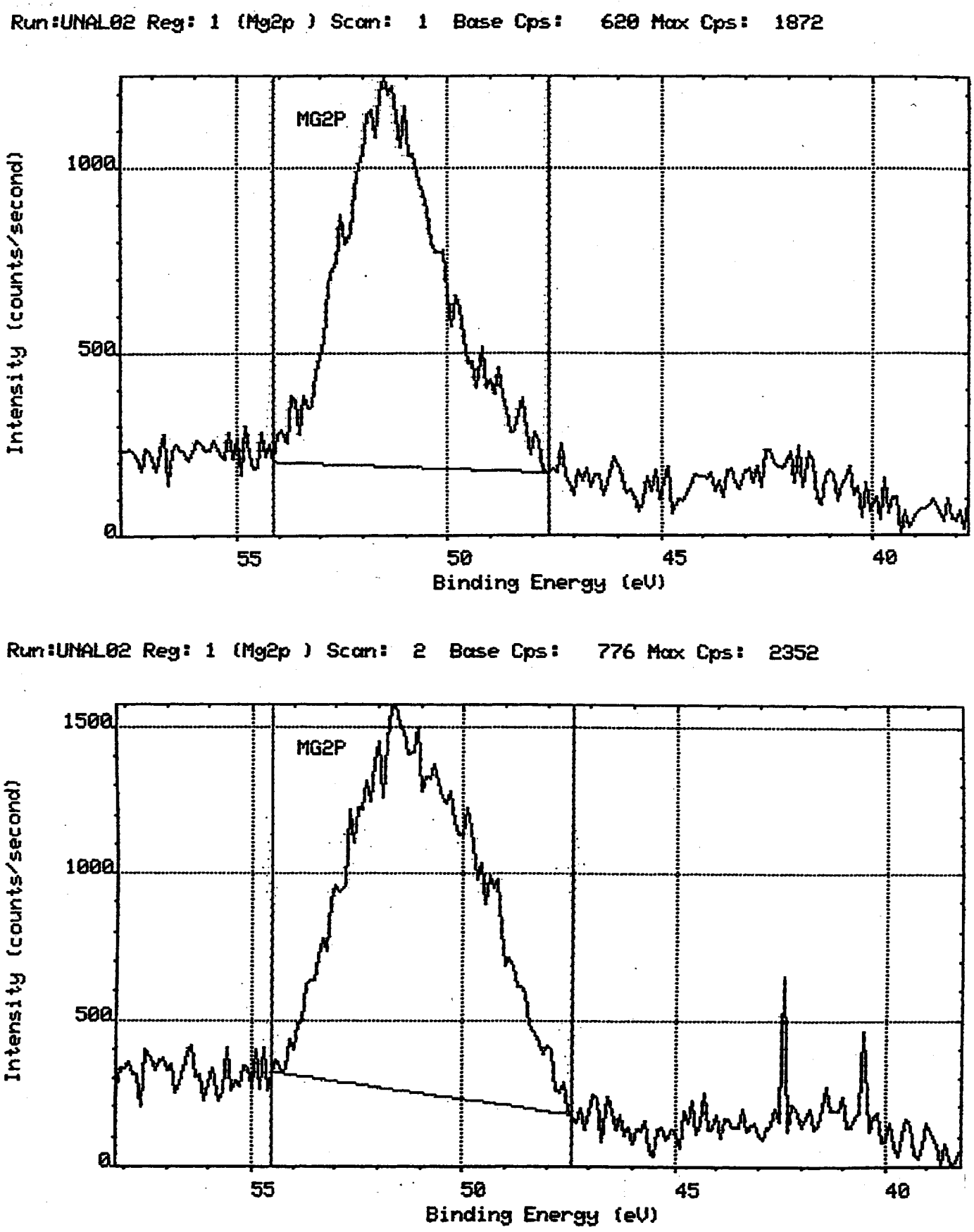

Figure 1. Mg 2p peak in the XPS spectrum of as-received magnesium nickel alloy. Top-before etching; Bottom – after 20 min etch.

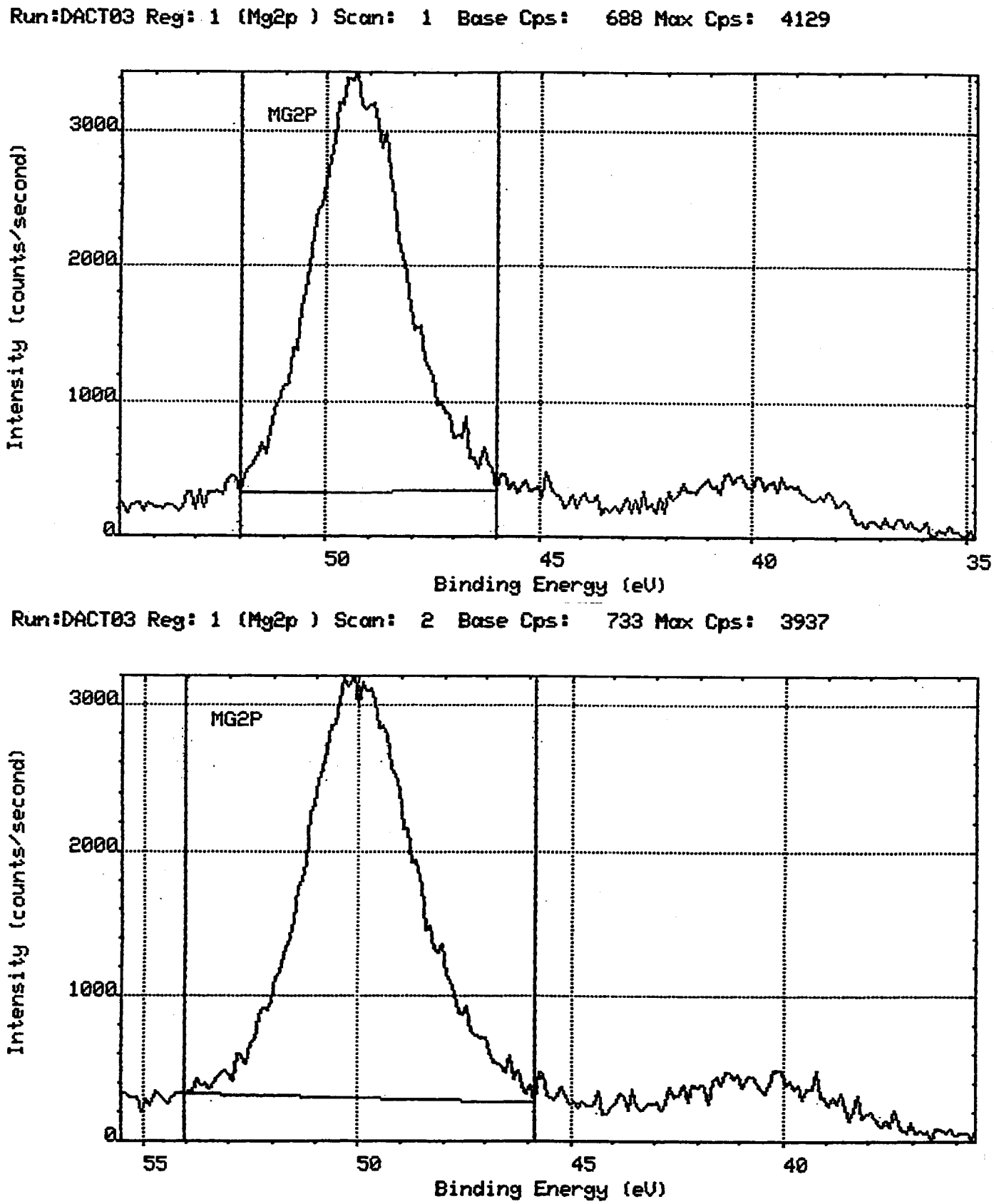

Figure 2. Mg 2p peak in the XPS spectrum of deactivated magnesium nickel alloy. Top-before etching; Bottom – after 20 min etch.

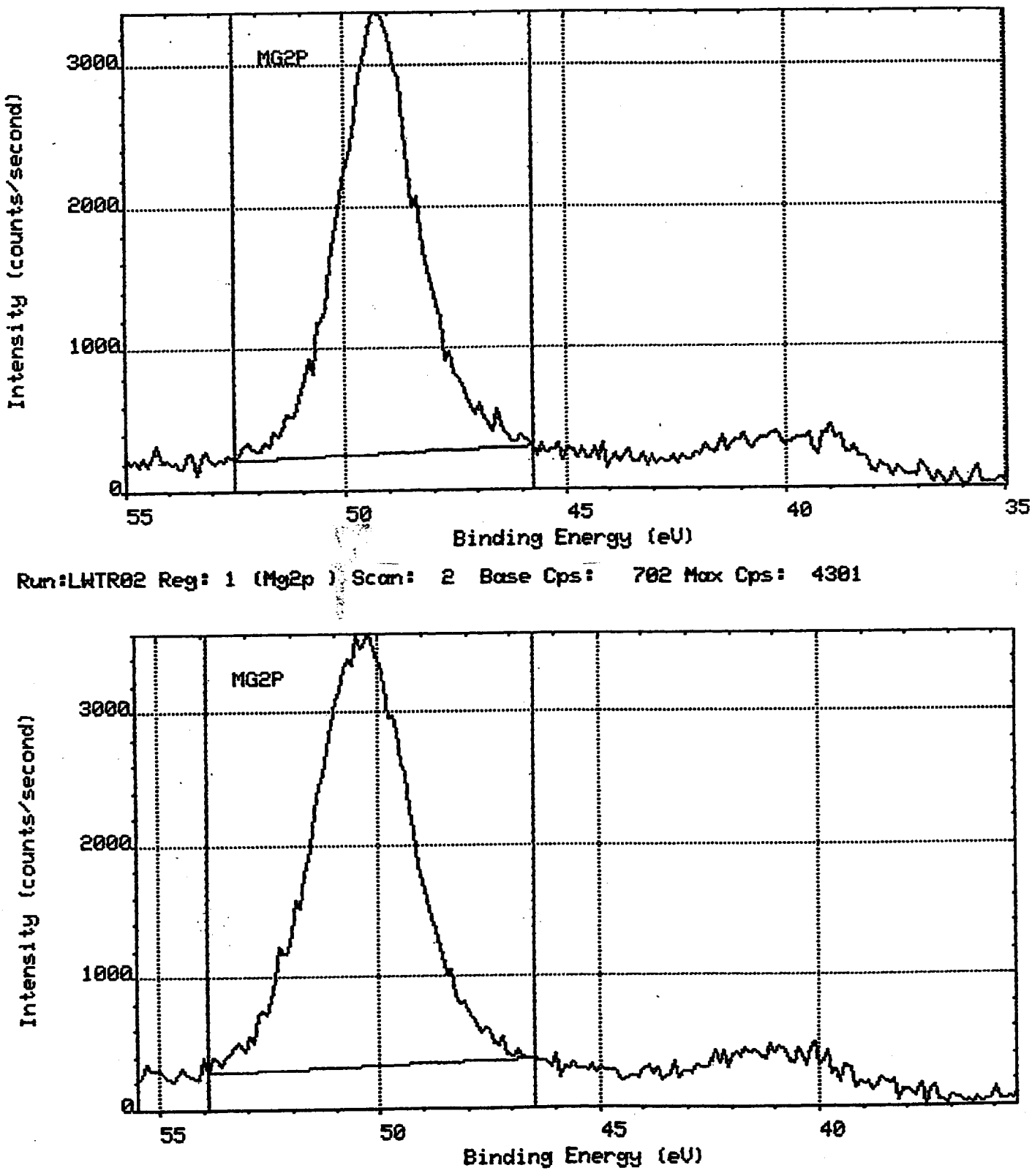

Figure 3. Mg 2p peak in the XPS spectrum of liquid water treated magnesium nickel alloy. Top- before etching; Bottom – after 20 min etch.

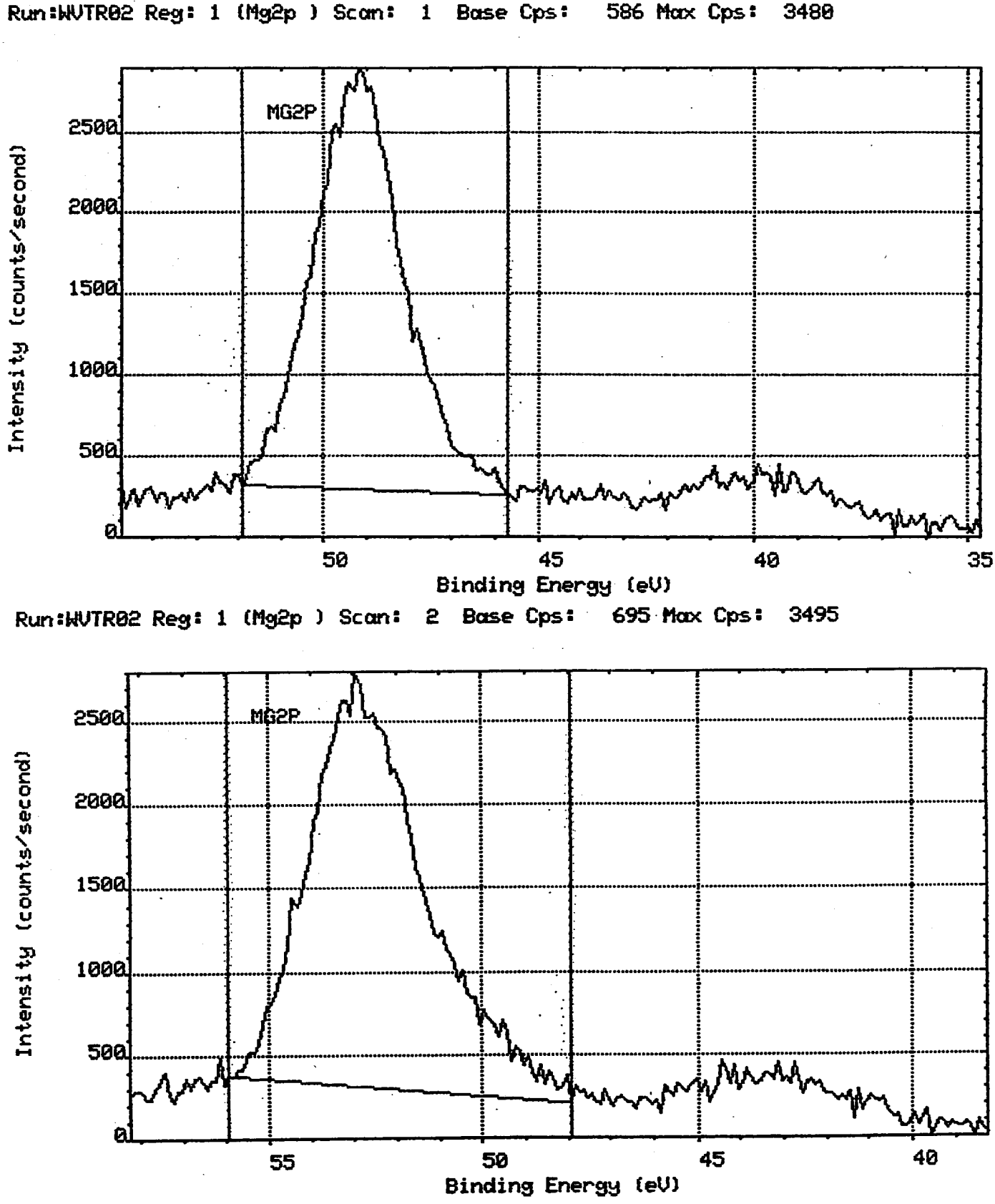

Figure 4. Mg 2p peak in the XPS spectrum of water vapor treated magnesium nickel alloy. Top- before etching; Bottom – after 20 min etch.

Figure 5. Bright field TEM image of deactivated magnesium nickel alloy sample.

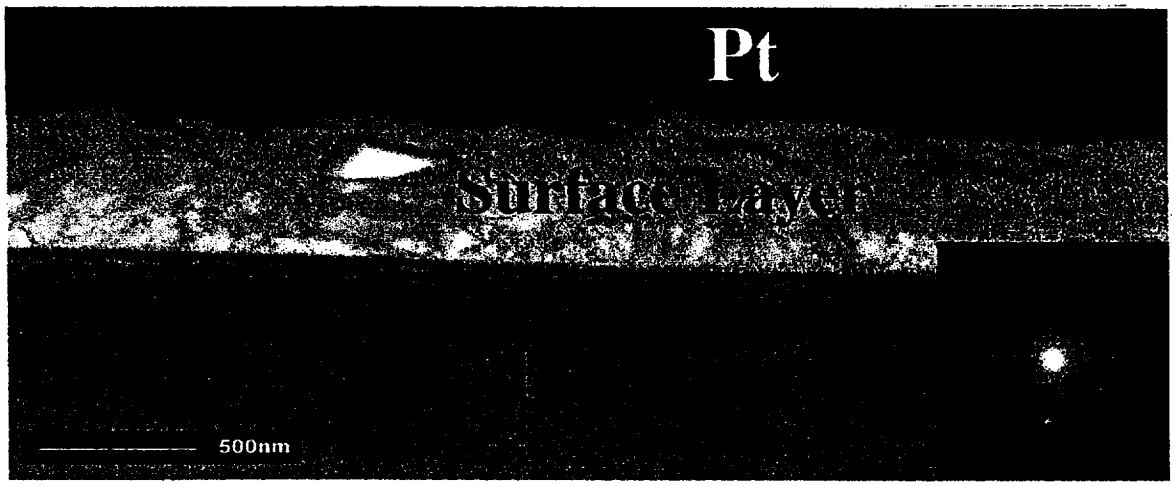

Figure 6. Bright field TEM image of liquid water treated magnesium nickel alloy sample.

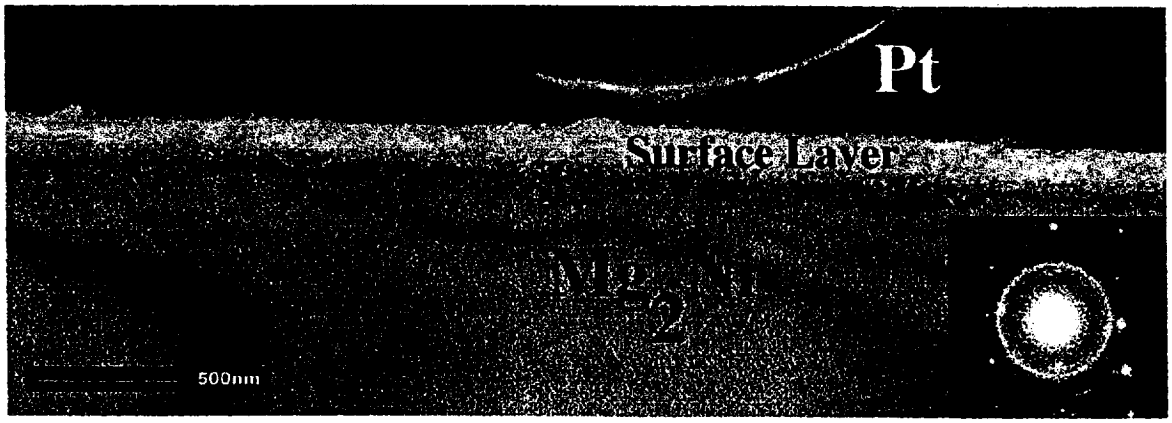

Figure 7. Bright field TEM image of water vapor treated magnesium nickel alloy sample.

2000 NASA/ASEE SUMMER FACULTY FELLOWSHIP PROGRAM

JOHN F. KENNEDY SPACE CENTER
UNIVERSITY OF CENTRAL FLORIDA

LYAPUNOV-BASED SENSOR FAILURE DETECTION AND RECOVERY FOR THE REVERSE WATER GAS SHIFT PROCESS

Michael G. Haralambous
School of Electrical Engineering and Computer Science
University of Central Florida
Brian Larson and Curtis Ihlefeld, KSC Colleagues
July 21, 2000

ABSTRACT

Livingstone, a model-based AI software system, is planned for use in the autonomous fault diagnosis, reconfiguration, and control of the oxygen-producing reverse water gas shift (RWGS) process test-bed located in the Applied Chemistry Laboratory at KSC. In this report the RWGS process is first briefly described and an overview of Livingstone is given. Next, a Lyapunov-based approach for detecting and recovering from sensor failures, differing significantly from that used by Livingstone, is presented. In this new method, models used are in terms of the defining differential equations of system components, thus differing from the qualitative, static models used by Livingstone. An easily computed scalar inequality constraint, expressed in terms of sensed system variables, is used to determine the existence of sensor failures. In the event of sensor failure, an observer/estimator is used for determining which sensors have failed. The theory underlying the new approach is developed. Finally, a recommendation is made to use the Lyapunov-based approach to complement the capability of Livingstone and to use this combination in the RWGS process.

INTRODUCTION

Livingstone is a reusable, model-based artificial intelligence system that is planned for use in the autonomous fault diagnosis, reconfiguration, and control of the oxygen-generating reverse water gas shift (RWGS) process test-bed located in the Applied Chemistry Laboratory at the Kennedy Space Center. The RWGS process is a candidate for the generation of oxygen on Mars. The test-bed was installed in May 2000. A target date of September 2000 has been set to begin testing the autonomous operation of the test-bed.

In this report the RWGS process is first described, then an overview of Livingstone is presented. The qualitative, static nature of the models used in Livingstone for representing dynamic system components is explained. Next the RWGS autonomous control architecture is described. Following this, a new approach for detecting and recovering from sensor failures is presented, wherein models used are in terms of the defining differential equations of system components, thus differing significantly from the models used by Livingstone. The models naturally represent transient as well as static modes of operation. An easily computed scalar inequality constraint, expressed in terms of sensed system variables, is used to determine whether sensor failures exist. The constraint is based upon an energy-like (Lyapunov) function. In the event of sensor failure, an observer/estimator is used for determining which sensors have failed. The theory underlying the new approach is developed. Finally, a recommendation is made for implementating the autonomous fault detection and recovery of the RWGS process using the new approach in combination with Livingstone.

THE RWGS PROCESS

The reverse water gas shift process, depicted in Figure 1, is a candidate for the production of oxygen on Mars. As such, autonomous control of the process is a necessity. A test-bed for the process was installed in May 2000 in the Applied Chemistry Laboratory of KSC, and is presently undergoing testing and modification.

The operation of the RWGS on Mars requires that hydrogen be transported from Earth. The hydrogen is combined with carbon dioxide from the Martian atmosphere in the RWGS reactor at an approximate temperature of 400 degrees Celsius. The carbon monoxide produced is vented off through a permeable membrane, while excess carbon dioxide and hydrogen are recycled to the reactor. Water vapor that is produced by the reaction is condensed and electrolyzed. Electrolysis produces hydrogen and oxygen. The oxygen is stored while the hydrogen is fed back into the RWGS reactor.

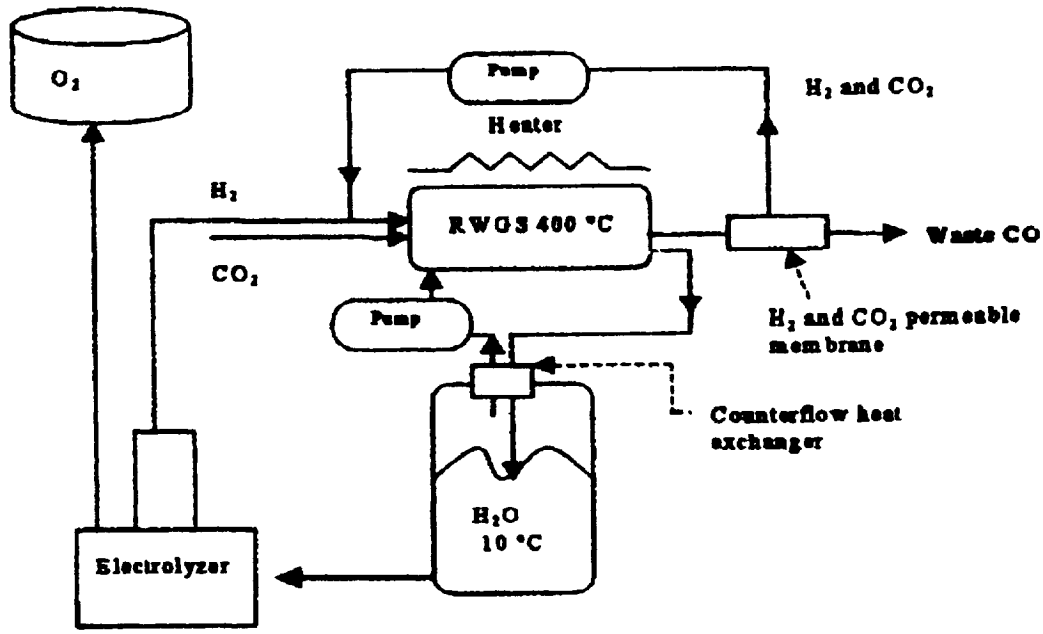

Figure 1. RWGS oxygen generating process

LIVINGSTONE OVERVIEW

A Planner and Scheduler (PS), a Smart Executive (EXEC) and Livingstone (also referred to as MIR, denoting Mode Identification and Reconfiguration) are the three components of an autonomous control architecture known as Remote Agent[1] [1,2]. Remote Agent may be used for controlling a system in deep space, such as a spacecraft, an oxygen generation plant situated on Mars, or a variety of other physical systems requiring autonomous control. For our purposes, Remote Agent, or a modification thereof, may be used to control the RWGS testbed.

PS produces flexible plans, specifying the basic activities that must take place in order to accomplish system goals. The Smart Executive carries out the planned activities. Livingstone, a reusable AI software system, assists the system in operating robustly with minimal human intervention, even when there are hardware failures and unexpected events. Livingstone, also called MIR, denoting mode identification and reconfiguration, constantly monitors the health of the system, and if it senses something unusual regarding the state of the system, will diagnose the problem and make a recommendation to EXEC

[1] Remote Agent was originally developed by the NASA Ames Research Center for controlling spacecraft systems in deep space. It was initially written using the Lisp programming language. A C++ version is also available.

regarding reconfiguring the system. EXEC executes the recovery action or requests a new plan from PS which will take into account the failure.

The Livingstone system consists of four software modules. The language module allows the user to specify a logical model of the system that is to be controlled. The language module then compiles this model into propositional logic. The interface module allows the user to interface Livingstone to other pieces of software, such as the low level control system. It also contains code for automatically hooking up Livingstone to a simulator written in Microsoft Excel. The inference engine module takes a system model compiled by the language module, together with sensor observations from the system provided by the interface module, and performs a diagnosis. It also computes the commands needed to work around a failure or to reconfigure the system into a desired state. The development module contains tools for debugging a model, automatically generating a web page describing the model.

RWGS AUTONOMOUS CONTROL ARCHITECTURE

Consider the RWGS control architecture shown in Figure 3. The real time Executive (EXEC) sends commands to the RWGS plant. The mode identification (MI) component of Livingstone monitors the commands to determine the expected state of the plant. Real-valued sensor data is converted by the Monitors to corresponding discrete values (such as low, medium, and high, or negative, zero, and positive, etc). When MI detects a difference between what it expects and what the sensed value is, i.e., when a failure is detected, Livingstone notifies EXEC. EXEC may request a sequence of reconfiguration commands from the MR component of Livingstone.

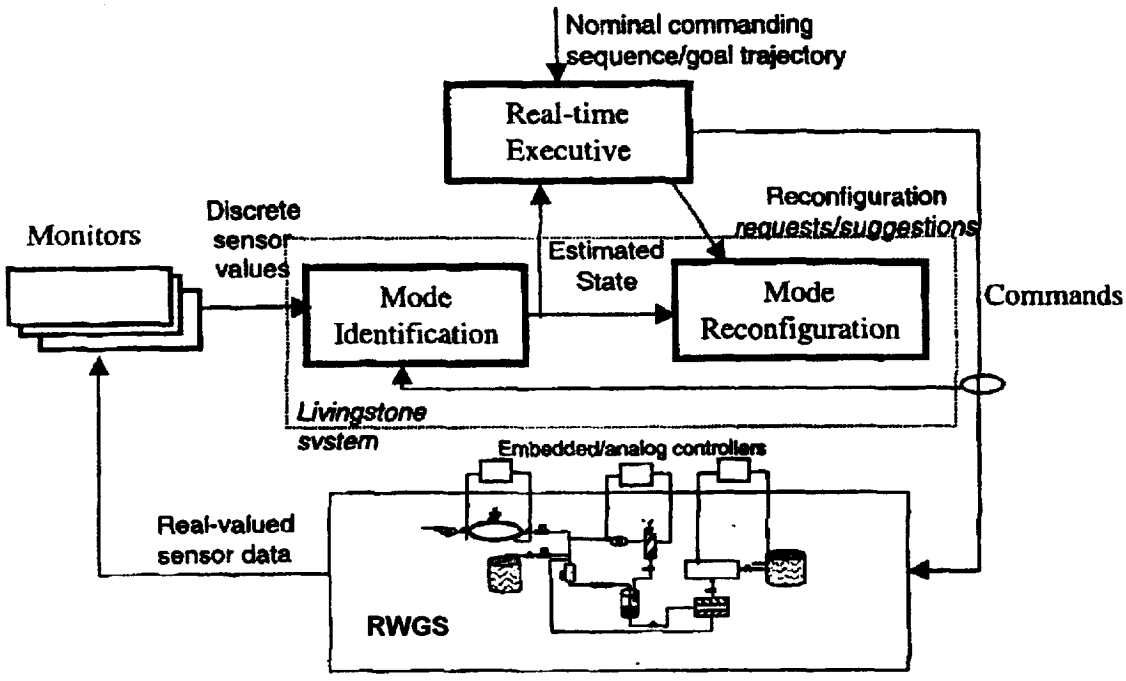

LIVINGSTONE MODELS

A Livingstone model is used for prediction, fault detection, isolation, and reconfiguration. It is qualitative, and static. It is composed of a set of components and their interconnections. Each component is modeled using a set of discrete valued variables, a set of modes, a set of constraints for each mode, and transitions between modes. For example, the valve component of Figure 2 might be modeled using the variables flow-in, flow-out, pressure-in, and pressure-out, with values such as zero, low, nominal, and high. For each component, we have nominal modes (open and closed) and failure modes (stuck open and stuck closed). For each mode, a set of constraints is specified that restrict the values of the component variables when the component is in that mode. There are also transitions between modes.

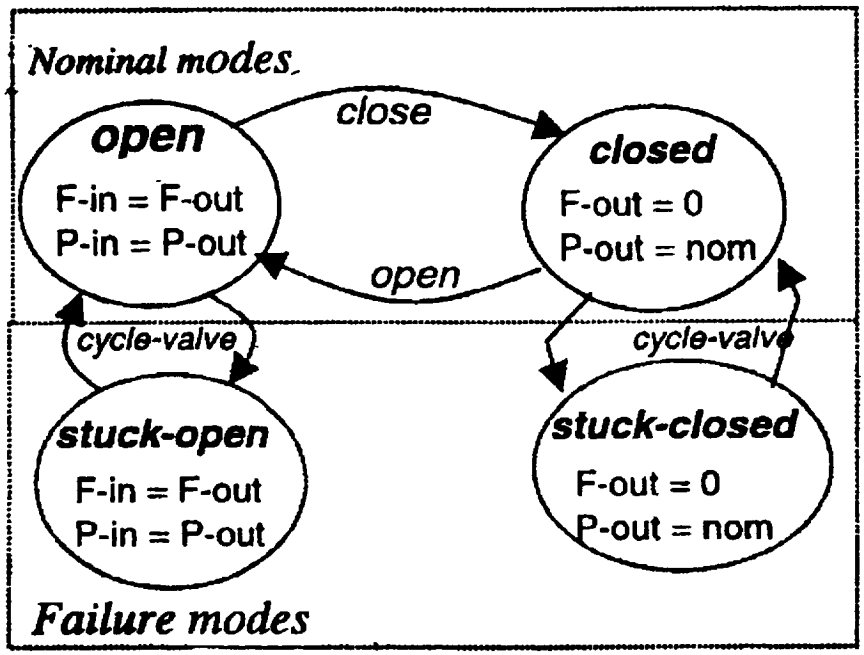

Figure 2. Valve model

LIMITATIONS OF LIVINGSTONE

Although Livingstone models are intuitively easy to understand and are effective in fault diagnosis while the system is in a static mode of operation, Livingstone cannot diagnose faults while the system is experiencing a transient. Furthermore, system components that must be described quantitatively, i.e., by differential equations, cannot be modeled using Livingstone alone. The computing power of the Monitors must be used. In the next section a novel approach to sensor failure detection and recovery is presented.

A LYAPUNOV-BASED APPROACH TO SENSOR FAILURE DETECTION

In this section a new approach is developed that is useful for the dynamic detection and recovery of sensor failures. A scalar inequality constraint is first derived that is used for determining the existence of sensor failures. The inequality constraint is based on an energy-like function known as a Lyapunov function that depends on the measured/sensed state variables of the system. If a sensor failure is detected, an observer is then used to estimate the measurement

Consider a plant described by the n[th] order differential equation

$$\frac{d^n\theta}{dt^n} + \cdots + a_1\frac{d\theta}{dt} + a_0\theta = u \qquad (1)$$

The corresponding state space representation (state equation and output equation) is given by[2]

$$\begin{aligned} \dot{x} &= A_1 x + Bu \\ y &= Cx \end{aligned} \qquad (2)$$

where $x^T = [x_1 \;\; x_2 \;\; \cdots \;\; x_n]$.

Using state variable feedback, $u = r - K_1x_1 - K_2x_2 - \cdots - K_nx_n = r - Kx$, where r is the commanded input, the resulting closed loop state space representation is given by

$$\begin{aligned} \dot{x} &= Ax + Br \\ y &= Cx \end{aligned} \qquad (3)$$

where $A = A_1 - BK$.

The closed loop system described by equation (3) is assumed to be stable. Consequently, the eigenvalues of matrix A will be negative.

The approach presented in this report is a special case of a general approach derived by Qu [3] for the dynamic detection of and recovery from sensor failures. It employs the direct method of Lyapunov [4]. The direct method is based on the concept of energy and dissipative systems. If the system has no input and its energy is always

---

[2] If the plant is described by a second order linear differential equation , then equation (1) becomes

$$\frac{d^2\theta}{dt^2} + 2\zeta\omega_n\frac{d\theta}{dt} + \omega_n{}^2\theta = u$$

This equation could describe a variety of physical systems, for example, the yaw dynamics of a satellite in orbit, in which case it gives the relation between the yaw axis angle θ (the output or response) and the applied torque u (the input). The corresponding state space representation is specified by

$$A_1 = \begin{bmatrix} 0 & 1 \\ -\omega_n{}^2 & -2\zeta\omega_n \end{bmatrix},\; B = \begin{bmatrix} 0 \\ 1 \end{bmatrix},\; \text{and } C = \begin{bmatrix} 1 & 0 \end{bmatrix},\; \text{where } x = \begin{bmatrix} x_1 \\ x_2 \end{bmatrix} = \begin{bmatrix} \theta \\ \dot{\theta} \end{bmatrix}.$$

decreasing, we think of it as being stable. If its energy increases, we think of it as being unstable.

If the system has a bounded input and its energy does not increase beyond that due to the input, we can think of the system as being stable; if, for bounded input, the system energy increases beyond that due to the input, we think of the system as being unstable. Because not all state space systems are descriptions of physical phenomena normally endowed with real energy, the concept of energy is generalized.

Consider an energy-like function called a Lyapunov function. For linear systems, a candidate Lyapunov functions has the following quadratic form

$$V(x) = x^T P x \tag{4}$$

where P is assumed to be a symmetric matrix. It follows that

$$\dot{V}(x) = x^T P \dot{x} + \dot{x}^T P x \tag{5}$$

According to Lyapunov, the system is stable if there exists a positive definite function $V(x)$ such that $\dot{V}(x)$ is negative definite.

Substituting state equation (3) into equation (5) and simplifying, this becomes

$$\dot{V}(x) = -x^T Q x + x^T P B r + r^T B^T P x \tag{6}$$

where Q is also a symmetric matrix defined by

$$-Q \equiv (A^T P + P A) \tag{7}$$

This is referred to as a Lyapunov equation[3]. Noting in equation (6) that

$$(r^T B^T P x)^T = x^T P B r ,$$

we can rewrite equation (6) as

$$\dot{V}(x) = -x^T Q x + 2 x^T P B r .$$

Rearranging,

$$-x^T Q x = \dot{V} - 2 x^T P B r \tag{8}$$

---

[3] A Lyapunov theorem that applies to linear time-invariant systems is as follows. The equilibrium state of equation (3) is asymptotically stable if and only if, given any positive definite matrix Q, P is positive definite. Consider an example in which we have a zero input $(r = 0)$ closed loop system that is critically damped, i.e., $A = \begin{bmatrix} 0 & 1 \\ -1 & -2 \end{bmatrix}$. Selecting positive definite $Q = \begin{bmatrix} 1 & 0 \\ 0 & 1 \end{bmatrix}$ results in positive definite $P = \begin{bmatrix} 3/2 & 1/2 \\ 1/2 & 1 \end{bmatrix}$. The system is therefore asymptotically stable.

It can be shown that $$x^T \lambda_{\min}(P)x \le x^T Px \le x^T \lambda_{\max}(P)x \quad (9)$$

where $\lambda(P)$ denotes an eigenvalue of P. Similarly,

$$x^T \lambda_{\min}(Q)x \le x^T Qx \le x^T \lambda_{\max}(Q)x \quad (10)$$

where $\lambda(Q)$ denotes an eigenvalue of Q. As matrices P and Q are positive definite, their corresponding eigenvalues will be positive.

It follows from equation (10) that

$$x^T Qx \ge x^T \lambda_{\min}(Q)x = \lambda_{\min}(Q)x^T x = \frac{\lambda_{\min}(Q)}{\lambda_{\max}(P)} x^T \lambda_{\max}(P)x \ge \gamma x^T Px = \gamma V(x)$$

where $$\gamma = \frac{\lambda_{\min}(Q)}{\lambda_{\max}(P)}.$$

Thus $$-x^T Qx \le \gamma V(x)$$

Substituting into equation (8)

$$\dot{V}(x) - 2x^T PBr \le -\gamma V(x).$$

Rearranging,

$$\dot{V}(x) \le -\gamma V(x) + 2x^T PBr$$

Taking the norm of the second term on the right hand side, the above inequality will continue to be satisfied. Thus,

$$\dot{V}(x) \le -\gamma V(x) + 2\|PBr\|\|x\|,$$

where $\|x\| = \sqrt{x^T x}$.

From equation (9), it can be shown that

$$\|x\| \le \frac{1}{\sqrt{\lambda_{\min}(P)}} \sqrt{V(x)}$$

It follows that

$$\dot{V}(x) \le -\gamma V(x) + 2\frac{\|PBr\|}{\sqrt{\lambda_{\min}(P)}} \sqrt{V(x)} \quad (11)$$

Terms in the inequality are functions of the sensed state vector x and of the known input r. Note that for $r = 0$ and positive definite $V(x)$, $\dot{V}(x)$ will always be negative definite. Furthermore, for non-zero, bounded input r, the second term in equation (11) will not

increase as quickly as the first term decreases, so $\dot{V}(x)$ will always be negative definite. Thus, the inequality given in equation (11) is a necessary and sufficient condition for stability of the closed loop system.

The inequality given in equation (11) forms the basis of the sensor failure detection scheme. That is, if one or more sensors fail, the inequality will not be satisfied.

Regarding recovery from sensor failures, an observer is utilized [5]. A closed loop observer is an algorithm for estimating the state (x) of the plant. Its inputs are the plant input (u) and the plant output (y). But because the observer's output should track the plant state, and the error in the outputs should drive the observer, it is also possible to think of the observer as having the same basic structure as the plant but with the additional input $y - \hat{y}$.

Thus the observer dynamic equation is given by

$$\dot{\hat{x}} = A_1\hat{x} + Bu + L(y - \hat{y}) \tag{12}$$

where $\hat{x}$ is the state estimate and $\hat{y} = C\hat{x}$. Equation (12) can be rewritten as

$$\dot{\hat{x}} = (A_1 - LC)\hat{x} + Bu + Ly \tag{13}$$

Matrix L is chosen to guarantee stability of the estimator, i.e., such that the eigenvalues of $A_1 - LC$ lie in the left half of the complex plane.

When one or more sensor faults exist, the state estimate provided by the observer may be used to isolate the faulty sensors. Concurrently, Livingstone may be notified that there are faulty sensors.

To summarize, in contrast to the qualitative, static models required by Livingstone, the system component models are quantitative and based upon an ordinary differential description. The new approach complements the qualitative, static models of Livingstone by providing dynamically changing information to it, thus allowing a more accurate diagnosis of component failure, and consequently, more effective control. The new approach also provides a simple scalar inequality test of the integrity of sensors. The results of the inequality test can be transmitted to Livingstone, which can diagnose the possibility of sensor failure.

SUGGESTED EXTENSIONS

Currently, models of components having an inherently discrete nature, such as valves, have been formulated, but models of complex components of the RWGS plant, such as those that perform system chemistry, must yet be developed in a manner utilizable by the autonomous software. If Livingstone does not contain a reactor model,

relating reactants with reactor health, it will be unable to consider the possibility of reactor failure as the potential problem.

Components such as the RWGS reactor and the separable membrane can be described by systems of complex differential and algebraic equations. The challenge is in converting these models to simpler, robust representations that retain their accuracy and to further convert these models toa representation useful to Livingstone.

The electrical engineering department of UCF has a grant from the Florida Space Grant Consortium for addressing the above problems. We plan to work with KSC in completing this project. In taking a team approach, we believe that both Kennedy Space Center and UCF will benefit.

REFERENCES

[1] A description of Livingstone can be found at the following website: http://ic-www.arc.nasa.gov/ic/projects/mba/projects/livingstone.html

[2] Williams, B. and Nayak, P. "A Model-based Approach to Reactive Self-Configuring Systems," *Proceedings* of AAAI-96.

[3] Qu, Z. and Ihlefeld, C. "Fault-Tolerant Robust Control of Nonlinear Systems and Its Application to the Reverse Water Gas Shift Plant for a Mars Mission," to be submitted.

[4] Slotine, J.& Li, W., *Applied Nonlinear Control*, Prentice-Hall, 1991.

[5] Bay, J., Fundamentals of Linear State Space Systems, WCB/McGraw-Hill, 1999.

2000 NASA/ASEE SUMMER FACULTY FELLOWSHIP PROGRAM

JOHN F. KENNEDY SPACE CENTER
UNIVERSITY OF CENTRAL FLORIDA

THERMAL ANALYSIS OF THE NASA INTEGRATED VEHICLE HEALTH MONITORING EXPERIMENT TECHNOLOGY FOR X-VEHICLES (NITEX)

Hisham E. Hegab, Ph.D., P.E.
Assistant Professor
Mechanical Engineering Program
Louisiana Tech University
KSC Colleague - Michael Lonergan, P.E.
Spaceport Engineering & Technology Directorate

ABSTRACT

The purpose of this project was to perform a thermal analysis for the NASA Integrated Vehicle Health Monitoring (IVHM) Technology Experiment for X-vehicles (NITEX). This electronics package monitors vehicle sensor information in flight and downlinks vehicle health summary information via telemetry. The experiment will be tested on the X-34 in an unpressurized compartment, in the vicinity of one of the vehicle's liquid oxygen tanks. The transient temperature profile for the electronics package has been determined using finite element analysis for possible mission profiles that will most likely expose the package to the most extreme hot and cold environmental conditions. From the analyses, it was determined that temperature limits for the electronics would be exceeded for the worst case cold environment mission profile. The finite element model used for the analyses was modified to examine the use of insulation to address this problem. Recommendations for insulating the experiment for the cold environment are presented, and were analyzed to determine their effect on a nominal mission profile.

THERMAL ANALYSIS OF THE NASA INTEGRATED VEHICLE HEALTH MONITORING TECHNOLOGY EXPERIMENT FOR X-VEHICLES (NITEX)

Hisham E. Hegab, Ph.D., P.E.

1. INTRODUCTION

The purpose of the NASA Integrated Vehicle Health Monitoring (IVHM) Technology Experiment for X-vehicles (NITEX) is to advance the development of selected IVHM technologies in a flight environment and to demonstrate the potential for reusable vehicle ground processing savings. Life-cycle costs for reusable space transportation vehicles are dominated by the cost of processing, operating, and maintaining the vehicle and the time required turning the vehicles around between missions. The objective of the NITEX flight experiment is to demonstrate the costs and benefits of an IVHM system. The experiment will provide real-time fault detection and isolation and suggest potential recovery actions of the X-34 vehicles throughout all mission phases. The experiment consists of a lightweight low power microelectronics data acquisition and processing platform with cabling linking to the X-34 flight and utility computers for passive monitoring of the vehicle command and data streams. The experiment interfaces to a ground computer via RF through the flight computer as well as direct connection when access is available. The experiment is activated by the flight computer using a pre-programmed command based on a mission elapsed time while the X-34 vehicle is still captive on the L1011. Processed system health data is internally recorded throughout captive carry, drop, engine burn, coast, propellant dump and autonomous approach and landing phases. Once installed, it is planned to refly the experiment through completion of the X-34 Program. IVHM technologies demonstrated by this experiment provide the potential for cost savings in vehicle maintenance by more efficient maintenance and turnaround processing and enhanced safety and reliability through better real-time visibility into system health.

This project report provides a thermal analysis of the NITEX experiment package for various possible mission profiles to determine if operating temperature limits for the experiment microelectronics would be exceeded. A finite element model of the NITEX experiment package, mounting interface, and honeycomb panel support structure for the experiment was constructed using ANSYS©, a commercial finite element analysis software package. A transient thermal analysis of the entire mission profile from ground operations before and after liquid oxygen loading, climb to captive carry, captive carry, and vehicle flight and reentry have been investigated to determine the most likely mission scenarios to provide the most extreme hot and cold environments for the NITEX experiment.

2. NITEX DESCRIPTION AND THERMAL ENVIRONMENT

The microelectronics for the NITEX experiment are contained in a ½-ATR conduction cooled box as shown in Figure 1. The ATR box dimensions are 13.25 cm x 17.49 cm x 33.15 cm. The microelectronics contained in the ATR box consist of a computer printed circuit board (PCB)

card, a power supply unit (PSU), a flash memory unit (FMU), and associated cabling and connectors. The ½-ATR box is side mounted onto a removable honeycomb panel using a mounting plate. The removable panel is mounted directly in the experiment bay of the X-34. The experiment bay is located in the strake of the X-34 wing and is adjacent to a liquid oxygen tank. Consequently, the thermal environment for the bay is fairly extreme. All experiment packages are required to provide their own thermal protection from the expected extremes of the environment. Table 1 lists expected internal experiment bay extreme temperatures for the inner skin surface (wall) and the ambient environment (environment) temperatures in the bay.

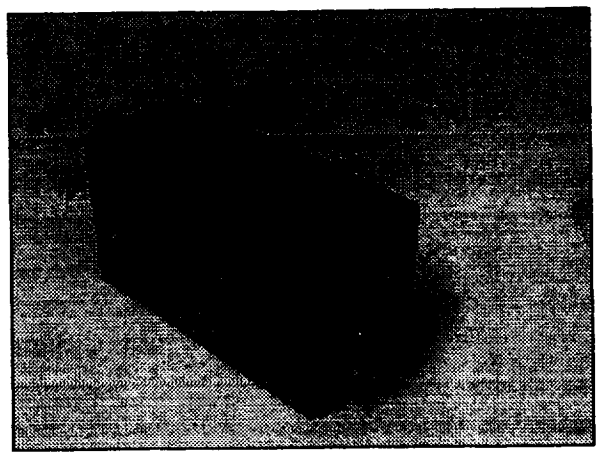

Figure 1. NITEX ATR

Table 1. Thermal environment of X-34 experiment bay.

Mission Phase	Minimum Temperature (°C)		Maximum Temperature (°C)	
	Environment	Wall	Environment	Wall
Ground Operations	-51.1	-34.4	52.8	54.4
Captive Carry	-67.8	-63.3	-45.6	-13.9
Ascent & Reentry	N/A	-6.7	N/A	80.6

The wide range of experiment bay temperatures for ground operations are a results of conditions before and after liquid oxygen loading. The expected maximum temperatures correspond to a hot day before liquid oxygen loading while the expected minimum temperature correspond to a cold day after liquid oxygen loading. Ambient environment temperature are not provided for ascent and reentry mission phases since the vehicle ascends to a peak altitude of 250,000 ft. Possible mission profiles for the X-34 were reviewed to determine the most likely extreme thermal environment mission profiles for the experiment bay. From this review, it was determined that ground operations before liquid oxygen loading on a hot day would provide the most extreme hot environment. The maximum bay temperature during ascent and reentry is higher than that for ground operations but the length of ascent and reentry is only approximately 15 minutes for the X-34. This brief exposure to a high wall temperature occurs after approximately a one hour exposure to the captive carry environment conditions (low temperature) so it was determined that this would not significantly affect the NITEX experiment due to its thermal capacity. Overheating during ground operations before liquid oxygen loading can be avoided simply by not turning on the NITEX experiment until liquid oxygen loading begins. An analysis was performed to determine the maximum time the experiment could be turned on before liquid oxygen loading just in case it would become necessary to do this.

From the review of the possible mission profiles, the most extreme cold environment would occur on a mission abort after a long captive carry of the vehicle. The transient variation of the environment and wall temperatures in the experiment bay for this scenario are shown in Figure 2.

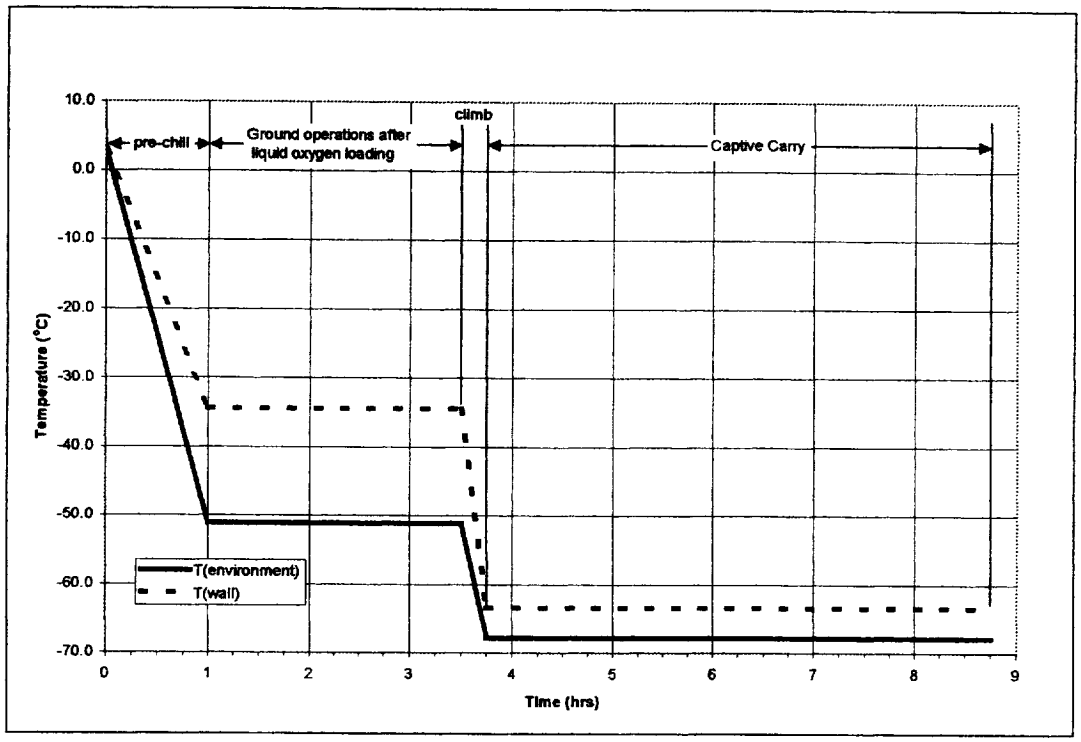

Figure 2. Extreme cold environment mission profile for experiment bay.

3. FINITE ELEMENT MODEL

A finite element model of the ATR box, PCB, PSU, FMU, mounting plate, and removable honeycomb panel that the NITEX experiment is mounted to in the experiment bay was created for the thermal analysis. The finite element mesh used in the analyses are shown in Figure 3 and Figure 4 for an uninsulated and an insulated ATR box, respectively. Shell elements were used to represent the walls of the ATR box, the PCB card, and the PSU. Solid brick element were used to represent the mounting plate for the ATR box, the removable honeycomb panel, and insulation added to the exterior of the ATR box. A thermal mass element is used to represent the FMU and it is thermally connected to the upper surface of the ATR box through thermal resistance links that represent the screws connecting the FMU to top surface of the ATR box. Thicknesses for the shell elements were determined from drawings of the ATR box. The ATR box is made of aluminum. Variations in the walls such as board mounting interfaces or connector slots result in the total mass predicted using the density of aluminum to over predict the actual mass of the ATR box. Consequently, the density the ATR box material was slightly reduced to accurately represent the measured total mass of the box. Properties of aluminum with adjustments to densities were also used to approximate the PCB card and PSU since both of these have an

aluminum core for mounting and thermal dissipation to the ATR box. Constant, isotropic properties are used for the thermal conductivity, density, and specific heat of the ATR box, PCB card, PSU, and the mounting plate. Constant, anisotropic properties are used for the thermal conductivity of the honeycomb removable panel. These directional properties for the thermal conductivity were calculated using a technique described by Gilmore [1]. Table 2 lists material properties used in the finite element model.

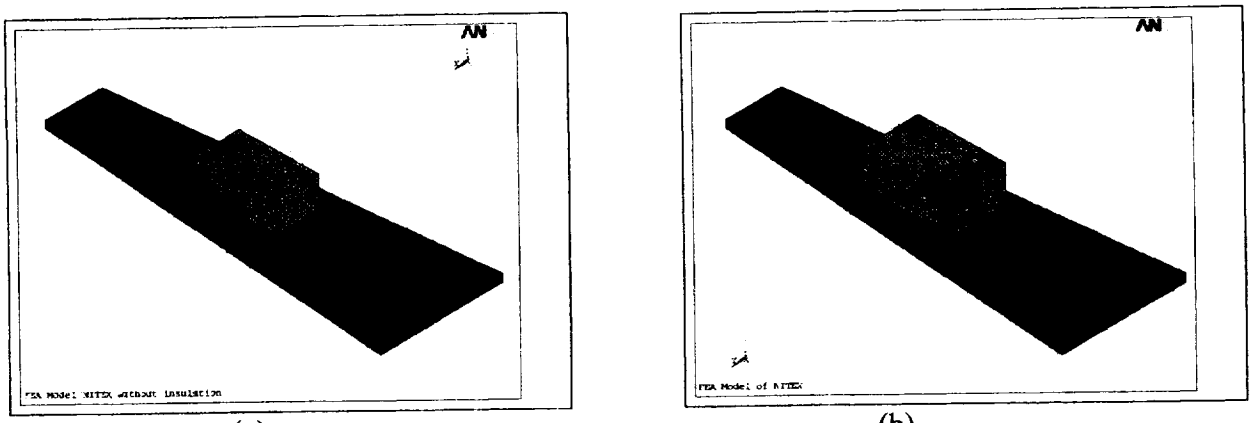

(a) (b)

Figure 3 Finite element model of NITEX experiment (a) without insulation (b) with insulation.

Table 2. Material properties used in FEM model.

Component	Material	Density (g/cm^3)	Specific Heat (J/g-K)	Thermal Conductivity (W/cm-K)
ATR Box	Aluminum	2.62	0.8792	1.80
PCB	Aluminum	2.62	0.8792	1.80
PSU	Aluminum	3.44	0.8792	1.80
Mounting Plate	Teflon	2.2	1.50	0.003
Insulation [2]	Polyurethane foam	0.032	1.045	0.00021
Removable Panel	Aluminum honeycomb with graphite/epoxy face sheets	0.344	1.147	$k_{x,y} = 0.028$, $k_z = 0.0175$

The expected total power dissipation for the NITEX experiment is 30 W. The power supply unit has a quoted efficiency of 67%. This results in 10 W being dissipated in the PSU and 20 W dissipated in the PCB and FMU. From the FMU specifications, it was estimated that approximately 1 W will be dissipated in the FMU so it was assumed that 19 W would be dissipated in the PCB. The power dissipations in the PCB and PSU were treated as heat fluxes applied to the shell elements representing these components. The FMU power dissipation was treated a nodal heat load on the thermal mass node representing the FMU.

In an initial analysis, convection and radiation boundary conditions from the exterior of the ATR box and the top and bottom surfaces of the removable panel were used. Convection boundary conditions used the transient environment temperature for the experiment bay (see Fig. 2) as the bulk fluid temperature. Ranges of convection coefficients for horizontal and vertical surfaces were calculated based upon the expected conditions in the experiment bay. Convection coefficients were also calculated at sea level as well as 39,000 ft which is the expected altitude for the captive carry portion of the mission profile. Ranges of the convection coefficients are listed in Table 3. The convection coefficients were made a function of time in the FEM since the altitude of the X-34 directly coincides with the mission timeline. To provide a conservative analysis, the upper range of the convection coefficients were used for the extreme cold environment analysis and the lower range of values were used for the extreme hot environment analysis. Mid-range values were used for analyzing a nominal mission profile.

Table 3. Expected range of convection coefficients.

Surface	Convection Coefficients (W/m^2-K)	
	Sea level	39,000 ft
Top of ATR Box	4.3 - 6.0	2.0 - 2.5
Sides of ATR Box	3.5 - 4.0	1.6 - 2.0
Top of removable panel	3.5 - 5.0	1.5 - 2.5
Bottom of removable panel	1.7 - 2.5	0.8 - 1.5

Radiation boundary conditions used a space node to represent the surroundings for the enclosure and the transient wall temperature for the experiment bay (see Fig. 2) was applied to this node. An emissivity of 0.9 was used for all painted surfaces. In cases where a reflective tape ($e \approx 0.05$) was used on surfaces, radiation from those surfaces were neglected. The radiosity method in ANSYS© [3] was used for performing radiation calculations in the enclosure.

4. RESULTS AND DISCUSSION

As previously mentioned, overheating of the NITEX experiment may be avoided by simply not turning the experiment on until after liquid oxygen loading during ground operations. Consequently, the extreme cold environment was simulated first to determine if the allowable operating temperature range of the microelectronics would be broken. Transient temperature profiles for the PCB and PSU thermal interfaces, the FMU, and the bottom surface of the ATR box are shown in Fig. 4. The allowable operating temperature limits for PCB, PSU, and FMU are –40°C to +75°C. From this initial analysis it was determined that the box needs to be insulated. From examining a variety of insulating materials and analyzing various thicknesses of insulation, it was determined that using a 2.54 cm (1 in.) thick sheet of teflon for the mounting plate would provide an adequate insulating barrier between the ATR box and the removable panel. It was also determined that insulation needs to be added to the exposed surface of the ATR box. A 2.54 cm (1 in.) thick layer of polyurethane foam insulation was added to all exterior surfaces except for one end where several connectors are located. In addition, low emissivity reflective tape is placed on the surface of the insulation to minimize radiation heat

transfer. These modifications were then analyzed for the extreme cold environment, extreme hot environment, and a nominal mission environment for the experiment bay.

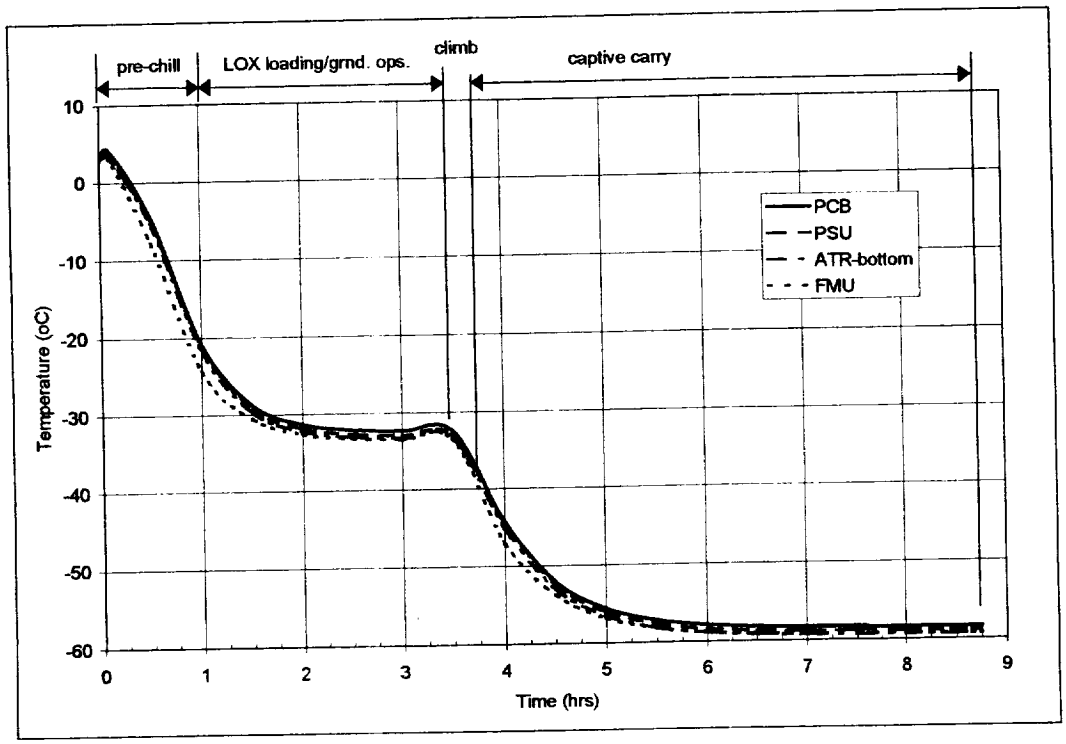

Figure 4. Transient temperature profile of uninsulated ATR box for extreme cold environment

The transient temperature profile for the PCB and PSU thermal interfaces, FMU, and the bottom surface of the ATR box are shown in Fig. 5 for the case of an extreme cold thermal environment described by Fig. 2. All of the temperature profiles follow each other rather closely since the box is very conductive. The temperatures are within the specified operating limits, but there is a very small margin of safety (2-3°C) near the end of the mission timeline. Any reductions in expected power dissipations or environmental conditions would need to be examined closely. The transient temperature profiles for the extreme hot thermal environment are shown in Fig. 6. In this case, the environmental and wall temperatures remain constant at 52.8°C and 54.4°C, respectively. From examining the results, the upper allowable operating temperature (+75°C) for the PCB is exceeded near the end of the simulation. It is recommended that the experiment only be powered for a maximum of two hours before liquid oxygen loading. The simulations examined in Fig. 5 and Fig. 6 represent extreme conditions that may occur in the X-34 experiment bay. An additional simulation was performed to examine the expected operating conditions for a nominal mission profile. This nominal mission profile consists of a one hour pre-chill phase, a one hour liquid oxygen loading phase, a one-half hour ground operations and taxi phase, a one-quarter hour climb to captive carry altitude, a one and quarter hour long captive carry phase, and a quarter hour flight and reentry phase. The expected thermal environment for the experiment bay for this nominal mission profile is shown in Fig. 7. The environmental

conditions is this case are not nearly as extreme as the others. A simulation of the insulated ATR box, shown in Fig. 8, demonstrates that the PCB, PSU, and FMU all remain within a range of 20°C to 45°C for a nominal mission profile. This temperature range is well within the required operating limits of the electronics.

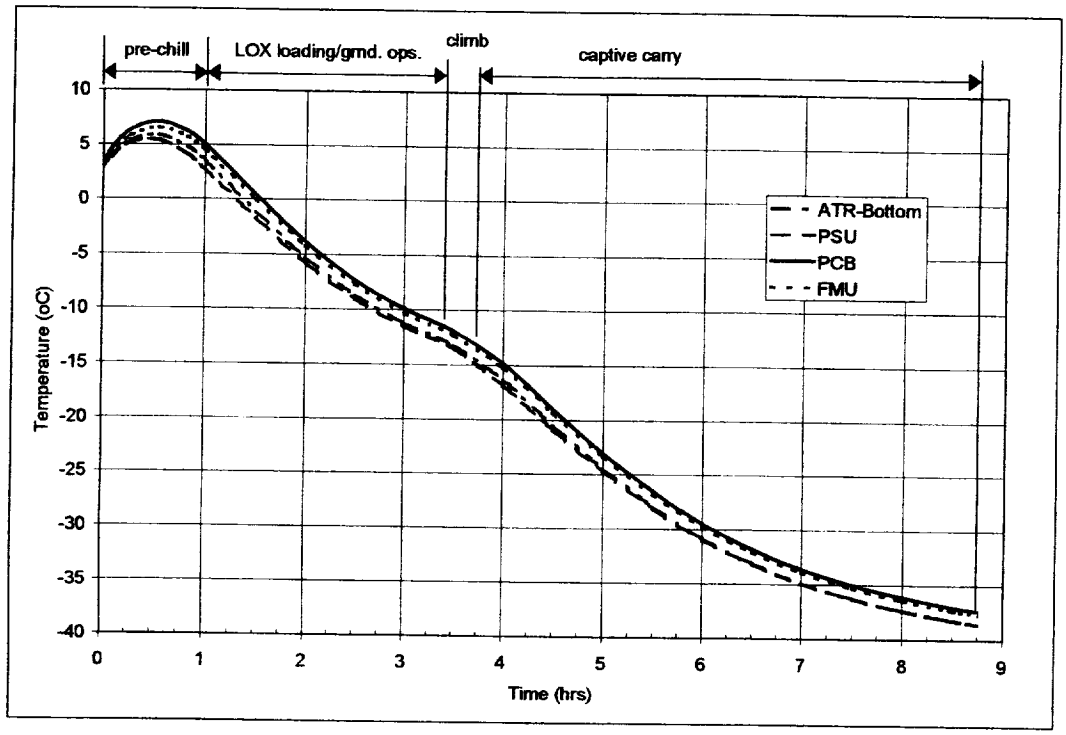

Figure 5. Transient temperature profile of insulated ATR box for extreme cold environment

5. CONCLUSIONS

A thermal model using finite element analysis was developed to predict the thermal condition of the NITEX experiment on the X-34. Simulations were performed to represent the worst expected hot and cold environment in the experiment bay where the NITEX would be mounted. Initial analyses revealed that the lower operating limits of the electronics would be exceeded. Subsequently, the model was modified to include insulation around the surface of the ATR box and an insulating layer of teflon between the ATR box and experiment bay mounting panel. Results from analyzing the expected extreme hot and cold environments demonstrated that the electronics would remain within the required operating limits subject to the assumed power dissipations and operating conditions. The cold environment simulation indicates that there is a very small margin of a few degrees Celsius from exceeding the lower operating limit of the electronics at the end of the mission profile. The assumed conditions for the simulation are based upon current expectations of the extreme temperatures in the experiment bay which may be relaxed upon obtaining experimental data on thermal environment of the bay. The hot environment simulation indicates that it should be safe to operate the NITEX experiment for

approximately two hours during ground operations on a hot day before pre-chill to liquid oxygen loading. A simulation of a nominal mission profile was also performed and indicates that the electronics within the NITEX experiment should remain well within their specified operating limits. All of the simulations presented are subject to the assumed environmental conditions, mission profile timelines, and estimated power dissipations. Any changes in these variables could significantly alter the predicted transient temperature profiles for the NITEX components.

ACKNOWLEDGEMENTS

I would like to express my sincere appreciation to my NASA-KSC colleague Mike Lonergan for his help and useful suggestions during this summer. I would also like to thank Ray Hosler, Cassie Spears, and Greg Buckingham for their efforts in supporting the Summer Faculty Fellowship Program at KSC. I have learned much about the center and its goals and operations during this program. Many thanks to everyone who help make this summer an enjoyable and professionally interesting experience.

REFERENCES

1. Gilmore, D. G., Satellite Thermal Control Handbook, The Aerospace Corporation Press, El Segunda, CA, 1994.
2. Augustynowicz, S. D., Fesmire, J. E., and J. P Wikstrom, Cryogenic Insulation Systems, 20th International Congress of Refrigeration, IIR/IIF, Sydney, 1999.
3. ANSYS© Theory Reference, Release 5.6, 11th ed., SAS IP, Inc., 1999.

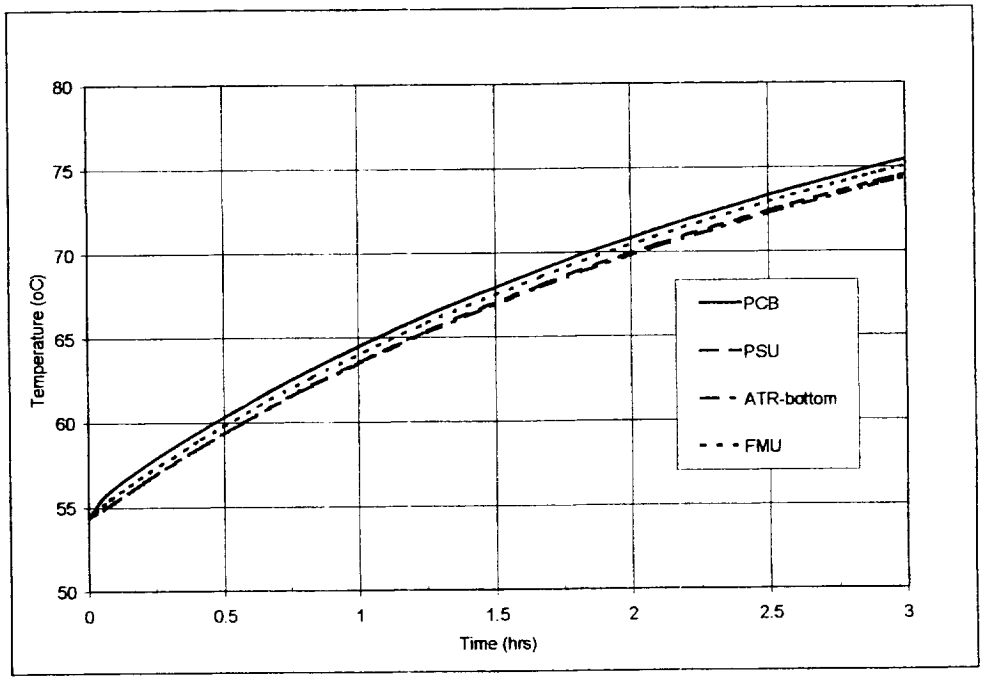

Figure 6. Transient temperature profile for insulated ATR box for extreme hot environment

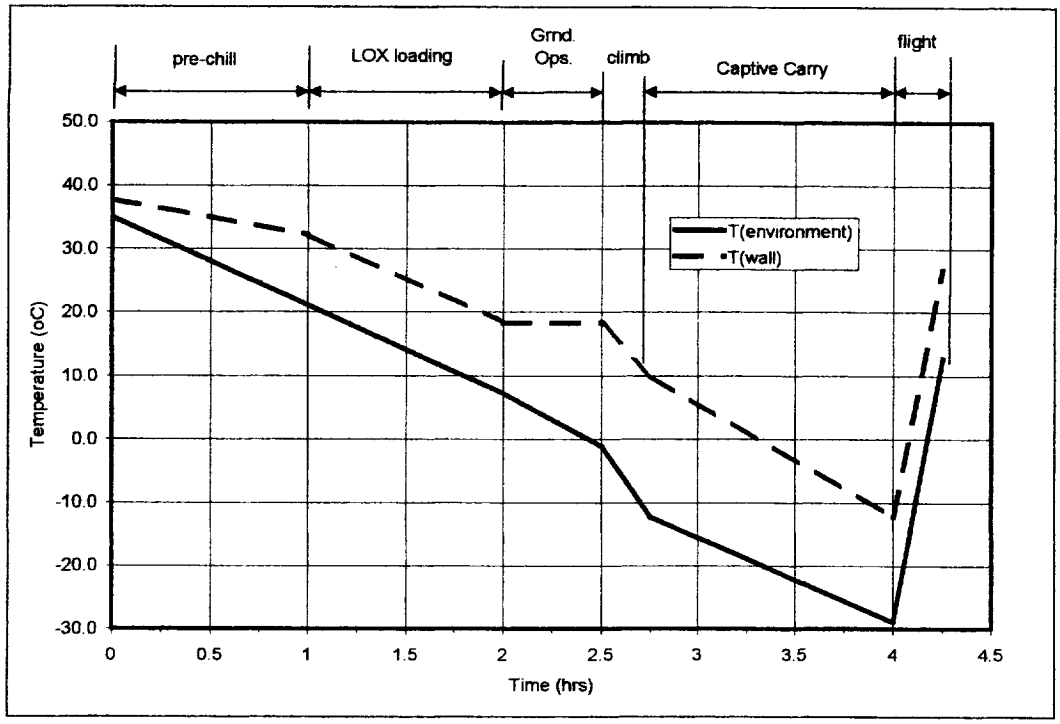

Figure 7. Thermal environment for a nominal mission profile

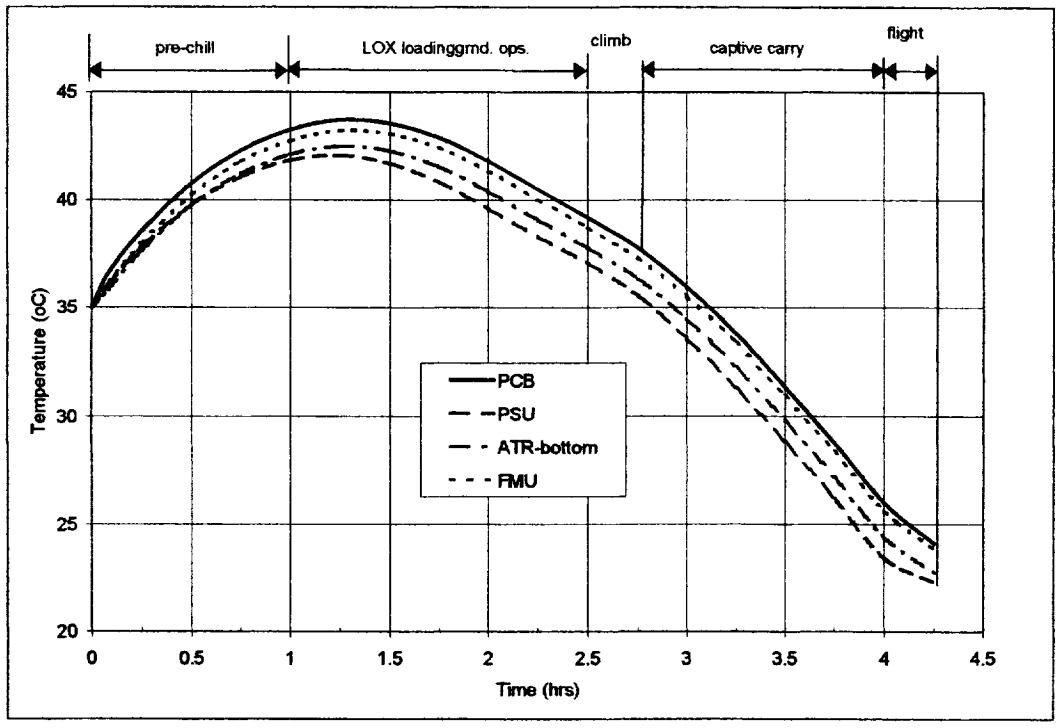

Figure 8. Transient temperature profile of insulated ATR box for nominal mission profile

5/0/cw/11/20

NASA/ASEE SUMMER FACULTY FELLOWSHIP PROGRAM

JOHN F. KENNEDY SPACE CENTER
UNIVERSITY OF CENTRAL FLORIDA

CORROSION RESEARCH AND WEB SITE ACTIVITIES

Robert H. Heidersbach
Professor and Department Chair
Materials Engineering Department
California Polytechnic State University
Louis MacDowell-KSC Colleague

ABSTRACT

This report covers corrosion-related activities at the NASA Kennedy Space Center during the summer of 2000. The NASA Kennedy Space Center's corrosion web site, corrosion.ksc.nasa.gov, was updated with new information based on feedback over the past two years. The methodology for a two-year atmospheric exposure testing program to study the effectiveness of commercial chemicals sold for rinsing aircraft and other equipment was developed and some preliminary laboratory chemical analyses are presented.

1. Introduction

This project had two parallel efforts, the refinement of the existing NASA KSC corrosion web site, corrosion.ksc.nasa.gov, and research efforts to start a testing program to evaluate commercial chemicals sold for use as additives to the rinse water for aircraft and other equipment. The two efforts are discussed separately below.

2. KSC Corrosion Web Site

The NASA KSC corrosion web site, corrosion.ksc.nasa.gov was extensively revised during a previous NASA/ASEE summer faculty fellowship in 1998. The purposes of that development were to provide a useful, informative site that would educate the general public and NASA personnel about corrosion. Another purpose of the web site was to publicize the availability of the NASA KSC corrosion facilities for use by outside government and other parties.

One test of the "visibility" of a web site is the ranking it receives from various browsers. The Kennedy Space Center corrosion web site was developed so that the home, or index, page would be picked up by various search engines and be made available to interested parties searching under the term "corrosion." At the start of the summer 2000 efforts the visibility of the site was tested by searching under "corrosion" under several widely-used browsers and the KSC site was generally the first government agency site to be ranked by these browsers—to include Google and other browsers that did not exist in 1998 when the site was developed. The site was deemed "adequately" visible and efforts to upgrade the site focused on other aspects.

Over the past two years hundreds of inquiries have been received as a result of the web site. Recent inquiries were examined for trends in the questions being asked, and these were used for guidance on the summer 2000 site development. The work during summer 2000 focused on the following:

Appearance of the pages: The appearance of the new site can be contrasted to the 1998 site by comparing the two similar pages below:

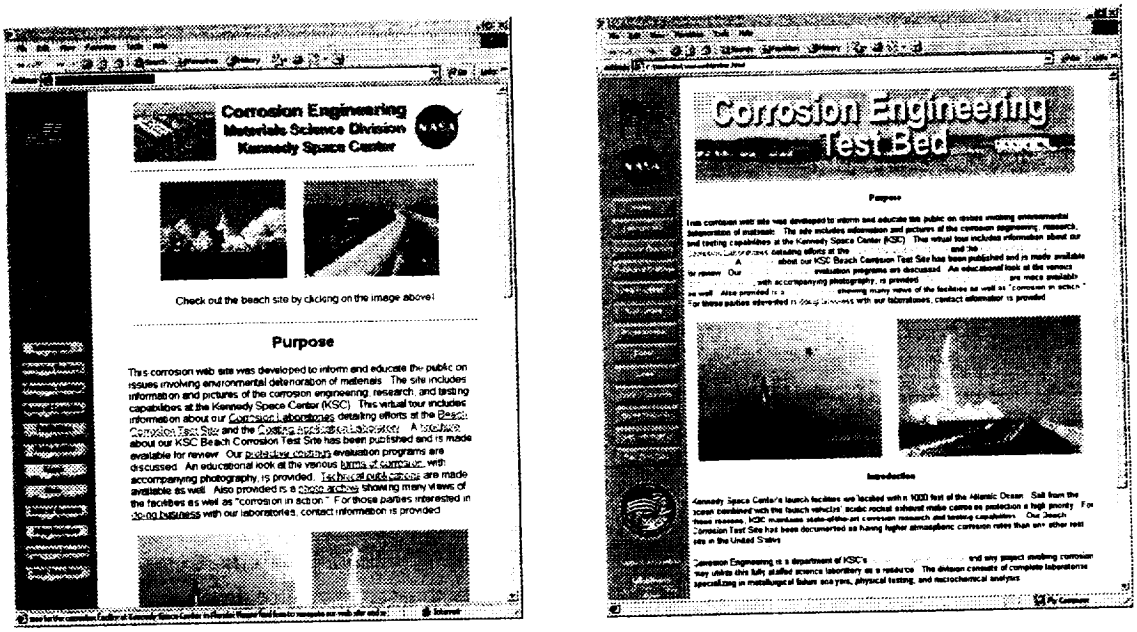

Figure 1: Comparison of the NASA KSC corrosion web site home pages from 1998 (left) and 2000 (right).

The new site has fewer colors in the outline, improved graphics on the heading, and loads faster on the major browsers.

Examples of industrial corrosion: Several examples of corrosion from industrial sites not related to NASA were added. The purposes of these additions were to improve the relevance of the NASA site to the general website user. Corrosion examples from elsewhere are also useful for NASA users, because they can compare what they see on the web with what they observe on NASA equipment.

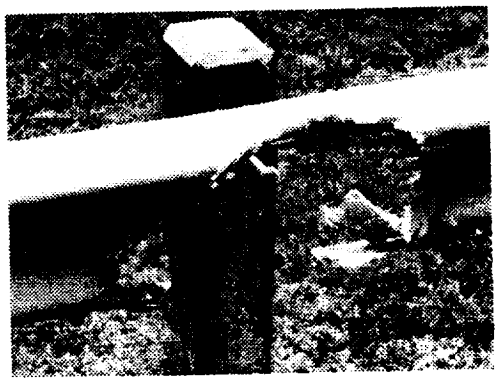

Figure 2. Intergranular corrosion of aluminum guard rail at Patrick Air Force Base.

Figure 2 shows the corrosion of a guard rail along Highway A!A at Patrick Air Force Base. This is just one example of corrosion included on the web site from sources not associated with NASA.

Corrosion fundamentals: Many inquiries have been received over the past two years for more information on corrosion fundamentals. These were incorporated into the web site by adding sections on the chemistry and electrochemistry basics—information useful to school children using the web site for science projects and for midcareer professionals who need brushing up on their chemistry knowledge.

Corrosion control: The following forms of corrosion control are briefly explained on the web site:

Design
Materials Selection
Protective Coatings
Inhibitors and other means of environmental alteration
Corrosion allowances
Cathodic Protection

3. Chloride rinse agent research

The U. S. Army has signed a Space Act agreement and contracted with the NASA Kennedy Space Center to conduct research and testing on commercially-available chemicals sold as additives to the rinse water used to clean helicopters and other equipment after deployment, during depot storage, and during shipment to remote operational locations.

Prior to the summer of 2000 four commercial chemical agents were selected for a two-year test at the NASA Kennedy Space Center beachside atmospheric corrosion site.

Efforts started during this summer will continue for a two year exposure program schedule to start in September 2000.

Preliminary efforts involved developing cleaning methods to insure sample uniformity prior to exposure, developing the rinsing protocol to be used during the weekly rinsing of the samples at the beach corrosion site, and chemical analysis of the commercial agents to determine their composition.

The chemical analyses are too preliminary to report in any detail in this report, but they do indicate that most of the agents contain surfactants—supposedly intended to reduce the viscosity of the diluted liquids and make them able to dissolve chemicals from crevices and other tight areas on equipment surfaces. One of the agents is approximately 3½% sodium fluoride—i.e. it seems to

substitute the fluoride ion for the more common chloride ion. Whether this is achieved or not remains to be determined, but there is no reason to think that substituting one halide ion for another would lower corrosion rates.

Ongoing work: The efforts on this project are part of a multiyear research project involving a two-year atmospheric testing program and associated evaluations of the chemicals and alloys tested.

Efforts will continue during the coming academic year on determining the most efficient ways of chemically analyzing surfactants, testing salt levels on exposed metal surfaces, and electrochemically monitoring corrosion rates of atmospherically-exposed metal samples. Dynacs, Inc, at KSC and DACCO Scientific in Maryland are cooperating with the authors of this report on these multiyear efforts.

4. Acknowledgements:

Louis MacDowell was the NASA Kennedy Space Center colleague who identified this project and secured the funding from the United States Army to conduct this work. J. Curran of Dynacs Incorporated did the preliminary work on this project and continues to direct the KSC efforts. G. Lillich, a Cal Poly materials engineering student did the programming of the web site and supplied many of the photographs for use on both the web site and the chloride rinse agent project.

In addition to the above-listed direct participants, we would like to acknowledge the support of G. Buckingham, NASA, and R. Hosler and C. Spears in the UCF NASA-ASEE program office.

Additional technical support and information was provided by:

W. Marshall and J. Palou, NASA—chemical analses and consulting
R. Springer and P. Read—corrosion technician support
S. Murray, V. Cummings, P. Faughan, P. Marciniak, S. McDanels, and D. Parker, NASA—interdisciplinary materials ideas
L. Levine, DYNAMAC—surfactant expertise
P. Stanstead and P. Bryden, United Space Alliance—insight into testing on other systems J. Martin and A, Webb—Naval Research Laboratory—information on Navy testing of similar chemicals

2000 NASA/ASEE SUMMER FACULTY FELLOWSHIP PROGRAM

JOHN F. KENNEDY SPACE CENTER
UNIVERSITY OF CENTRAL FLORIDA

Extending the Capability of Mars Umbilical Technology Demonstrator

Nasser Houshangi, Ph.D., P.E.
Associate Professor of Electrical Engineering
Department of Engineering
Purdue University Calumet

NASA/KSC Colleague: Thomas Lippitt
Mechanical System Branch

ABSTRACT

The objective of this project is to expand the capabilities of for the Mars Umbilical Technology Demonstrator (MUTD). The MUTD shall provide electrical power and fiber optic data cable connections between two simulated mars vehicles, 1000 m apart. The wheeled mobile robot Omnibot is used to provide the mobile base for the system. The mate-to umbilical plate is mounted on a Cartesian robot, which is installed on the Omnibot mobile base. It is desirable to provide the operator controlling the Omnibot, the distance and direction to the target. In this report, an approach for finding the position and orientation of the mobile robot using inertial sensors and beacons is investigated. First phase of the project considered the Omnibot being on the flat surface. To deal with the uneven Mars environment, the orientation as well as position needs to be controlled. During local positioning, the information received from four ultrasonic sensors installed at the four corner of the mate-in plate is used to identify the position of mate-to plate and mate the umbilical plates autonomously. The work proposed is the continuation of the principal investigator research effort as a participant in the 1999 NASA/ASEE Summer Faculty Fellowship Program.

1. Introduction

The ability to quickly and reliably mate and de-mate umbilical connections under automated control is needed in flights to mars. After review of mars reference mission [12], three umbilical (i) electrical power/fiber optic data cable umbilical; (ii) mars rover cryogenic servicing umbilical; and (iii) contingency in-situ propellant production water supply umbilical were identified. The electrical power/fiber optic data umbilical is mission critical since it must provide immediate power to the hab/crew vehicle and was chosen for a technology demonstration project.

The Mars Umbilical Technology Demonstrator (MUTD) shall provide electrical power and fiber optic data cable connections between two simulated mars vehicles (hab/lab vehicle and cargo vehicle) spaced 1 Km apart. The MUTD shall deploy 1 Km of electrical and fiber optic cables from the simulated hab/lab to the simulated cargo vehicle. The MUTD shall autonomously align the surface and the vehicle umbilical plates and parallel mate the connectors in an accurate manner.

The problem of automated umbilical mating is divided into two subproblems, global and local positioning. The global positioning is defined as when the two umbilical plates do not have any vertical common projection on each other, and the problem is to bring them close enough such as they do. If two plates are closer than 14 inches apart and have any common vertical projection on each other, to mate them from now on is refereed to as the local positioning problem.

Toward the completion of the phase 1, the teleoperated Omnibot picked up the cable reel using visual information, transported it 100 m, and placed the umbilical plates in the local positioning zone. Then, the operator switched the system to the autonomous mode. The umbilical positioning and mating performed autonomously. The demo of the system was successful and verified the approach.

The objective of the work presented in this report is to expand the MUTD capability. The operator navigates the mobile robot toward the target during global positioning. One problem especially on rough terrain is to guide the operator toward the target. The usual questions that need to be answered for the navigation are "where am I?", "where am I going", and "how should I get there?". The local visual information, which is provided to the operator, is not sufficient for navigating the Omnibot toward the target. The distance and direction to the target should also be provided to the operator.

As mentioned, the crew vehicle will land within 1 km of the cargo vehicle. It is reasonable to assume that the position of crew vehicle after landing and the cargo vehicle is known with respect to a world coordinate frame. The initial assumed known position and orientation of the Omnibot would also be calibrated with respect to world coordinate frame. Therefore, Omnibot initially knows where she is and also where it needs to go. The question is how to keep track of the Omnibot position during motion.

In the first phase of the project, the umbilical mating occurred during local positioning when the Omnibot was on a flat surface. Considering rough terrain, the orientation also needs to be controlled as well as the position for autonomous mating as discussed in this report. Mobile robot position and orientation determination for navigation on a rough terrain during global positioning is presented in section 2. In section 3, the autonomous local positioning problem is explained, and conclusion follows in section 4.

2. Navigation on Rough Terrain

As indicated, the wheeled mobile robot Omnibot is controlled in the teleoperated mode during global positioning. The operator needs the direction and distance to the target especially, when the target is not in the line of sight of the vision system. The optimal direction is defined to indicate the direction for the shortest path to arrive at the target. This information is calculated based on the Omnibot and the known cargo vehicle positions. Of course the operator may prefer to take different path (directions other than optimal direction), for example to avoid obstacles like steps, boulders, and craters.

To provide the position and orientation of the mobile robot with respect to the world coordinate frame, different coordinate frames are assigned. The mobile vehicle coordinate system is selected so that x is forward, lateral is y, and z is vertical up. Its origin is located at the kinematics center of the Omnibot in (x, y) and on the ground plane in the z direction. The initial position and orientation of mobile vehicle coordinate frame is refereed as vehicle reference coordinate frame. The sensor coordinate frame is defined at the center of the sensor with the same orientation with a displacement of d from vehicle coordinate frame. The world coordinate frame is attached to the simulated crew vehicle.

The position and orientation of the vehicle defined by the vector $P(kT) = [p(kT), \gamma(kT)]^T$ at time step kT, where k is a positive integer, and T is the sampling period. For simplicity T is dropped from notation after this point. The vector $p(k) = [p_x(k), p_y(k), p_z(k)]^T$ specifies the Cartesian position, and the vector $\gamma(k) = [\phi(k), \psi(k), \theta(k)]^T$ defines the orientation where $\phi, \psi, and\ \theta$ correspond to roll, pitch, and yaw angles, respectively. The position vector P(k) is updated during Omnibot motion.

The vehicle position p(k) is estimated incrementally by

$$p(k) = f[p(k-1), u(k)] = p(k-1) + R_{\phi,\psi,\theta}\ v_o(k)T \tag{1}$$

Where $v_o(k) = [v_x(k), v_y(k), v_z(k)]^T$ is the vehicle velocity in the vehicle coordinate system, and $R_{\phi,\psi,\theta}$ denotes the rotational transformation matrix from the vehicle coordinate system to the vehicle reference coordinate system:

$$R_{\phi,\psi,\theta} = \begin{bmatrix} c\phi & -s\phi & 0 \\ s\phi & c\phi & 0 \\ 0 & 0 & 1 \end{bmatrix} \begin{bmatrix} c\psi & 0 & s\psi \\ 0 & 1 & 0 \\ -s\psi & 0 & c\psi \end{bmatrix} \begin{bmatrix} 1 & 0 & 0 \\ 0 & c\theta & -s\theta \\ 0 & s\theta & c\theta \end{bmatrix} \tag{2}$$

For a wheeled robot, odometry is one of the important means of achieving the robot position p(k). Optical encoders mounted on drive wheels feed discretised wheel increments information to a processor, which continually updates the robot's position using the geometric equations. Odometry errors can be classified as being systematic or non-systematic [1]. The dominant sources for systematic error are identified as the difference in wheel diameter, the uncertainty about the effective wheel's base, the misalignment of wheels, and discretised sampling of wheel increments. Causes of nonsystematic errors are travel over rough terrain, wheel slippage, and floor roughness. Accumulation of orientation errors will usually cause large positional errors, which increase unbounded with the distance traveled by the vehicle. Therefore, the current direction and length of the path traveled can't be measured accurately using odometry especially for outdoor uneven environments.

Different approaches are used to overcome the problem with odometry as indicated in the literature [2-10]. One approach is to use the inertial systems, and the other being the use of landmarks or beacons as described in sections 2.1, and 2.2, respectfully.

2.1 Inertial Systems

Inertial navigation systems are self-contained and non-jammable. Complete inertial system for mobile robots application may contain three-axis accelerometer, a three-axis gyroscope, and roll and pitch inclinometers. Accelerometer measures acceleration along a single axis. Integrate the output once, and you have velocity. Integrate again, and you have relative position, or rather, change of position along the accelerometer's axis. If you know the direction of travel, you can deduce the current position. Gyroscopes measure rotational rate, which can be integrated to yield changes in orientation. Inclinometer provides the tilt information with respect to the x-y plane. The information obtained from these sensors may be used to cancel the gravity component projecting on each axis of accelerometer while vehicle is stationary.

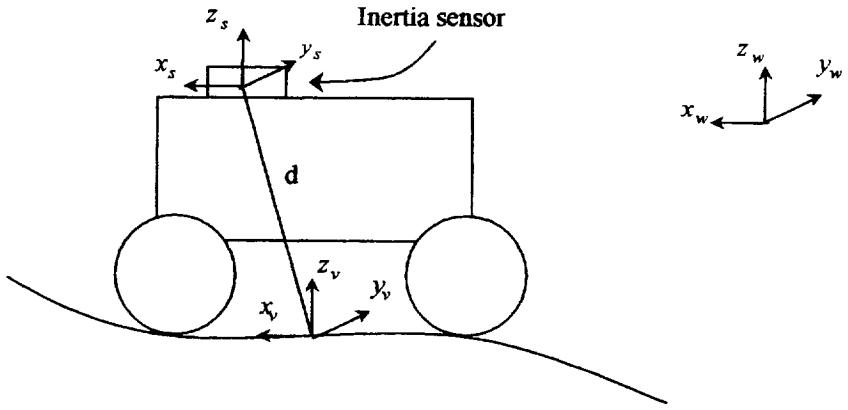

Figure 1: Coordinate frames assigned for the system

The measurements taken from rate output of the gyros, and the accelerometer are represented by:

$$\begin{bmatrix} G_x(k) \\ G_y(k) \\ G_z(k) \end{bmatrix} = \begin{bmatrix} \dot{\theta}(k) \\ \dot{\psi}(k) \\ \dot{\phi}(k) \end{bmatrix} + \begin{bmatrix} n_1(k) \\ n_2(k) \\ n_3(k) \end{bmatrix} \tag{3}$$

$$\begin{bmatrix} A_x(k) \\ A_y(k) \\ A_z(k) \end{bmatrix} = R^{-1}_{\phi,\psi,\theta} \begin{bmatrix} a_x(k) \\ a_y(k) \\ g \end{bmatrix} + \begin{bmatrix} n_4(k) \\ n_5(k) \\ n_6(k) \end{bmatrix} \tag{4}$$

Where the $G_x(k), G_y(k), G_z(k)$, and $A_x(k), A_y(k), A_z(k)$ corresponds to gyroscopes and accelerometer sensor readings, respectfully; a_x, a_y and g are the accelerations of the mobile robot in the vehicle reference coordinate frame; n_i, i=1...6 is the added white noise.

Tilt sensors provide more accurate angular information than the gyroscopes when the robot is not accelerating. As was suggested in [4], the output of Gyroscopes are reset by the output of tilt sensors whenever the absolute value of all acceleration component are less than a prefixed threshold determined by the noise level of the accelerometer outputs. Let β_x and β_y be the angles measured by the dual-axis tilt sensor lying along x, and y-axes with respect to the horizontal plane. The roll and pitch angles is calculated as follows:

$$\theta = \beta_x \tag{5}$$

$$\psi = \frac{\beta_y}{\cos\beta_x} \tag{6}$$

Inertial system provides the relative position and orientation of the mobile robot. It is widely understood that the foremost problem with gyros is their "bias-drift". Although, the drift rate for fiber optic gyros is very low which makes it suitable to mobile robot applications. The KVH E-core 2000 model RD 2030 is used in our system with the technical specification shown in table 1. Position estimation using accelerometer information is also susceptible to errors due to the double integration process. Experimental result showed [4] the position drift rate is between 1-8 cm/s, which is unacceptable over time. Therefore, other sensors are needed to reset inertial errors by providing absolute Omnibot position and orientation as explained in the next section.

Table 1: Technical specifications for KVH RD2030 gyroscope

Attribute	Value
Input rotation rate	±30 °/sec
Rate resolution	0.014 °/sec
Instantaneous bandwidth	100 HZ
Non-linearity	0.2 %rms
Bias stability over full temperature	0.12 °/sec P-P
Size	4.41"×4.27"×1.69"
Weight	12 OZ

2.2 Use of Beacons

Beacons are used [8-9] in determining the absolute position and orientation of the mobile robots. The main problems usually are the range, number of beacons, and complexity of infrastructure needed. There are number of commercially available system in the market. For example, MTI research corp. provides a Computerized Opto-electronic Navigation and Control (CONAC) laser tracking systems with 2D and 3D positional information. For this system three stationary NOADs are placed along one side of the target, and ideally should be connected to each other by cable. The STROAB (mobile robot beacon) emits a beam with approximately thirty-degree fan angle across the horizon. The NOADs need to be within this volume. The pulse transmitter transmits the NOAD signals to an optical receiver on the mobile robot.

A CONAC interface module on the mobile robot talks to the computer and the provided software converts module's data into 2D position and heading angle information. It is possible in the rough terrain to lose the communication between STROAB to NOAD. The laser tracker is based on triangulation of laser signals emitted by the beacons. The range of the system is between 3-300 m. Typical indoor precision is +/- 0.05 inches for position, and angular +/- 0.05 degrees for orientation. The price for this unit is about $15,000.

The configuration and the number of beacons increase in order to get 3D position and orientation information.

An inexpensive approach to receive positional information is to use popular Global Positioning System (GPS). The GPS accuracy usually is not sufficient for the mobile robot applications. The accuracy is improved considerably by using Differential GPS (DGPS). Commercial products like Starlink Incorporated Invicta 210 GPS/Beacon receiver board provide the positional accuracy of less than 1 m rms with differential signal as shown in table 2. For our application this kind of accuracy is sufficient. Because the operator will use the vision system to get close to umbilical plate when the target is in line of sight. The heading angle can also be calculated by measuring the position using DGPS at two different points. Of course use of DGPS on mars environment is not currently feasible. NASA is planning to place number of satellites around Mars to provide similar information like GPS on Mars.

Table 2: Technical specifications for Invicta 210 GPS/Beacon

Attribute	Value
Re-Acquisition	1 sec
Position Accuracy	< 1 m rms
Maximum Velocity	1000 knots
Acceleration	2 G
Altitude	60,000 feet
Size	6.67″×3.96″×0.5″
Weight	6.5 OZ

It is proposed to use DGPS in conjunction with inertial sensors to find the position and orientation of the Omnibot. The problem with the DGPS is that the signal may be blocked or fade from time to time. Inertial systems do not suffer from this problem. The problem with inertial system is that the positional errors grow with time and distance due to the gyroscopes drift, and the integration of sensor readings.

Therefore, the proposal is to use inertial system to keep track of Omnibot heading angle locally, and integrate the information with DGPS using Kalman filter to avoid the problem with growing errors. The Omnibot position and heading angle are estimated based on the single-axis fiber optic gyroscope, and the DGPS information.

The described system will provide the operator the distance and direction to the target in addition to the local visual information. Using the provided information, the operator will navigate the Omnibot and bring the umbilical plates to the local positioning zone. At this point, the system is switched to the autonomous mode. The umbilical local positioning and mating is described in the next section.

3. Local Positioning Problem

During local positioning, the position of mate-to plate is determined using ultrasonic sensors. The mate-in umbilical plate is mounted on a Cartesian robot on the Omnibot. Four ultrasonic sensors are installed in the four corner of the mate-in plate as shown in figure 2. The sensors are numbered clockwise. The edge 1 (E1) is defined across sensors 1 and 2. The following steps outline the procedure for local positioning of autonomous umbilical mating:

1. Align the orientation of the two umbilical plates
2. Obtain raw distance data d_1, d_2, d_3, and d_4 from the four ultrasonic sensors
3. Filter and separate the data according to constraints
4. Engage sensors and obtain the mate-to umbilical position
5. Align position of the two umbilical plates and mate

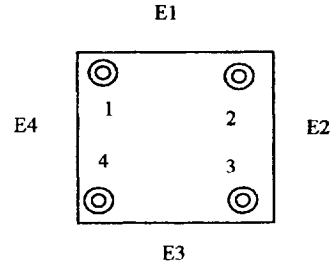

Figure 2. Location of four ultrasonic sensors

Considering a rough terrain, the Omnibot orientation is needed to determine the orientation of the mate-in umbilical plate. A dual-axis Applied Geomechanics tilt sensor with specification shown in table 3 is used to calculate the roll and pitch angles specifying the orientation of the Omnibot as described in section 2. Based on this information, the mate-in plate is oriented to align with the orientation of mate-to plate, which is known.

Table 3: Technical specification for Applied Geomechanics 900

Attribute	Value
Angular range	±45 deg
Resolution	0.01 deg arc
Repeatability	<0.02 deg arc
Linearity	6% of full span
Natural frequency	10 HZ
Size	2"×2"×0.64"
Weight	0.5 OZ

Assuming the same orientation for both umbilical plates, the position is calculated based on identifying the edge feature of the mate-to plate. The procedure to start determining the edges depends on if the four ultrasonic sensors are engaged as indicated in the flowchart in figure 3.

As shown in figure 3, the objective of the approach is to engage all four sensors and move the plates to about four inches apart from each other. At this point the algorithm to find the edges of the mate-to plate is initiated. To identify vertical edges (E2 and E4) shown in figure 2, the mate-in plate is moved in the right direction (positive x-axis) until sensors 2 and 3 are disengaged. This position is marked as x_pos_{23}. Then, the mate-in plate is moved in the left direction (negative x-axis), monitoring the sensors until sensors 1 and 4 miss the plate. This position is also marked as x_pos_{14}. The midpoint of the mate-to plate in the x-direction is determined by

$$x\_pos_m = \frac{x\_pos_{23} + x\_pos_{14}}{2} \tag{7}$$

The shape of umbilical plate is known. Therefore, with the obtained information, one point on both vertical edges is estimated. The same procedure is repeated in the z-direction to estimate a point on the top and

bottom edges (E1 and E3) of the plate. To estimate a line uniquely, with orientation uncertainty, at least two points are needed. To obtain the second point, the mentioned procedure is repeated.

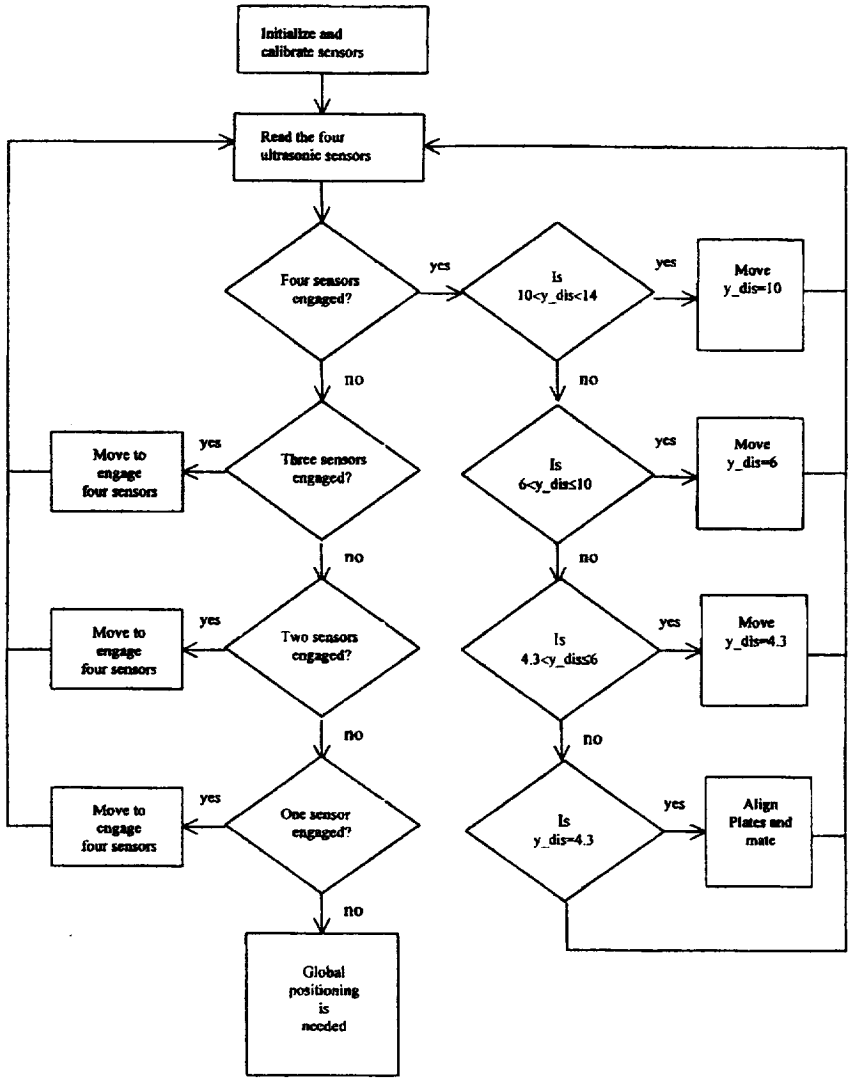

Figure 3. Flowchart of local positioning algorithm

An experiment is conducted to verify the feasibility of the proposed approach. The objective is to align umbilical plates autonomously during local positioning. The Omnibot with the umbilical positioning system is shown in figure 4. The position and orientation of receiving plate is fixed. The plates are made of aluminum. The mate-in plate is mounted on a three axis Cartesian table to simulate the Cartesian robot.

The program is written to perform the autonomous mating based on the flow chart shown in figure 3. The four sensors are engaged and the plate edges determined. The edges are estimated within ±0.05 inches by using only one point on each edge. By repeating the edge finding for 10 times, the edges can be estimated within ±0.042 inches. The improvement is minimal and the autonomous aligning can be performed based on one point. The results obtained detecting the edge position of the mate-to plate are graphed in figure 5.

Figure 4. Omnibot with umbilical positioning system

A passive compliance is build into mate-in umbilical plate with guided cones as shown in figure 4. This arrangement will insure to avoid excessive forces during umbilical plates mating for proper alignment. As experimentation showed the umbilical plates are aligned within 0.05 inches. Being able to align the plate this accurately means the guided cones are small on the compliance system. The passive compliance can also take care of orientation misalignment up to ten degrees in the system.

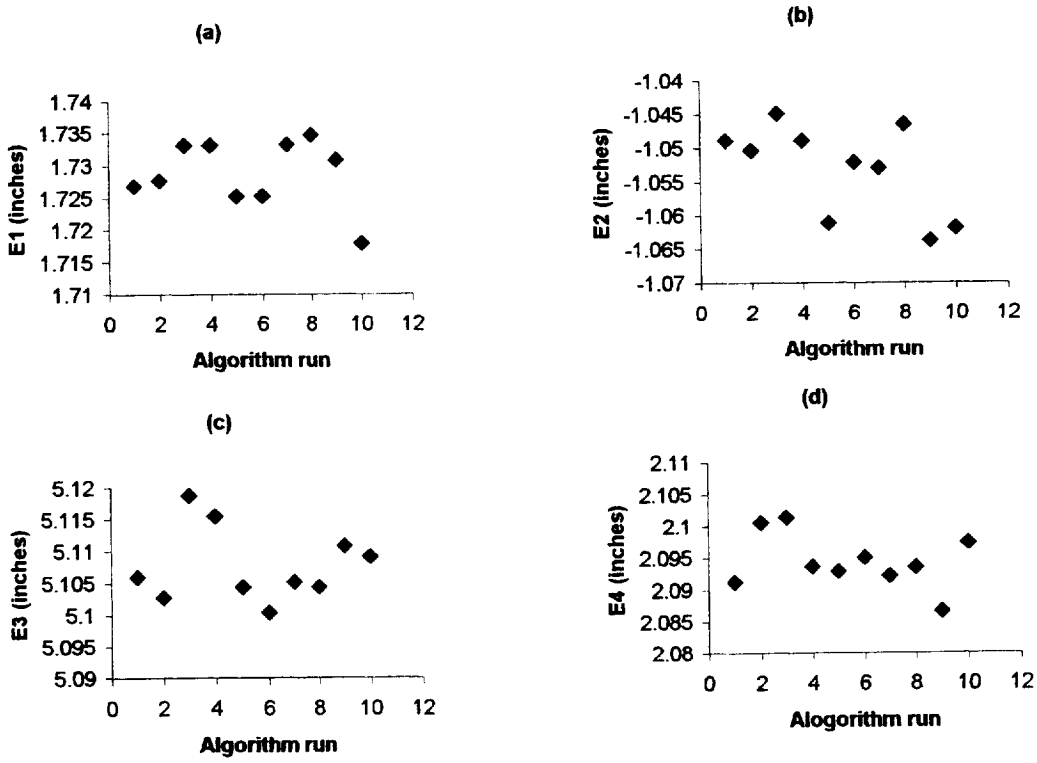

Figure 5. Sensors detecting edge position of mate-to plate (a) E1 (b) E2 (c) E3 (d) E4

4. Conclusion

As indicated, the problem of umbilical positioning system is divided to global and local positioning problem. The Omnibot will be initially 1000 m away from the target. To navigate the system toward target, the distance and direction to the target will be provided continuously to the operator. The proposed system will use the single axis gyroscope integrated with differential GPS information to provide the Omnibot position and orientation. For the mars environment, the DGPS system may be substituted with a beacon system.

For local positioning problem, considering the Omnibot is on a rough terrain, it is suggested to use dual-axis tilt sensor to find the Omnibot orientation. Based on this information, the orientation of the umbilical plates can be aligned. The algorithm indicated in figure 3 is then applied to autonomously position the umbilical plates and mate them. The approach for autonomous mating is verified experimentally.

Acknowledgements

I like to express my sincere appreciation to my NASA-KSC colleague Tom Lippitt for his help and useful suggestions during this summer. I also like to thank Ramon Hosler, Greg Buckingham, and Cassie Spears for their contributions to a successful Summer Faculty Program. I learned a lot about Kennedy Space Center facilities, operations, and goals. Thank you all, which made this summer both enjoyable and professionally interesting.

REFRENCES

[1] K. S. Chong and L. Kleeman, "Accurate Odometer and Error Modeling for a Mobile Robot", Proc. of the, IEEE Intl. Conference on Robotics and Automation Albuquerque, New Mexico, pp. 2783-2788, April 1997.

[2] J. Borenstein, "Experimental Evaluation of the Fiber Optics Gyroscope for Improving Dead-reckoning Accuracy in Mobile Robots", Proc. Of the IEEE Intl. Conference on Robotics and Automation, Leuven, Belgium, pp. 3456-3461, May 1998.

[3] S.Kotani, et.al., "Mobile Robot Navigation Based on Vision and DGPS Information", Proc. Of the IEEE Intl. Conference on Robotics and Automation, Leuven, Belgium, pp. 2524-2529, May 1998.

[4] B. Barshan, and H.F. Durrant-Whyte, "Inertial Navigation Systems for Mobile Robots", IEEE Transactions on Robotics and Automation, Vol. 11, No. 3, June 1995, pp. 328-342.

[5] K.C. Park, et. al., "Dead Reckoning Navigation for an Autonomous Mobile Robot Using a Differential Encoder and a Gyroscope", Proc. of the 8th Intl. Conference on Advanced Robotics, Monterey, CA, pp. 441-446, July 1997.

[6] J. Vaganay, and M.J. Aldon, and A. Fournier, "Mobile Robot Attitude Estimation by Fusion of Inertial Data", Proc. of IFAC Intl. Workshop on Intelligent Autonomous Vehicles, pp. 277-282,

[7] Y. Fuke, and E. Krotkov, "Dead Reckoning for a Lunar Rover on Uneven Terrain", Proc. of the IEEE Intl. Conference on Robotics and Automation, Minneapolis, Minnesota, April 1996.

[8] O. Kubitz, et.al, "Application of Radio Frequency Identification Devices to Support Navigation of autonomous Mobile Robots", Proc. of the IEEE 47th Vehicular Technology Conference, Vol 1, pp. 126-130, 1997.

[9] J.J. Leonard and H.F. Durrant-Whyte, "Mobile Robot Localization by Tracking Geometric Beacons", IEEE Transactions on Robotics and Automation, Vol. 7, No. 3, pp. 376-382.

[10] B.D. Hoffman, "Improved Rover State Estimation in Challenging Terrain", Autonomous Robots, 6, Kluwer Academic Publishers, Boston, pp. 113-130, 1999.

[11] N. Houshangi, and T. Lippitt, "Omnibot Mobile Base for Hazardous Environment", IEEE Canadian Conference on Electrical and Computer Engineering, Edmonton, Alberta, Canada, pp. 1357-1361, May 1999.

[12] NASA Mars Reference Mission Version 3.0, John F. Kennedy Space Center.

[13] N. Houshangi, "Mars Umbilical Technology Demonstrator", NASA/ASEE Summer Faculty Fellowship Program Report, Kennedy Space Center, August 1999.

[14] N. Houshangi, "Omnibot Mobile Base", NASA/ASEE Summer Faculty Fellowship Program Report, Kennedy Space Center, NASA CR-1999-208546, pp. 93-102, August 1998.

5/2/001/W/25

2000 NASA / ASEE SUMMER FACULTY FELLOWSHIP PROGRAM
JOHN F. KENNEDY SPACE CENTER
UNIVERSITY OF CENTRAL FLORIDA

MEMBRANE SEPARATION OF GASES FROM THE MARTIAN ATMOSPHERE

Paul A. Jennings, PhD
Assistant Professor and Head
Department of Chemical Engineering
Florida Institute of Technology

Clyde Parrish, PhD
NASA-KSC

ABSTRACT

A test bed has been constructed to test membrane modules for separation of gases under temperature and pressure conditions normally encountered on the surface of Mars. The test bed allows independent control of (1) feed flow rates, (2) feed composition, (3) feed pressure, (4) permeate pressure, and (5) operating temperature. Preliminary data obtained at a nominal feed pressure of 760 torr and permeate pressure of 10 torr has demonstrated the ability of one membrane module to operate at temperatures as low as –70 °C. At temperatures below –40 °C, however, significant loss of carbon dioxide and argon was observed, probably indicating condensation at the relatively high pressure used. As expected, permeation flow rates decreased with decreasing temperature, the flow at –30 °C approximately 37% of the value at +23 °C. Values of permeability for individual gas components showed similar decreases with decreasing temperature, but permeability ratios changed significantly. For example, the ratio of the permeabilities of carbon dioxide and nitrogen increased from 2.6 at 23 °C to 5.6 at –30 °C. Additional data at lower operating pressures and temperatures must be obtained in order to optimize design of a usable separation system.

1. INTRODUCTION

The Martian atmosphere is composed of 95.5% CO_2, 2.7% N_2, and 1.6% Ar at a pressure of approximately 6 torr (0.008 atm). It has been proposed to react hydrogen transported to Mars with atmospheric carbon dioxide to produce oxygen. The oxygen could then be used for either propulsion or life support. Although primary attention has been focused on utilization of carbon dioxide, the other components could also be used as purge gases or mixed with oxygen to form breathable mixtures if the carbon dioxide content can be sufficiently reduced. Any process for separation of atmospheric gases during a manned mission to mars should be low in weight, low in complexity (maintenance requirements), and low in power consumption. Membrane separation has the potential to satisfy all of these requirements.

Membrane separation has been studied for a number of industrial applications, including recovery of carbon dioxide from combustion processes at relatively high temperatures and removal of volatile organic compounds from waste gas streams at lower temperatures. No studies have yet been published on separation characteristics at the relatively low temperatures (- 70 ° C) encountered on the surface of Mars. Although permeabilities of all gases are expected to decrease with decreasing temperature, design and optimization of separation equipment for use on Mars requires definition of the magnitude of such decreases and any changes in relative permeation that may occur at low temperatures.

2. EXPERIMENTAL METHODS

Figure 1 is a schematic diagram of the experimental apparatus used in this study. The membrane module used was a hollow-fiber type with feed to the inside of the fibers and permeate withdrawn from the shell surrounding the fiber bundle. Pure gases (CO_2, Ar, and N_2) were combined using a manifold that employed three flow controllers (Sierra) that allowed control of both total flow rate and feed composition. Feed- and permeate-side pressure controllers (MKS Instruments, Inc.) allowed variation of pressure drop across the membrane. The membrane module was enclosed in an insulating box constructed from Styrofoam insulation panels. Temperature was controlled by bleeding liquid nitrogen into the box through a perforated stainless steel tube that distributed the nitrogen along the length of the membrane module. No significant differences were measured between the temperatures of the two effluent streams (*i.e.*, interior of the membrane module) and the temperature inside the box (*i.e.*, exterior of the module). The entire apparatus was installed under a fume hood, which ensured relatively constant ambient temperature conditions.

Flow rates of the permeate and reject streams were measured using direct volumetric measurement methods, a wet test meter and a electronic bubble meter respectively. The feed flow controllers were calibrated using the same wet test meter, and thus flow rates of all streams could be measured as liters per minute at ambient conditions of temperature and pressure (23°C and 1 atm). Samples of feed, permeate, and reject gas streams were fed directly to a gas chromatograph through a manifold that allowed real-time sampling of each stream. The gas chromatograph was calibrated by analysis of the feed gas (whose composition was controlled independently).

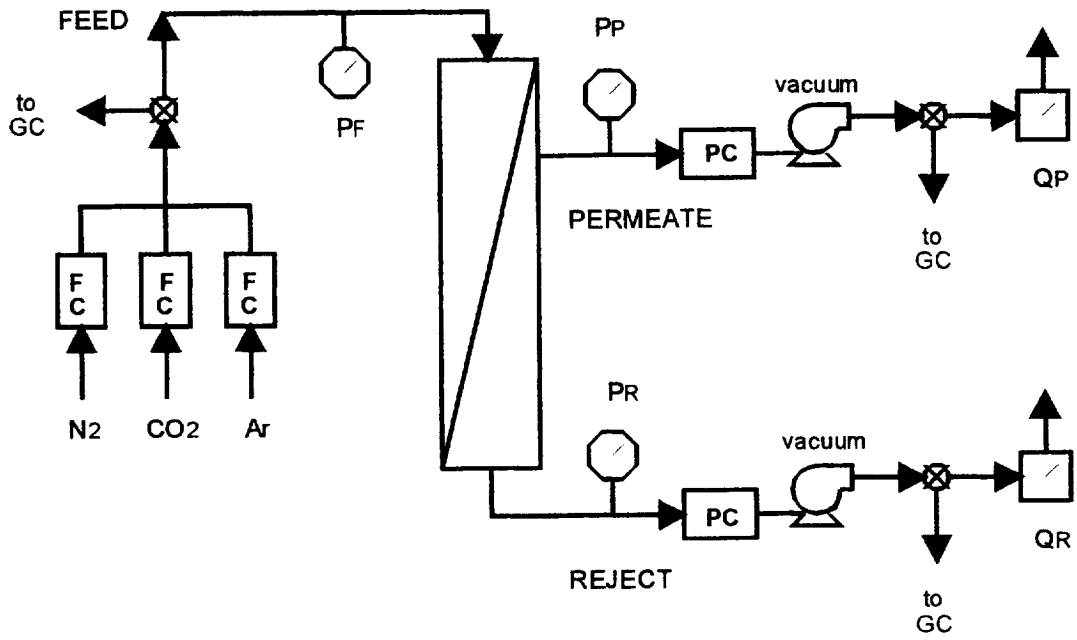

Figure 1 : Experimental Apparatus

3. THEORY

Assuming that ideal plug-flow conditions exist inside each membrane fiber and ideal mixed-flow conditions exist in the "shell" surrounding the fiber bundle, a material balance may be written on an individual fiber in the form:

$$\frac{d}{dx}\left(F\, y_k\right) \;+\; K_k\,(p_{k,F} - p_{k,P})\,a \;=\; 0 \qquad (1)$$

where
- F = total molar flow rate through the fiber,
- y_k = mole fraction of component "k",
- K_k = permeability of component k, mol / area – pressure – time
- $p_{k,F}$ = partial pressure of component k on the feed side of the membrane
- $p_{k,P}$ = partial pressure of component k on the permeate side
- a = membrane area per unit length of fiber
- x = axial length coordinate

Summing material balances on each component in the system yields an "overall" balance in the form:

$$\frac{dF}{dx} \;+\; \sum_k K_k\,(p_{k,F} - p_{k,P})\,a \;=\; 0 \qquad (2)$$

If L = the length of an individual fiber, a dimensionless axial coordinate may be defined as $z = x / L$. Let C_T° = total molar concentration at a reference temperature and pressure. A volumetric flow rate may then be defined (in units of volume at the reference conditions per unit time) as $Q = F / C_T^\circ$. Let $p_{k,F} = P_F y_{k,F}$ and $p_{k,P} = P_P y_{k,P}$, where P_F and P_P are the pressures on the feed and permeate sides of the membrane respectively. The material balances may be rewritten in the form:

$$\frac{d}{dz}(Q y_k) + \alpha_k (y_{k,F} - \beta y_{k,P}) = 0 \qquad (3)$$

$$\frac{dQ}{dz} + \sum_k \alpha_k (y_{k,F} - \beta y_{k,P}) = 0 \qquad (4)$$

where α = "reduced" permeability (in units of volume at reference conditions per unit time) = $K_k P_F a L / C_T^\circ$, and β = pressure ratio = P_P / P_F.

4. Results and Discussion

Several initial runs were made at room temperature (23 °C) and with varying flow rates and feed compositions to calibrate analytical equipment. The data obtained was subsequently with the above mathematical model to determine values of permeability for the three compounds in the gas mixture. Values of permeability (α) were found to be 3.4 lpm for CO_2, 1.4 lpm for Ar, and 0.42 lpm for N_2. Table 1 is a summary of those results. It should be noted that these runs were made before installation of pressure controllers on the feed and permeate. The values of feed-side and permeate side pressures (P_F and P_P) were assumed to be 760 and 10 torr respectively for modeling purposes.

Table 1. Room Temperature Data

	FEED	PERMEATE		RAFFINATE	
		measured	predicted	measured	Predicted
Flow, Lpm	0.947	0.808	0.817	0.139	0.130
% CO_2	24.1	29.6	27.9	0.2	0.4
% Ar	31.4	33.5	35.5	6.7	5.4
% N_2	44.5	37.5	36.6	92.7	94.1

	FEED	PERMEATE		RAFFINATE	
		Measured	predicted	measured	Predicted
Flow, Lpm	0.869	0.759	0.750	0.115	0.119
% CO_2	17.3	21.3	20.0	0.2	0.3
% Ar	34.2	38.9	38.9	5.2	4.8
% N_2	48.5	40.1	41.1	94.0	94.8

	FEED	PERMEATE		RAFFINATE	
		Measured	predicted	measured	Predicted
Flow, Lpm	1.021	0.892	0.880	0.127	0.140
% CO_2	29.6	36.7	34.2	0.5	0.6
% Ar	29.1	30.2	32.8	4.6	6.0
% N_2	41.3	33.4	33.0	94.2	93.4

	FEED	PERMEATE		RAFFINATE	
		Measured	predicted	measured	Predicted
Flow, Lpm	1.160	0.798	0.795	0.327	0.365
% CO_2	19.7	30.2	28.3	0.05	0.9
% Ar	25.6	28.6	32.8	4.8	9.9
% N_2	54.7	41.7	38.8	94.5	89.2

A set of data was then obtained for a constant feed composition (24.1% CO_2, 31.4% Ar, and 44.5% N_2) and volumetric flow rate (0.947 lpm) with varying temperature. Temperatures were controlled (by manual adjustment of liquid nitrogen flow) within +/- 0.5 °C of the values shown. As expected, permeate flow decreased with decreasing temperature. Below -30 °C, however, permeate flow rates began increasing due to pressure increases on the feed side of the membrane fibers. Below -40 °C, condensation of CO_2 and Ar appears to have occurred (material balances calculations resulted in values of percent recovery well below 100% at those temperatures) due to the combination of low temperature and high pressure. Table 2 is a summary of data obtained for temperatures between 23 °C and -30 °C. Although permeate flow rates were expected to decrease with decreasing temperature, little change in permeate composition was expected because diffusivities of gases normally show similar dependence upon temperature. (If permeation is a purely diffusive process, the permeation of each compound should decrease with temperature, but the ratio of permeabilities should remain relatively constant.)

Table 2. Low Temperature Data

23 °C

	PERMEATE		RAFFINATE		PERMEABILITY
	measured	predicted	measured	Predicted	(Lpm)
Flow, Lpm	0.808	0.817	0.139	0.130	
% CO_2	29.6	27.9	0.2	0.4	3.4
% Ar	33.5	35.5	6.7	5.4	1.4
% N_2	37.5	36.6	92.7	94.1	0.42

0 °C

	PERMEATE		RAFFINATE		PERMEABILITY
	measured	Predicted	measured	Predicted	(Lpm)
Flow, Lpm	0.49	0.478		0.469	
% CO_2	48.7	46.6	1.0	1.1	3.0
% Ar	27.5	28.4	34.2	34.4	0.39
% N_2	22.5	24.9	64.4	64.5	0.21

- 10 °C

	PERMEATE		RAFFINATE		PERMEABILITY
	measured	predicted	measured	Predicted	(Lpm)
Flow, Lpm	0.39	0.398		0.549	
% CO_2	56.1	55.0	3.5	1.7	2.8
% Ar	23.8	24.2	35.7	36.6	0.27
% N_2	19.6	20.8	60.7	61.7	0.15

- 20 °C

	PERMEATE		RAFFINATE		PERMEABILITY
	measured	predicted	measured	Predicted	(Lpm)
Flow, Lpm	0.34	0.323		0.624	
% CO_2	61.6	65.3	2.7	2.8	2.3
% Ar	18.2	18.9	37.1	37.9	0.17
% N_2	16.3	15.8	59.8	59.4	0.095

- 30 °C

	PERMEATE		RAFFINATE		PERMEABILITY
	measured	predicted	measured	Predicted	(Lpm)
Flow, Lpm	0.30	0.256		0.691	
% CO_2	68.7	68.9	7.6	7.5	1.3
% Ar	14.1	16.2	37.4	37.0	0.12
% N_2	14.4	14.8	56.4	55.5	0.075

Figure 2 is a plot of calculated permeability values as a function of temperature. Although the permeability of each compound decreases with decreasing temperature (as expected), the shape of the curve for CO_2 is significantly different from the shape of the curves for Ar and N_2. This may indicate that permeation of carbon dioxide may involve a different mechanism than permeation of argon and nitrogen. In addition, the variation of permeability with temperature implies that temperature may be used as an independently controlled variable to optimize separation in a multiple-stage system. For example, separation of carbon dioxide from nitrogen and argon may be optimal at moderate temperatures (0 to –10 °C), while separation of argon from nitrogen may be optimal at relatively high temperatures (20 °C).

Future experiments are planned to obtain additional data for the membrane module used in the above experiments as well as two other modules designed for gas separation. If significant differences in behavior are observed, it may be possible to relate permeation behavior to membrane composition.

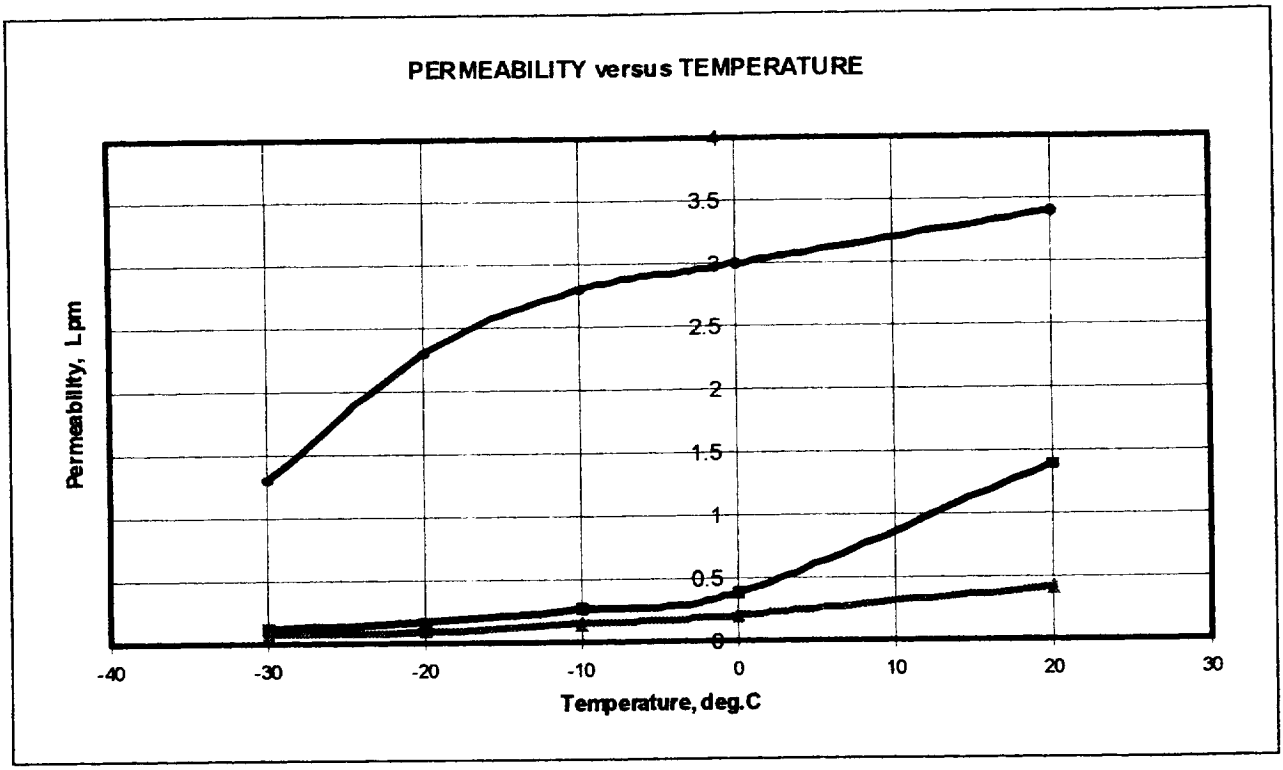

Figure 2. Permeability Data.

5. Conclusions

An experimental apparatus has been designed, constructed, and tested that allows operation of a membrane module for gas separation with independent control of multiple operating variables: (1) feed flow rate, (2) feed composition, (3) feed pressure, (4) permeate pressure, and (5) operating temperature. Volumetric flow rates and composition of permeate and reject streams can be independently measured, allowing calculation of percent recovery of each compound in the gas mixture.

A mathematical model has been derived and tested for the gas separation process under study. It contains one empirical constant ("reduced" permeability) for each component of the gas mixture which must be evaluated from experimental data. Once the values of these constants are determined, the model is capable of adequately predicting permeate flow rate and composition.

A preliminary analysis of the effects of low temperature operation on permeation rates has demonstrated significant differences in behavior among the three compounds studied. Both flow rate and composition of permeate may be expected to change with temperature as well as pressure. Optimum performance of process equipment may require operation at temperatures significantly greater than the ambient temperature on the Martian surface.

Membrane separation is capable of producing product gas streams with carbon dioxide concentrations well below the maximum contaminant level for breathable air or other applications. Due to low power requirements and simplicity of design and operation, membrane separation appears to be a practical process for a variety of applications of current interest to NASA.

6. REFERENCES

Membranes in Separations, Sun-Tak Hwang and Karl Kammermeyer, Wiley (1975).

"Separation of Multicomponent Mixtures by Gas Permeation," R.Rantenbach and W. Dahm, Chem.Eng.Prog., 19 (1985).

"Separation of Light Gas Mixtures Using SAPO-34 Membranes," J.C. Poshusta, V.A. Tuan, and J.L. Falconer, AIChE Jour., 46, 779 (2000).

ACKNOWLEDGEMENTS

I wish to thank Dr. Clyde Parrish for giving me the opportunity to participate in this project. I also wish to thank Mr. Paul Gamble and the other employees of Dynacs, Inc., for all the assistance they have given me in locating equipment and training me in the use of that equipment.

2000 NASA / ASEE SUMMER FACULTY FELLOWSHIP PROGRAM

JOHN F. KENNEDY SPACE CENTER
UNIVERSITY OF CENTRAL FLORIDA

Space Transportation Operations: Assessment of Methodologies and Models

Prafulla Joglekar
Lindback Professor of Operations Management
La Salle University, Philadelphia, PA 19141
Tel: (215) 951 1036 E-mail: Joglekar@lasalle.edu

NASA Colleagues:
Carey McCleskey: (321) 867 6370
Edgar Zapata: (321) 867 6234
Russ Rhodes: (321) 867 6298
Spaceport Technology Development Office (YA-C)
Kennedy Space Center, FL 32899

Abstract

The systems design process for future space transportation involves understanding multiple variables and their effect on lifecycle metrics. Variables such as technology readiness or potential environmental impact are qualitative, while variables such as reliability, operations costs or flight rates are quantitative. In deciding what new design concepts to fund, NASA needs a methodology that would assess the sum total of all relevant qualitative and quantitative lifecycle metrics resulting from each proposed concept. The objective of this research was to review the state of operations assessment methodologies and models used to evaluate proposed space transportation systems and to develop recommendations for improving them. It was found that, compared to the models available from other sources, the operations assessment methodology recently developed at Kennedy Space Center has the potential to produce a decision support tool that will serve as the industry standard. Towards that goal, a number of areas of improvement in the Kennedy Space Center's methodology are identified.

Space Transportation Operations: Assessment of Methodologies and Models

Prafulla Joglekar

INTRODUCTION

Today, at approximately $10,000 per pound of payload, cost is the major barrier to exploitation of scientific and commercial opportunities in space [1, 2]. Hence, NASA's strategic plan for second generation space transportation system aims at bringing these costs down by one order of magnitude (to $1,000/lb.) and its third generation plan aims for a reduction of two orders of magnitude (to $100/lb.). At the same time, NASA wants safety and flight rate capability to improve by similar orders of magnitude over the next two generations [3]. If we want to prudently invest in the right technologies that would realize these aspirations, the first thing we need is a model that would estimate the operations cost and performance metrics of alternative conceptual designs of space transportation systems (vehicle and spaceport facilities to support the vehicle). This is important since over 70% of a system's lifecycle costs are operations costs (OC) and although OC are actually incurred during the many years of operation of a system, over 70% of OC are *locked-in* by the end of the conceptual design phase of a system [4, 5].

Available literature provides a number of academic musings and theoretical prescriptions for building OC models [4, 5]. However, according to Hamaker [6], historically, most actual applications of cost models at NASA have been grossly inaccurate. They often use one or two key attributes of a proposed conceptual design (e.g., the weight budget, or degree of complexity) to estimate the resultant costs. Also, instead of truly estimating all components (particularly, operations and support) of a system's lifecycle costs, these models have concerned themselves primarily with the costs of design and construction of a vehicle and the necessary spaceport facilities. In a significant departure from this history, recently the Spaceport Synergy Team (a collaborative, jointly funded NASA/ Industry group) at the Kennedy Space Center (KSC) has developed a methodically rich, data and knowledge based approach to OC modeling.

The research reported here was aimed at:

- Critically examining available operations costs estimating models and methods to identify their strengths and weaknesses,
- Focusing particularly on KSC developed models and methodologies in this review,
- Proposing improvements in the existing models and methods as appropriate,
- Providing recommendations for new models or approaches, if necessary.

FINDINGS

Limitations of non-KSC operations costs models

While I examined over 25 different OC models from non-KSC sources, for want of space, I shall not detail them here. Since these non-KSC models have also been reviewed by others [5, 6, 7], I shall simply list their major limitations as:

- They are simplistic.
- They use primarily weight, size, and design complexity to arrive at the cost estimate.

- They often accept a designer's word for what would be the flight rate per year for a concept (rather than estimating the flight rate based on an estimation of the cycle time resulting from the concept).
- They are not based on detailed analysis of the existing operations cost data.

KSC's OC estimation effort

It has been very interesting for me this summer to study the evolutionary process as well as the product of the OC estimation effort at KSC. In response to NASA's "Access to Space" study [1], in the early 1990s KSC and its industry/ university partners set up "Reusable Launch Vehicle (RLV) Technology Development Program." Building on the knowledge of the operations experts at KSC, this program emphasized the need to *abandon* the traditional attitude of "*supporting the design*" in favor of an attitude of "*designing for support*." The RLV program also outlined a number of design principles that would minimize the operations and support costs of a space transportation system [8]. These principles included: Define the mission narrowly to transportation only, Apply advanced technology to design a simple vehicle, Avoid the need for flight-to-flight certification, and Reduce system integrity verification through automation.

In 1995, the RLV effort was followed by the team's Highly Reusable Space Transportation Study (HRST) which documented multiple, prioritized factors as drivers of recurring and non-recurring costs and other performance metrics of reusable space transportation systems [9]. In 1997, in order to assess as to how well a proposed design concept would do in terms of these cost drivers and performance metrics, an Architectural Assessment Tool (AAT) Form was developed. In 1998, Zapata [7] built an Excel based prototype, named Architectural Assessment Tool – enhanced (AATe), to estimate the operations costs resulting from a proposed design concept. This summer, the Spaceport Synergy Team (SST) (The names and the exact industry participants of the government/ industry/ university collaboration have changed over the years, SST being the latest manifestation of this effort) has released the first version of "Vision Spaceport Strategic Planning Tool" - a more comprehensive model for the assessment of operations costs and other performance metrics attributable to a design concept.

Unless otherwise specified, in the following discussion, I refer to both, the Strategic Planning Tool and AATe as simply "the Tool." A principal focus of my research this summer has been on assessing the strengths and limitations of the Tool.

Strengths of the Strategic Planning Tool/ AATe (or the Tool)

I shall not elaborate on the many strengths of the Tool here since SST has documented those strengths in many of its documents including [10]. However, I do want to note the following strengths:

- The Tool uses a systematic Quality Function Deployment (QFD) process to incorporate expert knowledge.
- It is based on detailed analysis of actual operations data (on costs as well as other performance dimensions, such as cycle time) from the Space Shuttle.
- It estimates both the costs and cycle times resulting from a design concept based on careful definition of 12 spaceport operations modules and 7 operability metrics.

- Insofar as collaboration among government, industry, and university participants is the hallmark of this effort, I believe that, when finished, it will provide a tool that would be an *industry standard.*
- Most importantly, the principles outlined by the RLV study, and reinforced by subsequent documents and tools, are already having a *significant impact on the design philosophy and the identification of the right technologies for funding by NASA.*

I also want to note that the process and product of the Spaceport Synergy Team's effort has two major purposes:

- To be *proactive in identifying the right directions* for future space transportation technology development, and
- To be *reasonably accurate in estimating the lifecycle costs* resulting from a proposed conceptual design.

While these two purposes are the most important strengths of this effort, as will be seen in the subsequent discussion, at times these two goals are in conflict.

Areas of Improvement for the Strategic Planning Tool / AATe (or the Tool)

Because the Spaceport Synergy Team is most interested in improving the Tool in its future releases, I have spent most of my effort on the preparation of this subsection of my report. As I see it, here are some major areas of improvement for the Tool:

1. **Strategic planning and Architectural Assessment**

   Although it claims to be a "strategic planning and architectural assessment tool," the Tool falls short of supporting the assessment of an architecture I visualize. I believe that the Third generation space transportation architecture (3G-STA) will consist of multiple types of vehicles (some manned, some unmanned, some highly reusable, some partially reusable, and some disposable, etc.), multiple types of spaceport facilities (some capable of handling any type of vehicle or cargo and others geared to specific vehicle types and/or cargo types, some commercially owned and others owned by governments of various countries, etc.). McCleskey's [11] concept of modifying Columbia to launch small commercially-operated devices to the moon while other shuttles continue to do what they do is consistent with my vision of a portfolio approach to STA design.

   In view of this vision, one serious limitation of the Tool is that it does not really aim to assess the entire architecture. It is aimed at assessing one vehicle and spaceport concept at a time. This is not a simple problem of using a wrong name for the tool. I think that when our mindset is to compare one design concept against others, we are looking for *the best general-purpose (one-size-fits-all) design,* instead of looking for *the best combination of several special-purpose designs.*

   The main lesson of industrial revolution is that, for productivity gains of an order of magnitude, it is important to have a few narrowly defined products (or services), each with a large, predictable, stable demand, and to design special machines, tools, and procedures to produce these narrowly defined products most efficiently at their predicted volumes.

   If STA objective is to attain costs of the order of $100/lb, we must recognize that it will not happen with a single general-purpose vehicle design. Several vehicles, each specially designed for a narrowly defined mission type (e.g., only passenger delivery to space station,

or only cargo delivery to Suntower, or only lab experiments no space walk, etc.) and appropriate spaceports, each designed to support only specific vehicles (but not all) is likely to be the key to the kinds of economies we are looking for. What NASA needs to do is to generate a list of narrowly defined missions with likely high volume in the future and then ask several developers to come up with vehicle design concepts for each specific mission. "Space Lift" – a Spacecast 2020 white paper [12] and Larson and Wertz's [13] "FireSat" concept are two good examples of narrowly defined Space Transportation System design concepts. To be able to evaluate such ideas, the Tool may have to be capable of adapting its criteria as appropriate for the design concepts under consideration.

JSC [14] has a model called "Advanced Missions Cost Model (AMCM)" which takes this kind of an approach. However, that model does not attempt to estimate operations costs. It estimates only R&D and production costs of the spacecraft and the space transportation system. Also, the methodology used by AMCM does not seem to incorporate true mass production scaling. In a true mass production situation, the cost of set up to produce even a single unit may be thousands of times the variable costs of production per unit. Thus, I believe that first AMCM needs to be modified to reflect true mass production scaling, and then the modified AMCM needs to be integrated with the Tool to account for the total system lifetime costs.

In integrating such models, one point to keep in mind is that while production costs often exhibit economies of scale, beyond a certain optimum level, operations costs of a transportation system are often characterized by diseconomies of scale. The reason is that in a transportation system, excessive traffic leads to congestion, accidents, long queue lengths, etc. It is important that the Tool accounts for such discontinuities in the cost patterns.

2. **Criteria Weighting**:

The Tool separates the criteria weighting of recurring (operations) costs from the criteria weighting of the non-recurring (technology R&D and programmatic) costs. However, many design choices (such as design life or reliability) may have cost implications in all three of the areas. For example, longer design life may lower maintenance frequency and hence operating costs, but it may increase technology R&D costs as well as acquisition (or programmatic) costs. It is therefore important that each method of design improvement is evaluated in terms of its impact on both the recurring and the non-recurring costs.

For no apparent reason, the method of analysis for generating the attribute weights for the non-recurrent cost factors is different from the method used for generating the attribute weights for the recurrent costs. Each of the components of operations costs along with those of safety, environmental compatibility, etc., are first rated on a 1 to 5 scale and then normalized. Whereas the components of Technology R&D are given a percentage weight each within its own category. Similarly, the components of programmatics are given a percentage weight each within its own category. I believe that use of a single integrated method to analyze all of the cost factors together would bring greater consistency and credibility to the Tool.

The Tool uses a simple additive utility function to capture the multiple attributes of concern. I believe that because of the go-no-go nature of some of the concerns, a combination of multiplicative and additive utility function may be appropriate. (See Appendix 1 for an elaboration of this point).

3. **Quality function deployment (QFD)**:

Quality function deployment (QFD) is an iterative method of systematically going from one level of "what"s and "how"s to the next level of "what"s and "how"s. In this process, the previous level's "how"s serve as the next level's "what"s [4, 5]. The Tool seems to have taken some shortcuts in the implementation of this QFD approach by trying to address several levels at once. Such shortcuts can distort (through double counting) the relative weights given to the attributes or criteria at each level. Shortcuts may also force us to use subjective weights for factors for which reasonably valid quantitative data may be available.

As I see it, in the space transportation industry, "Dependability" and "Responsiveness" are the "how"s of Affordability and Safety. Also, Environmental Compatibility is the "how" of Affordability, Safety, and Societal Benefit (including Public Perception). On the other hand, Technical and Political Feasibility is a make-or-break type criterion and hence needs to be dealt with at the highest level of QFD analysis. Hence, at Level 0 we should have just the four attributes: Affordability, Safety, and Societal Benefit (including Public Perception), Technical and Political Feasibility. In Appendix 1, I outline an idealized QFD approach. As can be seen from Sheet 1, I use a combination of multiplicative and additive utility (Figure of Merit) function.

It can be argued that "Responsiveness," or some other measure of performance (e.g., flight rate, vehicle turn around time, or throughput) is a value that the space program should seek in itself. The primary reason for this argument is the current dismal state of responsiveness of the space shuttle. If increasing the per vehicle per year flight rate is desirable in itself, then my list of Level 0 "whats" should be modified accordingly.

At Levels 1 and 2 (Appendix 1, Sheet 2) we identify the components and subcomponents of these Level 0 attributes and their relative weights within each attribute. As can be seen, for the components of Affordability, I suggest the *use of available lifecycle costs data* for the space shuttle to determine the weights (instead of the subjective weights derived by the Tool). For most of the other attributes, the component weights may have to be subjectively determined. One caveat about the use of shuttle cost data is that if there were a true paradigm shift (such as a demand for tens of thousands of launches per year using hundreds of vehicles for a narrowly defined or standard mission), the shuttle data would be irrelevant. Then the relevant cost data may be derived partly from the airline industry.

Where subjective methods must be used to assess the relative weights of attributes, pair wise comparisons would have been the better method to use than the method used by the Tool. NASA has often claimed that every dollar spent on space programs returns $9 in terms of direct and indirect contribution to GNP. In view of this claim, I believe that the Tool gives too small a weight to "Beneficial to GNP" attribute. (See Appendix 1 for an elaboration of this point).

Once the attributes (ends) are fully defined and their relatives weights are satisfactorily determined, from Level 3 on, we embark on an iterative process of determining the means to those ends and the correlations between the means and the ends. At level 3, the broad means of attaining safety may be minimal use of toxic materials, dependability, redundancy, auto system health monitoring and control, well defined procedures for abort and recovery, maintainability, management attitudes and practices, and properly trained personnel. These means should then be drilled down to the Level 4 means.

At level 3, the broad means of attaining affordability may be minimal use of toxic materials, dependability, responsiveness, use of COTS parts and subassemblies, auto system health monitoring and control, maintainability, and the several innovative approaches outlined in item # 5 below. These means should then be drilled down to the Level 4 means.

My Appendix 1 is incomplete. However, the idea is to apply the correlation scheme (-9, -3, -1, 0, 1, 3, 9) to the matrix of Level 2 ends and level 4 means across all factors -- technology R&D and programmatics not to be left out.

4. **Pareto Principle**:

The use of Pareto Principle is a good idea when one is looking for making a significant percent (30% to 50%) improvement in a system's performance by focusing only a few of the limitations of an existing system. However, when one wants an improvement of an order of magnitude or two, it seems important that almost all of the limitations of the existing system be addressed.

The Design guidelines for HRST identified 64 criteria. Yet, in assessing whether or not a design concept has the capacity to bring about an improvement of 2 orders of magnitude from the current level, the Tool focuses only on a small percentage of those criteria that account for a large percentage of the total weight of all 64 criteria. An improvement of 2 orders of magnitude is likely to require significant improvement in each one of the 64 criteria.

Of course, in order to keep the assessment manageable, it is important to focus on the few that will allow for the most improvement. But as the analysis proceeds further, it would be important to apply the Pareto principle in a dynamic way so that once the top 20% criteria are met, the remaining criteria are re-sorted to identify the new top 20% criteria to focus on. In other words, like a rolling horizon in a planning process, the Pareto criteria list should be a rolling list, updated in every round of assessment of alternative design concepts.

5. **The need for the creation of innovative alternatives**:

Coming up with the "right" list of "hows" (sometimes using a paradigm shift or other ways of creative thinking) is perhaps the most important part of the QFD process. As any successful businessman knows, *the greatest payoff of a decision comes from the creation of innovative alternatives*. While the Tool does address most of the obvious "hows" of affordability, I think that it misses some very important and innovative "hows" such as:

a) the degree of narrowness of the mission addressed
b) demand creation and economies of scale
c) sharing costs of research, development, and facility acquisition with international and or commercial partners
d) improved supply chain management
e) considering the possibility of a spaceport being simply another terminal at a major airport
f) airline type differential pricing policy to maximize the capacity utilization of a flight, etc.

Similarly, I think that the Tool misses some important "hows" of safety such as

a) redundancy

b) maintainability

c) management attitudes and practices

d) personnel training, motivation, and dedication, etc.

6. The correlation scale:

The current method of correlating the criteria ("means") with attributes ("ends") is to use a scale involving all positive values 0, 1, 3, 9. This scale assumes that no criterion will ever negatively impact an attribute. In reality, most criteria affect some attributes positively and some other attributes negatively. In order to capture both the positive and the negative correlations, the scale used should also allow negative values of –1, -3, and –9.

7. The proactive nature of "Improvement Ratio"

It seems that there is no standard QFD prescription on where and how to apply the "Improvement Ratio" and "the sales index." Some authors prescribe their use on the "whats"(or the rows of a QFD matrix), some others prescribe its use on the "hows" (or the columns of a QFD matrix) and still others on both. In quality control, the idea behind the improvement ratio or the "scale up" ratio (as Bossert [15] calls it) is to identify, attribute by attribute or engineering solution by engineering solution, how far our quality performance is behind the best competitor's performance. The larger the gap, the more important it would be to pursue a particular quality attribute or a specific engineering solution. Thus, the improvement ratio is used to focus management's attention on the top two or three quality problems that may offer the largest payoff in beating the competition. While this is an *excellent proactive strategy*, it should be realized that the Figure of Merit (FOM) resulting from the use of the improvement ratio is no longer an FOM that would assess accurately the original quality FOM resulting from a solution. In other words, the proactive nature of the "improvement ratio" conflicts with assessment purposes of a QFD analysis.

As I see it, the implications of this theoretical discussion in the context the Tool are:

a) If improvement ratio is to be used, I would rather see it *used on the "hows" (or the criteria) than on the "whats" (or the attributes)* of the final QFD matrix. After all, we want to identify the two or three proposed STA concepts that promise the best performance on the criteria (rather than the attributes).

b) Since it is difficult to define our competition precisely, the Tool has resorted to the notion of technology "Plan" versus "Now" concept. While this seems reasonable (although it stretches my imagination to conceptualize such things as "Technology Plan" for public perception), the Tool also assumes that Technology Plan index cannot exceed the importance rating attached to an attribute. I question this assumption. I believe that there need not be any relationship between the two. Since we are seeking orders of magnitude improvements, perhaps a rating of 5 for Technology Plan may be appropriate for every criterion, including criteria whose importance rating may be as low as 1.

However, note that some design dimensions are not to be pushed to their technological limits. For example, if we create a vehicle with a design life of 40 or 50 years, beyond the first half of the design life, we will be operating an obsolete vehicle. Thus for design life, it may be more appropriate to use a Technology Plan rating of 4 instead of 5.

c) The Tool should *use the FOM resulting from the improvement ratio only to select the promising design concepts. It must revert back to the original FOM to assess the actual utility function value accomplished* by each concept. Of course, the *cost estimation must be based on only the Affordability part of the original FOM.*

8. Formula for the improvement ratio (IR)

I find that the current formula for the improvement ratio (IR) is *intuitively unappealing*. At present, IR is defined as Plan/Now. I do not think this formula adequately reflects the increasing difficulty (and cost) of pushing a system's technology towards a 5. In the current method, going from 1 to 2 and going from 2 to 4 are both of equal value. I believe that going from 1 to 2 is considerably easier than going from a 2 to 4. Also, going from a 3 to 5 may be more difficult than going from a 2 to 4. Bossert [15, p. 25] has also raised similar concerns about his scale-up ratio. Perhaps we need to consider alternative formulae for the IR. In Appendix 2, I propose an alternate formula for calculating the IR.

9. The Tool's cost estimation procedure

So far, a complete understanding of the Tool's cost estimation procedure has eluded me. However, what I do know is that the Tool first translates a design concept's "Raw Score" to a "Facility Type," and plans to use that Facility Type to estimate a design's cost. At the June 5, 2000 meeting of the Functional Qualification Team, it became apparent that the then used method of translation of Raw Score to Facility Type was inadequate. In response to that meeting, I had proposed a new method for this translation requiring *proper calibration of the question by question Response Weights.* (See Appendix 3). I continue to believe that the method proposed in Appendix 3 would be more appropriate than the current method. However, I repeat that the use of my method will need proper design of the response choices for each question, and further work on conceptualizing how to handle the multiple response questions. Alternatively, experts can go question by question and estimate whether a particular response represents an improvement of an order of magnitude, or two, or somewhere in between, etc.

10. Associated Confidence Interval

At present, the Tool provides no indication of the confidence interval associated with its results. It is important that an analytical scheme is devised to provide that confidence interval. Apgar, Bearden and Wong's Chapter 20 in Larson and Wertz [13] has one approach to an estimate of the standard error associated with a cost estimate. The standard error can then be used to calculate the appropriate confidence interval.

11. One comment specific to AATe:

AATe's choice of 18 questions is based on a Pareto analysis of the total FOM. Given that AATe is focused on cost estimation, its choice of the 18 questions should have been based on a Pareto analysis of only the Affordability portion of the FOM.

CONCLUSION

This report has detailed a number of areas of improvement for the Tool. However, it should not detract the reader from the fact that the Tool, along with the process that produced it, represents a significant advancement over what is available from other sources. The principles outlined by the RLV study, and reinforced by subsequent documents and tools, are already having a *significant*

impact on the design philosophy and the identification of the right technologies for affordable space transportation in the future.

NOTE

For want of space, the Appendices mentioned in this report are not included here. They are available from the author or any one of his NASA colleagues.

REFERENCES

[1] CSTS Alliance (1994) The Commercial Space Transportation Study: Executive Summary and Final Report. Contract No. NAS1-19241 to 19247.

[2] Kennedy, F. and France, M. (1996) "Creating Space Mobility: A Vision for Our Twenty-First Century Spacelift Architecture," Proceedings of 33rd Space Congress, Canaveral Council of Technical Societies, FL, pp. 1.27 to 1.37.

[3] National Aeronautics and Space Administration (1994) Access to Space Study, January 1994.

[4] Blanchard B. J. and Fabrycky, W. J. (1998) Systems Engineering and Analysis, Prentice Hall, Upper Saddle River, NJ.

[5] NASA Systems Engineering Handbook (1995) National Aeronautics and Space Administration, Washington, DC. SP-6106.

[6] Hamaker, J. W. (1994) "But What Will it Cost? The History of NASA Cost Estimating," in Readings in Program Control, edited by F. T. Hoban, W. M. Lawbaugh, E. J. Hoffman, NASA SP-6103, National Space Administration, Washington DC.

[7] Zapata, E. and Torres, A. (1999) "Space Transportation Operations Cost Modeling and the Architectural Assessment Tool – Enhanced," Proceedings of the 1999 conference, American Institute of Aeronautics and Astronautics, Inc.

[8] Huether, J. E., Spears, J. M., McCleskey, C. M., and Rhodes, R. E. (1995) "Space Shuttle to Reusable Launch Vehicles," Proceedings of 32nd Space Congress, Canaveral Council of Technical Societies, FL, pp. 1.21 to 1.28.

[9] Highly Reusable Space Transportation (1997). A Catalog of Architectural Elements. Unpublished NASA document.

[10] Strategic Planning Tool Release 1.0: Milestone Briefing to Ken Payne (2000), Unpublished NASA document, June 28, 2000.

[11] McCleskey, C. M. (1996) "Using the Space Shuttle Columbia to Begin Bringing the Moon to America," Proceedings of 33rd Space Congress, Canaveral Council of Technical Societies, FL, pp. 7.16 to 7.23.

[12] Daehnick, C., (1996) "Space Lift: Suborbital, Earth to Orbit, and On Orbit" A SpaceCast White Paper, available at www.im.lcs.mit.edu/bh/spacecast3.html.

[13] Larson W. J. and Wertz, J. R. (editors) (1999) Space Mission Analysis and Design, Third edition, Microcosm Inc., Torrance, CA.

[14] Johnson Space Center (1999), "Advanced Missions Cost Model (AMCM)" available at www.jsc.gov/bu2/AMCM.html

[15] Bossert, J. L. (1991) Quality Function Deployment: A Practitioner's Approach, ASQC Quality Press, Milwaukee, Wisconsin.

514/cw/1w/17

2000 NASA/ASEE SUMMER FACULTY FELLOWSHIP PROGRAM

JOHN F. KENNEDY SPACE CENTER
UNIVERSITY OF CENTRAL FLORIDA

Space-based Encoded Telemetry for Range Safety

Sam Kozaitis
Associate Professor
Department of Electrical and Computer Engineering
Florida Institute of Technology, Melbourne, FL 32901

KSC Colleague: Richard Nelson, Advanced Range Technologies Manager/YA-E6

ABSTRACT

This work involves the analysis of a communication system that uses the NASA Tracking and Data Relay Satellite/Space Network (TDRSS/SN) to provide range safety and flight termination system support for expendable launch vehicles and the space shuttle. We examined the high-alphabet scheme for flight termination, and considered an analogous digital system. We also considered the bit-rate needed for a flight termination system using the TDRSS system based on the received signal-to-noise ratio, and link margin. We found that a TDRSS spread-spectrum communication system operating in the vicinity of 150 bits/second could satisfy the requirements for flight termination.

1.0 Introduction

This work involves the analysis of the communication system used for the NASA Tracking and Data Relay Satellite/Space Network (TDRSS/SN) to provide range safety and flight termination system support for expendable launch vehicles and the space shuttle. The concept and feasibility study of this approach can be found in Ref. 1.

Currently the Eastern range (ER), and the Western range (WR) rely on multiple ground stations to support the command destruct system. The range operations control centers (ROCCs), one at the WR, and one at the ER evaluate real-time tracking and telemetry data and provide command sequences for range safety. Some of these stations reside in foreign locations, with the associated rules, regulations, and logistics issues. New concepts for providing range safety have been investigated because of the costs associated with maintaining range safety stations, ground station horizon coverage limitations, and UHF frequency band crowding.

The TDRSS/SN has been studied to support range safety. The space portion of TDRSS/SN fleet consists of six satellites in geosynchronous orbit, and can provide hemispheric coverage for the ER and WR. The ground segment in located near Las Cruces, NM and consists of several ground terminals including one in Guam. Use of the TDRSS/SN would eliminate downrange stations and provide "seamless" coverage between launch-head (local) and space-based communications. The TDRSS/SN would provide maximum coverage for all potential launch trajectories, and provide centralized control.

2.0 NASA Tracking and Data Relay Satellite/Space Network (TDRSS/SN) [2]

The TDRSS/SN is a communication signal relay system that provides tracking and data acquisition services between low earth orbiting spacecraft and NASA/customer control and/or data processing facilities. The system is capable of transmitting to and receiving data from customer spacecraft's over at least 85% of the customer's orbit.

The TDRSS space segment consists of six on-orbit satellites located in geosynchronous orbit. Three TDRSs are available for operational support at any given time. The operational spacecraft are located at 41, 174 and 275 degrees west longitude. The other TDRSs in the constellation provide ready backup in the event of a failure to an operational spacecraft and, in some specialized cases, resources for target of opportunity activities.

The TDRSS ground segment is located near Las Cruces, New Mexico and consists of two functionally identical ground terminals known collectively as the White Sands Complex. Customer forwarded data is uplinked from the ground segment to the TDRS, and from the TDRS to the customer spacecraft. Customer return data is downlinked from the customer spacecraft via the TDRS to the ground segment and then on to the customer designated data collection location.

The TDRSS/SN offers several services that are summarized in Table 1. Forward service is defined as the communication path that generally originates at the customer control center and is routed through the TDRSS to the customer spacecraft. Return service is defined as the communication path that originates at the customer spacecraft and is routed through the TDRSS back to the customer control center or other customer-specified destination. single access service, as the name implies is a dedicated customer service utilizing the steerable single access antennas. Single access services support higher forward and return customer data rates. Services are available within a specified range of S or Ku band frequencies unlike the multiple access service that is fixed frequency. Multiple access service is a shared capability from which up to five return services can be run simultaneously. The multiple access service are more readily available than the single access service however they support lower forward and return data rates.

	FREQUENCY	SERVICE	MAX. DATA RATE	SERVICES PER TDRS
SINGLE ACCESS S-BAND	2020.4 MHz - 2123.3 MHz	FORWARD	300 k bps	2
	2200 MHz - 2300 MHz	RETURN	6 Mbps	2
K-BAND	13.747 GHz - 13.802 GHz	FORWARD	25 Mbps	2
	14.887 GHz - 15.119 GHz	RETURN	300 Mbps	2
MULTIPLE ACCESS S-BAND	2103.1 MHz - 2109.7 MHz	FORWARD	10 k bps	1
	2284.5 MHz - 2290.5 MHz	RETURN	100 k bps	5*

* GROUND STATION LIMITED

Table 1 Services of TDRSS system

TDRSS supports the following modulation schemes: bi-phase shift keying (BPSK), qudrature phase shift keying (QPSK) and staggered qudrature phase shift keying (SQPSK). Data formats supported are non-return to zero and Bi-Ø - Level (BiØ-L), also known as Manchester.

TDRSS utilizes two data groups, DG-1, and DG-2, and several operating modes within the data groups. DG-1 is psuedonoise (PN) spread, while DG-2 is non-spread. DG-1 transmission is beneficial in reducing interference to other customers or terrestrial communication systems, and allows for meeting flux density constraints for lower data rate services. DG-1 transmission also provides the means by which TDRSS supports ranging services. The characteristics of the data groups are listed below.

Data Group 1/Mode 1 - Coherent PN Epoch and Carrier
Provides ranging and two - way Doppler measurement
Provides low rate telemetry (300 Kbps maximum)
Long PN Code (2E10 - 1) X 256

Data Group 1/Mode 2 - Non Coherent
Provides low rate telemetry (300 Kbps/channel maximum)
Short PN Code (2E11- 1)
Provides one-way Doppler measurement only

Data Group 1/Mode 3 - Coherent-Combination (Coherent carrier for two-way Doppler)
I Channel
PN Spread to provide coherent long code PN epoch for ranging
Provides low rate telemetry (300 Kbps maximum)
Q Channel
Non Spread
High Rate Telemetry

Data Group 2 (DG-2) - Non PN Spread
High Rate telemetry (>300Kbps) data modulation provides necessary RF spectrum spreading to meet flux density restrictions

One or Two way Doppler Measurement (No ranging provided)

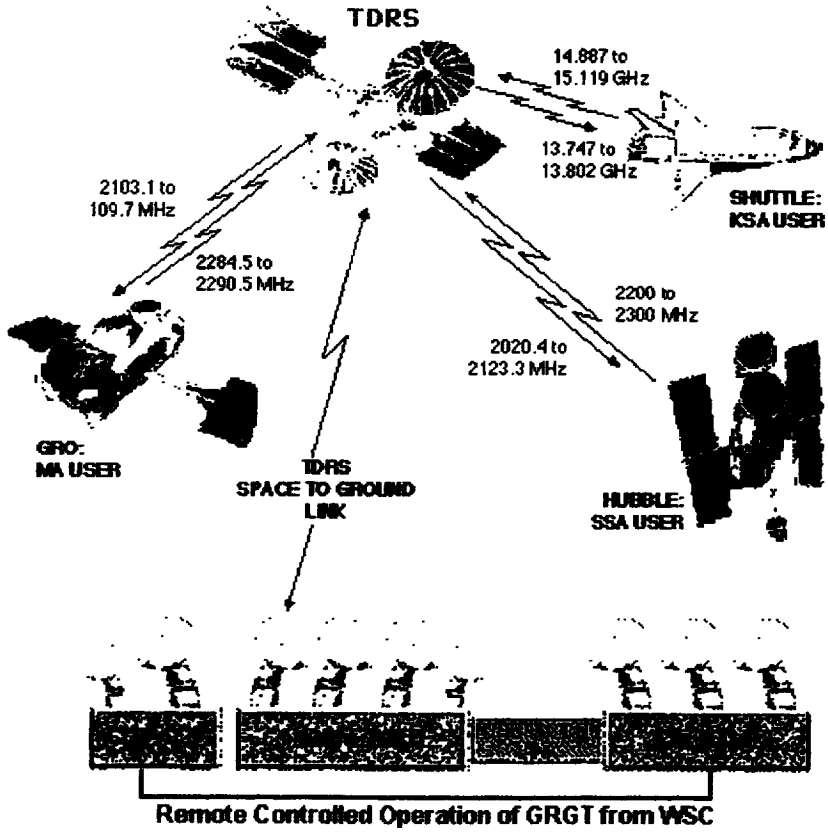

Figure 1 Overview of TDRSS system-showing control from the Western Range.

3.0 Spread spectrum communications [3]

The TDRSS/SN uses the spread spectrum (SS) method of communication. Spread spectrum describes a modulation technique that makes the sacrifice of bandwidth in order to gain signal-to-noise performance. Basically, the SS system is a system in which the transmitted signal is spread over a frequency much wider than the minimum bandwidth required to send the signal. The fundamental premise is that, in channels with narrowband noise, increasing the transmitted signal bandwidth results in an increased probability that the received information will be correct. If total signal power is interpreted as the area under the spectral density curve then signals with equivalent total power may have either a large signal power concentrated in a small bandwidth or a small signal power spread over a large bandwidth.

The process gain (Gp) is what actually provides increased system performance without requiring a high SNR. This is described mathematically as:

$$Gp = BW/R \tag{1}$$

where, BW = RF Bandwidth, and R = data rate in bits/second. The baseband signal is spread out to BW over the channel. Then at the receiving end, the signal is de-spread by the same amount by a correlation with a desired signal generated by the spreading technique. When the received signal is matched to the desired signal the baseband/information signal is retrieved.

Direct sequence spread spectrum (DSSS) is probably the most widely recognized form of spread spectrum. The DSSS process is performed by effectively multiplying a RF carrier and a pseudo-noise (PN) digital signal. First the PN code is modulated onto the information signal using one of several modulation techniques (e.g. BPSK, QPSK, etc). Then, a mixer is used to multiply the RF carrier and PN modulated information signal as shown in Fig. 2. This process causes the RF signal to be replaced with a very wide bandwidth signal with the spectral equivalent of a noise signal. The signals generated with this technique appear as noise in the frequency domain. The wide bandwidth provided by the PN code allows the signal power to drop below the noise threshold without loss of information.

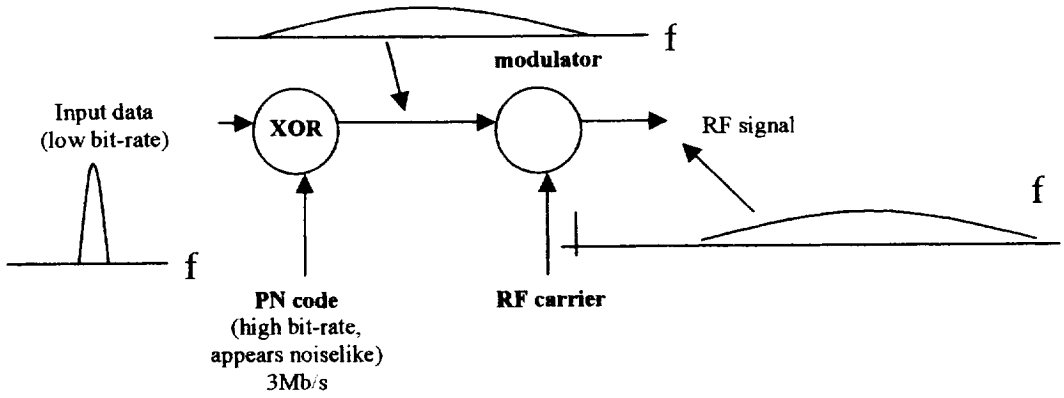

Figure 2 Schematic diagram of a DSSS transmitter

The demodulation process (for the BPSK case) is then simply the mixing/multiplying of the same PN modulated carrier with the incoming RF signal as shown in Fig. 3. The output is a signal that is a maximum when the two signals exactly equal one another or are "correlated." The correlated signal is then filtered and sent to a BPSK demodulator.

The bandwidth in DSSS systems is often taken as the null-to-null bandwidth of the main lobe of the power spectral density plot. The half power bandwidth of this lobe is 1.2 Rc, where Rc is the chip (PN code) rate. Therefore, the bandwidth of a DSSS system is a direct function of the chip rate; specifically 2Rc/R. This is just an extension of the previous equation for Gp. It should be noted that the power contained in the main lobe comprises 90 percent of the total power. This allows a narrower RF bandwidth to accommodate the received signal with the effect of rounding the received pulses in the time domain.

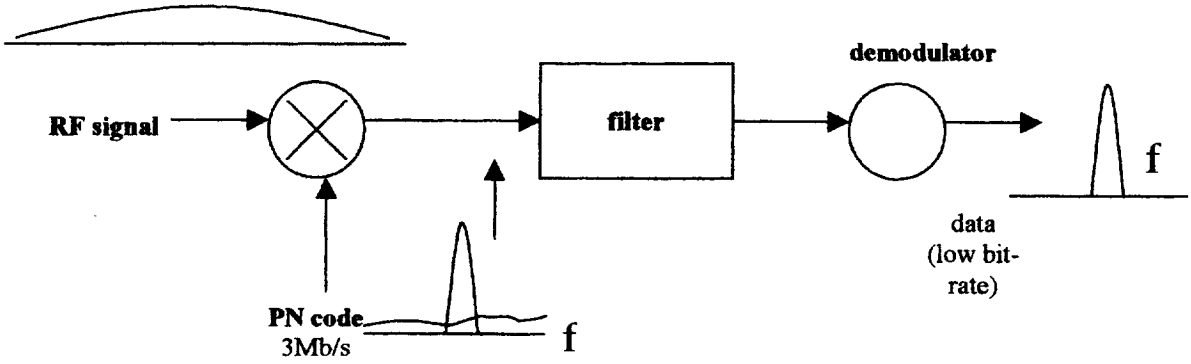

Figure 3 Schematic diagram of a DSSS receiver

The PN code is important because signals generated with different codes will not generally interfere. Actually, interference from multipath signals can result in severe interference. Therefore, correlated codes are used that are designed to be robust to multipath interference. Gold codes are often used because they have low crosscorrelations with other codes as well as low autocorrelation at nonzero shifts[4].

4.0 High-alphabet encoding

Currently, flight termination is provided by an analog FM system. Messages are encoded using a series of tones in what is known as a high-alphabet scheme. For use with TDRSS, the system will be digital.

Current system

There are 7 tones plus 1 pilot tone. The pilot tone is not used in the alphabet. Each character consists of two tones. Because the tones are sequence independent, the number of characters in the alphabet is

$$7^2 - \sum_{i=1}^{7} i = 21. \quad (1)$$

Each message consists of 11 characters. Because the message is sequence dependent, there are $21^{11} = 3.5 \times 10^{14}$ possible messages. A message is transmitted in 111.4mS, and the start between two messages is 180mS, for a rate of 5.5 messages/sec.

Digital analog of current system

There are two ways to directly implement the current system digitally. The first is to represent each character by five bits. Then, a message would consist of 5 bits/character x 11 characters = 55 bits.

Examining the number of messages, $\log_2 3.5 \times 10^{14} \approx 50$ bits are needed to represent all messages. Therefore, approximately 50-55 bits can be used to replace the high-alphabet method in a digital system. Note that the number of bits do not include any dead spaces or headers between characters or messages.

5.0 Data rates and results

A link budget analysis of the TDRSS forward and reverse links have already been performed.[1] However, it's not clear where all the parameters came from, and some may be added or changed for more detailed analysis. Therefore, we examined the bit-rate available for a given link margin. This allows the bit-rate to be dependent on only two parameters, the link margin, and the received signal-to-noise ratio (SNR) as,

$$\text{SNRin} + \text{Gp} - \text{SNRreq} = \text{Link margin (dB)}, \quad (3)$$

where SNRin is the RF input SNR, and SNRreq (4.2 dB), is the required SNR for a BER=10^{-5}, rate ½ code, BPSK modulation, Viterbi decoding with 32-bit path memory.[5] The value Gp is the process gain of the receiver in decibels which is

$$\text{Gp} = 10 \log (\text{BW/R}), \quad (4)$$

where BW = 6MHz for the ITT Industries Low Power Transceiver.

The bit-rate as a function of link margin is shown in Fig. 3. We considered link margins from 5 dB to 20 dB, and received SNRs of –30 dB to –40 dB. Note that a GPS receiver operates routinely at –30.5 dB SNR.

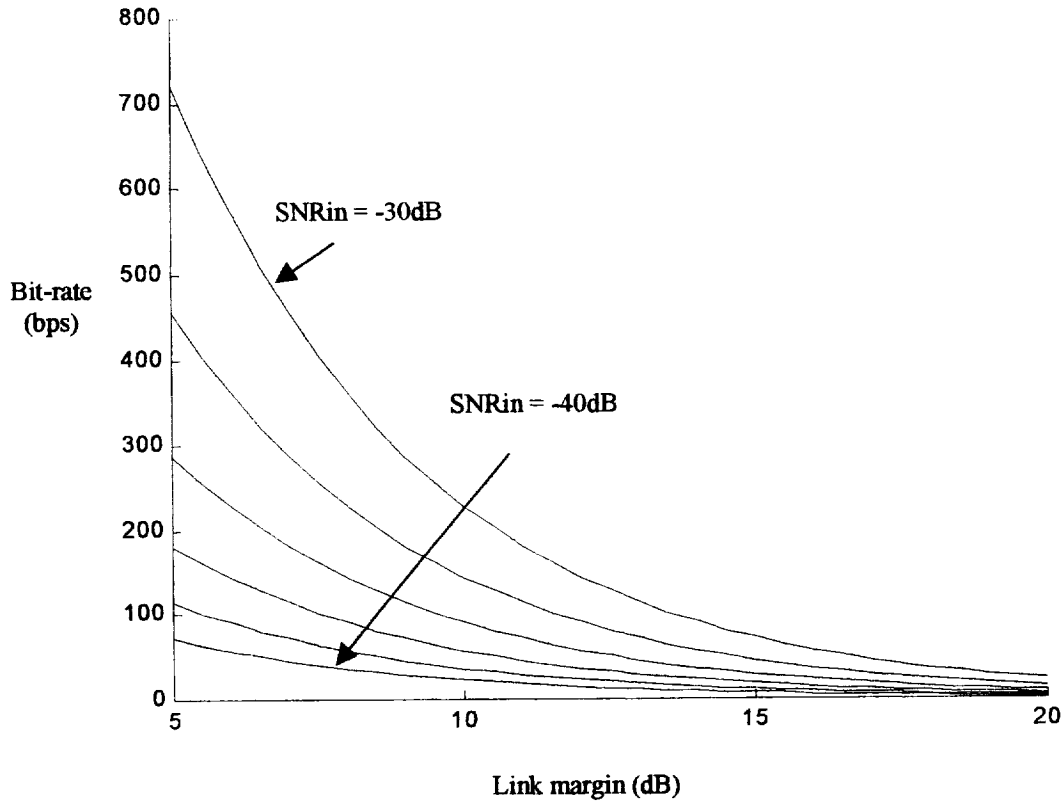

Figure 3 Bit-rate as a function of link margin for fixed receiver power

The graphs show that for a given SNRin, the bit-rate decreases as the link margin increases. This means that for a fixed amount of power, increasing the link margin decreases the bit rate. For a fixed input SNR, the data rate may be decreased to increase the link margin. Data rates between 25 and 300 bps are possible for a variety of parameters. Increasing the SNRin allows an increase in the data rate for the same link margin. Figure 4 shows the same data as in Fig. 3, but it is graphed as with respect to SNRin for different values of link margin.

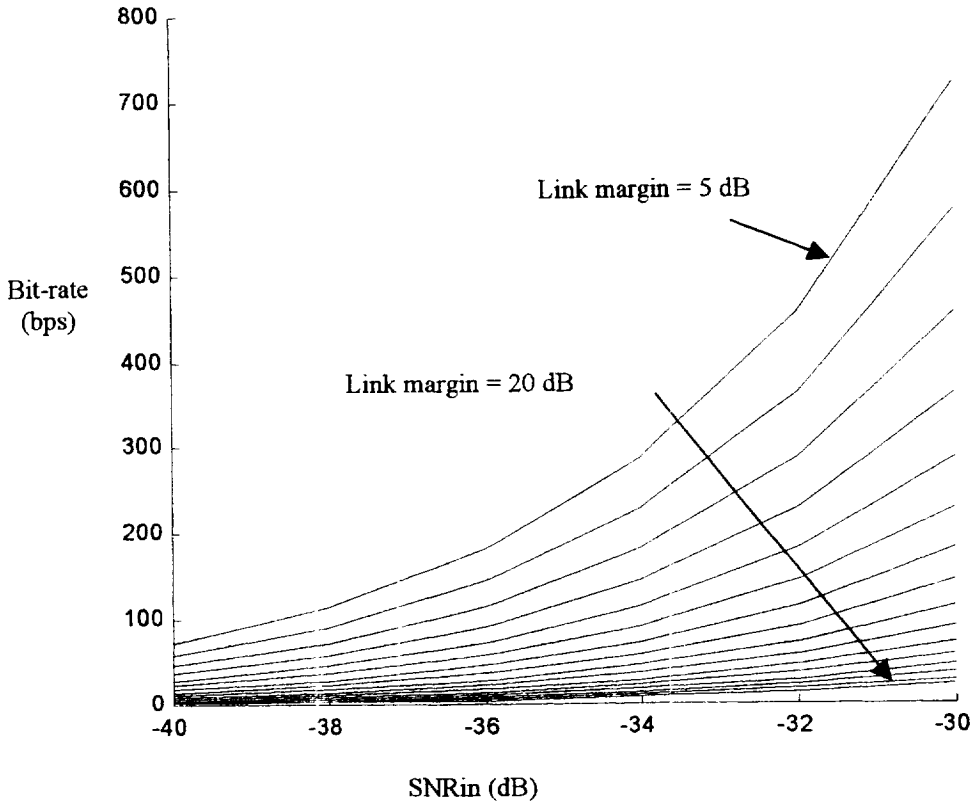

Figure 4 Bit-rate as a function of SNRin for different link margins.

Message rate

We can determine the equivalent message rate of the digital system from the graphs above. The data rata can be determined from,

$$\text{Bit-rate (bits/sec)} = \text{bits/message} \times \text{messages/sec}$$

$$= [(50 + \text{header}) \times (2 \text{ from encoding})] \times 5.5 \text{ messages/sec}$$

$$= 704 \text{ bits/sec.} \qquad (6)$$

This assumes a 14-bit header, and the bit-rate in increased by a factor of 2 due to convolutional encoding.

6.0 Conclusion

We found that a flight termination method using the digital spread-spectrum system available with the TDRSS system can meet the requirements for bit-rate and SNR. Bit-rates in the vicinity of 100-200 bps seem to the most probable with link margins in the vicinity of 10 dB. Increasing the received SNR, or lowering the bit-rate would be

ways increase the link margin. Decreasing the link margin or increasing the received SNR would be ways to increase the data rate.

7.0 References

1. J. A. Smith, T. Sobchak, and J. Walker, "NASA space network (SN) support for range safety: Concept and feasibility study," *NASA doc. 450-RSOPSCON-SN* (May 1998)

2. **http://nmsp.gsfc.nasa.gov/tdrss/**

3. **http://www.cwt.vt.edu/**

4. R. Gold, "Optimal binary sequences for spread spectrum multiplexing," *IEEE Transactions on Information Theory*," vol. 13, 619-621 (1967)

5. B. Sklar, "Digital Communications, Fundamentals and Applications," PTR Prentice Hall:New Jersey (1988)

Appendix

A Simulink model (tdrss.mdl) has been developed for the TDRSS system. The model is not complete, but currently works correctly. Each section is discussed below. Probably the use of the CDMA Blockset would be a better approach; this was not available during most of this effort.

Commands

Two blocks read an encoded message and a tone message that are contained in the files message1.m, and tone.m. They are multiplexed before going into the transmitter. It has been discussed that the tone message is not really needed.

Transmitter

The transmitter primarily consists of a convolutional encoder, a multiplexer to multiplex the 2 bit output of the encoder, and a BPSK modulator. The encoder uses the somewhat industry standard parameters of, feedforward encoding, constraint length = 7, and a code generator (octal) of [171 133].

Channel

Two blocks are used for the channel. They are for additive white Gaussian noise, (AWGN), and Rayleigh fading.

Receiver

The receiver combined the modulated PN code with the received signal, and demodulates and decodes the result. The decoding uses an industry standard Viterbi decoding. The memory is set to 50, but 32 may be a more appropriate number. It probably makes little or no difference. The hard decision may also be replaced with a soft decision.

Pilot Tone BER

The output signal is downsampled to separate the tone and message signals. The BER is currently measured for the tone signal only.

2000 NASA/ASEE SUMMER FACULTY FELLOWSHIP PROGRAM

JOHN F. KENNEDY SPACE CENTER
UNIVERSITY OF CENTRAL FORIDA

Using Neural Networks in Decision Making for a Reconfigurable Electro Mechanical Actuator (EMA)

Carl D. Latino
Associate Professor
Oklahoma State University
Stillwater Oklahoma

KSC Colleague
Jose Perotti

ABSTRACT

The objectives of this project were to demonstrate applicability and advantages of a neural network approach for evaluating the performance of an electro mechanical actuator (EMA). The EMA in question was intended for the X-37 Advanced Technology Vehicle. It will have redundant components for safety and reliability. The neural networks for this application are to monitor the operation of the redundant electronics that control the actuator in real time and decide on the operating configuration. The system we proposed consists of the actuator, sensors, control circuitry and dedicated (embedded) processors. The main purpose of the study was to develop suitable hardware and neural network capable of allowing real time reconfiguration decisions to be made. This approach was to be compared to others methods such as fuzzy logic and knowledge based systems considered for the same application. Over the course of the project a more general objective was the identification of other neural network applications and the education of interested NASA personnel on the topic of Neural Networks.

INTRODUCTION

For safety and reliability reasons the EMA's used on the X-37 Advanced Technology Vehicle will be designed with built in redundancy. These EMA's operate flight surfaces and thrust vectors. There are nine such EMA's, each provided with some degree of redundancy intended to ensure system functionality. If components of the primary system should fail or become unreliable, a decision must be made and ability to switch over to a backup system must occur in milliseconds. This requires the monitoring system to monitor, process, decide and affect switch over, if necessary, in a very short time period. Intelligent, embedded systems are the wave of the future. The actual X-37 EMA to be evaluated was not available. We did, however, acquire a linear actuator, control box and combined these with a PC with Lab View to have a platform for further system development. The actuator was connected to a simulated flight surface for demonstration purposes. As configured, the actuator could be controlled by commands given in Lab View. The A-B Servo Drive System operated in closed loop with the actuator using a PID controller. The system is shown in Fig. 1

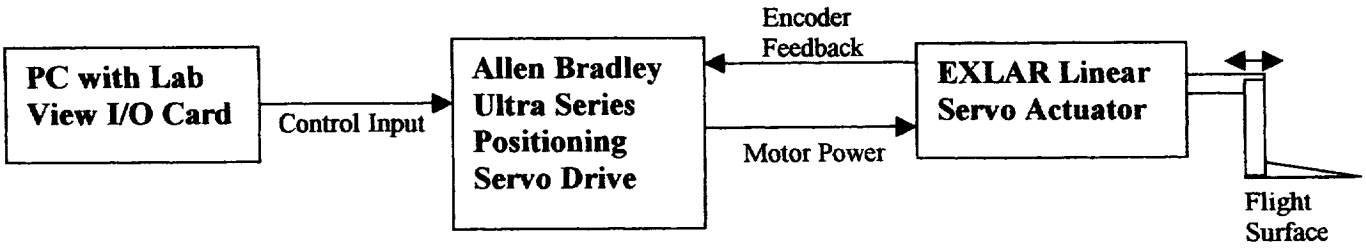

Block diagram of laboratory setup
Fig. 1

NEURAL NETWORKS

Neural networks are systems that can be trained to solve a large class of problems. One such application was demonstrated in the summer of 1998 for monitoring the health of the Gaseous Hydrogen Flow Control Valve. The system employed feed forward neural networks, embedded processing and software development tools. The EMA has added complexity in that temporal information is also a factor. Information about inputs and corresponding output conditions are needed. When sufficient input/output pairs have been given to the network, it can be trained, off line, using the commercially available Matlab Neural Network Toolbox. Once trained, the network gives outputs each time it is presented with the inputs. Challenging aspects of the problem include the selection of suitable network structures and a selection of input/output pairs. A practical solution is to replace the A-B controller box with a processor board capable of both control and neural network functions. This approach is similar to the 1998 GH2FCV project.

WHY NEURAL NETWORKS?

There are many different ways of approaching this problem. Why use NN? The NN solution is viable in this case because it can learn the behavior of the EMA without the need of accurate models. The NN, however, must be shown what constitutes nominal and anomalous behaviors. The NN must be given information regarding the different operating conditions and what they mean. For the sake of simplicity assume that all but one input variable are kept fixed. Varying this variable and observing the resultant curve trace gives the NN information about which portions of the curve are changed and by how much. For example, if an input parameter value is increased or decreased, it is reasonable to assume that a related output will increase or decrease by a related amount. The change in input may be nonlinear and have effects on the outputs that are not obvious. What effects do input value changes have on the outputs and by how much? If multiple input variables change, the closed form solution can quickly become intractable. These problems may be difficult to solve in closed form, but often not with neural networks. Neural networks can broaden the safe operating region, quantify critical parameters and reduce the occurrence of false alarms. Theoretically, if fault conditions and combinations of faults can be simulated, and if these cause unique outputs, the properly trained NN can tell what condition(s) occurred. A demonstration of such a system was made during the summer visit in 1998. The system combined dedicated hardware and software to evaluate the health of the Gaseous Hydrogen Flow Control Valve using feed forward neural networks. Indications are that the EMA is one of many suitable candidate for NN. Training the network means finding a set of weights and biases for each neuron in the network. Training is an operation which, if it converges, leads to the desired network. Assuming that a 5-N-2 Feed Forward NN has been selected, where N is the number of neurons in the hidden layer, the network is trained. Since the network has 5 inputs and N neurons, 5 x N weight values are needed to connect each input with each neuron in the hidden layer plus N more values for the bias. The five outputs are the inputs to the two neurons of the output layer. This requires N x 2 weights plus 2 more biases. In summary, the number of parameters to be determined is $5 \times N + 5 + N \times 2 + 2$. In general, for a NN with S input, N hidden layer neurons and Z output neurons the number of parameters that need to be determined are $= (S + Z) \times (N + 1)$. Therefore for a 5-6-2 FF NN there are $(5 + 2) \times (6 + 1) = 49$ parameters.
Without effective training procedures, finding the optimal solution for even small problems like these is difficult. Large problems quickly become prohibitive. Matlab and the Neural Network Toolbox are commercially available software packages capable of easily performing these tasks. Once the network has been trained, it is ready to evaluate the operation of the system in question. It should be stressed that the network is valid only if properly trained. It may be necessary to train a network for each EMA, if they are sufficiently different in operation. Testing the EMA with the trained NN is then automatic. The data is collected and pre processed to obtain the inputs for the NN. These values are then applied to the trained NN inputs. The output will then return information about the health of the EMA. The network just described generates a multi dimensional surface, which defines the valve for a given range of operating conditions. The network can execute quickly since it does not need to adapt once trained.

HOW IS THE NN IMPLEMENTED?

The NN can be implemented in software on a PC or other computer. It can also be implemented in hardware via custom VLSI or some type of PAL or PLA. Implementing a single neuron requires a device capable of performing floating point multiply operations, additions and transfer functions. A complex NN can, however, be realized by modeling a single, flexible structure neuron. Many neurons can then be simulated by repeated application of the neuron algorithm. A decision must be made regarding the issue of speed versus circuit complexity. If multiple neurons are built in hardware, higher operating speeds are possible. If fewer hardware neurons are used speed is compromised but circuit complexity is reduced. The optimal choice rests with the problem at hand. Building such a system, however, requires more than 10 weeks to develop. A neuron has S inputs and one bias, which may be considered another input with input value 1. A three input neuron is illustrated in Fig 2.

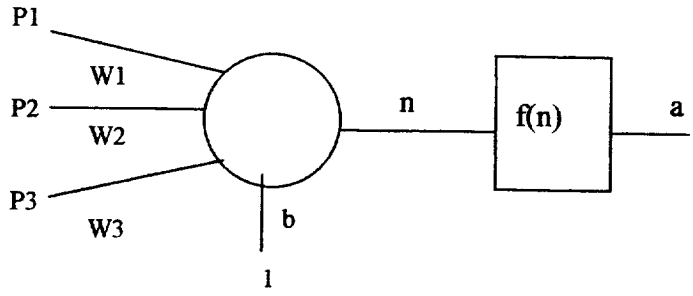

$$n = \sum_{i=1}^{3} w_i * p_i + b, \qquad a = f(n),$$ Where f(n) may be any desired function.

Three input neuron
Fig. 2

The inputs are multiplied by their associated weights and added together. There are S+1 such multiplications whose results must then be added together. This result is then fed through a transfer function. For the above figure assume b = 0.5, $p = [\,p1\ p2\ p3]^T = [\,1\ 2.5\ 4]^T$, w = [w1 w2 w3] = [0.2 –1.5 0.5] and f(n) = (exp(n)-exp(-n))/ (exp(n)+exp(-n)) then n = 1*0.2 + 2.5*(-1.5) +4*0.5 + 0.5 = -1
exp(-1) = 0.3679, exp(1) = 2.7183 therefore
f(n) = (0.3679-2.7183)/ (0.3679+2.7183) = -2.3504/3.0862 = -0.7616
The neuron output is obtained by performing three multiplies, the results are added together in addition to the bias value. This is the value used for the transfer function. The transfer function can be stored in a look up table to maximize execution speed. For this specific transfer function the output of the neuron is limited to a range of –1 to +1.

FUTURE OBJECTIVES

The reconfigurable EMA (REMA) seems like a viable application for neural networks. Often during flight, split second critical decisions must be made. In some cases a wrong decision or failure to act may be fatal. To deal with system complexities, and improve reliability, critical systems are often redundant and intelligent. The REMA is an Electro Mechanical Actuator with embedded intelligence and redundant electronics systems. The actuator controls flight surfaces, rocket thrust directions and thus are flight critical. Monitoring primary and secondary systems allows the selection of the "healthier" one to control the actuator. The appropriate one must be put on line within a short time of when the malfunction is detected. This implies the ability to monitor, evaluate in real time, make determinations of system conditions and act appropriately. An intelligent monitoring system needs a data acquisition system, signal processing capability and an ability to command system configuration. A system able to replace failing or defective components with ones that work has many real applications in deep space probes and long duration flights. Identifying one such system and building a demonstration unit seems like the next logical step.

CONCLUSIONS

The problem of using NN to solve the problem of evaluating a system requires the resolution of numerous issues. First and foremost the problem must be suitable. These include selecting a proper NN structure, training the neural network and ensuring that the solution is properly generalized. NN allows the evaluation of complex systems by letting the network learn by observation. This eliminates the need for the user to generate a complex system model. To evaluate a series of unique valves, such as the GH2FCV the same NN structure was used but each valve had its own specific values for weights and biases. The training is done off line allowing monitoring to occur in real time. Neural networks are applicable to a large class of complex problems. The Intelligent Electro Mechanical Actuator is an ideal application of embedded intelligent systems such as neural networks. One major obstacle to the development of such a system is the lack of understanding of what neural networks are their capabilities and limitations. A better understanding in this area will undoubtedly identify many practical applications of importance to NASA and contractors.

REFERENCES

[1] M. Hagan, H. Demuth and M. Beale, *Neural Network Design*, Boston, MA:PWS Publishing Company, 1996

[2] C. Latino, *Using Neural Networks for Evaluating the Health of the Gaseous Hydrogen Flow Control Valve*, 1998 Report

[3] Allen-Bradley Ultra Series (Catalog Numbers 1398-xxx)

2000 NASA/ASEE SUMMER FACULTY FELLOWSHIP PROGRAM

JOHN F. KENNEDY SPACE CENTER
UNIVERSITY OF CENTRAL FLORIDA

EVALUATION OF THE PERFORMANCE OF THE MARS ENVIRONMENTAL COMPATIBILITY ASSESSMENT ELECTROMETER

James G. Mantovani
Assistant Professor
Florida Institute of Technology
Department of Physics and Space Sciences
Melbourne, FL 32901

KSC Colleague: Carlos I. Calle

ABSTRACT

The Mars Environmental Compatibility Assessment (MECA) electrometer is an instrument that was designed jointly by researchers at the Jet Propulsion Laboratory and the Kennedy Space Center, and is intended to fly on a future space exploration mission of the surface of Mars. The electrometer was designed primarily to study (1) the electrostatic interaction between the Martian soil and five different types of insulators, which are attached to the electrometer, as the electrometer is rubbed over the Martian soil. The MECA/Electrometer is also capable of measuring (2) the presence of charged particles in the Martian atmosphere, (3) the local electric field strength, and (4) the local temperature. The goal of the research project described in this report was to test and evaluate the measurement capabilities of the MECA/Electrometer under simulated Martian surface conditions using facilities located in the Labs and Testbeds Division at the Kennedy Space Center. The results of this study indicate that the Martian soil simulant can triboelectrically charge up the insulator surface. However, the maximum charge buildup did not exceed 18% of the electrometer's full-range sensitivity when rubbed vigorously, and is more likely to be as low as 1% of the maximum range when rubbed through soil. This indicates that the overall gain of the MECA/Electrometer could be increased by a factor of 50 if measurements at the 50% level of full-range sensitivity are desired. The ion gauge, which detects the presence of charged particles, was also evaluated over a pressure range from 10 to 400 Torr (13 to 533 mbar). The electric field sensor was also evaluated. Although the temperature sensor was not evaluated due to project time constraints, it was previously reported to work properly.

EVALUATION OF THE PERFORMANCE OF THE MARS ENVIRONMENTAL COMPATIBILITY ASSESSMENT ELECTROMETER

James G. Mantovani

1. INTRODUCTION

The Mars Environmental Compatibility Assessment (MECA) Electrometer was designed jointly by researchers at the Jet Propulsion Laboratory and Kennedy Space Center to be a flight instrument on a future unmanned Mars mission (originally scheduled for Mars 2001) [1]. The MECA/Electrometer was designed primarily to characterize the electrostatic properties of insulating materials at the surface of Mars. The materials were selected for their known application on space missions. The five insulators chosen for the MECA/Electrometer were: Fiberglass/Epoxy, Polycarbonate (known as Lexan ™), Polytetraflouroethylene (Teflon ™), Rulon J ™, and Polymethylmethacrylate (Lucite ™ or PMMA).

The purpose of the research described in this report was not specifically to study the electrostatic properties of the five types of insulating materials mounted on the electrometer. Rather, the goal of the research was to test and evaluate the MECA/Electrometer and the four types of measurement sensors it has onboard: (1) triboelectric sensor array, (2) ion gauge (charged particle sensor), (3) local electric field sensor, and (4) temperature sensor.

When testing the triboelectric sensor array (tribo), we studied the degree to which the materials became electrically charged when rubbed with Martian soil simulant (JSC Mars-1) either at low CO_2 pressure inside a vacuum chamber, or at atmospheric pressure using dry air in a glovebox. Ottawa quartz sand and, at the end of the project, Lunar soil simulant were also studied as abrasive mediums that could triboelectrically charge the surfaces of the insulating materials.

The ion gauge (IG) was tested using a reliable source of atmospheric ions. The IG output was studied as a function of CO_2 pressure inside a small vacuum chamber.

We tested the electric field sensor (ELF) by applying a fixed voltage to a flat metal electrode that was placed above the ELF electrode. These measurements were conducted at various CO_2 pressures inside a vacuum chamber.

Finally, the temperature sensor could not be studied because the Mars vacuum chamber that could provide temperature control was under construction in the Labs and Testbeds Division at KSC. The temperature sensor was observed to work properly at room temperature, where all of our measurements were conducted.

The data and results of our testing of the MECA/Electrometer are presented in the following sections. We conclude with a summary of our evaluations of the MECA/Electrometer, and our recommendations for how MECA/Electrometer's performance might be enhanced.

2. RESULTS AND DISCUSSIONS

In this section, we describe the four types of measurement sensors contained within the MECA/ Electrometer. Data taken with the sensors is presented and sensor performance is discussed.

2.1 EVALUATION OF THE TRIBOELECTRIC SENSORS

The triboelectric sensor array consists of five insulating materials placed above metal electrodes that are connected to five independent electrometer circuits, one circuit for each type of insulator. The tribo sensors are housed inside the MECA/Electrometer, whose case is made of titanium of volume ~50 cm^3, total mass of ~50 g, and power consumption of <250 mW. Figure 1 contains a picture of the electrometer, and shows how it is mounted to the heel of the Mars lander's scoop.

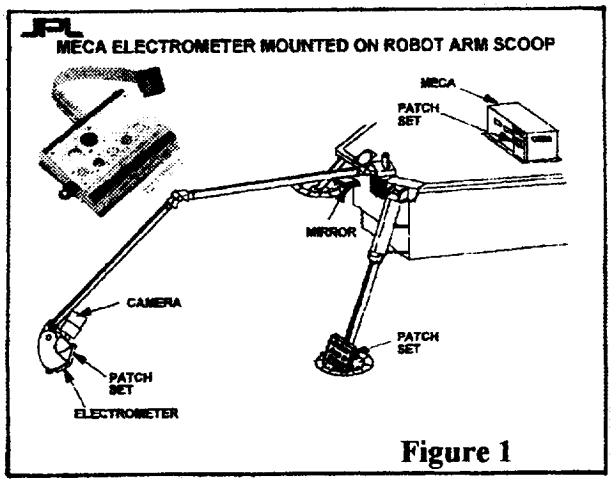

Figure 1

The five circular patches shown in Fig. 1 are the five types of insulators, below which are the electrometer circuitry that measures the amount of electric charge that develops on the insulator surfaces after the scoop drags the electrometer through the Martian soil. The two openings shown above the five insulators in the electrometer photo are the local electric field sensor (ELF) on the left, and the ion gauge (IG) on the right. The temperature sensor is a dedicated integrated circuit chip that is mounted inside the case and is not shown in the photo of the MECA/Electrometer.

The electronics contained within the MECA/Electrometer housing have been described in detail elsewhere [2], and will only be discussed as needed in this report.

The tribo sensor circuit's output voltage, V_{out}, is proportional to the electric charge that develops on the surface of the insulator. This is shown schematically in Fig. 2. The overall gain of the tribo circuit (not shown) is 4x. Thus, $V_{out} = 4Q/C$, where the fixed capacitor C = 1 nF. The charge Q on the surface of the insulator will be given by $Q = V_{out}/(4x10^9)$ C (C = Coulomb). Hence, the tribo circuit's gain is 0.25 nC/V as measured at the output. If the A/D converter has a 2mV/bit resolution, then the device can detect electric charge as small as 0.5 pC, which is numerically equivalent to $3.1x10^6$ electrons or protons.

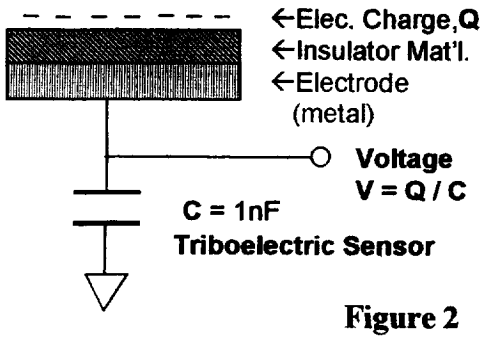

Figure 2

2.1.1 Electrostatic Rubbing Experiment

The tribo sensors were tested using two methods. The first method, described here, used a "rubbing" machine that allowed the MECA/Electrometer to be dragged through soil with the tribo sensors face down in the soil. The horizontal motion of the electrometer was under computer control, which allowed the speed and travel distance to be set separately. A speed of 10 mm/sec was suggested as the speed at which the Mars Lander will drag the electrometer through the Martian soil. The size of the rubbing machine did not allow us to perform this type of experiment in a low pressure CO_2 atmosphere in the small vacuum chamber. However, we were able to conduct this rubbing experiment inside a plastic glovebox, into which dry air flowed so as to reduce the humidity within the box. The relative humidity could be brought as low as 30% by continuously flowing bottled dry air into the box. An air ionizer was used to neutralize the charges that develop on the tribo materials after each measurement was made. Data was taken using the Parallax Basic Stamp II™ controlled by a PC laptop running MS-Windows 95™.

Using this experimental setup, the MECA/Electrometer could be rubbed over various types of soils, including quartz sand (SiO_2), Martian soil simulant (JSC Mars-1) [3], and Lunar soil simulant [4]. Only Martian soil simulant was investigated using the rubbing machine. A typical graph of the tribo sensor output voltages versus time are shown in Figure 3. This data was taken at atmospheric pressure in dry air at a relative humidity of 43% with the MECA/Electrometer being rubbed over the Martian soil simulant at 10 mm/s. The time between points is 1.4 seconds.

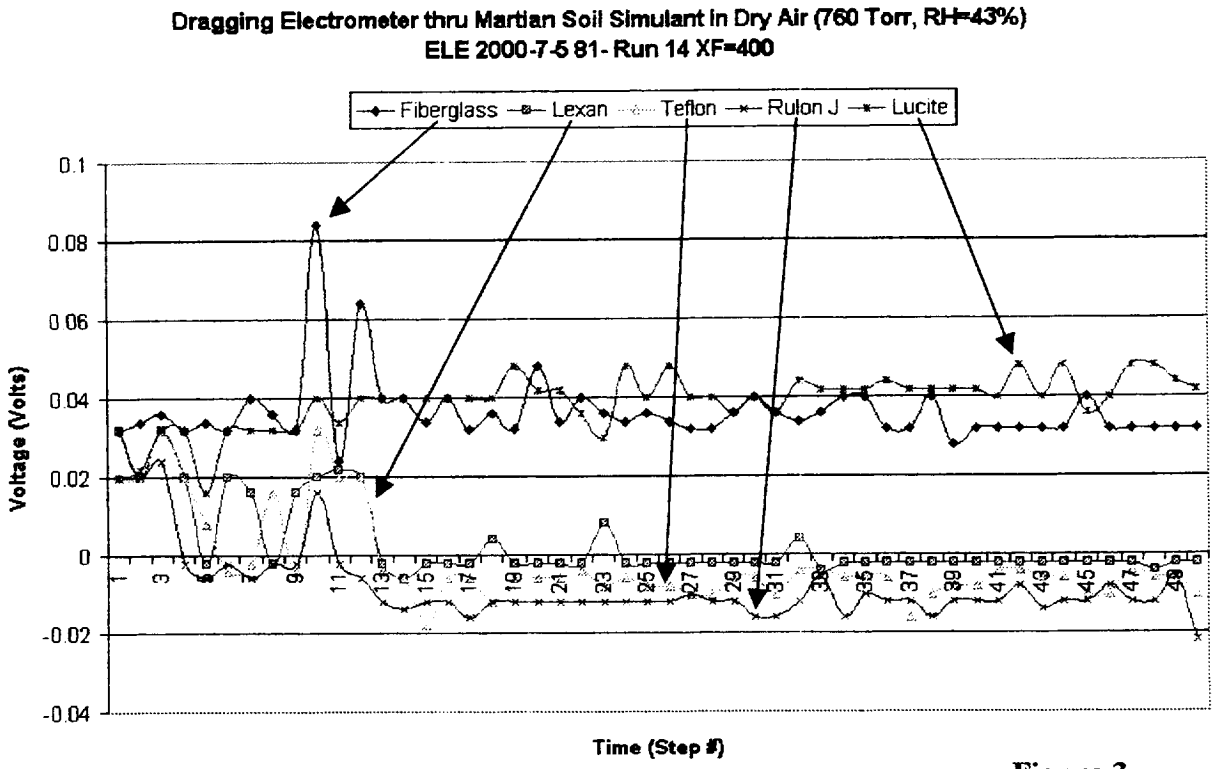

Figure 3

Figure 3 indicates that only small amounts of triboelectric charging will occur when the Martian soil simulant is used. The Rulon J™ insulator appears to charge up the most. The tribo voltage for this material changed by -0.04 V, which corresponds to a charge buildup of –10 pC. This is close to the A/D converter resolution of 0.5 pC/bit.

2.1.2 Electrostatic Rocking Experiment

Since the rubbing machine could only be operated in dry air at atmospheric pressure, an alternative method of triboelectrically charging the insulators was needed that would work at low CO_2 pressures. A rotary feedthrough mounted on a vacuum chamber was used to rotate an aluminum box containing Martian soil simulant back and forth. The MECA/Electrometer was mounted flush with the bottom of the box, and the tribo sensors were facing upwards. As the box was manually rocked back and forth, the soil was able to flow over the tribo sensors and cause the insulators to charge up. Using this experimental setup, it was possible to place 50 g of Martian soil simulant in the box. The vacuum chamber was evacuated of air using a mechanical pump. When a pressure of 1 Torr was reached, CO_2 from a gas cylinder was allowed to flow into the vacuum chamber through a microvalve mounted on the vacuum chamber. This microvalve and a gas regulator attached to the CO_2 cylinder allowed sufficient control of the flow of CO_2 into the chamber that any desired CO_2 pressure could be maintained. Figure 4 shows the tribo sensor responses (data acquired at 1.4 sec time intervals) for the five insulators at 7 Torr CO_2

pressure when Martian soil simulant is used in the rocking experiment. An air ionizer was placed in the vacuum chamber to neutralize any charge buildup on the tribo material's surfaces.

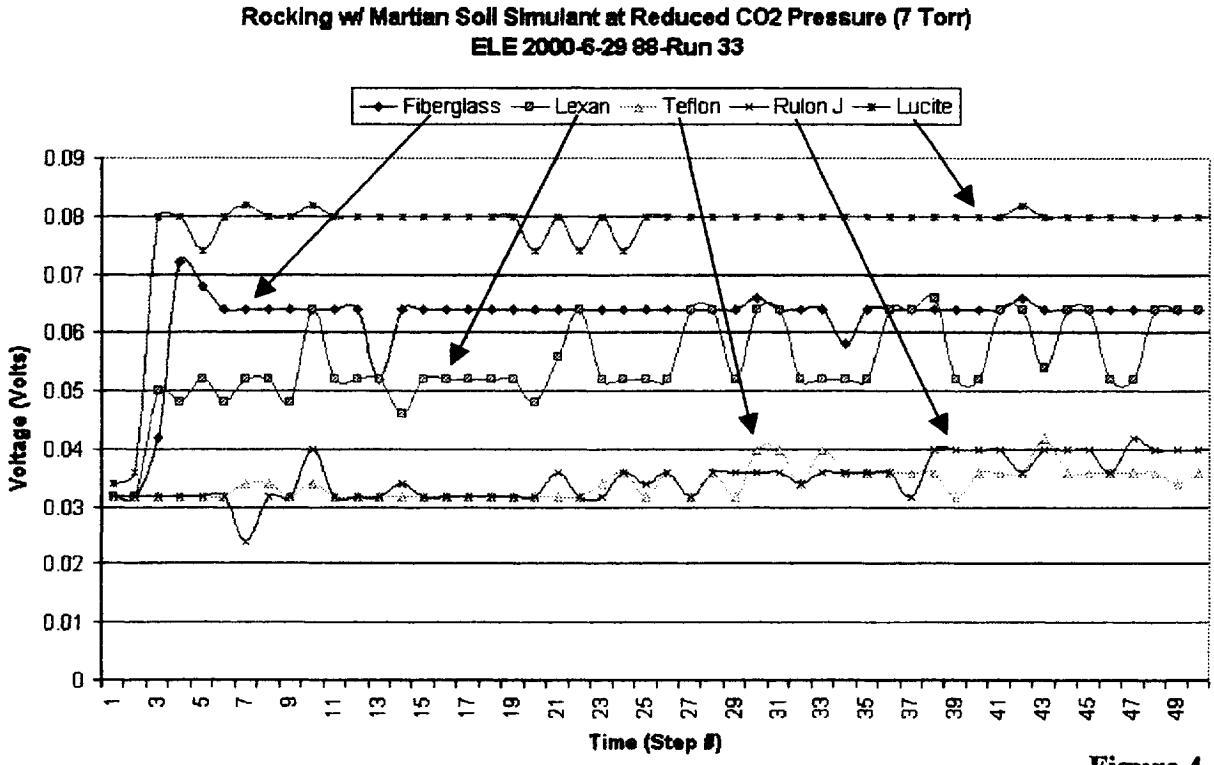

Figure 4

This rocking experiment was repeated at increasing CO_2 pressures with the Martian soil simulant and little change in the tribo sensor responses was discerned. Different and larger responses were obtained when Ottawa quartz sand was used. Whereas the Martian soil simulant tended to charge the tribo sensors positively, the Ottawa sand charged the same materials negatively, or not at all. Lunar soil simulant was also used in the rocking experiment, but only in dry air at atmospheric pressure in the glovebox due to time constraints and lateness in arrival of the lunar soil simulant.

2.2 EVALUATION OF THE ION GAUGE

The ion gauge measures the presence of charged particles and atmospheric ions in the vicinity of the MECA/Electrometer. The ion gauge circuit is basically a current-to-voltage converter as shown in Figure 5. In the actual circuit, the electrode is held at either a positive or a negative

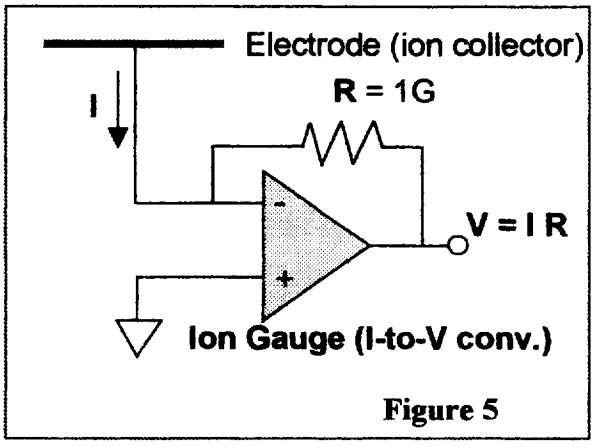

Figure 5

voltage. This causes negative or positive charges, respectively, to accelerate towards the electrode, thus producing the electric current that the circuit detects. The ion gauge was tested by introducing a weak Am 241 source at a fixed distance above the electrode. The source produces alpha particles that ionize any CO_2 molecule they collide with. In order to detect the presence of both positive and negative charges, the voltage at the electrode was cycled between the values +3V, 0V, -3V, and 0V. A typical ion gauge sensor response is shown in Figure 6 with the data taken at 5 sec time intervals.

From the actual ion gauge circuit, the overall circuit gain was calculated to be 42.2 pA/V. In Figure 6, an output voltage of 420 mV would thus correspond to an ion current of 18 pA. If we assume an A/D converter resolution of 2 mV/bit, the minimum current sensitivity of the ion gauge is found to be 84 fA, which exceeds the input bias current of the operational amplifier.

The dependence of the deduced ion gauge current on CO_2 pressure is shown in Figure 7. Ion current values due to both positive and negative currents are shown.

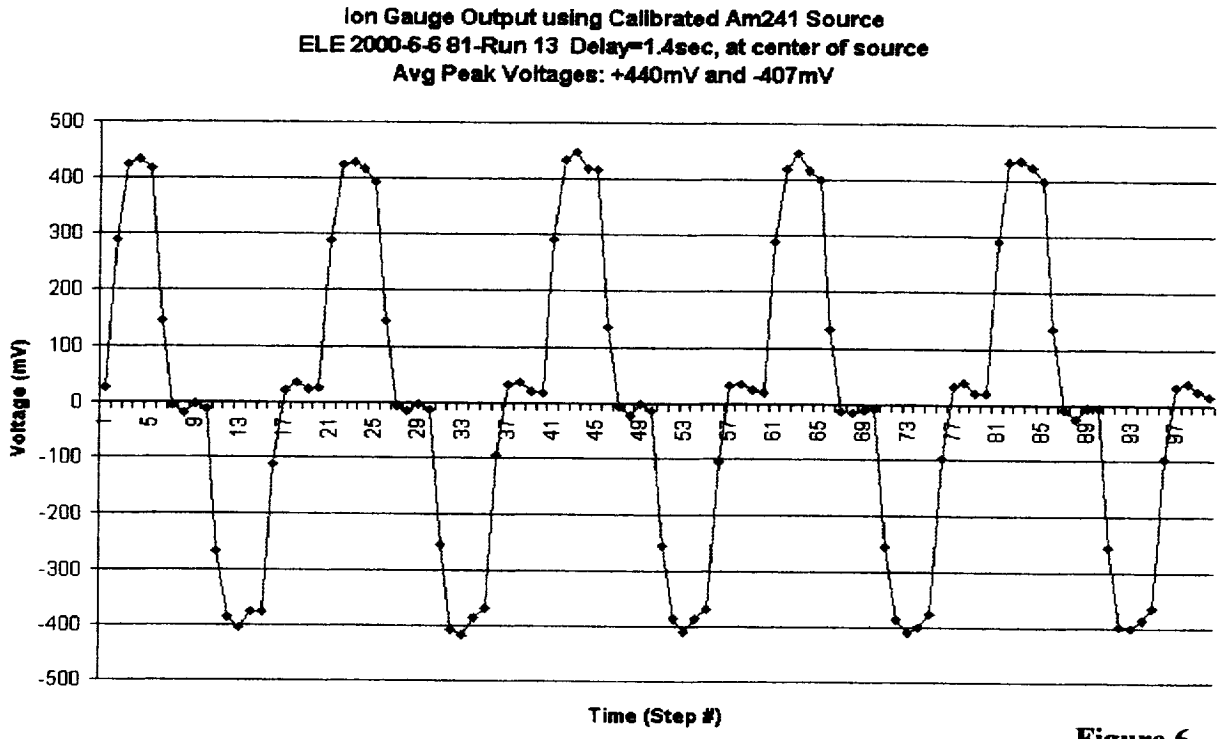

Figure 6

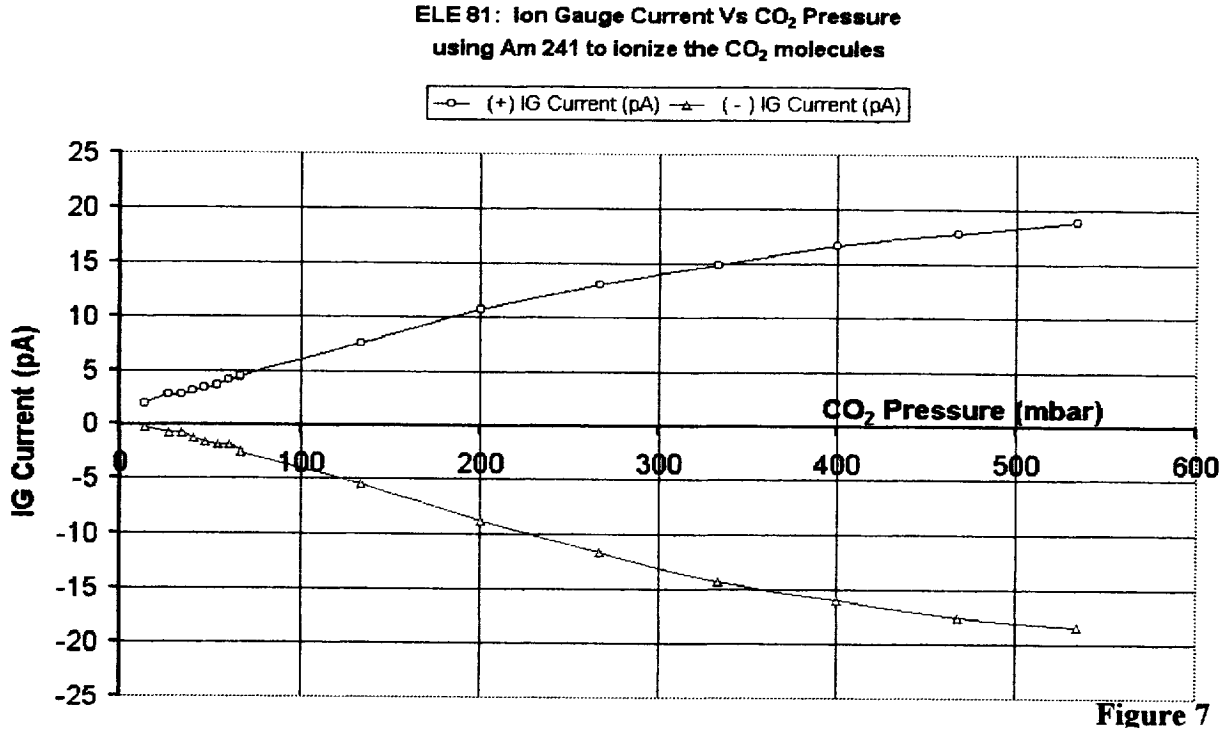

Figure 7

2.3 EVALUATION OF THE LOCAL ELECTRIC FIELD SENSOR

The electric field sensor (ELF) circuit is the same as the tribo sensor circuit, except that the insulator is absent from the top of the electrode. To test the ELF, a metal plate at a fixed voltage is placed at a known distance above the electrode. For the MECA/Electrometer, the distance between the plates is approximately 0.3 cm. The ELF sensitivity is calculated using the expression $(V_{plate}/d)/V_{ELF}$ where V_{ELF} is the potential difference between the plate and the electrode. The ELF circuit had a voltage offset of +0.032 V. When +1000 V was applied to the plate, the ELF output voltage was measured to be +0.265 V. And when V_{plate} = -1000 V was used, V_{out} = -0.199 V. After the offset voltage is taken into account, we find $| V_{ELF} |$ = 0.231 V. The sensitivity of the ELF is then calculated to be (1000V)/(0.3cm)/(0.231V) = 14.4 kV/cm / V.

2.4 EVALUATION OF THE TEMPERATURE SENSOR

The temperature sensor was not specifically tested due to project time constraints. All measurements were conducted at room temperature, which appeared to have been measured correctly by the temperature sensor. The Mars vacuum chamber, which will be able to simulate the range of temperatures and atmosphere, was under construction during this project and can be used to test the entire MECA/Electrometer in the future.

3. CONCLUSIONS

Although the rubbing experiment using Martian soil simulant (JSC Mars-1) could not be performed in a low CO_2 atmosphere, the rocking experiment described in Section 2.1.2 could be conducted in either the glove box in dry air, or in the small vacuum chamber in a low CO_2 atmosphere. We found that there was not a significant amount of difference observed in the tribo sensor output using the rocking chamber in a low CO_2 atmosphere or in dry air at atmospheric pressure. This would suggest that if the rubbing experiment had been performed in a low CO_2 atmosphere, then the tribo sensor responses would not be much different than in the dry air environment. The observation that the tribo sensors developed such little electric charge would indicate that the MECA/Electrometer's triboelectric sensor circuitry should be modified to provide a larger gain (increased sensitivity) that would allow the charge buildup to be more accurately measured. From Fig. 3, we see that when the maximum tribo output voltage change is measured to be 0.04 V for Rulon J ™, it appears that as little as (40 mV/ 4096 mV x100%) = 1% of the A/D converter's range is being utilized. If a utilization of 50% of the full range is desired, then the overall tribo circuit's gain should be increased by a factor of 50. Finally, the largest output voltage that could be obtained by vigorously rubbing the tribo materials was 1.5 V, which corresponds to only 18% of the full range of the A/D converter.

The performance of the ion gauge was found to be near ideal. The current sensitivity was calculated to be 42.2 pA/V. That is, if the ion gauge output voltage was measured to be 0.002 V (2mV) corresponding to the bit resolution of the A/D converter, then the ion current would be 84.4 fA, which is very close to the input bias current of the LMC 6044 op amp used in the current-to-voltage converter.

The sensitivity of the local electric field sensor was measured to be 14.4 kV/cm / V. That is, at a plate separation distance of 0.3 cm and with a 1 kV potential difference between parallel plates, the electric field sensor produced an output voltage of 0.231 V.

The temperature sensor consisted of a dedicated integrated circuit chip. Since all experiments that were conducted during this project were at room temperature, the temperature sensor's performance could not be determined.

ACKNOWLEDGMENTS

I would especially like to thank Carlos Calle for inviting me to work with him on this project, and for all of the assistance and support he provided during my stay at KSC. I would also like to thank Martin Buehler, Ray Gompf, and Jeff Rauwerdink for many helpful conversations, and the undergraduate students who helped participate in the research, especially Ellen Groop (Florida Tech) and Aaron Linville (Wilkes University). Finally, I would like to thank Ray Hosler and Cassie Spears of the University of Central Florida, and Cassandra Black of KSC for running an enjoyable summer program for all of the university faculty who participated in 2000.

REFERENCES

[1] M. Buehler, L.-J. Cheng, O. Orient, M. Thelen, R. Gompf, J. Bayliss, J.Rauwerdink, "MECA Electrometer: Initial Calibration Experiments", Inst. Phys. Conf., Ser. No. 163, pp. 189-196, Proceedings of the 10th Int. Conf., Cambridge, 28-31 March 1999.

[2] M.G. Buehler, et al., "From Order to Flight in Eighteen Months: The MECA/Electrometer Case Study", IEEE Aerospace Conference, March 2000.

[3] C.C. Allen, et al., "Martian Regolith Simulant JSC MARS-1", Lunar and Planetary Science Conference XXIV, Houston, TX, 1998.

[4] D.S. McKay, et al., "JSC-1: A New Lunar Regolith Simulant", Lunar and Planetary Science Conference XXIV, Houston, TX, 1998.

2000 NASA/ASEE SUMMER FACULTY FELLOWSHIP PROGRAM
JOHN F. KENNEDY SPACE CENTER
UNIVERSITY OF CENTRAL FLORIDA

ESTABLISHING A GEOLOGIC BASELINE OF CAPE CANAVERAL'S NATURAL LANDSCAPE: BLACK POINT DRIVE

Randall W. Parkinson, Ph.D., P.G.[1]
Florida Institute of Technology, Melbourne, Florida 32901
KSC Colleague: Kelly Gorman, Division of Safety, Occupational Health & Environment

ABSTRACT

The goal of this project is to identify the process responsible for the formation of geomorphic features in the Black Point Drive area of Merritt Island National Wildlife Refuge/Kennedy Space Center (MINWR/KSC), northwest Cape Canaveral. This study confirms the principal landscape components (geomorphology) of Black Point Drive reflect interaction between surficial sediments deposited in association with late-Quaternary sea-level highstands and the chemical evolution of late-Cenozoic sub-surface limestone formations.

The Black Point Drive landscape consists of an undulatory mesic terrain which dips westward into myriad circular and channel-like depression marshes and lakes. This geomorphic gradient may reflect: (1) spatial distinctions in the elevation, character or age of buried (pre-Miocene) limestone formations, (2) dissolution history of late-Quaternary coquina and/or (3) thickness of unconsolidated surface sediment. More detailed evaluation of subsurface data will be necessary before this uncertainty can be resolved.

1.0 INTRODUCTION

The origin of Merritt Island National Wildlife Refuge and Kennedy Space Center's (MINWF/KSC) unique ecosystems can be attributed in large part to the region's distinct geomorphology and associated geologic processes. The goal of this project is to identify the processes responsible for the formation of geomorphic features in the Black Point Drive area of MINWR/KSC, northwest Cape Canaveral (Figure 1). Without a basic knowledge of the origin and evolution of these features, any effort to manage the landscape or restore the function and value of an ecosystem becomes problematic. For example:

---

[1]current address - Coastal Technology Corporation, P.O. Box 361386, Melbourne, Florida 32936-1386

a. What did the *natural* landscape look like before human alteration?
b. What *natural* processes contributed to the formation of this landscape?
c. How do we recognize a *disturbed* landscape?
d. How is success quantified in a restoration or management program?

This project is designed to provide baseline geologic information useful to a land manager charged with maintaining functional ecosystems and restoring those altered by human activity. The decision to focus on Black Point Drive (Figure 1) was based upon (1) logistics and (2) prompt applicability. Much of the landscape in the area is accessible from numerous improved and unimproved roads, making field inspection of points of interest relatively easy. In addition, the information gathered during this project could immediately be applied to an ongoing investigation of wetland management practices funded by the US Environmental Protection Agency (EPA). In due time, other quadrants could be investigated following the format developed herein.

1.1 Objectives

In order to successfully complete this project, 5 objectives were pursued:

a. (1) Review relevant literature, surveys, maps, and aerial photography, and (2) interview field scientists active in study area.

b. Establish (1) principal landscape components and (2) a practical field program capable of being completed within time allotted.

c. Conduct fieldwork on select landscape components complimented with data obtained from the (1) surface (i.e., historical photography, thematic maps) and (2) subsurface (i.e., drill logs, core borings).

d. Analyze data and construct summary documents as an initial step in understanding the geomorphology and geologic processes.

e. Test the utility of this study by applying the results to an ongoing *EPA Wetlands Initiative* currently underway within the MINWR and awarded to this NASA Summer Faculty Fellow (Randall W. Parkinson).

1.2 Operational Hypothesis

Prior to the initiation of this project, the following operational hypothesis was established:

The principal landscape components (geomorphology) of Black Point Drive

reflect interaction between surficial sediments deposited in association with late-Quaternary sea-level highstands and the evolution of late-Cenozoic sub-surface karstic formations.

This interaction requires the presence of sub-surface limestone formations and should be most obvious in the western portion of MINWR/KSC, where the sandy late-Quaternary overburden is thinnest and where landscape features generally indicative of pervasive limestone dissolution are most apparent (Figure 1).

2.0 BACKGROUND

2.1 Description of Study Area

Surface. The geomorphology of MINWR/KSC has been previously described by Brooks (1972) and references cited therein. More recently, Clark (1987) proposed four surface aquifer terrains (Figure 1): (1) dune, (2) ridge[2] & swale, (3) western, and (4) marsh. The soils and sediments of this region have just been reviewed by Schmalzer and others (2000). The *dune* terrain is located along the eastern margin of Cape Canaveral. The terrain consists of recent, wave-dominated shorelines and aeolian dunes reaching elevations in excess of 10 m. Sediments consist of mid- to late-Holocene skeletal quartz sand; soil formation is minimal and classified as coastal by Schmalzer and others (2000). The *rigde & swale* terrain occupies most of the landscape east of the NASA Parkway. In this region, an undulatory topography is present and known to have formed as a progradational beach ridge complex during a late-Pleistocene sea-level high stand (110,000 yrbp, see Brooks 1972). Landscape elevation and local relief are diagnostic of this terrain and responsible for the presence of narrow, parallel bands of xeric, mesic, and hydric habitats. Distinct soil types also map as parallel bands corresponding to recent plant communities and generally consist of shelly quartz sand with varying amounts of organic matter (coastal, acid scrub, flatwood or hammock soils). Quartz-rich silt and clay, associated with fresh- and salt-water soils are encountered in the hydric habitats of the ridge & swale terrain.

The Black Point Drive area lies primarily in the *western* terrain, located landward of the NASA Parkway. It consists of subdued to indistinguishable beach ridges and sink hole depressions (Brooks 1972). The area now hosts flatwood, hardwood hammock and freshwater-wetland plant communities. Surface sediments consist of shelly quartz sand, locally organic rich or muddy. These correspond to flatwood, hammock or freshwater wetland soils (Schmalzer and others 2000). Thin and discontinuous coquina rock formations have also been described from this area. There is ample evidence of limestone dissolution, including the presence of a micritic cap

[2] As positive relief features in this terrain are no longer active aeolian dunes, Clark's (1987) label has been changed from dune & swale to ridge & swale.

rock, caliche crusts, and circular depressions (Figure 1). The depressions contain freshwater wetland or open water. The landward margin of MINWR/KSC consists of *marsh* terrain. Blackish-water wetlands are the principal plant community as the landscape is <1 m above sea level. Perhaps the most diagnostic feature of the marsh terrain is the presence of open water features, such as circular lakes and dissolution(?) channels. The area's surface sediment consists of shelly quartz sand and silt, locally enriched in organic matter or mud, and grouped into the saltwater wetland soil class.

Subsurface. Based upon the work of Brown and others (1962) and Clark (1987), the subsurface stratigraphy of MINWR/KSC is known to consist of five geologic age groups: (1) Recent, (2) Pleistocene, (3) Pliocene, (4) Miocene, and (5) Eocene (Table 1 and Figure 2). The Quaternary (Recent and Pleistocene) consist of undifferentiated marine quartz sand deposited in association with sea-level high stands and intermittently subjected to the subaerial processes of weathering and erosion. Radio-isotopic analysis (Brooks 1972) yields the following ages for prominent geologic features along a regional west to east transect: 110,000 yrbp, mainland and Atlantic Coastal Ridge; western Merritt Island, 240,000 yrbp; eastern Merritt Island, 110,000 yrbp; Banana River, 20,000 to 45,000 yrbp; Cape Canaveral, 7,000 yrbp to Recent. Black Point Drive is located in western Merritt Island and therefore upon a 240,000 year old succession of inter-bedded clastic and biogenic sediments.

Table 1. Stratigraphic units of northwest Merritt Island. After Brown and others (1962).

Geologic Age	Stratigraphic Unit	Depth (m)	Description
Recent Pleistocene	Pleistocene & Recent deposits	0 - 15	Skeletal quartz sand; locally organic-rich or coquina
Pliocene	Upper Miocene or Pliocene deposits	15 - 25	Greenish-gray, sandy fossiliferous marl
Miocene	Hawthorn Formation	25 - 40	Phosphatic greenish-gray, sandy marl or clay
Eocene	Ocala Group	40 - ?	White to cream, friable and porous coquina; soft, chalky marine limestones

The underlying Pliocene to late-Miocene consists of sandy silt, clay, and marl known locally as the confining layer because it separates the surface aquifer from the regional (Floridan) aquifer. This contact is encountered at ~15 m. These sediments were deposited upon the Hawthorn Formation, a fine-grained, phosphatic Miocene marine deposit. Eocene limestones are encountered ~40 m below sea level. Geologic cross-sections (see Figure 12 and 13 in Brown 1962) suggest the contact between Eocene and Miocene deposits is very irregular, while the overlying contacts between the younger geologic age groups are nearly horizontal.

2.2 Methods

Surface. This project was initiated by undertaking a survey of historical photography. Images depicting various portions of Black Point Drive were obtained for the following years: 1943, 1973, 1984, 1995, and 1999. Inspection of photography provided information on natural (i.e., landscape submergence) and anthropogenic (mining, impoundment construction) processes which were active during historical times.

A field program was then designed to catalog (1) surface sediments and soils, (2) plant communities, (3) submergent and emergent terrains, and (4) presence or absence of limestone beds exposed by natural (i.e., erosion) or anthropogenic (i.e., ditching) means. All sites were accessed using existing improved and unimproved roads.

Subsurface. Investigation of the subsurface geology was undertaken using: (1) remediation and groundwater monitoring well reports (i.e., Clark 1987, Universal 1998), (2) core samples (i.e., Wilson Corners Groundwater Remediation Site, provided by HSA Engineers & Scientists), (3) outcrops, and (4) literature (i.e., Brown and others1962).

3.0 RESULTS

3.1 Surface

The Black Point Drive area of MINWR/KSC consists of a featureless sandy surface gently dipping westward from ~3 m above sea level to ~0.5 m at the boundary with the marsh terrain. Inspection of surficial sediments indicates the presence of a shelly organic-rich quartz sand. The poor preservation of shell material (i.e., corroded, chalky) suggests this component of the sediment is actively undergoing dissolution. High organic content is a result of *in situ* production of roots and above-ground litterfall; both of which are probably contributing to acidic surface-water conditions and the chemical weathering of biogenic sediment.

Plant communities within the Black Point Drive area consist primarily of slash pine flatwood, hardwood hammock, and freshwater wetlands. Flatwood plant communities are the most extensive habitat, extending from the eastern boundary of the study area westward into hardwood hammock and freshwater wetland. Towards the marsh terrain, flatwood plant communities become increasingly isolated and occur as patches within freshwater wetlands. Inspection of a number of these patches revealed an apparent association with coquina rock at or very near (<1 m) the surface. Open water is present at a limited number of sites and is generally indicative of the presence of an inactive, shallow limestone quarry. Inspection of historical photographs

suggests mining operations were activated during the construction of impoundment dikes (late 1950s and early 1960s) and after completion of unimproved roads and drainage ditches (pre-1943). All but one of the mines are located in the flatwood habitat, an observation consistent with the possible affinity of this plant community towards coquina outcrops.

Along the western margin of Black Point Drive open water is widespread and associated with topographic depressions. These too represent alterations to the natural landscape as they formed by management induced water level elevation. In areas of submergence, the surface sediment layer is often sandy and subjected to wave-induced physical reworking. Organic-matter accumulation is minimal and restricted to a basin's low-energy embayments or "leeward" margins.

3.2 Subsurface

Inspection of well logs and core borings obtained from the Black Point Drive area revealed the presence of a stratigraphic succession consistent with that first published by Brown and others (1962). Late-Quaternary sediments are present in the upper ~15 m of the succession. Sedimentology, stratigraphy, and a knowledge of sea-level history suggests these marine sands were deposited during a late-Pleistocene (110,000 yrbp) sea-level highstand and subjected thereafter to subaerial processes of weathering and erosion. As the area has not yet been submerged during the most recent interval of deglaciation and concomitant sea-level rise, sediment *deposition* has been minimal. The only processes to modify the stratigraphic succession of Black Point Drive over the past 15,000 yrs are: (1) *in situ* production of organic material and (2) reduction of skeletal content through dissolution. In select (n~3) core borings obtained from the Wilsons Corner groundwater remediation site (Figure 1) a thin (<0.5 m), highly weathered (chalky) limestone layer was observed in the upper 2 m.

The effects of sub-aerial exposure are minimal below ~5 m. The preservation of marine molluscs is phenomenal at depths of 5 to 15 m. Many of the shells still retain their delicate architecture and color; they could easily be mis-identified as modern sediments if the stratigraphic context and local sea-level history were not known. Clay-rich beds of Pliocene-Miocene time are generally encountered at -15 m and these are clearly delineated from the overlying sediments by texture, composition, and color.

No recent cores have penetrated pre-Pliocene or Miocene sediments and therefore no new data were collected. Drilling to depths >15 m may compromise the integrity of the confining layer and induce contamination of the regional aquifer. All data describing these older sediments were obtained from Brown and others (1962). According to these authors, sediments deposited during Miocene and older times are present beneath the MINWR/KSC at a depth of ~25 m. The first occurrence of limestone was encountered within Eocene beds (Ocala Group) at a depth of at least 40

m (Figure 2). The limestone surface is highly irregular (c.f. Figures 12 and 13, Brown and others 1962), suggesting weathering and erosion lowered elevations significantly. The extremely high permeability of these marine limestones is indicative of karstification via groundwater dissolution. The relief of this irregular contact is not translated in the overlying beds, suggesting the karstification processes ceased prior to their deposition.

4.0 DISCUSSION

4.1 Relevance to Operational Hypothesis

There is abundant geomorphic evidence in the *western* and *marsh* terrains of Black Point Drive to infer limestone dissolution and the subsequent formation of a karstic landscape. This type of weathering requires a humid climate and the presence of limestone bedrock in close proximity to the surface. East central Florida is subjected to humid climatic conditions, however the first appearance of contiguous limestone formation within the stratigraphic succession of MINWR/KSC is at a depth of ~40 m. This is inconsistent with the operational hypothesis of this investigation; a karstic imprint on the landscape requires the presence of much shallower limestone beds undergoing dissolution during late-Quaternary times.

Numerous limestone outcrops are present within Black Point Drive and evidence of chemical weathering is abundant, including: micritic cap rock, caliche crust, and circular depressions. However, the coquina layers are relatively thin (<1 - 2 m) and it is difficult to envision how their dissolution could produce extensive circular or channel-like depressions with a diameter or length in excess of 1 km (Figure 1).

4.2 Management Implications

This investigation collected data applicable to understanding the paleo-environmental evolution of Black Point Drive and the surrounding area. The mainland coast, Merritt Island, and Cape Canaveral are geomorphic features that formed in association with the following late-Pleistocene sea-level highstands: (1) 240,000 yrbp, (2) 110,000 to 125,000 yrbp, (3) 20,000 to 45,000 yrbp, and (4) modern. During these times, skeletal quartz sand accumulated along at the coastline, in some cases prograding seaward as an undulatory beach ridge complex. During intervening lowstands, these deposits were subjected to chemical weathering and erosion. The presence of extensive dissolution features within ~5 m of the surface indicates weathering initially induced pervasive near-surface leaching and localized cementation at greater depths. Subsequent lowstands subjected lithified shell beds to dissolution and the formation of karstic features thereafter. These landforms are most abundant in the western region of Merritt Island, decreasing eastward towards the ridge & swale terrain. The processes responsible for the observed gradient in karstic landform

distribution are unclear at present. The gradient may reflect: (1) spatial distinctions in the elevation, character or age of buried (pre-Miocene) limestone formations, (2) dissolution history of late-Quaternary coquina, and/or (3) thickness of unconsolidated surface sediment. More detailed evaluation of *subsurface* data will be necessary before this uncertainty can be resolved.

The recent acceleration in late-Holocene sea-level rise, complemented by elevated water level management strategies, has prompted the formation of extensive wetlands during historical times. In areas of higher elevation, slash pine flatwood and hardwood hammock habitats remain. If these conditions persist, the expansion of brackish-water wetlands and invasion of hydric plant communities into mesic terrains can be expected.

From a technical point of view, sedimentation within MINWR/KSC has been minimal and restricted primarily to the *in situ* production of organic matter and accumulation of surface litter. *Destructional* processes are widespread. In submerged areas, the surface layer is being reworked by wave-induced circulation. Soils beneath mesic terrains are undergoing dissolution via downward percolation of acidic surface water. Hydrologic conditions created by the most recent sea-level highstand and managed water-level elevations have probably minimized the potential effects of karstification on the area's landscape.

The long-term (decades) prognosis of wetlands will be solely dependant upon biogenic processes. In contrast to wetland areas of the Gulf of Mexico or the more northern Atlantic coasts, fine-grained inorganic sediment is not a significant component of the sediment budget. Wetlands will persist or even expand into adjacent areas only if organic-matter production and accumulation can keep pace with rising water level. Managers must therefore work to understand the biogenic processes of sedimentation and the potential effects of water level management.

5.0 CONCLUDING REMARKS

The Black Point Drive area of MINWR/KSC consists of extensive flatwoods, hardwood hammock and wetland habitats that have colonized late-Quaternary skeletal quartz sands. These sediments were deposited during a preceding sea-level highstand and are currently undergoing localized physical reworking and pervasive chemical dissolution. Although there is abundant geomorphic evidence of karstification in the western portion of Merritt Island, the conditions responsible for the formation of these landforms remain enigmatic. These features may have formed via the chemical dissolution of near-surface coquina beds and/or buried Eocene limestone. The effects of Holocene sea-level rise and water-level management have probably reduced the potential for continued karstification and expanded the distribution of brackish- and fresh-water wetlands. The long-term prognosis of wetland persistence will be

dependent solely upon the rate of biogenic sediment production and accumulation relative to the change in water-level elevation induced by natural and anthropogenic factors. Therefore, land managers must consider the effects of current water management strategies on organic-matter production and accumulation if wetland protection is one of their mandates.

6.0 ACKNOWLEDGMENTS

The following scientists are acknowledged for their assistance: Melissa Hensley, Ross Hinkle, Mark Provancha, and Paul Schmalzer. Support was also provided by my NASA Colleague, Kelly Gorman. Inspection of subsurface data was made possible by Jim Hayman and Darcie McGee (HSA Engineers & Scientists). Access to field sites and permitting was granted by the US Fish and Wildlife Service and in particular Gary Popotnik and Mark Epstien. Ron Brockmeyer, St. Johns River Water Management District, is acknowledged for his support.

7.0 REFERENCES

Brooks, H.K., 1972. Geology of Cape Canaveral, p. 35-44, *in* T.E. Garner (ed.), Space-age geology. Southeastern Geology Society. Tallahassee, Florida.

Brown, D.W., Kenner, W.E, Crooks, J.W., and Foster, J.B., 1962. Water resources of Brevard County, Florida. Report of Investigations no. 28. Florida Geological Survey. Tallahassee, Florida. 104 pg.

Clark, E.E., Engineers-Scientists, Inc., 1987. KSC subsurface hydrology and groundwater survey. Volume IV. The areawide groundwater survey program. KSC-DF-3081. Unpublished report by Edward E. Clark Engineers-Scientists, Inc., Kennedy Space Center, Florida. Contract no. NAS10-11293. NASA, John F. Kennedy Space Center, Florida.

Schmalzer, P.A., Hensley, M.A., Mota, M., Hall, C.R., and Dunlevy, C.A., 2000. Soil, groundwater, surface water, and sediments of Kennedy Space Center, Florida: background chemical and physical characteristics. Unpublished Open File Report, NASA Environmental Program Office, Mail Code JJ-D, Kennedy Space Center, Florida. 44 pg.

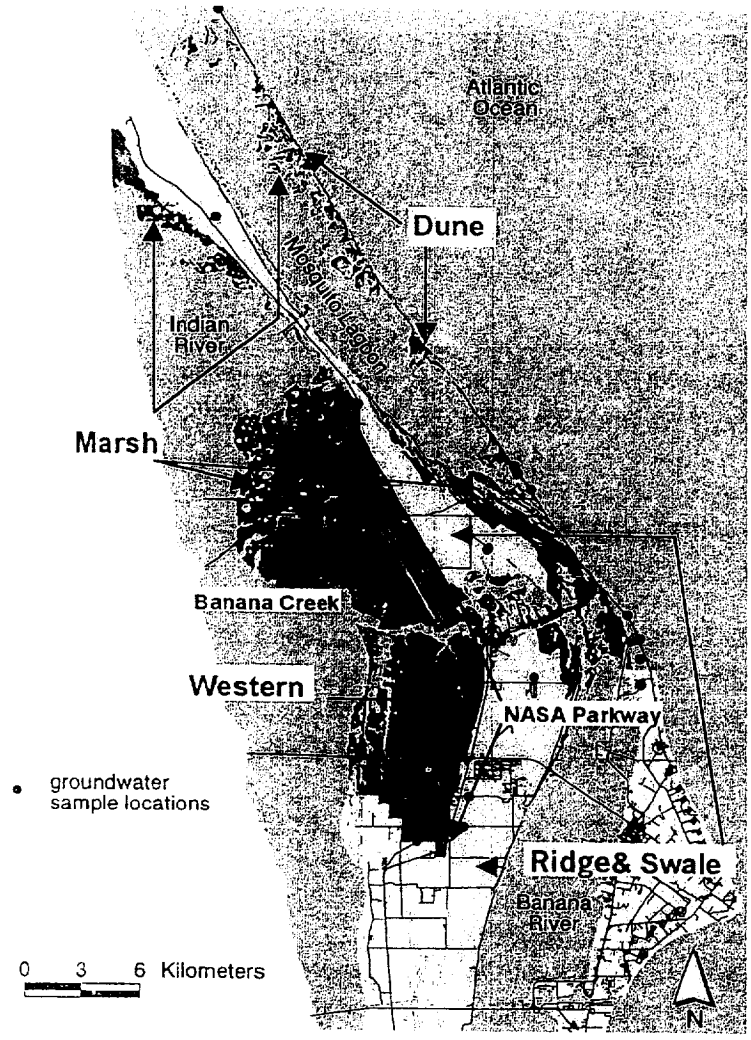

Figure 1. Cape Canaveral's principal geomorphic terrains: (1) dune, (2) ridge & swale, (3) western, and (4) marsh (after Clark 1987). Black Point Drive located north of Banana Creek and west of NASA Parkway. Wilson Corners located across road at north end of landing strip. **Figure 2 (below).** Cross-section of coastal stratigraphy in Brevard County, Florida, constructed using wells shown in inset. Asterisks (*) denote Black Point Drive. Vertical scale in ft (50 ft ~ 15 m). After Brown and others (1962).

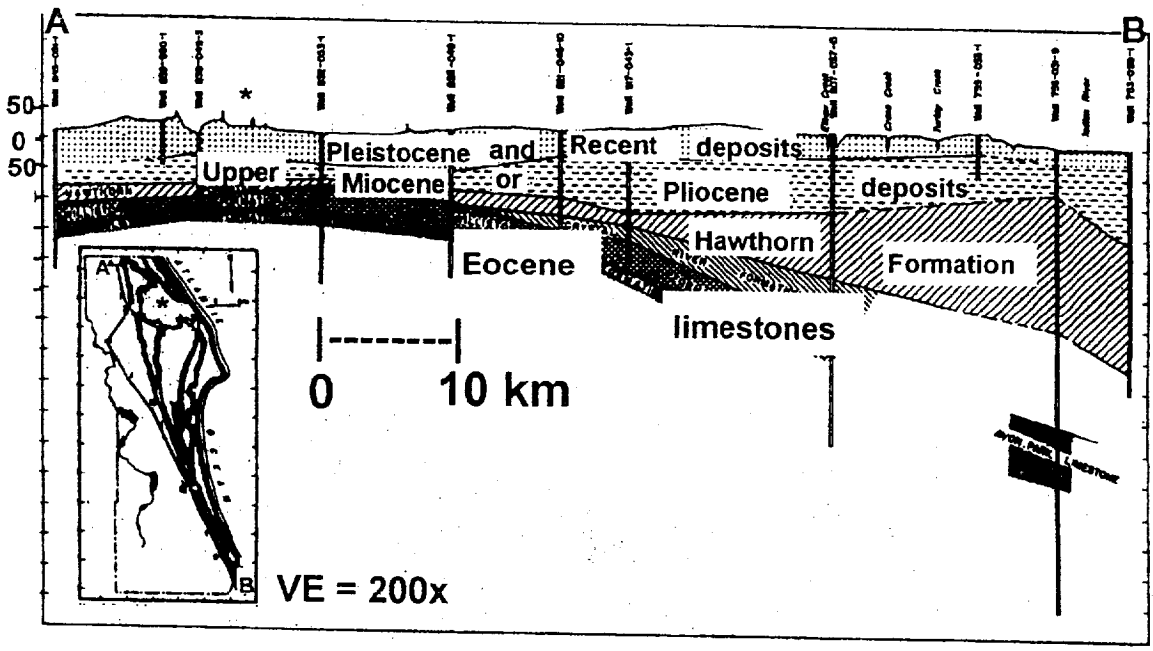

2000 NASA/ASEE SUMMER FACULTY FELLOWSHIP PROGRAM

JOHN F. KENNEDY SPACE CENTER
UNIVERSITY OF CENTRAL FLORIDA

CONTROL FOR NOx EMISSIONS FROM COMBUSTION SOURCES

Maria E. Pozo de Fernandez, Ph.D.
Assistant Professor
Department of Chemical Engineering
Florida Institute of Technology

Michelle M. Collins, Ph.D., P.E.
NASA-KSC
Environmental Program Office

ABSTRACT

The Environmental Program Office at the Kennedy Space Center is interested in finding solutions and to promote R&D that could contribute to solve the problems of air, soil and groundwater contamination. This study is undertaken as part of NASA's environmental stewardship program. The objective of this study involves the removal of nitrogen oxides from the flue gases of the boilers at KSC using hydrogen peroxide. Phases 1 and 2 of this study have shown the potential of this process to be used as an alternative to the current methods of treatment used in the power industry.

This report summarizes the research done during the 10-week summer program. During this period, support has been given to implement the modifications suggested for Phase 3 of the project, which focus on oxidation reactions carried at lower temperatures using a microwave source. The redesign of the flue gas inlet and optimization for the scrubbing system was the main objective of this research.

CONTROL FOR NOx EMISSIONS FROM COMBUSTION SOURCES

Maria E. Pozo de Fernandez, Ph.D.

1. Introduction

NASA launches the Space Shuttle from a 149,000 acre Wildlife refuge. NASA is committed to Environmental Stewardship and has explicitly stated this commitment in the NASA Strategic Plan. Nitrogen Oxide (NOx) emissions are a primary criteria pollutant regulated by the USEPA. The Kennedy Space Center is permitted to emit approximately 60 tons of NOx annually under their Title V air permit. NASA is pursuing R&D to minimize the detrimental environmental effects of KSC operations on the environment. This study is undertaken as part of NASA's environmental stewardship program.

This study involves the removal of nitrogen oxides from the flue gases of the boilers at KSC. The primary focus of the research is the conversion of NOx to nitrogen acids for the purpose of scrubbing them from the gas stream. NO is virtually non-soluble and NO_2 is only slightly soluble; however, nitrogen acids (HNO_2 and HNO_3) are highly soluble and can be removed via scrubbing.

Phase 1 of this study was completed in December 1998 and consisted of oxidation of the NOx at high temperatures (~930 °F). Phase 2 focused on oxidation at lower temperatures utilizing an ultraviolet (UV) light source. Key to the success of this study was the redesign, operation and optimization of the scrubber operation. The redesign included the following: 1. Conversion of batch to continuous reservoir flow. 2. Lower temperatures in the scrubber recirculation system. 3. Continuous and Batch caustic feed. 4. Providing for sampling and analysis in-line. 5. Increase recirculation flow rate.

Phase 3 started on January 1, 2000 and should conclude by December 31, 2001. This will focus on oxidation at low temperatures utilizing a Microwave source. Laboratory experiments have shown that microwaves promote the conversion of H_2O_2 into hydroxyl radicals, thus helping the desired NO to NO_2 conversion.

The Summer Faculty provided support in the coordination, implementation, logistics and follow-on procedures for the changes needed in the experimental setting. The changes for phase 3 will take place in the reaction zone, changing the UV lights Unit with the Microwave unit. Due to the installation of a new convection section at boiler #2, calculations were performed to determine the best option for re-connection from the boiler to the reactor. This report summarizes the research done during the 10-week program at NASA-KSC.

2. Background

Laboratory studies have demonstrated that hydrogen peroxide (H_2O_2) when injected under proper conditions into hot gases of the exhaust stream it oxidizes nitric oxide (NO) into NO_2, HNO_2 and HNO_3. The formation of nitrogen acids allows for more inexpensive methods of post treatment for nitrogen removal, such as, scrubbing. Sulfur dioxide can also be added to the combustion source to simulate the exhaust of an industrial power plant.

The primary reactions that are expected to occur during this process are as follows:

$$H_2O_2 \Rightarrow 2\,OH \quad [2.1]$$

$$NO_2 + SO_2 \Rightarrow NO + SO_3 \quad [2.2]$$

Hydroxyl-Radical Reactions:

$$H_2O_2 + OH \Rightarrow HO_2 + H_2O \quad [2.3]$$

$$NO + OH \Rightarrow NO_2 + H \quad [2.4]$$

$$NO + OH \Rightarrow HNO_2 \quad [2.5]$$

$$NO_2 + OH \Rightarrow HNO_3 \quad [2.6]$$

$$SO_2 + H_2O + OH \Rightarrow HSO_3 \bullet H_2O \quad [2.7]$$

Hydroperoxyl-Radical Reactions:

$$NO + HO_2 \Rightarrow HNO_3 \quad [2.8]$$

$$NO_2 + HO_2 \Rightarrow HO_2NO_2 \quad [2.9]$$

$$SO_2 + HO_2 \Rightarrow SO_3 + OH \quad [2.10]$$

To demonstrate the viability of such process in an industrial setting, researchers at NASA-KSC and the University of Central Florida (UCF) joint efforts to implement this process from a laboratory scale to a pilot plant scale. The experimental setting is located at the KSC Central Heat Plant (CHP). This study is part of Phase III of the BES Project. Highlights of Phase I and Phase II results are given below.

BES Phase 1: Phase 1 of this project was performed on a 35 mmBTUH natural gas boiler. The fuel used in the boiler consists mainly of methane and varying amounts of ethane, propane, butane, a sulfur-containing mercaptan added to natural gas, and inerts, such as, nitrogen, carbon dioxide and helium. When burning natural gas the major pollutant in the exhaust gases is mainly NOx. The percentage of NOx presence depends on the temperature of the combustion chamber as well on the fuel/oxygen ratio.

Part of the flue gas was diverted to the experimental apparatus consisting of different sections: Injection Zone, Reaction Zone, Quenching and Scrubbing. At the Injection Zone hydrogen peroxide (H_2O_2) was injected to the system. NO and SO_2 was added to the exhaust gases to simulate the composition of a flue gas from an industrial power plant. Once passed the Injection Zone the mixture of flue gas, NO, SO_2 and (H_2O_2) went through an auxiliary gas burner to bring the slipstream gases to the desired reaction temperature. From this point, the gases went through the Reaction Zone, where the conversion of NO to NOx and nitric acids took place. The Reaction Zone consisted of a 12-inch diameter, 8-ft long stainless steel pipe, having sampling ports and thermocouples distributed along its length. Reactions were carried out up to 500 °C. The reaction

products and by-products passed then through the Quenching system, where water was added to cool off the gas mixture before entering the Scrubbing System. The scrubber was a packed column consisted of an 8-ft tall acrylic column with a 6-ft bed depth. 1-inch Hyflow 25-7 polypropylene rings were used as packing material. The scrubber had a 30x60x30 inch^3 reservoir, a 1¼ - inch PVC recirculation line with a Hayward diaphragm valve, a by-pass valve, a ½ HP submersible pump and reservoir drain and sampling port. Sodium bicarbonate was used to control the pH of the fluid at the reservoir.

Figure 2.1 shows the process schematics for Phase 1. A Data Acquisition System (DAQ) using LabView software from National Instruments was used to obtain instant readings of the key parameters in the process. Figure 2.2 shows the schematics of the experimental system as the computer monitor displays it.

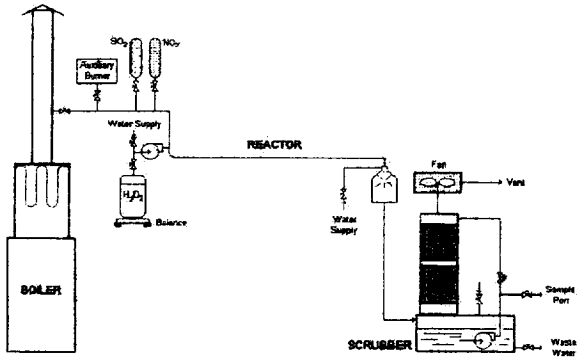

Figure 2.1. Process Schematics (Phase I)

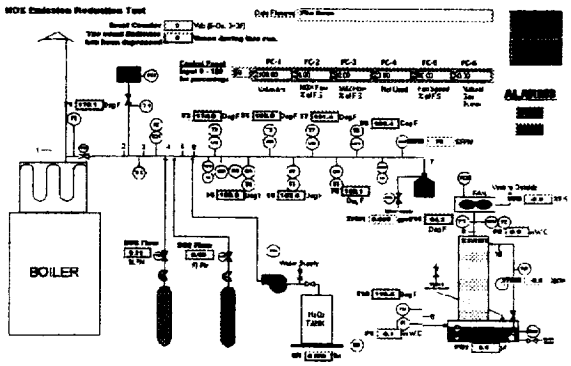

Figure 2.2. LabView Diagram (Phase I)

Several runs were made with this experimental configuration changing the following variables: Reaction temperature, NO, SO_2 and H_2O_2 concentration, NO/H_2O_2 ratio, SO_2/H_2O_2 ratio and residence time. The results obtained during Phase 1 were encouraging but some modifications were required in order for the system to perform to the optimum expected values. The conversion from NO to NOx worked very well, getting conversions greater than 96% for NO/ H_2O_2 ratios of 1:1. Conversion from NO_2 to nitric acids was not as high as expected. Operating the reactor at high temperatures and having the surface of the stainless steel reactor without any type of coating could have been part of the problem. The removal of the nitric acids by the scrubber was not as efficient as expected. The scrubbing system was never optimized for the kind of removal required by the process. The submersible pump provided was under-specified, since the rates of liquid flow recommended for optimal scrubbing operation were never achieved. The implementation of these modifications led to Phase 2 of the project.

BES Phase 2: Based on the results obtained during Phase I, several modifications were proposed for Phase 2 of the project. The sections to be re-designed were the Reaction Zone and the Scrubbing System. The reaction zone pipe (12" diameter, 8' long SS pipe) was coated with a boron-nitride paint to prevent the release of iron during the reaction.

The paint selected was high temperature ceramic boron nitride paint from Carborundum. UV lights were used as a heat source to carry the reaction at lower temperatures.

Scrubbing System: The scrubber used during Phase 1 of the project was designed and manufactured by Rauschert Industries, Inc. Based on the parameters supplied, they estimated the size, material, packing material, optimum gas and liquid rate within the column and the operation temperature. The packing material selected by the vendor was 1-inch Hyflow 25-7 polypropylene rings. This packing material is proprietary, meaning that its characteristics and hydraulic behavior can not be found in the open literature. Once the vendor specified the unit, he recommended 500 scfm for the gas rate and 35 gpm for the liquid rate. Since the recirculation pump provided with the unit was under-specified the maximum liquid flow achieved was approximately 15 gpm, which proved to be too low for the scrubber operation.

The scrubber was re-designed for continuous operation having inlet, outlet and recirculation lines. Fresh water was introduced in the system through the inlet line. Two Hayward diaphragm valves control the flow through the outlet line and the recirculation line in the system. Mass flowmeters hooked up to the DAQ provided accurate flow measurement at the inlet, outlet and recirculation lines. Liquid recirculation was provided through a new 1-HP pump, able to deliver 35 gpm if desired. A continuous and batch caustic feed was also added to the system. The submersible pump at the reservoir provided continuous mixing of the tank fluid and the caustic solution added to the tank. Figure 2.3 shows the process schematics of Phase 2 and Figure 2.4. shows the scrubber with the modifications.

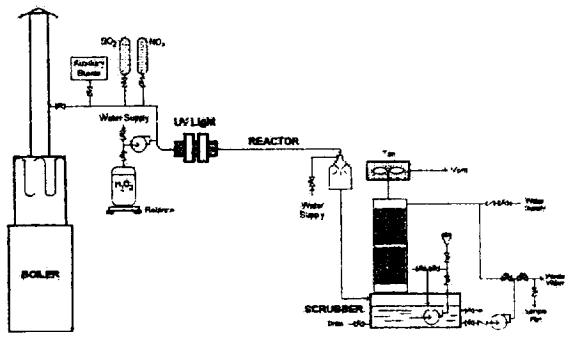

Figure 2.3. Process Schematics (Phase 2)

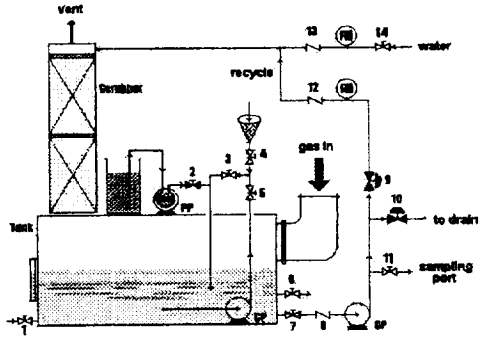

Figure 2.4. Scrubber Modifications

Many tests were performed during Phase 2 of the project. The parameters varied included: the reaction temperature (350, 400 and 450 °F), the injection point location, the NO_2/H_2O_2 ratio, and SO_2/H_2O_2 ratio, the pH of the scrubber reservoir solution and the recycle flow at the scrubber.

The Phase 2 data showed that the use of UV lights was slightly to moderately effective in oxidizing NO to NO_2. The improvements in the scrubber re-design provided a better temperature control and the capability to perform steady state operations.

3. Experimental

For Phase 3 of the project a microwave source will replace the UV lights unit. The commercial unit is being built by Tiberian, one of the industrial partners of this project. The size of the unit is such, that it can be easily bolted to the existing apparatus configuration. Laboratory experiments at Tiberian and at UCF have shown that microwaves promote the conversion of H_2O_2 into hydroxyl radicals, thus helping the desired NO to NO_2 conversion.

Another issue was presented while getting ready to implement the changes for Phase 3, a new convection section on Boiler #2 was installed at the beginning of the project. Installing the convection section required to dismantle the flue gas inlet gas section from the boiler to the reactor, then all the piping, valves, auxiliary burner, flanges, and fittings were taken apart. Figures 3.1 show the inside chamber of the boiler and Figure 3.2 shows a view of the top of the boiler without the convection section.

Figure 3.1. Boiler Internal Chamber

Figure 3.2. Boiler Top

Once the installation of the convection section was finished, several options were presented to re-connect the inlet gas to the reactor. In the past, the use of the auxiliary burner presented some problems, and then this was the right time to look into new options.

The options presented are as follows:

1. Heat the flue gas pipe using external heaters (band heaters)
2. Heat the flue gas using heaters inside.
3. Mix two flue gas streams at different temperatures from different locations in the boiler.
4. Re-connect the system as it was previously.

To select the best option, calculations on the heat load required were made based on the following restrictions:

1. Flue gas composition: 72% N_2, 17% H_2O (steam), 9% CO_2 and 2% O_2
2. A gas velocity ν =10 ft/s is required at the reaction chamber.
3. The flue gas from the convection section should be heated from 320 to 500 °F
4. $\Delta P < 5$ inches of H_2O

Heat Load Calculations:

Sectional area of the reactor pipe $\Rightarrow$ A= 121.5 in^2
Volumetric rate $\Rightarrow$ q = ν A = 506.3 ft^3/ min
Flue gas density at 400 °F $\Rightarrow$ $\rho_{flue\ gas}$ = 0.044309 lb/ft^3
Reactor mass flow rate $\Rightarrow$ m = ρ q = 22.4 lb/min

Heat requirements to heat the flue gas mixture from 170 °C to 260 °C :

Table 3.1: Flue Gas Mixture Cp Calculations

$Cp = a + bT + cT^2 + dT^3$

Cp -> J/ gmol C T -> C

Component	MW	X_i (molar)	a	b x 10^2	c x 10^5	d x 10^9	T Range C
N2	28	0.72	29.00	0.2199	0.5723	-2.8710	0 - 1500
CO2	44	0.09	36.11	4.2330	-2.8870	7.4640	0 - 1500
O2	32	0.02	29.10	1.1580	-0.6076	1.3110	0 - 1500
H2O	18	0.17	33.46	0.6880	0.7604	-3.5930	0 - 1500

	a_m	b_m x 10^2	c_m x 10^5	d_m x 10^9
Cp mixture =	30.40	0.6794	0.2693	-1.9800

MW Ave = 27.82

Heat required per unit mass $\Rightarrow$ $q = \int Cp_{FlueGas}\, dT \Rightarrow 102.16 \frac{kJ}{kg}$

Reactor mass flow rate $\Rightarrow$ $\dot{m} = 0.154 \frac{kg}{s}$

Energy required $\Rightarrow Q = q\dot{m} = 15.7 \frac{kJ}{s} = 15.7\,kW$

Total energy required to heat flue gas from 320 to 500 °F = 15.7 kW

Based on these results, vendors for external and internal pipe heaters were contacted. The use of external heaters could have met the heat load requirements, but the cost was outside the budget. The use of internal heaters could have also met the heat load requirements, but not the required ΔP. It was then decided to perform calculations to check the viability of mixing streams taken from points at different temperatures in the boiler.

Temperature requirements to mix two flue gas streams at different locations in the boiler:

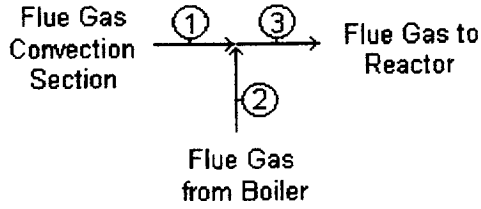

Two streams taken from different points in the boiler will be mixed. One stream will be taken form the convection section at 320 °F. The other stream will be taken from the "furnace" section and its temperature will be considered to be between 600 – 1000 °F, for the calculations.

Mass Balance: $\dot{m}_1 + \dot{m}_2 = \dot{m}_3$

Energy Balance $\Rightarrow$ assuming δQ = 0 $\dot{m}_1 h_1 + \dot{m}_2 h_2 = \dot{m}_3 h_3$

The gas mixture enthalpy can be calculated as function of the heat capacity (Cp):

$$h_i = \int_{T_{REF}}^{T_i} Cp_i\, dT + h_{REF} \Rightarrow m_1 Cp_1 (T_1 - T_{REF}) + m_2 Cp_2 (T_2 - T_{REF}) = m_3 Cp_3 (T_3 - T_{REF})$$

For the required temperature range, it can be assumed that $Cp_1 \approx Cp_2 \approx Cp_3$ then,

$$\dot{m}_1 T_1 + \dot{m}_2 T_2 = \dot{m}_3 T_3 = (\dot{m}_1 + \dot{m}_2) T_3 \qquad \Rightarrow \qquad \frac{\dot{m}_2}{\dot{m}_1} = \frac{T_3 - T_1}{T_2 - T_3}$$

For temperature values $T_3 = 400$ °F; $T_1 = 340$ °F and 600 °F $< T_2 <$ 1000 °F, the ratio "m_2/m_1" is within $0.1 < [m_2/m_1] < 0.3$ The calculations performed for the pressure losses in the pipes using a $\phi = 4$" for the flue gas from the "furnace"(T_2) and a $\phi = 6$" for the flue gas from the convection section (T_3) shown that the pressure losses will be within 1 inch of water. Based on the previous calculations, the flue gas inlet to the reactor will be re-connected to the boiler using option 3. The schematic diagram of the process for Phase 3 is presented below.

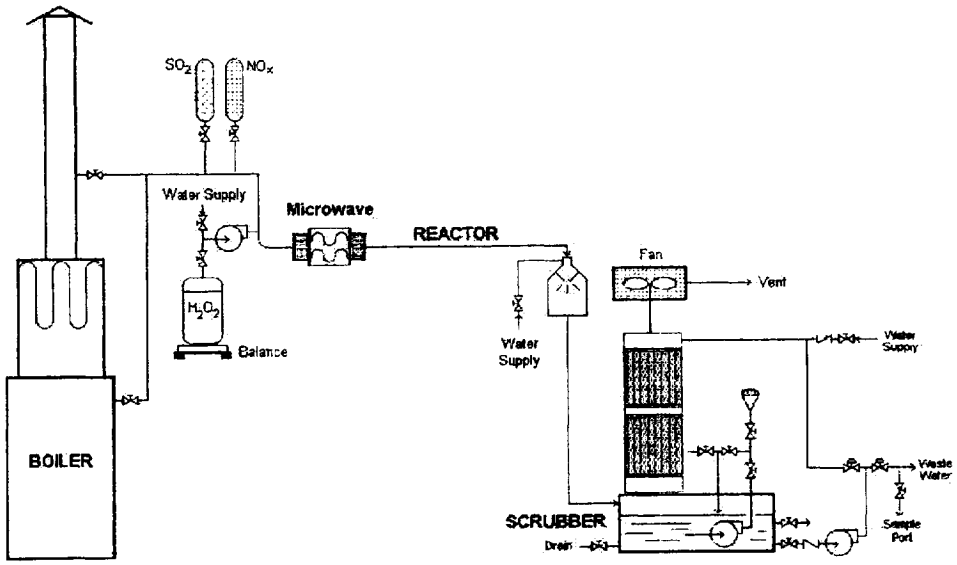

Figure 3.3. Schematic Diagram Phase 3

Different tasks must be performed before starting experiments on Phase 3. These task are presented as follows:

Table 3.2. BES Phase III: New Component Installation and Preparation for experimental Work

#	Tasks	In Charge
1	Ordering Materials	BES Team
2	Delivering Materials	Vendors
3	CHP Reactor Area Clean-Up	BES Team
4	Fabricate flue gas inlet piping	Metal Shop
5	Erect Scaffolding (2 levels)	Scaff. Shop
6	Install and weld flue gas piping	Metal Shop, CHP
7	Test gas inlet system	CHP
8	Electrical Supply & installation	Elect. Shop
9	Pipe Insulation	Insulation Shop
10	Check Instrumentation	BES Team
11	Experiments	BES Team, CHP

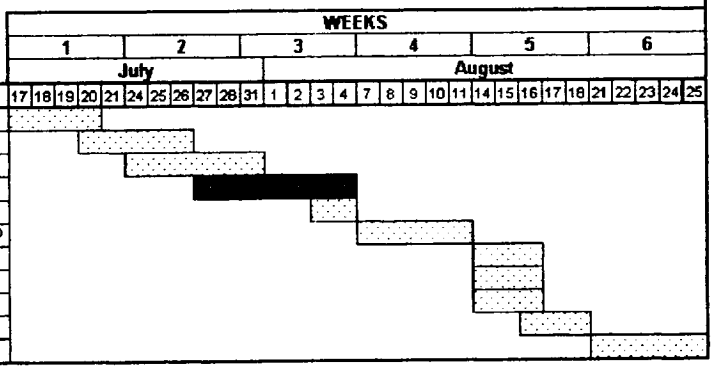

Scrubbing System Optimization: Due to the installation of the convection section in boiler # 2, and since the reactor was not connected to the boiler, experiments on the scrubber could not be performed at this time.

4. Conclusions

Calculations were performed and recommendations were made to implement the changes on the gas inlet delivery system from the boiler to the reactor. Once the gas inlet system and the microwave unit are properly connected, the whole system will be ready for testing and validation.

5. References

[1] Collins, M. M. (1998) Ph.D. Dissertation. University of Central Florida.

[2] Collins, J. G. (1999) M.S. Thesis. University of Central Florida.

[3] Coulson, J. M. and J. F. Richardson (1991) *Chemical Engineering*, Volume 2, Pergamon Press, USA.

[4] McCabe, W. L.; J. C. Smith and P. Harriot (1985) Unit Operations in Chemical Engineering, 4th Edition, McGraw-Hill, Inc., USA.

[5] Orioles, J. J. (1999) M.S. Thesis. University of Central Florida.

6. Acknowledgments

I would like to thank my NASA colleague Dr. Michelle M. Collins for providing the opportunity to work in this project. Special thanks to the members of the BES Group: Jennifer Murray , Debra Erving, Dr. Chris Clausen, Dr. David Cooper, Dr. John Dietz and the UCF graduate students for their help and support. My sincere appreciation to the personnel of the Central Heat Plant, especially George Broyles and Tom Petelle. Without their help, support and expertise it would have been impossible to accomplish the tasks of this project. Special thanks to the members of the Remediation Group at KSC for providing a friendly working environment. Special thanks to Dr. Ramon Hosler, Gregg Buckingham and Cassie Spears from the NASA/ASEE Summer Program for all their efforts. This has been a great research experience.

2000 NASA/ASEE SUMMER FACULTY FELLOWSHIP PROGRAM

JOHN F. KENNEDY SPACE CENTER
UNIVERSITY OF CENTRAL FLORIDA

OUTLINE OF A TWENTY-FIVE YEAR PLAN FOR DEVELOPMENT AND DEPLOYMENT OF A CATAPULT FOR A THIRD GENERATION SPACE SHUTTLE

JOHN M. RUSSELL
Associate Professor, Aerospace Engineering
Florida Institute of Technology
NASA colleague: FREDERICK W. ADAMS, YA-D2

ABSTRACT

This report reviews the rationale for catapult assist in the launching a third generation space shuttle. It then furnishes lists of early design decisions, questions whose answers are prerequisite to later design decisions, preliminary inventories of carriage levitation and carriage propulsion concepts, phases of the project and major milestones, and some sources of expertise to support the project.

OUTLINE OF A TWENTY-FIVE YEAR PLAN FOR DEVELOPMENT AND DEPLOYMENT OF A CATAPULT FOR A THIRD GENERATION SPACE SHUTTLE

JOHN M. RUSSELL

1. INTRODUCTION

The cost of launching a unit mass of payload into orbit with the present generation space shuttle is higher than one would like. Let $i \in \{0, 1, 2 \ldots, n\}$ be an index that counts vehicle states. Then vehicle state i will differ from vehicle state $i+1$ if there is an engine burn in between. The number n thus represents the total number of engine burns. A classical equation in the theory of aircraft or rocket propulsion asserts that

$$\frac{m_i}{m_{i+1}} = \exp\left(\frac{v_{i+1} - v_i}{I_{i,i+1} g_0}\right) , \qquad (1)$$

in which:

- m_i, The mass of the vehicle in state i;
- v_i, The speed of the vehicle in state i;
- $I_{i,i+1}$, The specific impulse of the powerplant during an engine burn between state i and state $i+1$. The specific impulse is defined to be the ratio whose numerator is the thrust produced during the burn (in units of force) and whose denominator is the net rate of consumption of the weight of stored matter (in units of force per unit time). Thus $I_{i,i+1}$ has the units of *time*;
- g_0, The value of the acceleration due to gravity at the surface of the Earth (9.807 m/s^2).

The overall ratio of initial mass to final mass after n engine burns is thus

$$\frac{m_0}{m_n} = \prod_{i=0}^{n-1} \frac{m_i}{m_{i+1}} = \exp\left(\sum_{i=0}^{n-1} \frac{v_{i+1} - v_i}{I_{i,i+1} g_0}\right) . \qquad (2)$$

In the case of a chemical rocket the term $I_{i,i+1}$ is bounded above by fuel chemistry. Thus, for example, $I_{i,i+1}$ is about 387 s for a Hydrogen-Oxygen rocket which discharges into an atmosphere at 1 atm pressure(*cf.* SUTTON, 1992, p194)[1]. Discharge into a vacuum raises $I_{i,i+1}$ to about 470s (this figure was taken from the Pratt and Whitney Engine Gallery web page, http://www.pratt-whitney.com/engines/gallery, in reference to the SPW2000 upper stage engine). Alternatively, in the case of an airbreathing engine supplied by a hydrocarbon based fuel, the values of $I_{i,i+1}$ can be much higher. Thus, for a ramjet at Mach 3, $I_{i,i+1}$ can be 2,000 s. For a turbofan jet at high subsonic speeds, $I_{i,i+1}$ can be 7,000 s or higher. The advantage of the airbreathing engine, of course, is that it draws the oxidizer from the atmosphere and thus avoids the need to carry it aboard the vehicle. If a vehicle boosts to Earth orbit (at an altitude of 556 km or 300 nautical miles), then v_n is 7.582 km/s. If the vehicle is boosted to an orbit inclined to the equator at an angle 28.5° and is launched due East from a point whose latitude is 28.5° then v_0 is 0.409 km/s. If all of the energy used to boost the vehicle is supplied by fuel on board at blast off from a standing start (due East) on the Earth's surface, then $v_n - v_0$ is equal to 7.582-0.409=7.173 km/s (plus a small correction due to aerodynamic drag and the change in potential energy between the Earth's surface and the orbit). Thus, for a single stage to orbit vehicle, an optimistic estimate of the ratio m_0/m_1 (Hydrogen/Oxygen discharging into a vacuum) is $\exp[7,173/(470 \cdot 9.807)]$, or 4.741. Thus, the dry mass of the vehicle and payload once in orbit is 1/4.741 or 21.1% of its lift-off mass.

The factor $v_n - v_0$ can be less than the value given above if*the first stage of the vehicle acceleration is the result of boost by an external force*, delivered, for example, by a movable carriage that accelerates horizontally along a track. The larger the velocity increment supplied by the carriage, the smaller the velocity increment supplied by the orbiter's powerplant and, hence, the smaller the ratio m_0/m_n. If, therefore, the carriage accelerates the vehicle to 268 m/s (600 mi/hr), then the total speed increment to be supplied by the powerplant is now 7,173-268=6,904 m/s. The ratio of initial mass to final mass thus reduces to $\exp[6,904/(470 \cdot 9.807)]$, or 4.473. This time the dry mass of the vehicle and payload once in orbit is 1/4.473 or 22.4% of its lift-off mass. The liftoff mass needed to deliver a mass m_1 into low Earth orbit has thus been reduced by (4.473-4.741)m_1=-0.268 m_1. In other words, by accelerating the orbiter to 268 m/s before liftoff, one may reduce the gross liftoff mass of the vehicle by an amount equal to about 27% of the delivered mass. Of course, the foregoing calculation is based on the assumption that the orbiter is propelled by a rocket engine. Equation (2) above shows that further reductions in the ratio m_0/m_n are to be expected if

the orbiter is propelled by an airbreathing engine during part of its boost.

NASA personnel, aware of the foregoing facts, have proposed the consideration of a third generation space shuttle that exploits the notion of external boost. The time scale for the first flight of such a third generation vehicle would be twenty-five years from the *kickoff* (KO) of the project.

Kennedy Space Center is officially a Center of Excellence in the field of *Launch Technology*. Consequently, it now has primary responsibility (within NASA) for managing the exploration of externally energized boost concepts. KSC is working in cooperation with NASA/DRYDEN Flight Research Center in California regarding the development of the part of the vehicle which detaches (hereinafter called *the orbiter*)

SCOPE OF THIS REPORT:

The scope of the present report will be limited to the research, development and deployment of the catapult (consisting of the launch carriage, track and related hardware.)

2. EARLY DESIGN DECISIONS

Some design decisions seems to be sufficiently principled to state at the outset. They are:

D1. The orbiter powerplant may operate in a variety of modes—such as turbojet, subsonic combustion ram jet, supersonic combustion ram jet (a.k.a SCRAMJET), or chemical rocket—but there will be only one *stage*.

D2. Owing to the hazard of detonation of explosive gases leaked from the orbiter during a flameout of the powerplant or rupture of a fuel line or tank, the external boost of the orbiter must not take place in a confined region (like a tube). For this reason, concepts of external boost of the fully-fueled orbiter down a barrel by differences of air pressure on its forward and aft sides (in the manner of an artillery shell) are *a-priori* unacceptable.

D3. One advantage of the external boost concept is to avoid using energy from the fuel-oxidizer to accelerate its own mass. Thus proposals in which the energy that propels the carriage while it is on the ground is supplied from sources external to the carriage are especially attractive.

D4. An advantage of concepts that involve horizontal acceleration on the ground is to avoid extra costs associated with a flying first stage booster. In particular, a reusable flying first-stage booster (as in the early conceptual development of the first generation space shuttle) is *a-priori* unacceptable.

3. QUESTIONS WHOSE ANSWERS ARE PREREQUISITE TO LATER DESIGN DECISIONS

Q1. *At what time in the launch sequence should the main engines of the orbiter by ignited?*

In regard to this question, most of the discussions I have had with NASA personnel here has been predicated on the assumption that the orbiter's main engines will be brought up to full power while the orbiter remains attached to the carriage. Early ignition allows ground controllers to confirm that the main engines are operating satisfactorily before committing to launch. In the mean time, the main point of the boost by an external launch carriage is to conserve fuel in the orbiter. To avoid defeating this purpose, a carriage that supports an early-ignition launch profile must serve as a *tanker* that continually resupplies the orbiter with fuel up to the instant of separation. Making the carriage *wet* in this way introduce complexities and attendant costs in the system (and its between-launch processing) that one might otherwise want to avoid.

Alternatively, the second stage of the Saturn V launch system was not ignited until shortly after separation from the first stage and the X-15 rocket plane operated in a captive-carry mode (with the engine off) prior to separation from a mother ship. These examples illustrates that a man-rated launch system may function satisfactorily even some of its engines do not begin to fire until after it attains both significant altitude and significant speed.

If one were to carry this reasoning to its logical conclusion, one should consider the option of a mission profile in which the orbiter is towed by a cable from a ground based *tug*. Such a tug might be along the lines of a launch carriage. The key difference, however, is to place sufficient distance between the tug and the orbiter to prevent wear and tear on the tug from the orbiter's exhaust plume.

Q2. *What limits the speed that the carriage-orbiter combination can attain on the ground prior to separation?*

The equations in §1 above show that for the orbiter the ratio, m_0/m_n, of mass at separation, m_0, to mass in orbit, m_n, depends upon the velocity increment, $v_n - v_0$, that the orbiter powerplant produces during its sequence of engine burns during that period. Here, $v_n = 7,582$ m/s for a 300 nautical mile low Earth orbit and v_0 is the carriage velocity at separation. Since v_n is fixed by natural phenomena (*e.g.* the Earth's radius and gravitational constant) any increase in v_0 carries over to a drop in $v_n - v_0$ and, hence, to a drop in m_n/m_0. The dependence of m_n/m_0 is, moreover, exponential. It is clearly desirable to make v_0 as large as possible.

The figure $v_0 = 600$ mi/hr seems to be the most common one mentioned in the literature on proposals for a catapult for a third generation space shuttle. The figure $v_0 = 600$ mi/hr is close enough to the velocity of sound at sea level to suggest that it arose from a feeling that supersonic speeds on the ground introduce technical difficulties that one would otherwise like to avoid. While it is clear that there will be technical difficulties associated with supersonic ground speeds, it is not clear that those difficulties would be insurmountable or that the cost of surmounting them would be prohibitive. Note that the aerospace industry has considerable experience designing inlets for jet engines that operate supersonically. A supersonic inlet which operates in close proximity to an airplane fuselage or wing is analogous to a launch carriage that operates in close proximity to the ground. Although the theory and software required to model such a flow accurately is not trivial, it is nevertheless available and does not require the discovery of any new physical principles. If one's only reason to limit the carriage speed to 600 mi/hr or less is the supposed lack of technology for modeling the compressible flow involved then that reason is not compelling.

There is a principled reason for setting a maximum tolerable velocity on any given carriage, however. This reason has to do with a species of dynamic instability known as *flutter*. In wing flutter, forces due to aerodynamics, elasticity and inertia all play essential roles. The so-called *typical section model* of bending torsion flutter of an airplane wing (see, for example, §2-7 on pp 36–40 and §6-6 on pp 258–277 of BISPLINGHOFF & ASHLEY, 1962)[2] furnishes a time honored example of dynamic instability. The seminal papers on the typical section model were THEODORSEN (1935)[3] and THEODORSEN & GARRICK (1940)[4], both of which resulted from work done at the NACA Langley Research Laboratory. In this model, one replaces a three-dimensional elastic airplane wing by a representative section, situated, say at a distance three-quarters of the way from the plane of symmetry to the tip. A unit span of wing at the typical section is then treated like a rigid body in two degrees of freedom (namely *plunge* and *pitch*). The section pivots about a hinge axis. This raises the question: Which point on the typical section should one take as the hinge axis? The standard choice is the so-called *shear center*, a familiar one in beam theory.

The plunge displacement of the typical section is resisted by a spring which, according to the model, represents the bending stiffness of the original wing. Likewise, the angular displacement of the typical section is resisted by a torque spring which represents the torsional stiffness of the wing. The center of mass of the typical section need not coincide with the shear center and the distance between these two points is a sensitive parameter in flutter theory.

In the absence of aerodynamic forces the typical section is a species of harmonic oscillator which is not subject to any dynamic instability as such. In addition to the shear center and the mass center the inclusion of aerodynamic forces brings a third special point into the analysis, namely the *aerodynamic center*. The aerodynamic center is a fulcrum point relative to which the aerodynamic pitching moment is independent of angle of attack (at least for angles of attack below the the condition of *stall*).

If one writes down the relevant equations of rigid body dynamics (namely the equation for the rate of change of translational momentum in plunge and the rate of change of rotational momentum in pitch), includes aerodynamic forces and restricts attention to disturbances of small amplitude, then one obtains a linear, homogeneous, constant coefficient system of ordinary different equations. One may reduce the system of differential equations to a system of algebraic equations by substituting trial solutions for the dependent variables each of which depends upon time, t, through the factor $e^{\lambda t}$, (in which λ is an unknown complex constant). Nontrivial solutions are mathematically possible only for special values of λ, which are *eigenvalues* of a linear algebraic system.

Typical results show that if the remote wind speed, v, varies parametrically, there will be a special value of v (denoted, v_f) such that the eigenvalues have negative real part (indicating damping) if $v < v_c$ and positive real part (indicating amplification) if $v > v_c$. This critical velocity is called the *flutter speed*. If the airplane were to fly faster than the flutter speed, then infinitesimal disturbances would amplify exponentially in time and the wing is in danger of shaking itself apart. the flutter speed is then a *red line* speed above which a wing must never fly.

What does all this have to do with catapults for launching third generation space shuttles? The elements present in the typical section model of wing flutter are all present when one models the dynamics of a carriage-orbiter combination during its acceleration down a catapult. The magnetic or aerodynamic forces present may be modeled as virtual spring stiffnesses and from them one may find a virtual hinge point analogous to the shear center discussed above.

Among the tasks that must be carried out in this project is: *The development of a suitable dynamic instability model for the flutter of an orbiter-carriage combination with a view toward calculating the dependence of the flutter speed.* Experience with flutter calculations on airplane wings shows that the flutter speed is strongly dependent upon the placement of the center of mass relative to the shear center and aerodynamic center.

One should also mention that a flutter analysis would include the modeling of the aerodynamic side force due to sideslip. In the present application, a disturbance velocity under the heading of sideslip would be caused a gust of wind whose velocity had a nonzero component perpendicular to the launch track. Such a gust would produce a side force directly proportional to the vehicle speed. An analysis of such a side forces is necessary in any case to establish stiffness and strength requirements for the launch track.

If the carriage of a launch catapult is wet, *i.e* it is used as a tanker to resupply the orbiter through a quick disconnect during the acceleration phase, then any shift of the center of mass of the carriage that results could affect the flutter speed. If, as I suspect, dynamic instability results in a red line speed for the catapult, then the ability to analyze and control that speed is of fundamental importance to the whole project and must not be allowed to fall through the cracks during the planning stage.

4. PRELIMINARY INVENTORY OF CATAPULT CONCEPTS

The concept of levitation and propulsion are distinct. Consequently, one may construct family of $m \times n$ boost concepts, in which m is the number of independent levitation concepts and n is the number of independent propulsion concepts. Thus, a short list of *levitation concepts* might include: *Magnetic levitation*, *Fixed-wing aerodynamic levitation*, and *Hovercraft levitation*. A hovercraft is a vehicle supported by an cushion of air. The sides of the air cushion are surrounded by a flexible skirt. The pressure in the air cushion is maintained at a value above that of the surrounding air by a ducted fan that pumps air into the cushion from the outside. Similarly, a short list of propulsion concepts might include: *Propulsion by a linear electric motor*, *Propulsion by a ducted fan*, and *Propulsion by pneumatic pressure on a piston in a long slotted cylinder*. I will elaborate briefly on each of these levitation and propulsion concepts in turn.

L1. Magnetic levitation. The present discussion is adapted from GIBBS & GEIM (1997)[6]. Let the term *static levitation* denote the case of stable suspension of an object against gravity. According to a theorem by EARNSHAW (1842)[7] there is no possible arrangement of fixed magnets or electric charges that enables static levitation in the foregoing sense.

GIBBS & GEIM (1997)[6] thus organize technologies for magnetic levitation into classes, each of which exploits one or another violation of the assumptions of EARNSHAW's theorem. They list five such loopholes, namely

1. Quantum effects (which apply only only atomic or subatomic scales);
2. Feedback (An electromagnet of controllable strength supplies the magnetic field while a sensor detects changes in position of the suspended body. Feedback of the information from the sensor to a actuator enables adjustment of the magnetic field to restore the body to its intended position);
3. Diamagnetism (which normally involves the use of superconducting materials and is effective only in very intense magnetic fields);
4. Oscillating fields;
5. Rotation.

Magnetic levitation trains built in Germany exploit feedback. Three NASA contractors have built technology-demonstration tracks intended to model the action of an external boost system for a spacecraft launcher. Of these, tracks built by FOSTER-MILLER of Waltham, Massachusetts and Lawrence Livermore National Laboratories produce magnetic fields that oscillate relative to an observer fixed to the track (The inventor of the Livermore system is Dr. RICHARD POST, who calls the device the *Inductrack*). The *Inductrack* and the FOSTER-MILLER track produce a time dependent magnetic field relative to the track by placing an array of permanent magnets *of alternating orientation* on the launch carriage. The track is equipped with wire coils. Movement of the magnetized carriage over the track induces electrical currents in the coils which thus set up magnetic fields of their own (that act to repel the carriage). In this way, forward motion of the track produces a levitating force even when neither the carriage nor the track is supplied by any external power source. A third technology-demonstration track, built for NASA by PRT Advanced Maglev Systems of Park Forest, Illinois (based on knowhow furnished by a team at the University of Sussex in Brighton, England) produces an oscillating magnetic field by electromagnets which require an external (alternating current) power supply to energize.

L2. Fixed-wing aerodynamic levitation. A fixed-wing airplane takes off horizontally by producing lift which exceeds its weight. In doing so, it produces a system of *trailing vortices* (having rotation axes parallel to the direction of flight) that continually add kinetic energy to the air. A body that continually feeds kinetic energy to the air does so by performing *work* on it. The force that does this work is called *induced drag*, *vortex drag* or *drag-due-to lift* (all of which are synonyms). Such vortex drag is in contrast to *wave drag* (due to the generation of bow shocks and other *compression waves* in supersonic flow) and *form drag* (which is a catch-all term that incorporates contributions to drag from *skin friction* and alteration of the pressure field due to the unsteady vortex shedding and other manifestations of *boundary-layer separation*).

Now the vortex drag of a wing of given span, b, flight speed and lift (moving through an incompressible fluid of uniform density) is dependent upon altitude, h, but varies with h only for values of the altitude-to-span ratio, h/b, that are small compared to one. In the limit $h/b \to 0$ (within the limits of the usual inviscid-fluid model) the vortex drag, D_v, tends to zero according to the rule $D_v \propto h$, while the lift, L, tends to infinity according to the rule $L \propto 1/h$. Classical works which demonstrate the foregoing assertions are WIESELBERGER (1921)[8] and DE HALLER (1936)[9]. For modern expositions of this theory and discussions of its relevance to the design of ram-wing vehicles for high-speed mass transportation I recommend BARROWS & WIDNALL (1970)[10] and WIDNALL & BARROWS (1970)[11]. Ram wing tube vehicles of the size of subway trains would cruise at an altitude on the order of one foot at speeds on the order of three hundred miles per hour. There is nothing in the principle of operation of such fixed-wing ground effect vehicles which exclude operation in an open channel (as would be the case when the vehicle is the carriage for external boost of a spacecraft). An article by YAFFEE (1967)[12] describes a small-scale technology demonstrator of a ram-wing tube vehicle built at Princeton under the direction of M.P. KNOWLTON. The vehicle was about six feet long. It was powered by a model airplane engine and it flew down a one-foot diameter two-hundred-yard-long channel at a speed of about fifty miles per hour with a clearance of about one inch. BARROWS & WIDNALL (1970)[10] (whose senior author was a member of the team that built the Princeton model) report that "[the model] was inherently stable and required no special devices to prevent it from drifting into the side of the tube."

As in the case of the *Inductrack* and the FOSTER-MILLER track mentioned in the preceding subsection, the channel in which a fixed-wing aerodynamically levitated carriage would run would be passive, that is, no external power source is needed to produce levitation other than the value needed to overcome aerodynamic drag. The aerodynamic drag would be small compared to the force needed to overcome inertia to accelerate the carriage and orbiter to the orbiter's release speed. The channel is even simpler than a maglev track, however, since it does not require that electrical coils be imbedded in it throughout its length. The spacing between the hull of the fixed-wing carriage (on the order of one foot) is larger than the spacing between the carriage and a maglev track (on the order of a centimeter). One may surmise that the manufacturing and maintenance of a maglev track to one centimeter tolerance and equipped with embedded coils will be more expensive than the manufacturing and maintenance

of a channel for a fixed-wing carriage (which is on the order of one foot and has no embedded coils).

L3. Hovercraft levitation. As I mentioned in at the beginning of §3 a hovercraft is a vehicle supported by an cushion of air. The sides of the air cushion are surrounded by a flexible skirt. The pressure in the air cushion is maintained at a value above that of the surrounding air by a ducted fan that pumps air into the cushion from the outside.

One disadvantage of hovercraft levitation is that it requires a power source to drive a fan that maintains an overpressure in the air enclosed by its bottom skirt. If one is willing to pay this price, however, hovercraft have the advantage that they can hover above the track even if there is no forward motion. The *Inductrack* and the fixed-wing aerodynamically levitated carriage options, by contrast, levitate only with some forward motion of the carriage thus necessitating the use of wheels at the start and at the end of the acceleration run when this forward motion is too small to produce lift.

P1. Propulsion by a linear electric motor. An ordinary electric motor converts electrical power to shaft power. Two broad categories of electric motors are *induction* motors and *synchronous* motors. Both kinds can be unwrapped in the sense that the parts that normally constitute the rotating spindle and its surrounding housing can be replaced by linear elements. The present versions of the maglev launch technology demonstators built by FOSTER-MILLER and the PRT Advanced Maglev Systems incorporate linear electric motors. So will the Phase-II version of the Lawrence Livermore device—the one which incorporates the *Inductrack* levitation system—when it is delivered (the Phase I version of the *Inductrack* device used a stretched bungee cord for propulsion).

The supply of electrical power to a linear electric motor in sufficient quantity and at sufficient switching speeds to launch a full-scale third generation space shuttle is a significant technical problem. Indeed, one may reasonably expect that the development of high-speed, high-capacity switching technology represents a major cost item for the magnetic levitation-magnetic propulsion option. At the same time such development effort, if sucessful, would yield spinoffs that promise to be valuable in the electric power industry.

P2. Propulsion by a ducted van. The simplest device for producing a large propulsive efficiency is a propeller. Now a propeller that drives a vehicle that cruises at a high subsonic Mach number will have tip speeds that are well above the speed of sound (since the speed of the propeller tip relative to the air is the resultant of an axial and a rotational component). Such supersonic tip speeds are noisy and rather inefficient. One can solve this problem, by situating the propeller at the aft end of a diffusor (a variable area duct designed to reduce the axial velocity of the fluid). Having a propeller inside a duct, one may then reduce vortex drag by allowing the propeller tips to extend all the way to the wall. The result is called a *ducted fan*.

Nearly all commercial jetliners (with the single exception of the *Concorde* supersonic transport) are propelled by engines that feature ducted fans. The shaft power to drive the fan is supplied by a turbine. Such engines are therefore called *turbofans*. It is important to realize, however, that the bulk of the thrust produced by a turbofan powered jetliner engine is produced by the fan.

Now shaft power to drive a ducted fan need not come from a turbine. In the case of a ducted fan that propels a catapult for a third generation space shuttle the shaft power may come from a conventional (rotary) electric motor. In such a design, the carriage need not carry any liquid or sold fuel *to supply its own powerplant*. Of course, if the mission profile is such that the engines of the orbiter are started sometime before separation, then the carriage must act as a tanker to refuel the orbiter through a quick disconnect. The weight penalty of this fuel is then quite independent of the weight—or lack of weight—of the energy that drives the catapult. If the catapult is indeed powered electrically, then there must be some sort of electrical contact between the carriage and a linear conducive element, such as a third rail of a subway train.

Of some interest here is the size of the ducted fans that would be required in the present application. For comparison, the Pratt and Whitney Engine Gallery web page (cited in §1 above) furnishes data for the PW4098 turbofan engine, which produces 98,000 lbf thrust at takeoff. The fan tip diameter is 112 in. If one estimates the diameter of the hub as 1/3 the diameter of the tip, then one can calculate the frontal area of the fan. The ratio of the thrust (98,000 lbf) to the frontal area (10,433 in^2) gives a *pressure loading* for the fan of about 9.39 lbf/in^2.

If one supposes the same pressure loading for

a twin pair of electrically powered ducted fans on a launch carriage, then one can estimate the diameters of those large fans in a straighforward manner. For this purpose assume that

1. The (wet) weight of the carriage and its powerplant equals the (wet) weight of the orbiter;
2. The (wet) weight of the orbiter is 1×10^6 lbf;
3. The thrust of the orbiter is 1.5 times the wet weight of the orbiter;
4. The horizontal acceleration of the orbiter and carriage when coupled equals $2g_0$;
5. The diameter of the hub is again 1/3 the tip diameter of the fan.

With these assumptions, I calculate a fan tip diameter of 35.26 ft. For comparison purposes, consider the size of the power rotor of the 16 ft transonic wind tunnel at NASA/Langley. According to the *Langley 16-foot transonic tunnel users guide* (on the web at http://wte.larc.nasa.gov/facility/16ft/16ft_user/16ft03.html#3.5) the outer diameter of the power fan is 34 ft and the inner diameter is 20 ft. The size of the ducted fans in above calculation is thus comparable with that of fans used in existing wind tunnels.

The most serious disadvantage of the ducted fan propulsion concept seems to be vulnerability of the fan to damage from foreign objects or from the exhaust plume produced by the orbiter powerplant following separation. A launch carriage design could deal with this problem by incorporating *blast shields* that would raise just prior to separation. As I mentioned in §3 above (at the end of the discussion of Question Q1) there is a possible mission profile in which the orbiter is towed by a cable from a ground based tug and that such a tug might be along the lines of the launch carriage. The lack of close proximity between the orbiter and the tug would eliminate the need for blast shields on the latter, even if it were propelled by ducted fans.

P3. Propulsion by pneumatic pressure on a piston in a long slotted cylinder. DALE LUECK and CLYDE PARRISH of Kennedy Space Center have considered the option of pneumatic propulsion of a launch carriage for a second generation space shuttle (I am indebted to DALE LUECK for furnishing me with unpublished documents describing their proposal). In their proposal the piston would be connected to the launch carriage by a slender pylon, the cylinder having a longitudinal slot which would be open on the downrange side. The pylon between the cylinder and the carriage transfers thrust load rather than weight, so a separate mechanism supports the weight of the carriage by outriggers. The air downrange of the piston is subject to compression by it, the resulting drag playing a role in post separation decelleration and abort scenarios. The cylinder slot uprange the piston must be closed after the piston passes by. LUECK and PARRISH point out that such sealing can be accomplished by a sequence of doors driven closed by a mechanism that exploits the pressure in the cylinder itself and that such devices fall under the heading of available technology (in the field of *fluidics*).

One advantage of piston propulsion is that the cylinder shelters the prime mover (in this case the piston) from the exhaust plume of the orbiter's engines, and thus eliminates the need for blast shields of the sort needed in the case of ducted fan propulsion.

LUECK and PARRISH propose the use of gas storage chambers in two locations, namely a stationary chamber at the uprange end of the cylinder and another in the piston itself. As the piston accelerates down the cylinder it will cause the driving pressure behind it to diminish and the resisting pressure ahead of it to increase. The maintenance of a constant acceleration down the track is thus not an automatic feature of the design.

There are other technical challenges that must be overcome to implement this concept, including:

1. The assurance that the bearing between the piston and the cylinder is of adequately low friction;
2. The assurance that the seal between the piston and the cylinder is of adequately low leakage;
3. The assurance that the capital cost of building a cylinder of adequate length strength and accuracy is not prohibitive.

5. PHASES OF THE PROJECT AND MAJOR MILESTONES

The overall project divides itself naturally into two major parts. The first part is devoted to research *in support of the development and evaluation of rival levitation and propulsion concepts*; The second part is research *in support of development of the operational system after the winning concept has been identified.* Between these two overall phases is what one might call the *design stabilization time.* The choice of when to fix the design stabilization time

is sensitive. The error of placing the design stabilization time too early is summarized by the ancient maxim *haste makes waste*. Thus, the more time one allows for the development of rival design options, the better those options should become (and the more likely one is to make a wise decision among alternatives).

Alternatively, the error associated with placing the design stabilization time too late is summarized by the more recent maxim *the perfect is the enemy of the good*. Thus, the longer one waits to fix the overall design the less time one has to finish the project within the overall twenty-five year time window. If one tried to resolve every conceivable question before committing oneself to a design the project would never get underway in earnest. One thus arrives at a

MANAGEMENT QUESTION:
At what point in the twenty-five year project cycle should the design be stabilized?

In the following straw-man timetable, I have set the design stabilization time (more or less arbitrarily) at the one-third point of the twenty-five year cycle. In round numbers, then, *the design stabilization time is eight years after kickoff* (The abbreviation "KO" denotes "kickoff." in the following).

Phase 1a: (KO $< t <$ KO + 4 years). Carry out a number of *small scale hardware demonstration projects*. The idea is *to filter the set of all reasonable suggestions for levitation and propulsion to determine which ones can be implemented in some form of hardware* (and, consequently, to weed out the ones which are so advanced that they exist only on paper).

Phase 1b: (KO $< t <$ KO + 4 years). Research to address questions whose answers are prerequisite to later design decisions (*cf.* §3 above). *e.g.* At what time in the launch sequence should the main engines of the orbiter be ignited? and What limits the speed that the carriage-orbiter combination can attain on the ground prior to separation? Research on the analysis of flutter of a launch carriage and on the aerodynamics of fixed wing ground-effect machines should be commence during this period. The research should lead to the development of models of sufficient detail and credibility to assess design tradeoffs quantitatively, though it will be limited by the lack of data from small-scale hardware projects to be carried out simultaneously.

Milestone 1: (t = KO + 4 years). Completion of Phases 1a and 1b and selection of levitation and propulsion concepts that make the *first cut*, *i.e.* advancement to Phase 2.

Phase 2a: (KO + 4 years $< t <$ KO + 8 years). Development and construction of a number of small-scale catapults, each of which is designed to launch a 1×10^3 lbm vehicle.

Phase 2b: (KO + 4 years $< t <$ KO + 8 years). Continuation of the work commenced in Phase 1b, this time taking account of the data produced by the hardware projects in Phase 1a. At the conclusion of this effort, project administrations will have all the information they will get prior to committing the project to one particular choice of levitation concept, propulsion concept, and mission profile.

Milestone 2: (t = KO + 8 years). **Design stabilization time:** Completion of Phase 2 and selection of the levitation and propulsion concept that make the *final cut*, *i.e.* advancement to Phases 3 and 4.

Phase 3: (KO $<$ 8 years $<$ KO + 12 years). Development and construction of the penultimate-scale external boost system designed to launch a 1.2×10^5 lbm vehicle

Milestone 3: (t = KO + 12 years). Completion of Phase 3. Review to determine whether the project should advance to Phase 4.

Phase 4: (KO + 12 years $< t <$ KO + 20 years). Development and construction of the full-scale external boost system designed to launch a 1×10^6 lbm vehicle

Milestone 4: (t = KO + 20 years). Completion of Phase 4. Begin integration of the external boost system with all of the other subsystems of the third generation space shuttle.

Phase 5: (KO + 20 years $< t <$ KO + 25 years). Integration of the external boost system with all of the other subsystems of the third generation space shuttle. Verification that they satisfy the requirements for successful interaction. Troubleshooting.

Milestone 5: (t = KO + 25 years). First flight of the third generation space shuttle.

6. SOME SOURCES OF EXPERTISE TO SUPPORT THE PROJECT

The development of a catapult to assist the launch of a third generation space shuttle can only be carried out by a team.

A list of organizations and individuals that have capabilities (and inclination) well suited to support this project would be long and would require frequent updating. The short list I present here thus makes no pretense to completeness. Having said that, there are a few organizations or categories of organizations that deserve mention in the present context.

1. Developers of prototype magnetic levitation tracks.
2. Defense contractors.
3. The Aerospace Corporation (Headquarters in El Segundo, California).
4. The Charles Stark Draper Laboratory in Cambridge, Massachussets.
5. Faculty and students at universities.

Of course, if this project becomes a reality and significant amounts of money change hands, one may expect that the market will respond and many organizations that have not shown any prior interest in bidding for contracts will do so at that time. One may assume and expect that such latecomers will include many that are highly capable and worthy of support. This observation merely underscores the disclaimer I made at that start of this section, namely that this short list makes no pretense of completeness.

ACKNOWLEDGEMENTS

I am indebted to my NASA colleagues RIC ADAMS and BOB YOUNGQUIST for suggesting this project and for providing much advice, access to documents moral support and tips.

REFERENCES

[1] SUTTON, G.P. 1992 *Rocket propulsion elements.* Sixth edition, Wiley-Interscience.

[2] BISPLINGHOFF, R.L. & ASHLEY, H. 1962 *Principles of Aeroelaticity.* New York: John Wiley and Sons [Reissued as a Dover Paperback in 1975].

[3] THEODORSEN, T. 1935 General theory of aerodynamic instability and the mechanism of flutter. National Advisory Committee for Aeronautics NACA Report 496.

[4] THEODORSEN, T. & GARRICK, I.E. 1940 Mechanism of flutter, a theoretical and experimental investigation of the flutter problem. National Advisory Committee for Aeronautics NACA Report 685.

[5] ETKIN, B. & REID, L.D. 1996 *Dynamics of flight, stability and control.* Third edition, John Wiley & Sons.

[6] GIBBS, P. & GEIM, A. 1997 Is magnetic levitation possible? Article posted on the World Wide Web by JOHN BAEZ of the Mathematics Department, University of California at Riverside (http://math.ucr.edu/home/baez/physics/levitation.html).

[7] EARNSHAW, S. 1842 On the nature of the molecular forces which regulate the constitution of the luminiferous ether. *Transactions of the Cambridge Philosophical Society*, 7, Part I, pp 97–112.

[8] WIESELBERGER, C. 1921 Über den Flügelwiderstand in der Nähe des Bodens. *Zeitschrift für Flugtechnik und Motorluftschiffahrt*, 10, S 145–147. [Translated as: Wing resistance near the ground. National Advisory Committee for Aeronautics NACA TM 77, April 1922]

[9] HALLER, P. DE 1936 La portance et la traînée induite minimum d'une aile au voisinage du sol. *Mitteilungen aus dem Institut für Aerodynamik. ETH Zürich*, 5, p99.

[10] BARROWS, T.M. & WIDNALL, S.E. 1970 Optimum lift-drag ratio for a ram wing tube vehicle. *AIAA Journal*, 8, pp 491–497.

[11] WIDNALL, S.E. & BARROWS, T.M. 1970 An analytic solution for two- and three-dimensional wings in ground effect. *J. Fluid Mech.*, 41, pp 769–792.

[12] YAFFEE, M.L. 1967 Ram wing studied as a transit vehicle. *Aviation Week & Space Technology*, January 2 issue.

2000 NASA/ASEE SUMMER FACULTY FELLOWSHIP PROGRAM

JOHN F. KENNEDY SPACE CENTER
UNIVERSITY OF CENTRAL FLORIDA

EVALUATION OF THE NASA QUALITY SURVEILLANCE SYSTEM PILOT IN MEETING REQUIREMENTS FOR CONTRACTOR SURVEILLANCE UNDER PERFORMANCE BASED CONTRACTING.

Karen E. Schmahl, Ph.D.
Associate Professor
Manufacturing Engineering Department
Miami University
Oxford, Ohio

KSC Colleague: William DeLoach

Abstract

The use of performance-based contracting at Kennedy Space Center has necessitated a shift from intrusive oversight of contractor activities to an insight surveillance role. This paper describes the results of a pilot implementation of the NASA Quality Surveillance System (NQSS) in the Space Shuttle Main Engines Processing Facility. The NQSS is a system to sample contractor activities using documented procedures, specifications, drawings and observations of work in progress to answer the question "Is the contractor doing what they said they would do?" The concepts of the NQSS are shown to be effective in providing assurance of contractor quality. Many of the concepts proven in the pilot are being considered for incorporation into an overall KSC Quality Surveillance System.

EVALUATION OF THE NASA QUALITY SURVEILLANCE SYSTEM PILOT IN MEETING REQUIREMENTS FOR CONTRACTOR SURVEILLANCE UNDER PERFORMANCE BASED CONTRACTING.

Karen E. Schmahl, Ph.D.

1.0 Introduction

In an effort to enhance the government's ability to acquire services of requisite quality, to ensure adequate contractor performance and ultimately reduce the cost of services, the government is promoting the use of performance based contracting.[1] Under performance based contracting, all aspects of an acquisition are structured around the purpose of work to be performed and measurable performance standards should be applicable to the requirements.[2]

One of the key aspects of performance based contracting relative to quality assurance is that contractors should be given as much responsibility for quality performance as possible. The agency must develop a quality assurance surveillance plan to determine that supplies or services conform to contract requirements. According to Stanley Kaufman of the Office of Federal Procurement Policy, "The use of formal, measurable performance standards and surveillance plans should pay off in the long run by saving contract administration effort through clearer oversight, less government micro-management, and fewer performance problems and cost overruns." [3]

At NASA's Kennedy Space Center, the move to performance based contracting required backing out of detailed oversight of contractor activities to an insight role. According to the NASA Shuttle Restructuring: Safety and Mission Assurance Plan the terms oversight and insight are explained as follows:

Oversight – An intrusive process of gathering contractor product or process data through on-site in-series involvement in the process.

Insight – A process of gathering a minimum set of product or process data that provide adequate visibility into the integrity of the product or process.

One of the primary methods of contractor oversight was performed by means of inspections at Mandatory Inspection Points (MIPs) through out the process. NASA guidelines for MIPs state "Mandatory Inspection Points are specific points during a process where an inspection by the Government is required before the process can proceed." Prior to performance based contracting initiatives, approximately 25,000 inspection points were called out in the contractor's work documents for processing of the shuttle between flights.

Due to the critical and complex nature of manned flight systems, detailed inspections are still a necessary part of the NASA Quality Assurance program. For performance based contracting, however, a process was undertaken to review the MIPs for flight risk and criticality to mission success. Approximately two thirds of the mandatory inspection points were removed with an estimated 8,500 MIPs remaining on the most critical processing jobs. Insight concepts are applied to review contractor activity associated with the remaining areas of shuttle processing.

Johnson Space Center is the lead NASA center for the Shuttle Program and has design authority for the orbiter. Marshall Space Flight Center is the design authority for the propulsion systems. Kennedy Space Center (KSC) is where actual orbiter processing takes place with United Space Alliance as the prime contractor. The NASA design teams and KSC worked together to review the MIPs in the MIP reduction effort.

One of the most significant reductions in MIPs occurred in Space Shuttle Main Engines (SSME) processing. In this area, Boeing Rocketdyne, as a subcontractor to United Space Alliance, is responsible for refurbishment of the engines between shuttle flights. The mandatory inspection points were reduced 90% from approximately 6000 to 600 MIPs. This was enabled due to the outstanding track record of the contractor and use of a pilot approach to surveillance called the NASA Quality Surveillance System.

2.0 NASA Quality Surveillance System

Under the concepts of performance based contracting, it is important to allow the contractor systems to function to deliver a quality product (hardware). The contractor is also "delivering" an activity that should be consistent with their documented procedures and contract requirements. The NASA Quality Surveillance System NQSS was designed as a surveillance approach to evaluate contractor performance in processing the shuttle between flights. The NQSS is a system to sample/audit contractor activities. It uses documented procedures, specifications, drawings and observations of work in progress to answer the question "Is the contractor doing what they said they would do?"

The NQSS is structured to gather information about contractor adherence to their documented systems and procedures in three areas.

- Key Process Surveillance - General Inspection of work in progress for adherence to the Work Authorization Document (WAD).
- Support Process Surveillance – Detailed review of processes to requirements found in specifications.
- Quality System Elements - Review of overall system procedures within the contractor's ISO Quality System.

Development of these system components for SSME was a combined effort of NASA Marshall Space Flight Center Resident Office, NASA Safety and Mission Assurance and Boeing Rocketdyne Quality Engineering. Each of the areas is discussed below.

2.1 Key Process Surveillance

The term "Key Process" in the NQSS system refers to an overall category of work. All work performed by the contractor, as represented in the standard flow Work Authorization Documents, was reviewed and categorized through process mapping. The term "standard flow" means all activities planned for processing of one set of engines (three engines) for an orbiter to prepare them for the next flight. (Additional unplanned activity occurs each flow as flight degradation and other needs are assessed.) The Work Authorization Document (WAD) provides detailed work instruction to the contractor technicians and authorizes them to perform the work during the flow.

Figure 1 depicts an example of the process mapping performed for Space Shuttle Engine Processing. The top-level process is shown with more detail mapping provided of the "Post Flight Inspection and Test" process block. Two checklists are noted as associated with the detail process blocks. Generally, one work authorization document would contain the set of process activities that compose the "key process" as covered by one checklist. Multiple WADs could use the same key process checklist. The checklists are relatively generic and refer to the WAD for specific requirements for which the NASA Quality Assurance Specialist (QAS) should be looking. Figure 2 shows the checklist associated with the key process Post Flight Inspections.

The checklists are representative of what the NASA QAS would be verifying whether inspecting for a MIP or using the NQSS. Therefore, the specialists are not asked to do more than they would do with a MIP inspection. The key difference is the input of data to a quality system. Under the MIP system, only conformance or non-conformance at the inspection point is recorded. Under NQSS, conformance or non-conformance for each item of the checklist is required. This allows greater amounts of information about contractor performance, both positive and negative, to be obtained. Further levels of detail are provided when incorporating Support Process Surveillance.

Figure 1.

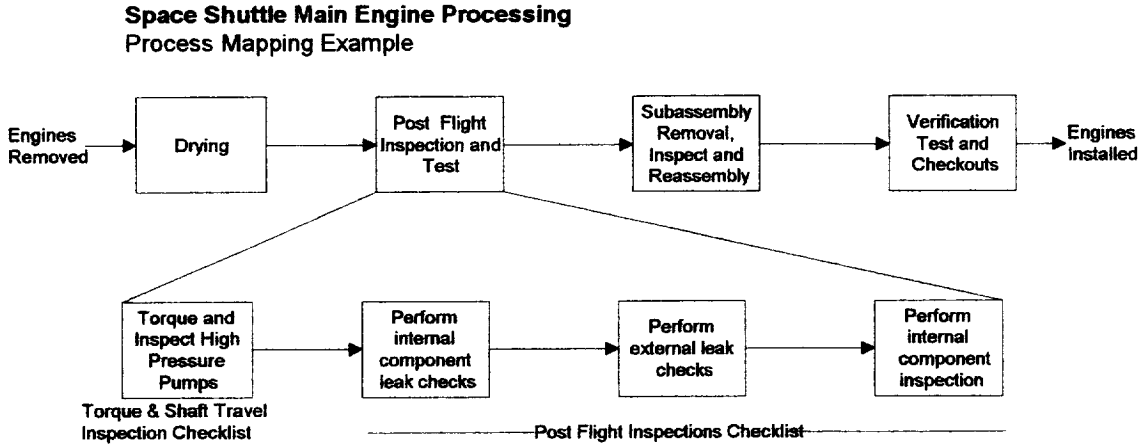

2.2. Support Process Surveillance

"Support processes" refer to those processes that are controlled by standards or specifications. They tend to be common across key process areas. Examples include bolt elongation, nondestructive testing and fusion welding.

In the NQSS system, checklists are made for each support process based on attributes in the associated specifications that could adversely affect process outcome if not correctly performed. The checklist is relatively generic in that it refers to paragraphs within the specification. Changes to the overall structure of a specification, i.e., the paragraph numbers, are infrequent. Therefore, by referring to paragraph numbers, the checklist need not be updated for content changes in the specification. The specialist must obtain the current specification for reference during this type of inspection. Figure 3 shows an example of a support process checklist.

Figure 2. Post Flight Inspections Checklist

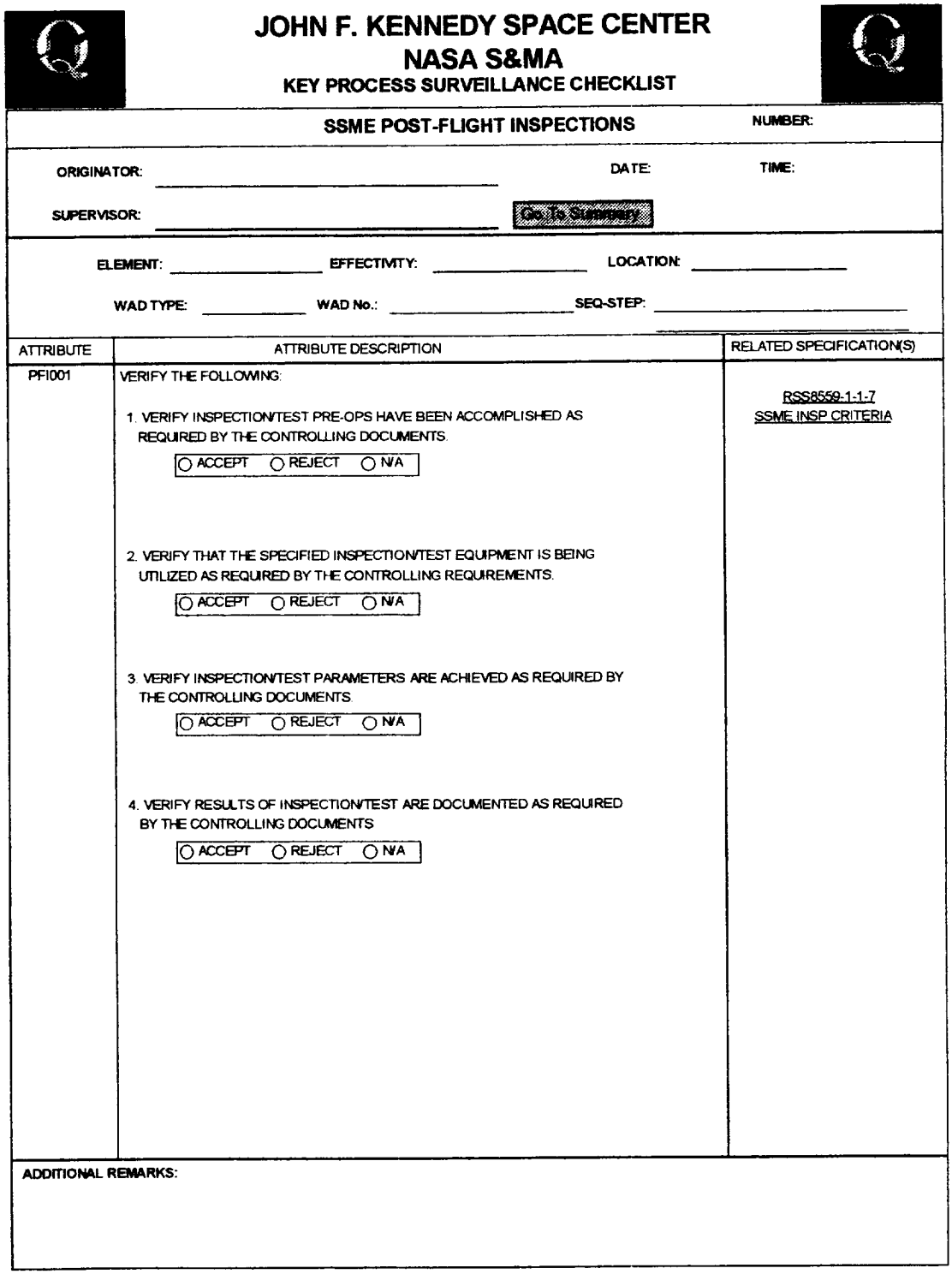

JOHN F. KENNEDY SPACE CENTER
NASA S&MA
KEY PROCESS SURVEILLANCE CHECKLIST

SSME POST-FLIGHT INSPECTIONS NUMBER:

ORIGINATOR: _____ DATE: TIME:

SUPERVISOR: _____ Quality Signature

ELEMENT: _____ EFFECTIVITY: _____ LOCATION: _____

WAD TYPE: _____ WAD No.: _____ SEQ-STEP: _____

ATTRIBUTE	ATTRIBUTE DESCRIPTION	RELATED SPECIFICATION(S)
PFI001	VERIFY THE FOLLOWING: 1. VERIFY INSPECTION/TEST PRE-OPS HAVE BEEN ACCOMPLISHED AS REQUIRED BY THE CONTROLLING DOCUMENTS. ○ ACCEPT ○ REJECT ○ N/A 2. VERIFY THAT THE SPECIFIED INSPECTION/TEST EQUIPMENT IS BEING UTILIZED AS REQUIRED BY THE CONTROLLING REQUIREMENTS. ○ ACCEPT ○ REJECT ○ N/A 3. VERIFY INSPECTION/TEST PARAMETERS ARE ACHIEVED AS REQUIRED BY THE CONTROLLING DOCUMENTS. ○ ACCEPT ○ REJECT ○ N/A 4. VERIFY RESULTS OF INSPECTION/TEST ARE DOCUMENTED AS REQUIRED BY THE CONTROLLING DOCUMENTS ○ ACCEPT ○ REJECT ○ N/A	RSS8559-1-1-7 SSME INSP CRITERIA

ADDITIONAL REMARKS:

Figure 3. Support Process Checklist

JOHN F. KENNEDY SPACE CENTER
NASA S&MA
SUPPORT PROCESS SURVEILLANCE CHECKLIST

LIQUID PENETRANT (ROC) **NUMBER:**

ORIGINATOR: _____ **DATE:** **TIME:**

SUPERVISOR: _____

ELEMENT: _____ **EFFECTIVITY:** _____ **LOCATION:** _____

WAD TYPE: _____ **WAD No.:** _____ **SEQ-STEP:** _____

ATTRIBUTE	ATTRIBUTE DESCRIPTION	RELATED SPECIFICATION(S)
LP001	VERIFY THE FOLLOWING: 1. VERIFY THAT THE EQUIPMENT USED MEET THE REQUIREMENTS OF PARAGRAPH 3.2 ○ ACCEPT ○ REJECT ○ N/A 2. VERIFY PERSONNEL CERTIFICATION REUIREMENTS OF PARAGRAPH 3.3 ○ ACCEPT ○ REJECT ○ N/A 3. VERIFY THE WRITTEN REQUIREMENTS PER PARAGRAPH 3.5 ○ ACCEPT ○ REJECT ○ N/A 4. VERIFY THE PREPARATION OF PARTS PER PARAGRAPH 3.6 ○ ACCEPT ○ REJECT ○ N/A 5. VERIFY INSPECTION PROCEDURES ARE PERFORMED PER PARAGRAPH 3.7 ○ ACCEPT ○ REJECT ○ N/A 6. VERIFY THAT QUALITY ASSURANCE PROVISIONS IN SECTION 4 ARE MET ○ ACCEPT ○ REJECT ○ N/A	RA0115-116 PENETRANT INSPECTION

ADDITIONAL REMARKS:

The difference between inspection as a support process and as a key process or MIP can be illustrated using a liquid penetrant example. In a liquid penetrant operation to check for cracks in high pressure fuel pumps the part is first cleaned, then penetrant is applied and left on for a specified time, a developer is applied, then the part is inspected under a black light for visible defects. Under a MIP, the QAS would look at the final result of the process to verify that the contractor technician detected the surface continuities under the black light. With support process sampling under NQSS, the applicable specification would be obtained. The checklist would direct the QAS to verify a list of the critical attributes of the specification. The QAS would now be verifying such requirements as operator certification, use of the correct cleaner and penetrant and that the dwell time was correct. The entire process would be reviewed in detail relative to the specification.

2.3. Quality System Elements

The NQSS Quality System Elements provides a mechanism for review of overall system procedures within the contractor's ISO Quality System. For NQSS, the contractor Standard Practice Instructions (SPIs) were grouped according to the ISO 9000 elements as shown in Figure 4. Checklists in this portion of the system are developed based on the requirements of the SPIs in a manner similar to the support process checklists derived from the specifications.

Figure 4. Quality System Process screen from NQSS

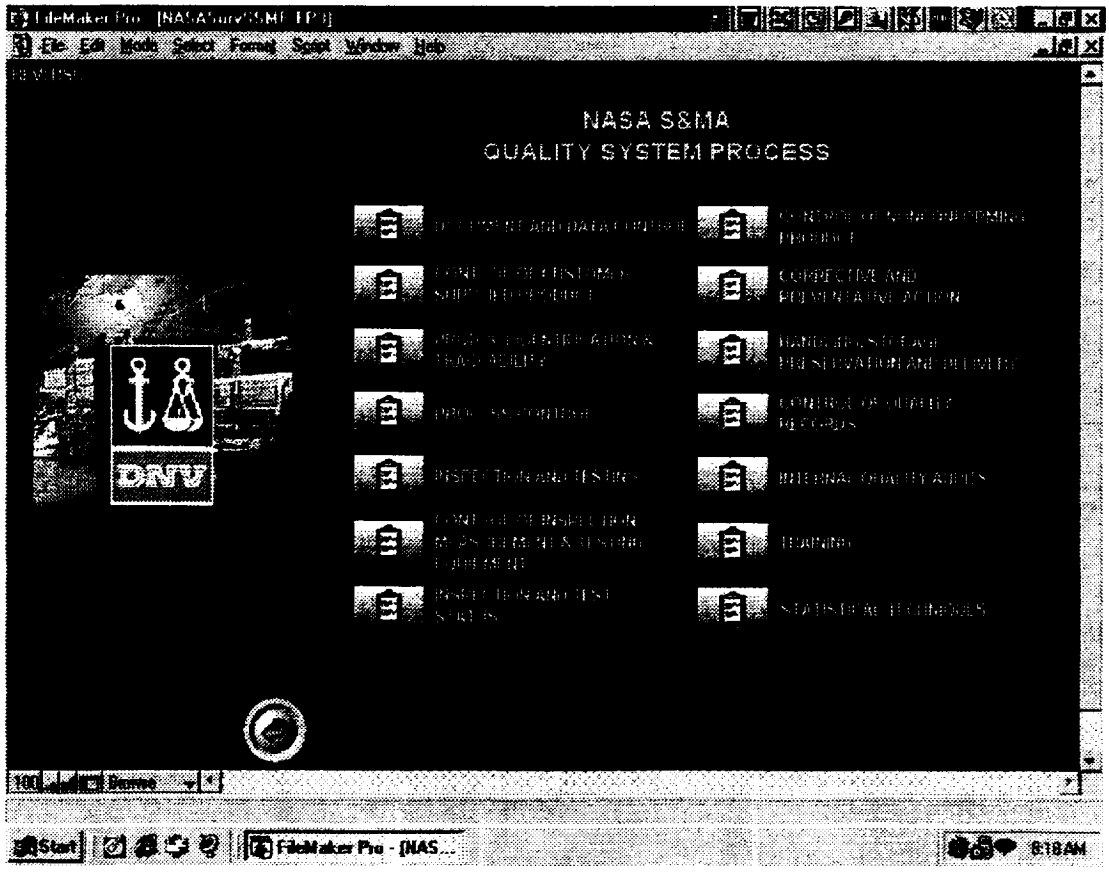

3.0 The NQSS Pilot Project

For the pilot project in the Space Shuttle Main Engine Processing Facility, the Key Process and Support Process checklists were fully developed. (The Quality System Elements were not incorporated.) From January 1999 through January 2000, 111 key and 37 support samples were taken. The numbers of samples are lower than initially requested due to a reduced number of flights. Figures 5 and 6 show the number of samples taken in each category and the number of nonconformances found.

Figure 5 – Key Process Sample Data

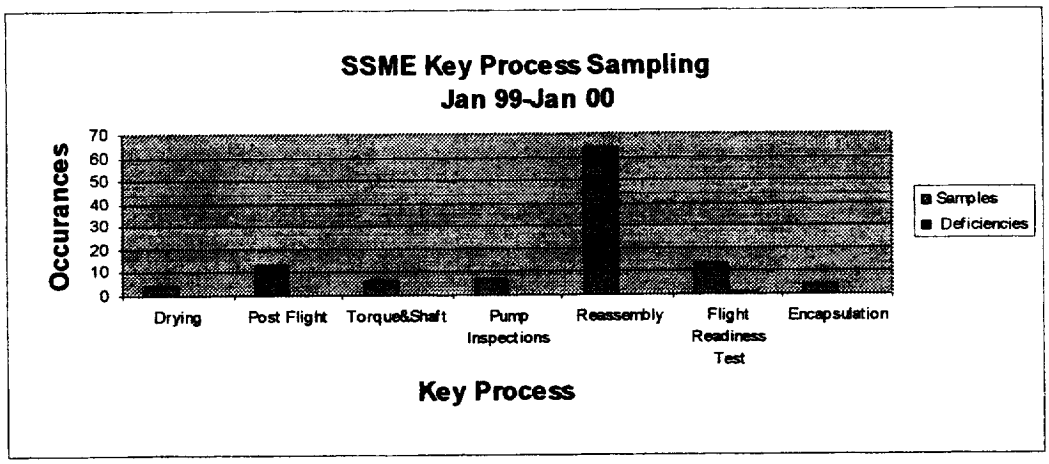

Figure 6 – Support Process Sample Data

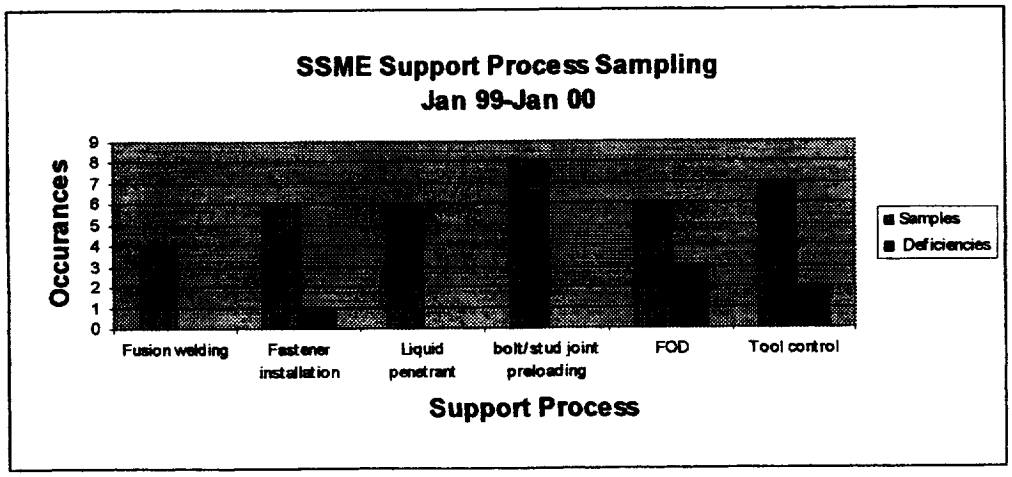

3.1 Key Process Sampling

The key process sampling was designed to provide a level of assurance of process integrity primarily where MIPs were removed. Opportunity was taken to capture adherence to overall processes/procedure on a sampling or audit basis rather than single points in time such as with the MIPs.

The NQSS demonstrated the use of sample data from NQSS to conclude that the SSME processes are in control and performing adequately. The sample data from the key process Reassembly is illustrative of this. Sixty samples were taken with no nonconformances. Using the exact method for binomial proportions in MINITAB, [4] this would indicate that with 95% confidence the true percent defective could be said to be between 0% and 4.87%. This indicates that the contractor meets the expectation of 95% first time quality as required in the contract. (Generally, MIP data and data from the contractor's quality system are also used in determining process adequacy.)

The pilot also validated the concept that the data could be used to assess the accuracy of data in the contractor's system. Based on 111 key process observations with 1 nonconformance, the 95% confidence interval for the true percent defective is 0.02% to 4.91%. The contractor reported first time quality at 99.76%, a nonconformance rate of 0.24%, for the same time period. (More data is desirable to increase the power of such a test.)

Each sample actually verified from four to six attributes for the process. This approach provided some structure to the inspection process that had previously been dependent on and varied by the inspector. By providing the structure, the inspection process was standardized and provided data from which more detailed analysis could be performed.

3.2 Support Process Sampling

Relative to the support process samples, the violations recorded for FOD (foreign object debris) and Tool Control were for workplace rule issues that were corrected at the time they were identified. Of significance in the Support Process sampling is the single violation found under Fastener Installation. By methodically reviewing the specification entitled "Installation of bolts, nuts, screws and studs" it was discovered that an unacceptable configuration safety cable was being utilized on fasteners. This discovery would most likely have been overlooked by traditional government surveillance and inspection methods. An internal letter of appreciation from Boeing-Rocketdyne to KSC management noted:

> NASA's proactive efforts prevented this issue from becoming a fleet-wide problem and saved many man-hours that would have been required to document, remove and replace the incorrect safety cable. During the cause and corrective action investigation it was determine that systemic concerns existed that required further investigation and resolution. Due to NASA's discovery of the initial violation, Boeing-Rocketdyne has made system enhancements to prevent further recurrence of similar escapes.

While anecdotal, the above example does illustrate the potential of specification audits to identify systematic problems that can be addressed to prevent future problems. In the case of the florescent penetrant example, if the dwell time was incorrect, the indicators may not show a crack resulting in a defective component being installed on an engine. The support process surveillance is proactive in preventing such an occurrence.

An additional benefit of the support process sampling was noted by one of the NASA inspectors. He indicated that having to do audits of the specification was a good refresher for him of the specific process requirements. He then brings this increased awareness to MIP and key process sample inspections. The contractor technician also know that they are subject to audit at the specification level so their awareness of requirements is also increased.

4.0 Next Steps for NASA

The concepts of the NQSS approach for surveillance of contractor quality have proved to be effective during the pilot program. To institutionalize the system as a method of surveillance for Space Shuttle Main Engines, several management issues must be addressed. A good quality assurance plan should include a surveillance schedule and clearly define the resources needed to implement the plan. Feedback and corrective action mechanisms should also be incorporated. [5]

A systematic process must be developed for determining how often and where in the flow of the orbiter samples should be collected. For the pilot, it was specified that a certain number of each type of sample be taken every 90 day period. This approach should be reviewed as the launch schedule increases. Criteria must be developed to determine the number of samples per process within a flow or time period and when to make adjustments to the sample sizes based on previous data.

A more formal procedure is needed for assigning specialists to the sampling jobs and for keeping track of the number and type of sample taken. Additional specialists must be trained in the system.

As more data is generated, a method for systematic analysis of the data and feedback of results should be employed. The Quality System checklists also need to be developed and implemented into the surveillance system.

While the NQSS system continues for use in surveillance in the Space Shuttle Main Engines Facility, other areas at Kennedy Space Center are evaluating the system. Many of the concepts proven in the NQSS pilot at being considered for incorporation into an overall KSC Quality Surveillance System.

References

[1] Office of Federal Procurement Policy, Policy Letter 91-2.

[2] Federal Acquisition Regulation, Part 37 Service Contracting, FAC 97-17 including amendments effective as of April 5, 2000.

[3] Kaufman, Stanley, "Federal Policy on Performance Based Contracting for Services", *Contract Management*, July 1993.

[4] MINITAB Statistical Software, Version 13, ©2000 MINITAB.

[5] Office of Federal Procurement Policy, Office of Management and Budget, *A Guide to Best Practices for Performance-Based Service Contracting*, October 1998.

2000 NASA/ASEE SUMMER FACULTY FELLOWSHIP PROGRAM

JOHN F. KENNEDY SPACE CENTER
UNIVERSITY OF CENTRAL FLORIDA

GOES-MICROBURST PRODUCTS PERFORMANCE ANALYSIS IN THE CAPE CANAVERAL AND KENNEDY SPACE CENTER AREAS

Michael R. Witiw
Associate Professor
School of Aeronautics
Florida Institute of Technology
KSC Colleague – Richard Nelson

ABSTRACT

In the past few years, the capabilities of NOAA Geostationary Operational Environmental Satellites (GOES) have increased dramatically. Hourly vertical sounder data is now generally available, but may be unavailable depending upon cloud conditions, satellite operations, and computer system problems at NOAA's National Environmental Satellite Display and Information Service (NESDIS). Meteorologists at NESDIS have used vertical sounder data to develop experimental products for forecasting the probability of convective downbursts. The two products of interest are the Microburst Day Predictive Index (MDPI), which provides an indication of microburst potential and the WINDEX which is a forecast of maximum winds assuming a microburst does occur. Data analyses were made for the central Florida convective season, that is, the period beginning May 1 and ending September 30. The MDPI showed significant potential as an aid in forecasting convective downbursts. MDPI calculated from GOES soundings were well correlated with those calculated from Cape Canaveral RAOBs.

GOES MICROBURST PRODUCTS PERFORMANCE ANALYSIS IN THE CAPE CANAVERAL AND KENNEDY SPACE CENTER AREAS

Michael R. Witiw

1. INTRODUCTION

Microbursts are the concentrated down rushes of air that frequently accompany showers and thunderstorms associated with atmospheric convection. Their definition is "small downbursts, less than 4 km in diameter, with peak winds lasting only 2 to 5 minutes." [1]. In the western United States, microbursts are often associated with precipitation that evaporates below the base of the cloud. This type of microburst that reaches Earth's surface unaccompanied by precipitation is termed a "dry" microburst [2]. In Florida, however, our concern is with "wet" microbursts that are usually accompanied by heavy precipitation.

On August 16, 1994, a thunderstorm produced winds of 33.5 ms^{-1} (65 knots) at the Shuttle Landing Facility. Although thunderstorms were forecasted that day, the strength of the winds was greatly under estimated [3]. Techniques for forecasting the occurrence of thunderstorms at Kennedy Space Center were well developed and described in technical memoranda by Neuman as early as 1970[4] and 1971[5]. However, the ability to forecast the occurrence of a microburst on a particular day was not well established. Likewise, forecasting the strength of winds resulting from the microbursts was problematic.

Equivalent potential temperature, θ_E is the temperature a parcel of air would have, if all the moisture contained in the parcel were condensed out, and the parcel was brought dry adiabatically to a pressure of 1000 millibars. Typically, during summer in Florida, θ_E reaches a maximum in the lower troposphere, and a minimum in the mid-troposphere, typically at an altitude of 14,000 to 16,000 feet. Early studies [3] indicated that a difference of 20^0 C or more indicated a high potential for wet microbursts, while a difference less than 13^0 C implied little likelihood of a microburst event. However, these thresholds were based upon studies conducted elsewhere, and it was thought that they might vary depending upon geographical location. In their 1996 study [3] Wheeler and Roeder refined these limits for the Kennedy Space Center (KSC), and determined that the critical difference for KSC was 30^0 C, with microburst occurrence unlikely when this difference falls below 20^0 C. This difference in θ_E is referred to as TED. The Microburst Day Predictive Index (MDPI) was defined as the difference between θ_E in the lowest 150 millibars of the atmosphere and θ_E higher in the troposphere divided by 30, or TED/30. Converting TED values to MDPI, microburst occurrence is thought to be most likely when MDPI exceeds 1, and unlikekly when MDPI falls below .65. Calculating MDPI from the 1000 UTC and 1500 UTC KSC RAOBs , they showed MDPI to be an aid in forecasting microbursts, provided thunderstorms were already in the forecast, and then later observed.

The Wind Index (WINDEX) is a parameter derived to help forecast the maximum wind speed on days that convection occurs. Its formula is: $WI = 5[H_M R_Q(\Gamma^2 - 30 + Q_L - 2Q_M)]^{0.5}$.
WI is the maximum forecasted wind speed. H_M is the melting level; Q_L is the mean mixing ratio in the lowest 1 km; Q_M is the mixing ratio at the melting level, R_Q is Q_L divided by 12; and Γ is the lapse rate from the surface to the melting level. Mixing ratios are in g/kg, and lapse rates are in deg C per km [6]. Wheeler [7], in examining some selected cases from 1995, determined WINDEX had potential for use as an aid in forecasting maximum wind gusts contingent upon occurrence of a microburst.

Other indicators of microbursts can be found in the radar depictions. These depictions allow for a nowcast of microbursts. Hoffert and Pearce [8] found a relationship between microbursts, lightning, and descending precipitation cores. Descending precipitation cores are associated with both lightning and microbursts. Maximum in cloud lightning occurs 10 minutes prior to a microburst and peak cloud to ground lightning is coincident with microburst occurrence. Microbursts are likely when a maximum precipitation core with a radar reflectivity exceeding 55DBz reaches the level of minimum θ_E [7].

2. METHODS

Previous studies of microburst forecasting at KSC were largely based upon radar and MDPI and WINDEX calculated from local vertical atmospheric soundings (RAOBs). The purpose of this study is to assess the value of the MDPI and WINDEX calculated from GOES soundings. On a typical day at KSC, RAOBs are launched at 1000 UTC and 1500 UTC. GOES soundings are frequently available hourly and have the potential of being useful in updating information obtained from the last KSC RAOB.

GOES data for the Kennedy Space Center convective season (May through September) were archived beginning at the end of July, 1998. The National Environmental Satellite Display and Information Service (NESDIS), a component of the National Oceanic and Atmospheric Administration (NOAA) provided these satellite images as well as the calculated difference in θ_E between the lowest layer of the troposphere and mid-troposphere. WINDEX values were also provided on the satellite images. TED and WINDEX were calculated from the satellite soundings. The TED and WINDEX values were then separately archived. (At KSC, MDPI = TED/30.) Data through the end of June, 2000 were used for this study. NOAA/NESDIS super imposed verification boxes for Cape Canaveral, an off shore location and the Orlando area. Figure 1 shows an example of the data with the boxes drawn for the Cape Canaveral area, an offshore location, and the Orlando area. The numbers plotted are TED values, centered on 10 kilometer by 10 kilometer squares (satellite sounder resolution). Values can vary, both spatially and temporally.

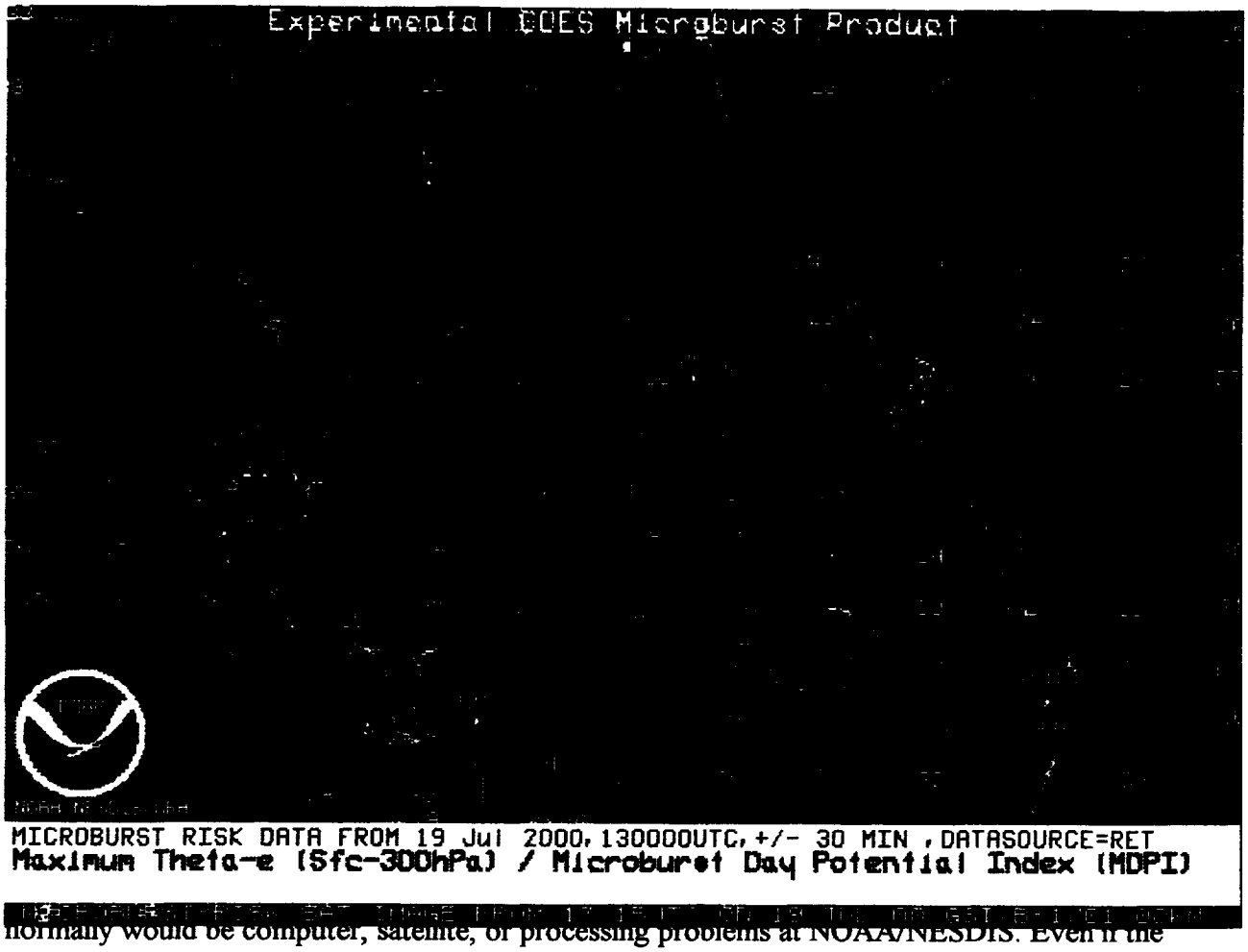

normally would be computer, satellite, or processing problems at NOAA/NESDIS. Even if the product were successfully generated by NESDIS, clouds could prevent the taking of an actual sounding and the calculation of TED and WINDEX.

Two Excel files were then established. In one file, for each day complete data were available, the following information was entered: GOES calculated MDPI and WINDEX; whether or not a microburst occurred on that particular day; and if a microburst did occur, the maximum wind gust associated with the event. The second file contained MDPI calculated from the KSC RAOB at 1500 UTC along with the MDPI calculated from GOES soundings at 1445 UTC and 1615 UTC. Both Excel files were exported to the SPSS statistical program where the data were analyzed.

3. DESCRIPTIVE STATISTICS

GOES satellite data were used for obtaining forecasts. Inclusive periods included 31 July – 28 September 1998; 8 May – 31 August, 1999; and 1 May – 29 June, 2000. From these periods, 169 days were determined to have sufficient data to make a determination whether or not a microburst occurred on that day. For 1998, microburst occurrences were verified using data from Sanger's thesis [10]. For 1999 and 2000, data determined to be adequate to verify a prediction included: TED values available at 1300 UTC or later, and KSC wind tower data from the KSC meteorological information site. For an unknown reason, WINDEX values were not available for 25 of the 169 days analyzed. Other helpful data included lightning strike data, and hourly weather observations. On six occasions when wind verification data were not available, lightning strike data and weather observations were used to rule out microburst occurrence. Positive verification of a microburst event however, could only be made if wind tower data were available for all suspect hours on the day to be verified. Cases were not included in the analysis if these data were not available, and microburst occurrence could not otherwise be ruled out. Thirteen days were eliminated from the analysis due to the lack of wind data. Of the 169 days analyzed, microbursts were determined to have occurred on 37 days. This was determined using Sanger's data [10] for 1998, and applying Fujita's algorithm [9] for 1999 and 2000. Microbursts were categorized according to Kennedy Space Center/Cape Canaveral Air Force Station warning criteria. Category 1 included microbursts where the maximum wind gust was less than 35 knots. There is no warning required for this category. Both categories 2 and 3 require warnings. Category 2 included events where winds were at least 35 knots but less than 50 knots, while category 3 included events that occurred with maximum gusts of at least 50 knots. Table 1 shows the distribution of these events.

Microburst category	**Frequency**	**Percent**
1	21	12.4
2	13	7.7
3	3	1.8

Table 1

In table 2, the descriptive statistics for the analyzed variables are given. Two values for TED and WINDEX were entered into the spreadsheet. On days that microbursts were verified, these included the highest values from 1300 UTC to just before occurrence time, and the value that was computed closest to occurrence time. On days that no microburst occurred, the highest values computed between 1300 UTC and 2000 UTC were entered as well as the values computed closest to, but not later than 2000 UTC.

	N	**Minimum**	**Maximum**	**Mean**	**Standard Deviation**
Max gust	37	22	61	35.65	9.88
Max MDPI	169	10	54	27.50	7.21

Closest MDPI	169	10	54	24.89	7.03
Max WINDEX	144	21	66	44.86	8.05
Closest WINDEX	144	21	64	43.97	7.84

Table 2

2. RESULTS

Simple and multiple linear regressions were then accomplished using the SPSS statistical program. The data indicated that microburst occurrence was related to the highest TED ($p<.01$) computed from GOES soundings between 1300 UTC until just before microburst occurrence. It also showed that microburst occurrence was related to the TED computed closest to occurrence time ($p<.05$). WINDEX values did not add significantly to the variance explained by TED. No variable explained well the wind gusts. However, it should be considered that there were only 37 microburst events and WINDEX was only available for 29 of these events. Table 1 shows the number of microbursts that occurred in each category of TED and what is termed adjusted TED. Adjusted TEDs were calculate from a relationship that appears between the 1445 UTC GOES sounding and the 1500 UTC Cape Canaveral RAOB. Twenty two cases were available where KSC RAOB MDPI were available at 1500UTC. It is interesting that the threshold where the likelihood of a microburst based solely upon TED is 0% when adjusted TED is less than 22; 11.8% when adjusted TED is greater or equal to 22, but less than 30; and 24.5% when adjusted TED exceeds 30. Also interesting is the fact that percent occurrences are fairly evenly distributed above an adjusted TED value of 30. (Recall that 45th Weather Squadron uses a TED threshold of 30 as a first cut on microburst prediction.) The equation developed to calculate an adjusted TED from GOES data is: Adjusted TED = 1.257xTED - 3.422 (1).

TED	**Adjusted TED**	**Microburst days/ total days**
>=40	>=48	2/8
>=35; <40	>=41; <48	5/17
>=30; <35	>=35; <41	10/32
>=27; <30	>=30; <35	14/41
>=20; <27	>=22; <30	6/51
<20	<22	0/20

Table 3

The availability of the data was also evaluated. This is shown in Table 4. Total products available is the percentage of actual products received compared to the number that were scheduled. Products available for Cape Canaveral are the percent of available products that contained data for the Cape Canaveral area. Twenty four products were usually scheduled, however for most of May and June 2000, only 13 products were scheduled per day as there was some question as to

the value of nighttime production. Scheduled production increased to 24 images per day again at the end of June, 2000. From 1998 to 2000 there is an upward trend in the percentage of products that contained data for Cape Canaveral. The total products available in 2000 went down. The over six percent drop however, can be explained by a three day period (May 27 – May 29) for which no products were available. If these three days are subtracted out, the total products available for May and June, 2000 become 94.8%, comparable to the 1999 figure.

Year	**Total products available (% of scheduled)**	**Products Available for Cape Canaveral (% of available)**
1998	73.9%	19.3%
1999	95.4%	43.8%
2000	89.2%	72.8%
All years	87.8%	41.7%

Table 4

5. CONCLUSIONS

Microbursts are hazardous events and finding a method to better forecast their occurrence would benefit operations at Cape Canaveral. Although MDPI or TED calculated from the Cape RAOB has been seen to be an effective forecasting tool on days when convective activity is forecast, the ability to have updated information via GOES satellite soundings has the potential of increasing this effectiveness. An increase of MDPI after 1500 UTC through the predictive threshold can be an indicator of greatly increased microburst probability. Our data shows that a TED adjusted using equation (1) can help update the 1500 UTC RAOB, if it indicates an increase. GOES satellite sounding data, however, are not always available, although the year 2000 shows an increase of availability over the two prior years.

6. ACKNOWLEDGEMENTS

Many people worked to make the NASA summer faculty program a success. I would especially like to thank Rich Nelson of Range Systems for sponsoring my study and Bill Roeder of 45th Weather Squadron for making available an interesting and important project. Dr. Ramon Hosler and Cassie Spears provided superb administrative support and scheduled many interesting meeting and social events.

7. REFERENCES

[1] Wakimoto, R.M., 1985: Forecasting dry microburst activity over the high plains. *Mon. Wea. Rev.*, **116**, 1521-1539.

[2] Nelson, J.P. III, and Ellrod, G.P., 1997: Recent developments in a microburst risk image product derived from GOES I-M satellite sounder data. *Proceedings of the 7th Conference on Aviation, Range, and Aerospace Meteorology.*

[3] Wheeler, M.M. and Roeder, W.P., 1996: Forecasting wet microburst on the central Florida Atlantic coast in support of the United States space program. *NASA CR-203136.*

[4] Neumann, C.J., 1970: Frequency and duration of thunderstorms at Cape Kennedy, Part II (application to forecasting). *ESSA Technical Memorandum WBTM SOS 6.*

[5] Neumann, C.J., 1970: Thunderstorm forecasting at Cape Kennedy, Florida, utilizing multiple regression techniques. *NOAA Technical Memorandum NWS SOS-8.*

[6] Ellrod, G.P., Nelson, J.P. III, Witiw, M.R., Bottos, L., and Roeder, W.P. , In Press: Use of experimental products derived from GOES sounder data in the assessment of microburst potential. *Weather Analysis and Forecasting.*

[7] Wheeler, M., 1997: Verification and implementation of Microburst Day Potential Index (MDPI) and Wind Index (WINDEX) forecasting tools at Cape Canaveral Air Station. *NASA CR-201354.*

[8] Hoffert, S.G., and Pearce, M.L., 1996: The 29 july 1994 Merritt Island, FL microburst: A case study intercomparing Kennedy Space Center three-dimensional lightning data (LDAR) and WSR-88D radar data. *Proceedings of the 18th Conference on Severe Local Storms.*

[9] Fujita, T.T., 1985: The Downburst , 122 pp., Chicago: University of Chicago Press.

[10] Sanger,N.T.,1999: A four-year summertime microburst climatology and reationship between microbursts and cloud-to ground lightning flash rate for the NASA Kennedy Space Center, Florida: 1995-1998: M.S. Thesis, Texas A&M University.

REPORT DOCUMENTATION PAGE

Form Approved
OMB No. 0704-0188

1. AGENCY USE ONLY (Leave blank)	2. REPORT DATE	3. REPORT TYPE AND DATES COVERED
	October 2001	Contractor Report - Summer 2000

4. TITLE AND SUBTITLE

2000 Research Reports
NASA/ASEE Summer Faculty Fellowship Program

5. FUNDING NUMBERS

NASA Grant
NAG10-280

6. AUTHOR(S)

See attached list

7. PERFORMING ORGANIZATION NAME(S) AND ADDRESS(ES)

University of Central Florida
Orlando, Florida 32816-2450
John F. Kennedy Space Center
Kennedy Space Center, Florida 32899

8. PERFORMING ORGANIZATION REPORT NUMBER

NASA CR-2001-210260

9. SPONSORING / MONITORING AGENCY NAME(S) AND ADDRESS(ES)

National Aeronautics and Space Administration
Washington, D.C. 20546

10. SPONSORING / MONITORING AGENCY REPORT NUMBER

11. SUPPLEMENTARY NOTES

12a. DISTRIBUTION / AVAILABILITY STATEMENT

Unclassified - Unlimited
Subject Category 99

12b. DISTRIBUTION CODE

13. ABSTRACT (Maximum 200 words)

This document is a collection of technical reports on research conducted by the participants in the 2000 NASA/ASEE Summer Faculty Fellowship Program at the Kennedy Space Center (KSC). This was the 16th year that a NASA/ASEE program has been conducted at KSC. The 2000 program was administered by the University of Central Florida in cooperation with KSC. The program was operated under the auspices of the American Society for Engineering Education (ASEE) with sponsorship and funding from the Education Division, NASA Headquarters, Washington, D.C., and KSC. The KSC Program was one of nine such Aeronautics and Space Research Programs funded by NASA in 2000. The NASA/ASEE Program is intended to be a two-year program to allow in-depth research by the university faculty member. The editors of this document were responsible for selecting appropriately qualified faculty to address some of the many problems of current interest to NASA/KSC.

14. SUBJECT TERMS	15. NUMBER OF PAGES
Research and Technology	200
	16. PRICE CODE

17. SECURITY CLASSIFICATION OF REPORT	18. SECURITY CLASSIFICATION OF THIS PAGE	19. SECURITY CLASSIFICATION OF ABSTRACT	20. LIMITATION OF ABSTRACT
Unclassified	Unclassified	Unclassified	UL